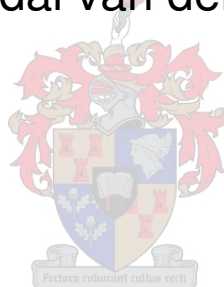


**Spontaneous metathesis of bis-chelated
 $\text{Pd}^{\text{II}}(\text{L-S},\text{O})_2$ complexes in solution:
a *rp*-HPLC study**

Lynndal van der Molen




Thesis presented in partial fulfilment of the requirements for the degree of
Master of Science at Stellenbosch University

Supervisor: Professor Klaus R. Koch

March 2008

Declaration

I, the undersigned, hereby declare that the work contained in this thesis is my own original work and that I have not previously in its entirety or in part submitted it at any university for a degree.

Signature: 

Date: 05 March 2008

Abstract

N,N-dialkyl-*N*-acyl(aryl)thiourea ligands form stable chelated complexes in a *cis* configuration with the platinum group metals. Such chelated complexes are generally considered substitutionally “inert” in solution, however, it was found that *cis*-bis(*N,N*-dialkyl-*N*-acyl(aryl)thioureato)M(II) complexes (M = Ni(II), Pd(II) or Pt(II)) readily undergo facile chelate metathesis reactions in solution at room temperature. Upon mixing two different parent complexes, a mixed-ligand product formed in solution, with an equilibrium, or steady state, between the two parent complexes and the mixed-ligand product being attained after a period of time: $M(L^A)_2 + M(L^B)_2 \rightleftharpoons M(L^A)(L^B)$. All three complexes remained in solution even with a ten-fold excess of one parent complex.

The presence of the mixed-ligand products in solution was confirmed by liquid chromatography-mass spectrometry (LC-MS), nuclear magnetic resonance (NMR) spectra and a crystal structure of the mixed-ligand complex *cis*-Pd(L³-S,O)(L⁴-S,O). Though a number of attempts were made, it was not possible to either isolate or synthesise the mixed-ligand complexes exclusively.

The equilibrium distribution and the rate of the metathesis reaction were influenced by a number of factors, including the central metal ion, the substituents on the complexed ligands and the reaction medium. In addition to these, a number of other factors, some unexpected, also played a role in the rate of the reaction. Initial concentration of the parent complexes, the age of the solutions upon mixing and the presence of impurities or additives all contributed to the overall rate of reaction. The results from these rate studies highlighted the necessity for extensively purified compounds.

In addition to chelate metathesis reactions, the exchange between a *cis*-Pd(L-S,O)₂ complex and an unbound HL ligand in solution was also investigated. Again, even with an excess of unbound ligand, all three possible complexes were present in solution.

It has been shown previously that these complexes undergo a photoinduced *cis-trans* isomerisation under intense light, and it has been proposed that the reverse *trans-cis* process, which occurs in the dark, may be a metathesis reaction. In light of this, the relationship between these chelate metathesis reactions and the reverse *trans-cis* reaction was briefly investigated.

Though the metathesis reactions were a general phenomenon in the Ni(II), Pd(II) and Pt(II) complexes of the aforementioned ligands, the experiments focused mainly on the *cis*-Pd(L-S,O)₂ complexes due to the favourable timescales of their metathesis reactions. The primary technique to observe these reactions was reversed-phase high-performance liquid chromatography (*rp*-HPLC). The timescales involved in the *cis*-Pd(L-S,O)₂ metathesis reactions as well as the stability of the Pd(II) complexes under the HPLC conditions made this technique ideal.

Opsomming

N,N-dialkiel-*N*-asiel(aroïel)tioüreum ligande koördineer in 'n *cis* konfigurasie met die platinum groep metale om stabiele kelaatkomplekse te vorm. Dit word oor die algemeen aanvaar dat kelaatkomplekse in oplossing "inert" teenoor substitusie reaksies is. Ewewel is daar ontdek dat *cis*-bis(*N,N*-dialkiel-*N*-asiel(aroïel)tioüreato)M(II) komplekse (M = Ni(II), Pd(II) or Pt(II)) maklik kelaat metatesisreaksies in oplossing by kamertemperatuur ondergaan. Binne 'n bepaalde tydperk, is daar 'n ewewig, of bestendige toestand, tussen die twee oorspronklike ("parent") komplekse en die gemengde-ligand produk kompleks bereik: $M(L^A)_2 + M(L^B)_2 \rightleftharpoons M(L^A)(L^B)$. Hierdie drie komplekse is altyd teenwoordig in die oplossing selfs wanneer daar 'n tienvoudige oormaat van een van die oorspronklike komplekse teenwoordig is.

Die teenwoordigheid van die gemengde-ligand komplekse in oplossing was bevestig deur vloeistof-kromatografie-massa spektrometrie (LC-MS), kern magnetiese resonans (KMR) spectra en 'n kristalstruktuur van die gemengde-ligand kompleks *cis*-Pd(L³-S,O)(L⁴-S,O). Alhoewel 'n aantal pogings aangewend was, was die isoleering of sintese van uitsluitlik die gemengde-ligand kompleks, nie moontlik nie.

Die ewewigsverspreiding en die tempo van die metatesisreaksies was deur 'n aantal faktore beïnvloed, onder andere die sentrale metaal ioon, die substitüente op die gekomplekseerde ligande en die reaksie medium. Boonop het 'n aantal ander, soms onverwagse faktore, ook 'n rol gespeel in die tempo van die reaksie. Die aanvangskonsentrasie van die oorspronklike komplekse, die ouderdom van die oplossings teen die tyd dat hulle gemeng is en die teenwoordigheid van onsuiverhede

of byvoegings het almal bygedra tot die algehele reaksietempo. Die tempo-eksperimente het klem gelê op die noodsaaklikheid van uiters suiwer komplekse.

Die *cis*-Pd(L-S,O)₂ komplekse ondergaan nie net kelaat-metatesisreaksies nie, maar kan ook hul gebonde ligande met ongebonde ligande in oplossing uitruil. Al is daar 'n oormaat van ongebonde ligand, kom al drie moontlike komplekse nog steeds in die oplossing voor.

Dit is al voorheen gevind dat hierdie komplekse 'n foto-geïnduseerde *cis-trans*-isomerisasie onder intense lig ondergaan. Die moontlikheid dat die terugwaardse *trans-cis* reaksie, wat in donkerte plaasvind, 'n metatesisreaksie is, is voorgestel. Aan die hand hiervan, was die verhouding tussen kelaatmetatesis en die terugwaardse *trans-cis* reaksie, kortliks ondersoek.

Alhoewel die metatesisreaksies in die Ni(II), Pd(II) en Pt(II) komplekse van die genoemde ligande 'n algemene verskynsel was, het die eksperimente hoofsaaklik op die *cis*-Pd(L-S,O)₂ komplekse gefokus as gevolg van die gunstige tydsbestek van hul metatesisreaksies. *rp*-HPLC was die primêre tegniek vir die waarneming van dié reaksies. Die tydsbestek van die *cis*-Pd(L-S,O)₂ metatesisreaksies asook die stabiliteit van die Pd(II) komplekse onder die HPLC kondisies het dié tegniek ideal gemaak.

—oOo—

Sections of this work were presented in the form of a Poster Presentation (*“Metathesis of bis-Chelated [Pd^{II}(L-S,O)₂] Complexes in Solution”*) at the 37th International Conference on Coordination Chemistry in August 2006 held in Cape Town, South Africa.

A article encompassing this work is currently being prepared for publication.

Acknowledgments

- To Prof. Klaus R. Koch for the opportunity to study these “dancing molecules” and for his invaluable guidance and insight
- To the University of Stellenbosch, the National Research Foundation (NRF) and Anglo Platinum for financial support
- To the members of the PGM Research Group– especially Jean McKenzie and Maggie Burger – for the many helpful discussions
- To Jan-André Gertenbach and Bertie Barnard at the Inorganic Chemistry Department for all their help
- To my parents, Karel and Melinda, and sister, Nicole, for their constant love and encouragement
- And, to Jaco Badenhorst for the endless supply of moral support



Table of Contents

Abstract	i
Opsomming	ii
Acknowledgments	iv
Abbreviations	viii
CHAPTER 1	1
1.1 Metathesis	2
1.2 Metathesis reactions involving chelated metal complexes	4
1.2.1 Sulphur/Selenium donor atoms	4
1.2.1.1 Four-membered chelate rings.....	4
1.2.1.2 Five-membered chelate rings	10
1.2.2 N/O donor atoms – six-membered chelate rings	20
1.2.3 Summary and Conclusions.....	26
1.2.4 Instrumentation for the observation of metathesis reactions	27
1.3 Objectives of this study	28
1.4 High-performance liquid chromatography of metal complexes	29
1.5 Coordination chemistry of <i>N</i>-alkyl- and <i>N,N</i>-dialkyl-<i>N'</i>-aroyl(acyl)thiourea ligands towards Pd(II) and other transition metals	35
CHAPTER 2	39
2.1 Synthesis and characterisation of the <i>cis</i>-bis(<i>N,N</i>-dialkyl-<i>N'</i>-aroyl(acyl)thioureato)Pd(II) complexes	40
2.1.1 Ligand synthesis	40
2.1.2 Synthesis of palladium(II) complexes: <i>cis</i> -Pd ^{II} (L-S,O) ₂	41
2.1.2.1 Further purification.....	42
2.1.3 Palladium(II) complex characterisation.....	43
2.1.3.1 Summary of compounds and abbreviated names	51

2.2	Monitoring the metathesis reaction using high-performance liquid chromatography (HPLC)	52
2.2.1	Handling and preparation of samples	53
2.2.2	HPLC procedure	54
2.2.3	LC-MS procedure	58
2.3	Calculations	59
2.3.1	Calibration and calculation of concentrations and percentages	59
2.3.2	Possible sources of error	63
CHAPTER 3	68
3.1	The identification of mixed-ligand complexes	69
3.1.1	Nuclear magnetic resonance spectra (NMR) of mixed-ligand complexes	69
3.1.2	Liquid chromatographs-mass spectra (LC-MS) of mixed-ligand complexes	71
3.1.3	Crystal structure of the mixed-ligand <i>cis</i> -Pd(L ³ -S,O)(L ⁴ -S,O) complex.....	73
3.2	Chelate metathesis in Pd(II), Pt(II) and mixed-metal systems	74
3.2.1	Chelate metathesis in <i>cis</i> -Pd(L-S,O) ₂ complexes	75
3.2.2	Chelate metathesis in <i>cis</i> -Pt(L-S,O) ₂ complexes	76
3.2.3	Chelate metathesis in mixed-metal Pd(II)-Pt(II) systems.....	77
3.3	Attempted synthesis of a mixed-ligand complex	79
3.4	The effect of ligand structure on metathesis	81
3.4.1	Effect of substitution on the benzoyl ring of aroylthiourea Pd(II) complexes on the extent and rate of the metathesis reaction	81
3.4.2	Investigation into the extent and rate of reaction for a combinations of a variety of <i>cis</i> -Pd(L-S,O) ₂ complexes	83
3.5	Varying the ratio of the two complexes in solution	86
3.6	The effect of solvent on chelate metathesis	87
3.7	Ligand exchange between a complex and an unbound ligand	94
3.7.1	Ligand exchange between a complex and its identical ¹³ C-labelled ligand: NMR evidence	97
CHAPTER 4	101
4.1	Determining the rate characteristics of a reaction	102
4.1.1	Rate of reaction in the chelate metathesis of <i>cis</i> -Pd(L-S,O) ₂ complexes	105

4.2	Factors which affect the rate of the chelate metathesis reaction	107
4.2.1	The effect of concentration	107
4.2.1.1	Initial unsuccessful concentration-dependence study	107
4.2.1.2	Successful concentration-dependence study	108
4.2.2	The effect of age.....	109
4.2.3	The effect of the addition of unbound ligand.....	113
4.2.3.1	Addition of a different unbound ligand	117
4.2.4	The effect of the addition of a Brønsted acid.....	121
4.2.5	The effect of the addition of a Brønsted base.....	124
4.3	Metathesis and the photoisomerisation reaction	126
CHAPTER 5		130
5.1	Concluding remarks	131
5.2	Recommendations for further study	133
REFERENCES		134
APPENDICES		138
	Appendix A – Crystal structure and refinement data for <i>cis</i> -Pd(L ⁶ -S,O) ₂ , <i>cis</i> -Pd(L ⁹ -S,O) ₂ , <i>cis</i> -Pd(L ¹⁰ -S,O) ₂ and Pd(L ³ -S,O)(L ⁴ -S,O)	139
	Appendix B1 – Calculation of error on instrument signal replicates	140
	Appendix B2 – Estimation of error around calculated concentration values	140
	Appendix C – Calculation of 95 % confidence interval for calibration graphs	141
	Appendix D1 – “Cold” synthetic method adapted from Mautjana <i>et al.</i>	142
	Appendix D2 – Chromatograms and distributions of recrystallised crude synthesised product of Pd(II) salt with HL ³ /HL ⁴	142
	Appendix D3 – Chromatograms and distributions of crude and recrystallised synthesised product of Pd(II) salt with HL ¹ /HL ²	142
	Appendix E – Detection wavelengths.....	143
	Appendix F – Bodenstein’s numerical method	144
	Appendix G – Equilibrium constants and time taken to reach equilibrium for concentration/aging experiments	145
INDEX OF FIGURES, TABLES AND SCHEMES		146

ABBREVIATIONS

CCl ₄	carbon tetrachloride
CH ₂ Cl ₂	dichloromethane
CH ₃ CN	acetonitrile
CH ₃ OH	methanol
CHCl ₃	chloroform
<i>cis</i> -M(L-S,O) ₂	<i>cis</i> -bis(<i>N,N</i> -dialkyl- <i>N'</i> -acyl(aroyl)thioureato)M(II)
DMF	dimethyl formamide
DMSO	dimethyl sulfoxide
dppe	1,2-bis(diphenylphosphine)ethane
dsc	diselenocarbamate
dtc	dithiocarbamate
ESR	electron spin resonance spectroscopy
EtOH	ethanol
<i>fac</i>	facial ligand orientation
HPLC	high-performance liquid chromatography
HPTLC	high-performance thin-layer chromatography
<i>k</i> and <i>k'</i>	forward and reverse rate constants
K	equilibrium constant $K = \frac{[M(L^A)(L^B)]^2}{[M(L^A)_2][M(L^B)_2]}$
LC-MS	liquid chromatography-mass spectrometry
M	central metal ion of a chelated complex
<i>mer</i>	meridional ligand orientation
MQ water	milli-Q water (deionised, 18 MΩ)
NMR	nuclear magnetic resonance spectroscopy
PGMs	Platinum Group Metals
<i>rp</i> -HPLC	reversed phase high-performance liquid chromatography
sol	solvent
TLC	thin-layer chromatography
t _R	retention time
UV-Vis	ultra violet-visible spectroscopy

Chapter 1

Introduction

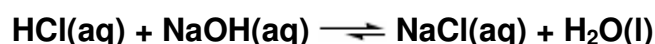
1.1 Metathesis

The term metathesis is defined in the *IUPAC Gold Book* as:

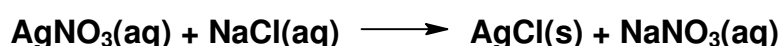
“A bimolecular process formally involving the exchange of a bond (or bonds) between similar interacting chemical species so that the bonding affiliations in the products are identical (or closely similar) to those in the reactants.”^[1]

In other words: $AB + CD \rightleftharpoons AD + CB$

The term has its origins in inorganic chemistry and the reacting species may be ionic or covalent. The position of the equilibrium is dependant upon the reactants.^[2] Surprisingly, one of the simplest reactions in inorganic chemistry can be considered to be a metathesis reaction – the neutralisation reaction between an acid and a base, for example:



A further example of a metathesis reaction is that between two inorganic salts in aqueous solution, where one product is insoluble in water, thereby driving the reaction forward. An example of this is:



The metathesis reaction, however, has found its greatest application in the field of organic chemistry with the metathesis of olefins or transalkyldation. The double bond of the alkene is cleaved and the alkylidene fragments reorganise in a statistical distribution (Figure 1.1).

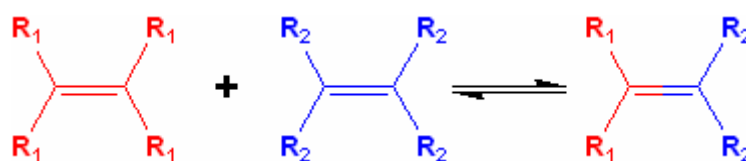
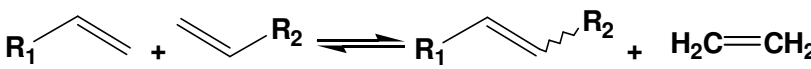
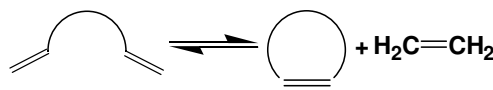
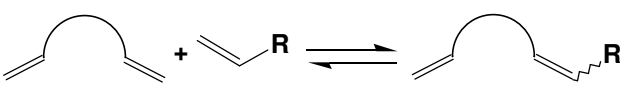
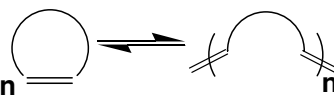



Figure 1.1. Olefin metathesis.

The reaction is catalysed by organometallic complexes of nickel, molybdenum, ruthenium or tungsten and has found widespread use in the manufacture of new compounds, fuels, medicines and polymers.^[3] The catalysts are remarkably selective for carbon-carbon double bonds even in the presence of other functional groups such as alcohols, carboxylic acids or amides, resulting in fewer unwanted side products. Hazardous waste is also reduced as the catalysts allow the olefin metathesis reaction to take place under mild conditions and in some cases, even in aqueous solutions. Due to the revolutionary nature of this reaction, three of its pioneers, Yves Chauvin, Robert H. Grubbs and Richard R. Schrock, received the Nobel Prize for Chemistry in 2005.^[4]

By correctly choosing the structure of the starting compounds, various products with diverse structures are possible (Table 1.1).

Table 1.1. Possible products from olefin metathesis reactions.^[3]

Cross metathesis	
	
Ring-closing metathesis	Ring-closing metathesis polymerisation
	
Ring-opening metathesis	Ring-opening metathesis polymerisation
	

While metathesis reactions are common in simple inorganic chemistry and organic synthesis, one does not immediately associate chelated metal complexes with metathesis reactions. However instances of metathesis reactions involving chelated metal complexes do exist in the literature, though these are few in number.

1.2 Metathesis reactions involving chelated metal complexes

Chelate metathesis – also known as scrambling, ligand exchange or ligand redistribution reactions – has not been studied in much detail and only a few reports of this type of reaction exist in the literature. In almost all cases, studies have focused on the metathesis of chelates of the more labile four-coordinate metals such as Cu(II)^[5-10] and Ni(II).^[5-7, 9, 11-18] Only three cases involving Pd(II) complexes^[9, 19, 20] have been reported and a limited number of cases dealt with six- and eight-coordinate metal complexes.^[21-25] The bidentate chelating ligands focused on in the literature studies of chelate metathesis can be broadly divided into two categories, namely:

1. systems with four- or five-membered chelate rings and S/Se donor atom sets;
and
2. systems with 6-membered chelate rings and N/O donor atom sets.

As part of the systematic study of the coordination chemistry of *N*-alkyl- and *N,N*-dialkyl-*N'*-aroyl(acyl)thioureas (Figure 1.2 adjacent), we have discovered that the complexes *cis*-Pd(L^A-S,O)₂ and *cis*-Pd(L^B-S,O)₂ undergo facile metathesis reactions in solution.

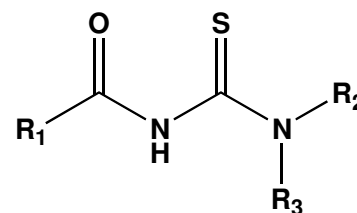


Figure 1.2. *N,N*-dialkyl-*N'*-aroyl(acyl)thiourea ligand.

No previous reports of chelate metathesis in *N*-alkyl- or *N,N*-dialkyl-*N'*-aroyl(acyl)thioureato or other similar S,O donor complexes have been reported in the literature to the best of our knowledge. What follows is a brief literature review of related systems.

1.2.1 *Sulphur/Selenium donor atoms*

1.2.1.1 Four-membered chelate rings

It is generally accepted that the geometry of a four-membered chelating ring is strained,^[26] resulting in a metal complex that is less stable than one with a larger chelate ring, so it is not surprising that systems of this type exhibit chelate metathesis.

The only complexes falling into this category that have been studied in the literature were those of the *N,N*-disubstituted dithio- and diselenocarbamic acids (Figure 1.3).

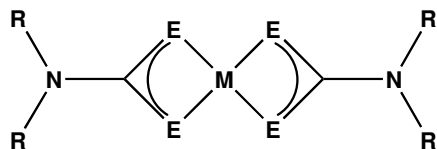


Figure 1.3. bis(*N,N*-disubstituted dithio- or diselenocarbamato)M(II) complex (E = S or Se)
M = Fe, Co Ni, Cu.

A few studies involving intramolecular exchange of coordination sites^[27-29] and exchange between an unbound ligand and a corresponding complex^[13] have been published. However, until 1979, metathesis between two chelated complexes of this type was only mentioned briefly by Chant and co-workers during their electrochemical study of tris(dithiocarbamato)Fe(III) complexes.^[11]

In 1979, while attempting a high-performance liquid chromatography (HPLC) separation of a mixture of Ni(II) bis-*N,N*-dialkyldithiocarbamates with differing *N*-alkyl substituents, Liška and co-workers noticed that each pair of complexes produced three distinct peaks in the chromatogram.^[17, 18] It was observed that metathesis in chloroform was a general phenomenon for all combinations of these compounds, with *N*-alkyl chains ranging from ethyl to octyl. In an attempt to isolate a mixed ligand complex, they focused their attention on the reaction between bis(*N,N*-diethyl-) and bis(*N,N*-dihexyldithiocarbamato)Ni(II). As both these complexes are crystalline, it was anticipated that the mixed ligand complex would prove to be the same.

However, conventional preparative chromatography with silica or alumina columns proved unsuccessful, as the mixed-ligand complex did not separate well from the two parent complexes and was unstable, undergoing rapid redistribution on the column back to the parent complexes. The same rapid redistribution was observed even when using thin-layer chromatography (TLC), which allowed for faster separation. A two-dimensional TLC separation revealed that the centre, mixed-ligand spot again separated into three spots corresponding to the equilibrium mixture of two parent complexes and the mixed ligand species (Figure 1.4 on the following page).

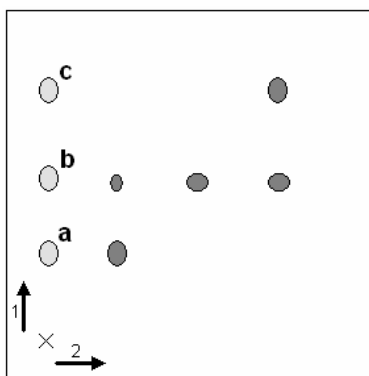


Figure 1.4. Two-dimensional TLC separation of mixture of (a) bis(*N,N*-diethyldithiocarbamato)Ni(II) (c) bis(*N,N*-dihexyldithiocarbamato)Ni(II) and (b) their mixed ligand complex. *Silufol silica gel plate with mobile phase chloroform/cyclohexane (3:4 v/v).*^[18]

The kinetics of the metathesis for these compounds were examined a year later by Moriyasu and Hashimoto.^[16] Using a normal phase-HPLC (*np*-HPLC) system of their own design,^[30] with a *np*-silica column and hexane/cyclohexane/isopropylacetate mobile phase, they obtained good chromatograms of *N,N*-dialkyldithiocarbamic acid complexes of a number of metals with no evidence of complex dissociation during chromatography. Moriyasu and Hashimoto then turned their attention to the metathesis reactions between the very labile bis(*N,N*-dialkyldithiocarbamato)Ni(II) complexes. After establishing that no further reaction took place during elution (see Section 2.2 for more detail), the reaction was followed over time by injecting small samples of the reaction mixture at specific time intervals into the HPLC system (Figure 1.5).

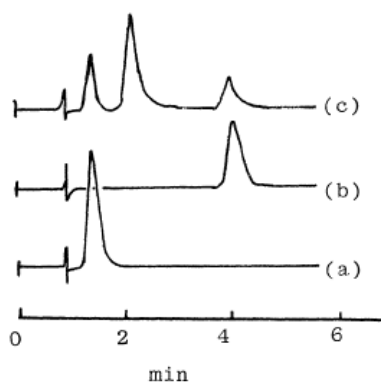


Figure 1.5. Chromatograms of the two individual parent complexes as well as the mixture.
 (a) 1.0 mM bis(*N,N*-di-*n*-propyldithiocarbamato)Ni(II)
 (b) 1.0 mM bis(*N,N*-tetramethylenedithiocarbamato)Ni(II)
 (c) Mixture of 1.0 mM (a) and 1.0 mM (b)

Column: LiChrosorb SI 100 (4 x 250 mm)

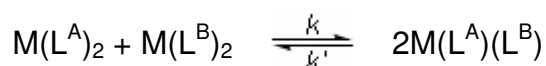
Mobile phase: hexane/cyclohexane/isopropylacetate (50:50:15, water saturated), 1.8 ml/min

Detection: UV, 323 nm.^[16]

When the starting concentrations of the parent complexes were very low, the mixed-ligand complex peak was not observed on the first chromatogram after mixing, though, as time progressed, the middle peak, corresponding to the mixed-ligand complex grew, while the parent complex peaks decreased in height until equilibrium was reached.

It was observed, at equilibrium, for all combinations of two different Ni(II) dithiocarbamate complexes, that exactly half of the parent complexes had metathesised to the mixed-ligand complex, resulting in an equilibrium constant (K) of 4. From this they concluded that the redistribution is controlled solely by a statistical factor as there were no other factors such as steric hindrance within the ligands or favourable hydrogen bonding which could give preference to the mixed-ligand complex.^[31]

The forward and reverse rate constants, k and k' , were calculated by a graphical method (see Section 4.1 for more detail) for the reaction:



For example, in the case of 100 μM solutions of the parent compounds bis(N,N -di- n -propyl-) and bis(N,N -tetramethylenedithiocarbamato)Ni(II), the rate constants were found to be 14 $\text{M}^{-1}.\text{s}^{-1}$ for the forward reaction and 3.5 $\text{M}^{-1}.\text{s}^{-1}$ for the reverse reaction in chloroform at 25 $^\circ\text{C}$.

For combinations of a bis(N,N -dialkyl dithiocarbamato)Ni(II) ($\text{Ni}(\text{dtc})_2$) and a Ni(II) complex of a substantially different ligand (Figure 1.6), a change in the equilibrium distribution was observed (Table 1.2 on the following page).^[15]

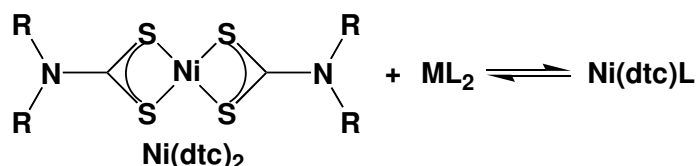
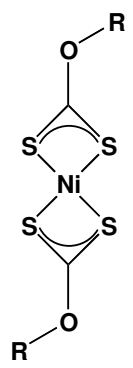
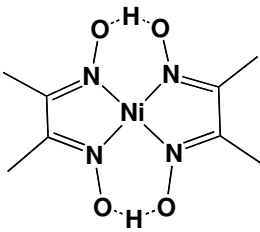
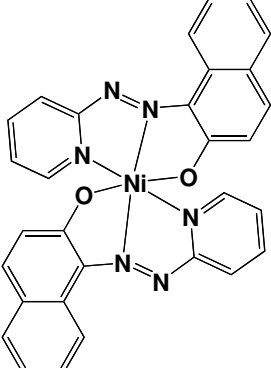
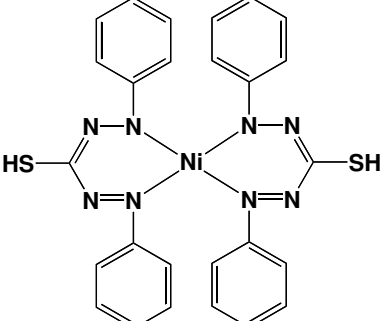


Figure 1.6. Reaction between a bis(N,N -dialkyl dithiocarbamato)Ni(II) complex and a Ni(II) complex of a different ligand (see Table 1.2).

Table 1.2. Complexes reacted with the bis-(*N,N*-dialkyl dithiocarbamato)Ni(II) complexes.^[15]

xanthates	dimethylgloxime	1-(2-pyridylazo)- 2-naphthol	dithizone
			
K ≈ 8	No mixed-ligand complex formed		Complete conversion to mixed-ligand complex
	stable hydrogen bonds in ligand	stable 6-coordinate structure	

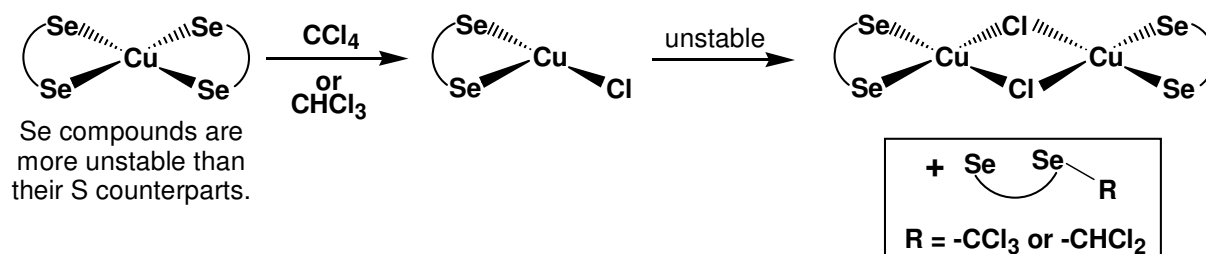
Although Liška *et al.* had claimed that metathesis did not take place for similar Cu(II) and Co(III) complexes of the *N,N*-disubstituted dithiocarbamic acids,^[32] Moriyasu and Hashimoto reported observing such metathesis.^[7, 16] A mixture of two Co(III)L₃ complexes (where L is a dithiocarbamate ligand) could, however, only be coaxed into metathesis upon addition of unbound ligand, yielding four peaks corresponding to Co(L^A)₃, Co(L^A)₂(L^B), Co(L^A)(L^B)₂ and Co(L^B)₃. At the other extreme, since the Cu(II) chelates are more labile than their Ni(II) or Co(III) counterparts, significant disproportionation occurred during separation, with the mixed-ligand species only visible with extremely low starting concentrations of the parent complexes and high mobile phase flow rates.^[7, 16]

While HPLC may not be the most effective tool to study the fast metathesis reactions of Cu(II) complexes, a recent study by Yordanov and Dimitrova has shown that electron spin resonance spectroscopy (ESR) is ideal when the complexes of interest are paramagnetic.^[10] When bis(*N,N*-diethyldithiocarbamato)Cu(II) (Cu(dtc)₂) and bis(*N,N*-diethyldiselenocarbamato)Cu(II) complexes (Cu(dsc)₂) were mixed, it was discovered that the structure of the mixed-ligand products was dependent upon the solvent used. When hexane, heptane, benzene, toluene, acetone, dimethylformamide (DMF), dimethylsulphoxide (DMSO) or dichloromethane (CH₂Cl₂) were used, a stable equilibrium between Cu(dtc)₂, Cu(dsc)₂ and Cu(dtc)(dsc) was observed. This steady state remained so for more than a month, as indicated by an unchanged ESR spectrum.

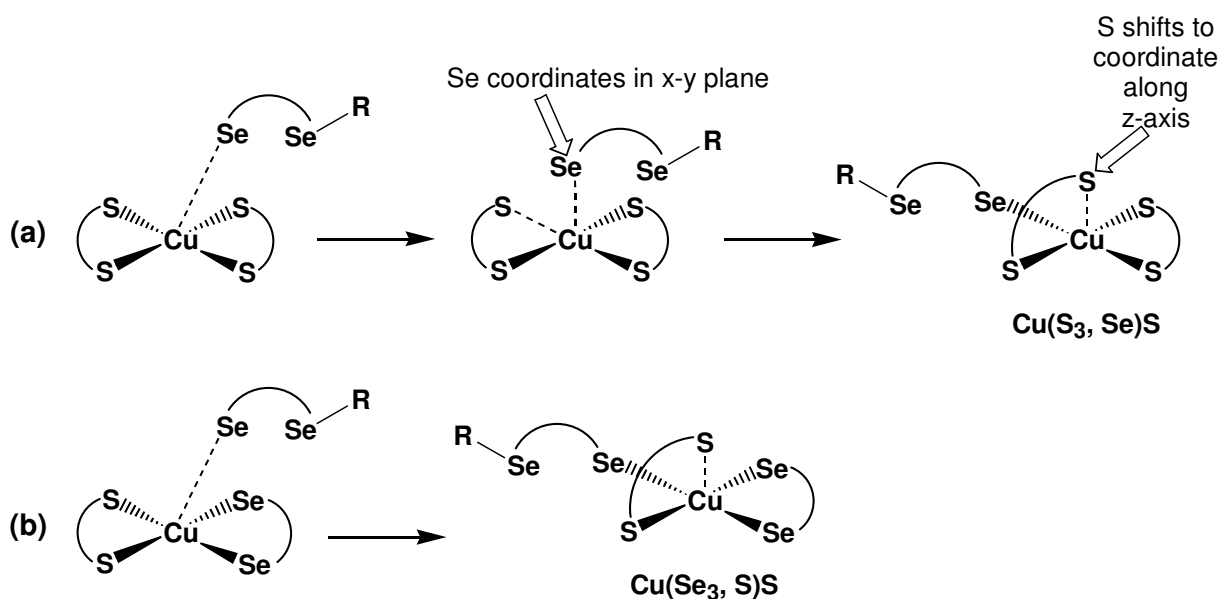
However, when solvents with a higher chlorine content, such as chloroform (CHCl_3) or carbontetrachloride (CCl_4), were used, two new complexes – identified as five-coordinate complexes with a coordination sphere configuration of $\text{Cu}(\text{S}, \text{Se}_3)\text{S}$ and $\text{Cu}(\text{S}_3, \text{Se})\text{S}$ – began to appear with time. The bracketed atoms indicate those coordinated in the xy plane in a square planar configuration, while the atom outside the bracket is coordinated axially along the z-axis.

A proposed mechanism for the formation of these complexes is shown below. Firstly, as the diseleno complexes are not as stable as their dithio counterparts, an unbound diseleno ligand is released into solution through the reaction of a $\text{Cu}(\text{dsc})_2$ complex with the solvent (Scheme 1.1). This unbound ligand can then react with either (a) $\text{Cu}(\text{dsc})_2$, or (b) $\text{Cu}(\text{dsc})(\text{dsc})$ to form the five-coordinate complexes mentioned above (Scheme 1.2). This mechanism, ending with a ligand coordinated in the axial position, is supported by an upward shift in the g-values (gyromagnetic ratios) of the ESR spectra. Similar upward shifts in g-values have been observed in other cases where a Lewis base is coordinated in the axial position of a $\text{Cu}(\text{II})$ chelate.^[33, 34]

Scheme 1.1. The release of an unbound diseleno ligand into solution.



Scheme 1.2. Formation of the 5-coordinate complexes.



1.2.1.2 Five-membered chelate rings

The earliest work investigating chelate metathesis took place in the late 1960's with the study of complexes of *cis*-1,2-disubstituted dithiolene (Figure 1.7).

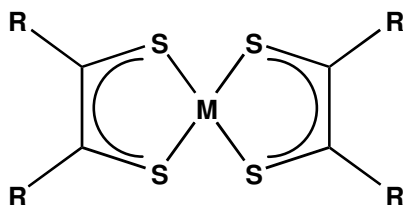


Figure 1.7. bis(*cis*-1,2 disubstituted dithiolato)M(II) complex.

These ligands form five-membered chelate rings with suitable metal ions and, as five-membered chelate rings are more stable than their four-membered counterparts,^[26] one would not immediately assume that metathesis will take place. In fact, prior to 1967, it was widely assumed that these complexes were not able to take part in metathesis reactions.^[12]

Complexes of such ligands undergo discrete one-electron-transfer reactions and it is possible to isolate various members of the electron-transfer series.^[35] The ease with which these electron-transfer reactions occur make it ideal to study these complexes using electrochemical methods.

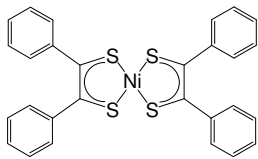
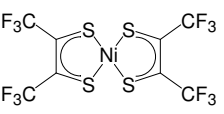
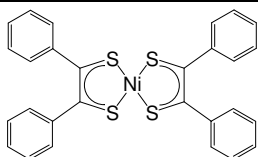
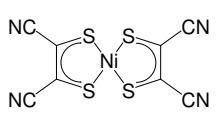
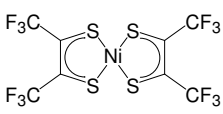
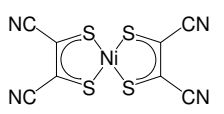
In the first study undertaken by Davison *et al.* on the negatively charged bis(*cis*-1,2-disubstituted-ethylene-1,2-dithiolato)Ni(II) complexes with C₆H₅, CF₃ or CN as the substituents, it was established that chelate metathesis took place in dichloromethane, acetonitrile and acetone.^[12]

Equimolar amounts of two different bis(*cis*-1,2-disubstituted-ethylene-1,2-dithiolato)Ni(II) complexes of about 1 mM in concentration in different solvents, together with the supporting electrolyte necessary for polarographic measurements, were mixed and polarograms recorded periodically. Initially, only the characteristic waves of the starting materials were observed, but over time, a new wave with a potential between those of the parent complexes appeared in the polarogram.

The relative percentage mixed-ligand species formed was dependent upon the solvent, whilst the time needed to reach equilibration was dependent upon temperature.

Refluxing the reaction mixture greatly increased the rate of reaction. In all the solvent systems, it was found that a greater percentage mixed complex formed than one would expect from a purely statistical reorganisation. Selected results from the study by Davison *et al.* are shown below in Table 1.3.

Table 1.3. Selected results from the study by Davison *et al.*^[12]

Parent Complexes (all have a charge of -1)		Solvent	Temperature	Equilibrium Time	% Mixed-ligand species at equilibrium
		CH ₃ CN	25 °C	13 days	92
		CH ₂ Cl ₂	40 °C	6 days	77
		CH ₃ CN	82 °C	4 hours	88
		CH ₂ Cl ₂	40 °C	6 days	81
		CH ₂ Cl ₂	40 °C	37 days	74

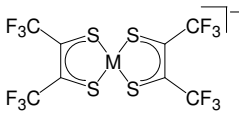
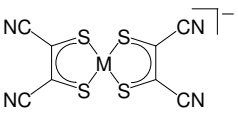
The fact that the mixed-ligand complex was favoured during the metathesis reaction made it possible to design a synthetic route to obtain this complex. Four to six hours in refluxing acetonitrile or acetone was sufficient to allow the reaction to reach equilibrium. The three species present at equilibrium could be separated at room temperature due to their differing solubilities (with suitable counter-ions). When freshly prepared solutions of these isolated mixed-ligand complexes were examined, they exhibited only those polarographic waves attributable to the mixed-ligand species. However, upon being left to stand, the mixed-ligand complex underwent metathesis and settled into the previously observed equilibrium distribution of all three species. After studying this data, the authors tentatively suggested that the transient intermediate species in the metathesis reaction may be a dimeric species (see Figure 1.8 on page 13 for an example).^[12]

Davison *et al.* also briefly mentioned observing metathesis in mixed-metal systems containing equimolar amounts of Pt(II) and Ni(II) *cis*-1,2-disubstituted dithiolato

complexes. While the rate of reaction was far slower than that for two Ni(II) complexes, mixed-ligand complexes for each of the metals were observed.^[12]

Balch extended the number of metals studied when he published data on the equilibrium times and percentage mixed-ligand species formed for Cu(II), Au(II), Ni(II), Pt(II) and Pd(II) dithiolato complexes as well as five-coordinate Co(III) and Fe(III) complexes with a base coordinated in the axial position (base)-M^{III}S₄C₄R₄⁻.^[19] In each of the metal systems studied, Balch used complexes of the CF₃- and CN- disubstituted dithiolene ligands. The reactions were carried out at room temperature with 1 mM dichloromethane solutions of the complexes and were monitored using the polarographic method developed by Davison *et al.*^[12] Selected results are tabulated below (Table 1.4). As one would expect, the more labile Cu(II) complexes reach equilibrium first, with 61% mixed-ligand complex forming within 15 days. No discernable reaction occurred in the more substitutionally inert Au(II) and Pt(II) complex mixtures during the 74 and 99 days they were respectively monitored. Surprisingly, the same mixture of Ni(II) complexes studied by Davison *et al.* at 40 °C (see the last row of Table 1.3)^[12] did not result in any discernable formation of mixed-ligand complex when the reaction was carried out at room temperature.

Table 1.4. Selected results from the study by Balch.^[19]

Complex 1		Complex 2	Equilibrium Time (days)	% Mixed-ligand Species
				
Metal	Ni(II)		72	<i>none discernable</i>
	Cu(II)		15	61
	Pd(II)		27	16
	Pt(II)		99	<i>none discernable</i>
	Au(II)		74	<i>none discernable</i>

Balch also carried out a study into the dimeric, dianionic bis-dithiolato complexes of Fe(III) and Co(III) such as those seen in Figure 1.8 on the following page. Immediately after mixing equimolar amounts of the CF₃- and CN- substituted dimeric complexes, three distinct waves were clearly visible on the polarogram. These

corresponded to the two parent complexes as well as a single mixed-ligand dimer (Figure 1.8).

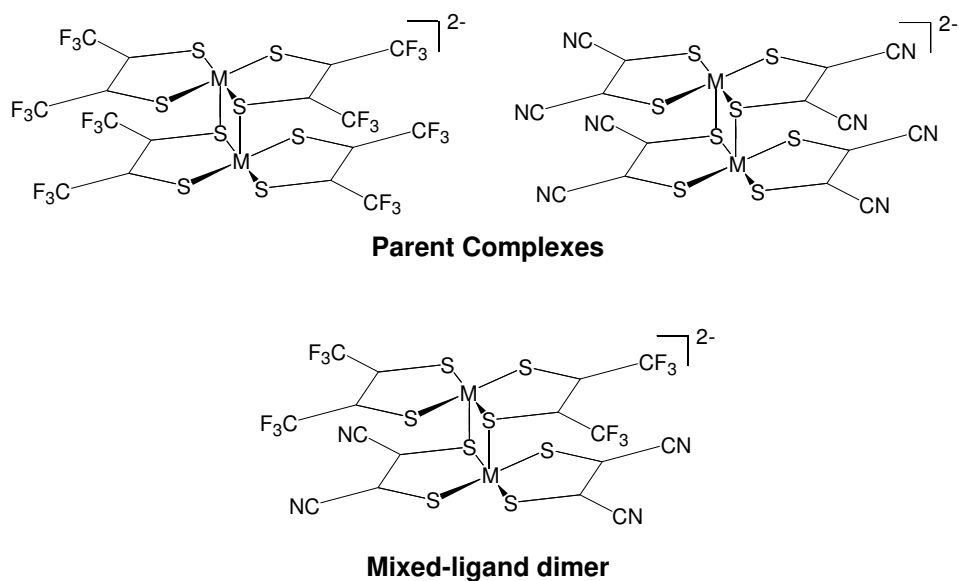


Figure 1.8. The three complexes in solution present immediately after mixing.

Over time, the polarogram wave gradually broadened, with the structure of the three distinct waves disappearing, and exhibited no further change after five hours. With four ligands per dimeric complex, statistically ten combinations are possible (Figure 1.9) and the gradual broadening of the polarographic wave can be attributed to the formation of all ten dimers.

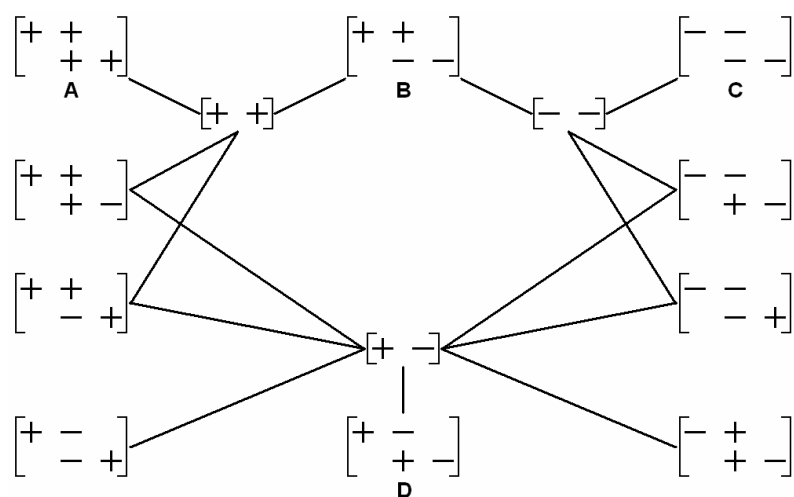


Figure 1.9. Diagram illustrating the relationship between the ten possible dimeric complexes and the three monomeric complexes. The two different ligands are indicated by + and -.^[19]

From Balch's data, it is clear that the cleavage and reassociation of the extraplanar M-S dimer bonds is extremely rapid in contrast with the metathesis of the monomeric dithiolene complexes – a reaction which requires days to reach equilibrium. With the formation of all ten dimers complete after only five hours, Balch concluded that there must be a different mechanism at work.

Balch proposed that the first step in this process involved the intramolecular rearrangement of the mixed-ligand dimer B into D (Figure 1.9). However, this rearrangement alone cannot generate all ten dimers. These dimeric complexes are known to undergo a degree of dissociation in solution through the cleavage of the extraplanar M-S bonds, to form two monomers.^[36] A combination of the cleavage and reassociation of the dimers as well as the intramolecular rearrangement can be envisaged to produce all ten dimers as seen in Figure 1.9.

Whilst most authors focused on the metathesis of complexes with identical coordination spheres and ligands, varying only the substituents on the ligands, four exceptions to this trend exist, including the study by Moriyasu and Hashimoto already discussed in Table 1.2 on page 8. The first case discussed here involves ligands where the coordinating atoms are similar while the size and structure of the chelating ring differs, whereas in the second case, the ligands are near-identical in structure, but with differing coordinating donor-atoms. In the final case, both the coordinating atoms and the ligand structure differs.

Case 1 – Difference in ligand structure

Chelate metathesis can also occur when the coordinated ligands are not identical, such as the metathesis between a four-membered and five-membered chelate ring complex as studied by Olk *et al.* (Figure 1.10).^[9]

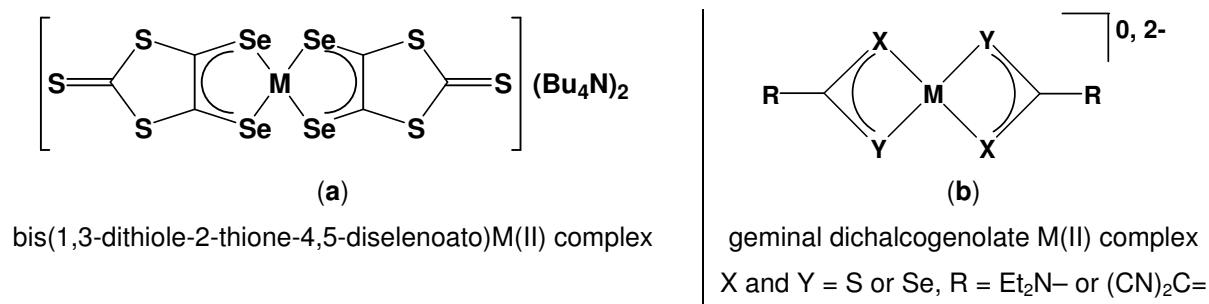


Figure 1.10. (a) Vicinal and (b) geminal dichalcogen complexes studied by Olk *et al.* M = Cu, Ni or Pd.^[9]

When equimolar amounts of a vicinal and a geminal dichalcogen complex (a and b respectively in Figure 1.10) are mixed, the mixed-ligand product was formed quantitatively in a suitable solvent. Complexes of Cu(II), Ni(II) and Pd(II) were studied, with the reaction rates varying predictably according to the known lability of the metal centre. For the highly labile Cu(II) complexes, metathesis took place spontaneously in acetone at room temperature, while the less labile Ni(II) and Pd(II) complexes required additional heat to begin the reaction. The metathesis reaction for the Ni(II) complexes was complete after one to eight hours in acetone under reflux, whereas the reaction between the Pd(II) complexes required three to four days at reflux in acetonitrile to reach completion.

Each reaction was monitored using a different technique. Cu(II) complexes are paramagnetic, making ESR spectroscopy ideal. In the Ni(II) complexes, striking differences between the ultra-violet-visible (UV-Vis) spectra of the two parent complexes and the mixed-ligand complex allowed this reaction to be monitored by UV-Vis spectrometry (Figure 1.11).

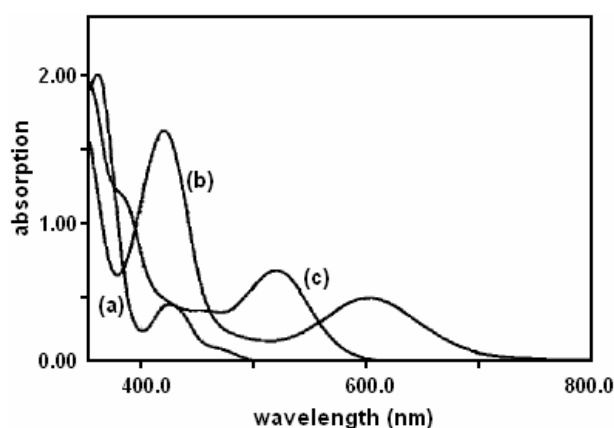


Figure 1.11. UV-Vis spectra of the two parent Ni(II) complexes (a) bis(*N,N*-diethyldiselenocarbamato)Ni(II) and (b) (1,3-dithiole-2-thione-4,5-diselenolato)Ni(II) and (c) the mixed-ligand complex.^[9]

In the case of the Pd(II) complexes, the metathesis reaction was observed with ^{13}C and ^{77}Se NMR spectroscopy. Additionally, chelate metathesis in these compounds was confirmed by the crystal structure of a mixed-ligand (1,3-dithiole-2-thione-4,5-diselenolato)(*N,N*-diethyldiselenocarbamato)Pd(II) complex (Figure 1.12 on the following page).

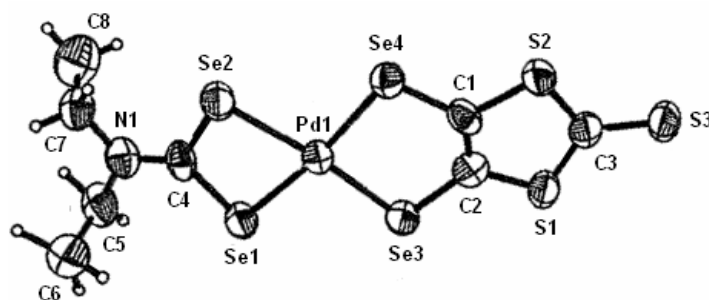


Figure 1.12. Crystal structure of the anionic mixed-ligand Pd(II) complex studied by Olk *et al.*^[9]

The counter-ion has been omitted

Olk *et al.* concluded from their data, as well as other literature,^[8] that mixed-ligand complexes will not form if the parent complexes have different geometrical configurations, such as square planar *versus* tetrahedral. As is illustrated in the crystal structure above (Figure 1.12), the planar geometry present in both parent complexes is maintained in the mixed-ligand product. In addition, bond distances and angles are similar to those observed in the two parent complexes.^[37, 38]

Olk *et al.* suggested that mixed-ligand complexes possess the average electronic and bonding properties of the parent chelates. The changes in the coordination sphere of the metal when metathesis occurs result in significant differences in the ESR, NMR and UV-Vis spectra and therefore these techniques can be utilised to detect the mixed-ligand chelates and observe the extent of their formation. They also cited these electronic changes in the coordination sphere as a possible reason why chelate metathesis occurs in this case. ESR and computational studies of the mixed-ligand chelates showed that, while the metal-sulphur bonds lost some spin density, the metal-selenium bonds gained some spin density, increasing their covalent character, and consequently, increasing the strength of the M-Se bond. Additionally, while the spin density of the Se atom had increased, its charge had decreased slightly, suggesting that significant back-bonding was occurring. These back-bonding effects could contribute to the stabilisation of the mixed-ligand product. Comparison of the total electron energies calculated for the parent and mixed-ligand complexes indicated that the formation of the mixed-ligand complex was energetically favoured.^[39]

Case 2 – Difference in coordinating atoms

Continuing in the vein of *cis*-1,2-disubstituted dithiolene complexes, Miller and Dance extended the investigation to the metathesis reaction of dithiolene Ni(II) complexes and the similarly structured nitrogen-coordinating α -diimine Ni(II) complexes (Figure 1.13).^[14]



Figure 1.13. Structure of (a) bis(dithiolato)Ni(II) complex and (b) bis(α -diiminato)Ni(II) complex.

The ligands focused on in this study included the α -diimine ligands biacetylbisaniil, 2,2'-dipyridal, *o*-phenylenediimine and 1,10-phenanthroline and its 5-nitro derivative (Figure 1.14), as well as the $C_6H_5^-$, CF_3^- and CN^- disubstituted dithiolenes used by both Balch^[19] and Davison *et al.*^[12]

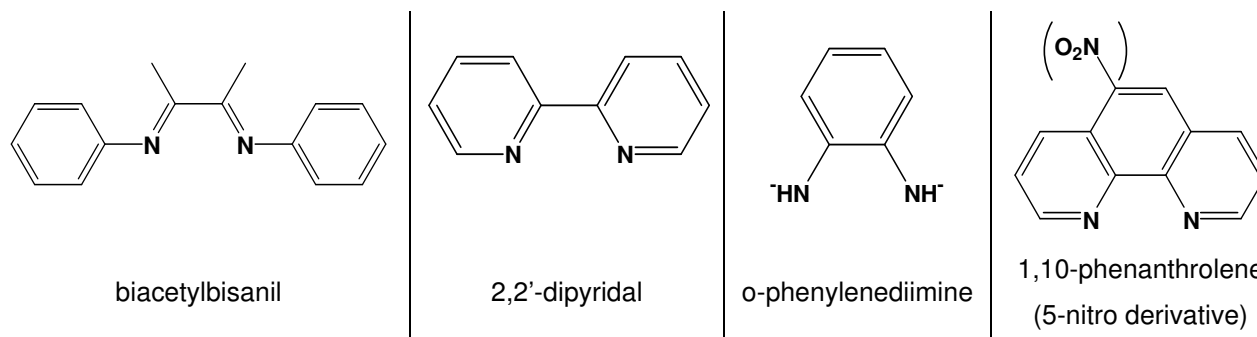


Figure 1.14. α -diimine ligands studied by Miller and Dance.

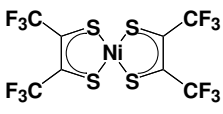
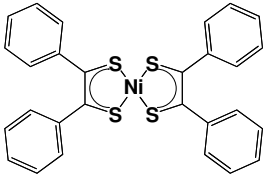
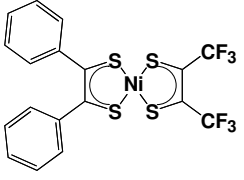
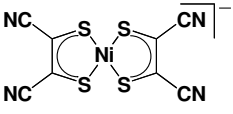
Like the dithiolato complexes, complexes of the α -diimine ligands can also undergo discrete one electron transfer reactions, making it possible to study these metathesis reactions using cyclic voltametry.

To obtain a mixed-ligand complex, three different combinations can be used:

1. a bis(dithiolato)Ni(II) complex and an unbound α -diimine ligand;
2. a bis(α -diiminato)Ni(II) complex and an unbound dithiolene ligand; or
3. a bis(dithiolato)Ni(II) complex and a bis(α -diiminato) Ni(II) complex.

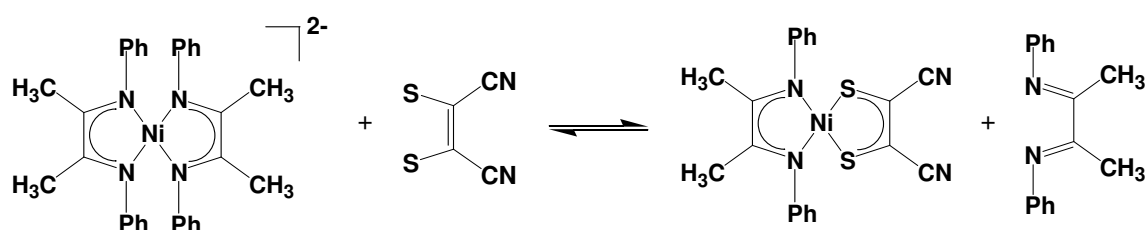
Using the first possible route, Miller and Dance observed that only the neutral dithiolene complexes with C_6H_5- or CF_3- as substituents, as well as the monoanionic CN-substituted dithiolene complex underwent metathesis. The dianionic complexes appeared to be totally inert to ligand substitution by α -diimine ligands. The rates of exchange varied greatly, from the reactions between the CF_3- disubstituted dithiolene complex and any of the diimine ligands complete within minutes, to the combinations containing the C_6H_5- disubstituted dithiolene complex, inert even after several hours at reflux. Selected results are tabulated below (Table 1.5).

Table 1.5. Selected results from the study by Miller and Dance (using route 1).^[14]

Complex	Ligand	Solvent	Temperature	Observations
	all diimine ligands investigated	toluene CH ₂ Cl ₂	room temperature	very fast reaction (complete within minutes)
	biacetylbisaniil (N-N, CH ₃ , Ph) and derivatives	toluene	reflux	several hours – no discernable reaction
	1,10-phenanthroline (phen) and biacetylbisaniil	CH ₂ Cl ₂	room temperature	very fast reaction. 80% Ni(S-S, CF ₃)(phen) formed, with only a trace of Ni(S-S, Ph)(phen)
	biacetylbisaniil	CH ₃ CN o-dichloro benzene	60 °C	mixture of Ni(S-S, CN)(N-N, CH ₃ , Ph) and dianionic (CN ⁻) substituted complex

* Davison *et al.* demonstrated that it is possible to precipitate these mixed-ligand complexes from a metathesis reaction mixture.^[12]

Using the second possible route to obtain a mixed-ligand complex, only the combination illustrated below yielded any results:



The final route, chelate metathesis, allowed for the formation of mixed-ligand complexes that could not be prepared by any other route. The metathesis reaction could be used to obtain mixed-ligand complexes containing an *o*-phenylenediimine ligand (this ligand has limited stability when not coordinated to a metal ion).^[14]

Miller and Dance briefly mentioned the metathesis reaction between $C_6H_5^-$ and CF_3^- -disubstituted dithiolene Ni(II) complexes. They studied both the monoanionic complexes focused on by Davison *et al.*^[12] as well as the neutral complexes. Miller and Dance observed that, while the monoanionic complexes required six days at 40 °C in dichloromethane to attain equilibrium, the reaction between the neutral complexes was complete within about half an hour under the same conditions.

Another form of chelate metathesis studied by Miller and Dance was the ligand exchange within the crystalline salts $[Ni(N-N)_2^{z+}][Ni(S-S)_2^{z-}]$ where (N-N) denotes an α -diimine ligand, and (S-S), a dithiolene ligand and $z = 2, 1$ or 0 . Two equivalents of the neutral mixed-ligand complex could be obtained when the solid salt was heated to 180 °C or refluxed in an aprotic polar organic solvent for an hour. In all the cases investigated by Miller and Dance, the equilibrium between the mixed-ligand complex and the parent complexes was stable, with the distribution remaining unchanged in dichloromethane solution over a period of several weeks.

Case 3 – Difference in both ligand structure and coordinating donor-atoms

The ligands in the complexes studied by Ohya *et al.* differed in both their structure and their coordinating atoms.^[8] These authors focused on the Cu(II) complexes of *N,N*-diethyldithiocarbamic acid, which complexes through its sulphur donor-atoms, forming a four-membered chelate ring; and acetylacetonate which contains oxygen donors and forms a six-membered ring (Figure 1.15).

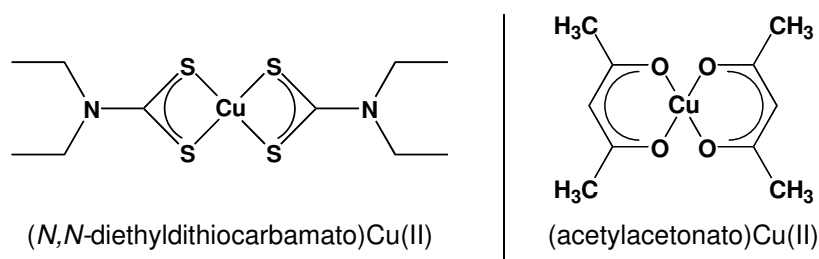


Figure 1.15. The complexes studied by Ohya *et al.*

The metathesis reaction was monitored by UV-Vis and ESR spectrometry at a number of temperatures between 0 °C and 60 °C in single solvents, as well as mixed-solvent systems. It was found that, in general, the higher the dielectric constant (κ) of the solvent, the less mixed-ligand product formed and the smaller equilibrium constant (Table 1.6).

Table 1.6. Dielectric constant of solvent vs. equilibrium constant of metathesis reaction.^[8]

Solvent	Dielectric constant (κ)	Equilibrium constant (K)
CCl ₄	2.24	0.32
benzene	2.28	0.45
toluene	2.38	0.39
chlorobenzene	5.62	0.30
CH ₂ Cl ₂	9.08	0.17
o-dichlorobenzene	9.93	0.21
acetone	20.7	0.17
CH ₃ OH	32.6	0.0045
CH ₃ CN	37.5	0.0034

The mixed-solvent system, dichloromethane-carbon tetrachloride, in the example below (Figure 1.16), illustrates that the natural logarithm of the equilibrium constant ($\ln K$) is almost directly proportional to κ^{-1} .

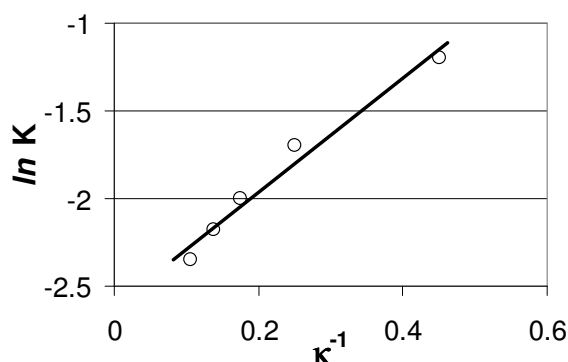


Figure 1.16. Dependence of K on the dielectric constant of the solvent.^[8]

1.2.2 N/O donor atoms – six-membered chelate rings

Along with five-membered chelate rings, six-membered chelate rings are considered amongst the most stable chelated metal complexes^[26] and one would not immediately expect metathesis to take place between complexes of this sort.

Nevertheless, a number of studies indicate that metathesis does indeed take place for nitrogen and/or oxygen donor complexes of the four-coordinate metals, Ni(II), Co(II), Cu(II) and Zn(II),^[5, 6] as well as the six-coordinate metals Al(III)^[22] and Ga(III)^[24, 25] and the eight coordinate metals Zr(IV)^[21, 23] and Hf(IV).^[21]

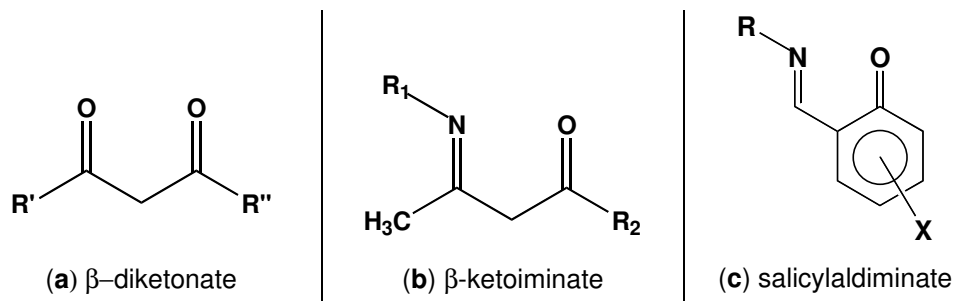


Figure 1.17. Metathesis reactions between metal complexes of these N/O donor ligands were studied

With the six- and eight-coordinate metals, studies focused on complexes of β -diketonate ligands (Figure 1.17a). In all the cases investigated, metathesis reactions occurred, with the mixed-ligand complexes greatly favoured in systems containing eight-coordinate metals, as well as in the six-coordinate metal systems when one ligand contained a fluorinated alkyl substituent.

Another type of complex not expected to undergo metathesis are those of the multidentate ligands ethylenediaminetetraacetate (EDTA) and triethylenetetramine and its derivatives. These ligands contain multiple coordinating atoms, which result in the central metal ion being encased by one single ligand which forms multiple chelate rings. A number of studies on metathesis between tetradentate triethylenetetramine (or similar derivatives) and ethylenediaminetetraacetate complexes of Cu(II) and Zn(II) or Ni(II) have been carried out.^[40-44] It has been proposed that the reaction proceeds via a coordination chain reaction mechanism, initiated by traces of unbound triethylenetetramine ligand present in solution.^[40] The reaction can be accelerated through addition of a trace of unbound ligand, and inhibited by the addition of metal ions.

Since the study described in this thesis is concerned with the metathesis of *cis*-bis(*N,N*-dialkyl-*N'*-aroyl(acyl)thioureato)Pd(II) complexes (see page 4) and this molecular motif most closely resembles those in Figure 1.17b and c, this discussion will be limited to

complexes of the four-coordinate metals Ni(II) and Zn(II) with the aforementioned ligands.

The thermodynamics and kinetics of chelate metathesis for Ni(II) complexes of the β -ketoiminates and substituted salicylaldiminates were studied by Lockhart and Mossop, using ^1H and ^{19}F NMR to follow the reaction and quantitatively measure the concentrations of reactants and products.^[5, 6]

Equimolar quantities of two β -ketoiminato and/or salicylaldiminato complexes (see Figure 1.18 for the combinations of complexes used) were dissolved in either deuteriochloroform or tetrachloroethylene, resulting in solutions within a concentration range of 0.1 to 0.001 M. Once dissolved, the mixture was transferred to an NMR tube, cooled to $-78\text{ }^\circ\text{C}$, sealed and placed in a temperature-controlled NMR spectrometer where spectra were recorded as soon as possible at a minimum of five different temperatures between $17\text{ }^\circ\text{C}$ and $107\text{ }^\circ\text{C}$ for the thermodynamic studies.^[5]

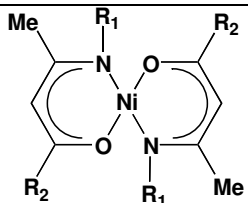
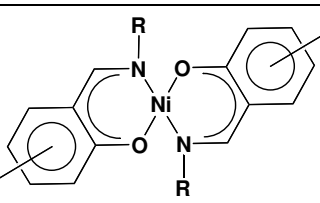
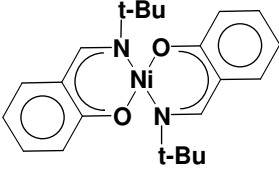
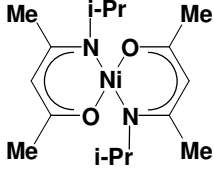
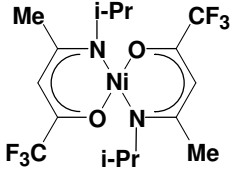
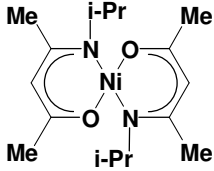
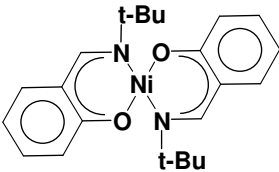
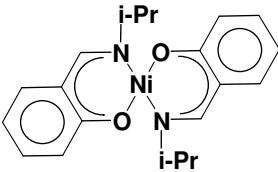
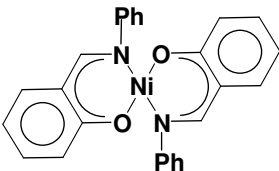
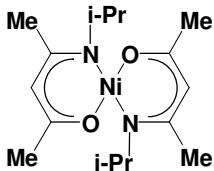
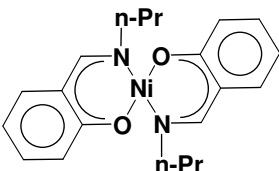
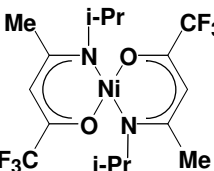
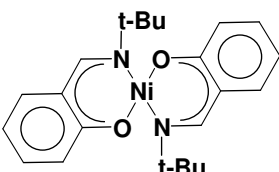
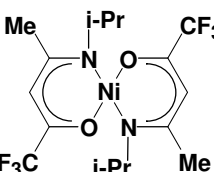
β -ketoiminato complex		salicylaldiminato complex	
			
R_1	R_2	R	X
^iPr	$\text{CF}_3, \text{Me}, \text{Ph}$	$^n\text{Pr}, ^i\text{Pr}, ^n\text{Bu},$ $^t\text{Bu}, \text{Et}_2\text{CH},$ Ph	$\text{H}, 4\text{- or }5\text{-Me},$ 3-MeO

Figure 1.18. Substituted Ni(II) complexes studied by Lockhart and Mossop.

Lockhart and Mossop observed striking differences in the time required to reach equilibrium for various combinations of the complexes in Figure 1.18. While some reactions were complete even before the first spectrum could be recorded, others required up to 30 hours to attain equilibrium. Still other combinations appeared not to react at all, even after being left to stand for several days at room temperature or heated for a number of hours at $87\text{ }^\circ\text{C}$. Selected representative results are shown in Table 1.7 on the following page, including the equilibrium constant (K) at $25\text{ }^\circ\text{C}$ and the enthalpy (ΔH) and entropy (ΔS) of the reaction. Interestingly, although some unreactive

combinations (not listed here) could not be coaxed into metathesis by any means, the combinations in the final two rows of Table 1.7 could be made to react extremely rapidly upon the addition of pyridine to combination 1, which alters the geometry of the metal complex; or unbound ligand in the case of combination 2.

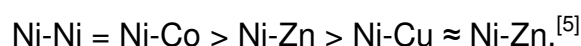
Table 1.7. Selected results from the thermodynamic studies by Lockhart and Mossop.^[5]

Complex 1	Complex 2	K (25 °C)	ΔH (kJ mol ⁻¹)	ΔS (J.K ⁻¹ .mol ⁻¹)	Reaction rate
		13	-2.8 ± 3	12 ± 9	slow
		4	-0.1 ± 0.5	11.2 ± 2	slow
		1.44	5.5 ± 2	21 ± 7	fast
		0.0087	38 ± 1	107 ± 3	fast
		—	—	—	no reaction (1)
		—	—	—	no reaction (2)

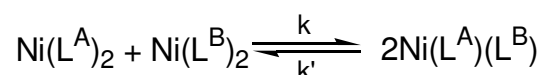
Lockhart and Mossop suggested that the unfavourable enthalpies and low equilibrium constants observed for certain combinations could be due to differences in the

geometry of the Ni(II) parent complexes. The geometry of Ni(II) complexes of β -ketoiminates and salicylaldiminates can be either tetrahedral or square planar depending on the nature of the R-substituent on the coordinating nitrogen atom. Metathesis between parent complexes of differing geometries occurred either to a very slight degree, or, most often, not at all. Similar conclusions regarding geometry and extent of reaction were made by Olk *et al.* in their studies of metathesis between vicinal and geminal dichalcogen complexes of Cu(II), Ni(II) and Pd(II).^[9]

Chelate metathesis was also possible for mixed-metal systems of the *N*-substituted salicylaldiminate ligands in deuteriochloroform.^[5] Reactions between a Ni(II) chelate and a Co(II), Cu(II) or Zn(II) chelate reached equilibrium within 20 minutes with all six possible complexes observed in the mass spectra of the mixtures: Ni(L^A)₂, Ni(L^B)₂, Ni(L^A)(L^B), M(L^A)(L^B), M(L^A)₂, M(L^B)₂ (where M = Co, Cu or Zn). It was, however, not possible to obtain sensible information from the NMR spectra for all combinations due to the broadness of the copper and cobalt signals. A qualitative comparison of reaction rates indicated that:



Lockhart and Mossop also conducted a more detailed kinetic study on the Ni(II) β -ketoiminato and salicylaldiminato complexes,^[6] determining both the forward (*k*) and reverse (*k'*) rate constants as well as activation energies (*E*^a) for the reaction:

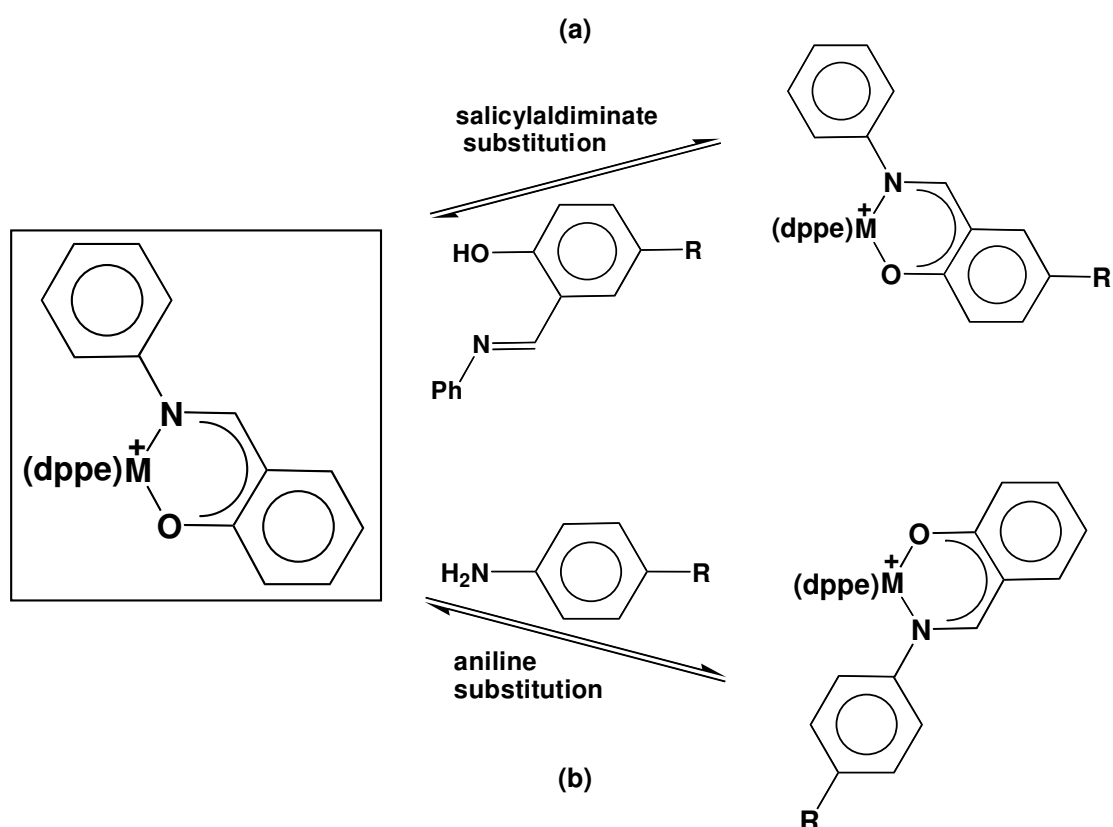


The same experimental procedures used in the thermodynamic studies were followed.^[5] Due to its greater liquid range, tetrachloroethylene was the preferred solvent, unless solubility became an issue, in which case, mixtures of deuteriochloroform and tetrachloroethylene were used. Selected results for the experiments carried out at 30 °C are tabulated in Table 1.8.

Table 1.8. Selected results from the kinetic studies by Lockhart and Mossop.^[6]

Complex 1	Complex 2	k	k'	E _a	E _a '
		L mol ⁻¹ s ⁻¹		kJ mol ⁻¹	
		4.8 x 10 ⁻⁴	1.1 x 10 ⁻⁴	100	101
		1.7 x 10 ⁻³	—	64	—
		2.7 x 10 ⁻³	6.8 x 10 ⁻⁴	89	79
after addition of pyridine (alters geometry)					
		9.9 x 10 ⁻⁵	3.1 x 10 ⁻⁵	118	117

A final example relevant to the study discussed in this thesis, although not chelate metathesis, illustrates labile ligand exchange in mixed-ligand, cationic Pt(II) and Pd(II) complexes of 1,2-bis(diphenylphosphine)ethane (dppe) and substituted salicylaldimine ligands.^[20] Kerber *et al.* showed that the N,O-donor ligands of these complexes could undergo two distinct types of exchange: (a) substitution of the entire salicylaldimine ligand; or (b) substitution of only the aniline fragment of the ligand (Scheme 1.3 on the following page). For both Pd(II) and Pt(II) complexes, the reaction occurred in a wide variety of both protic and aprotic solvents at 60 °C, with the Pd(II) complexes reaching equilibrium before their Pt(II) counterparts. The reactions were followed using ³¹P NMR. It was also noted that increasing the electron density at the nitrogen atom, by means of electron-donating groups (R) on the aniline fragment, stabilised the complexes, as indicated by lower free energy (ΔG). Altering the electron density at the oxygen donor, by varying the salicyl-ring substituent, had no effect.



Scheme 1.3. Two distinct types of ligand exchange possible for the Pt(II) and Pd(II) complexes of dppe and substituted salicylaldimines.^[20]

1.2.3 Summary and Conclusions

Information available on chelate metathesis in the literature varies widely, from some authors merely mentioning observing the reaction to others conducting more detailed studies of equilibrium distributions,^[5, 8, 12, 19] thermodynamics^[5] or kinetics.^[6, 16] Besides chelate metathesis studies, there have been investigations into exchange reactions between an unbound ligand and a complexed ligand.^[14, 20] On the whole, most of the metathesis reactions studied in the literature have been of labile Cu(II) and Ni(II) complexes, with a considerable variation in the structure, chelate-ring size and coordinating atoms of the ligands.

A general conclusion that can be drawn is that, for metathesis to occur, the geometry of the parent complexes must be identical.^[5, 8, 9] Notwithstanding this limitation, chelate metathesis has been reported in neutral, anionic and cationic complexes as well as in mixed-metal systems^[5, 12, 19] and in mixed-ligand systems.^[8, 9, 14] It has even been observed between dimeric complexes^[19] and in tetracoordinate ligand systems.^[40-44] In

many instances, the metathesis reaction was spontaneous and occurred at room temperature,^[7, 9, 15-18] while other cases required heat to initiate the reaction.^[9, 12, 14]

There is only one documented case where the mixed-ligand complex could be successfully separated from the reaction mixture^[12] and only one report where the mixed-ligand products formed quantitatively.^[9] In general a dynamic equilibrium exists in solution between the two parent complexes and the mixed-ligand product.^[12, 17, 18] The equilibrium constant was, in some cases, subject to the polarity of the solvent used;^[8, 12] and the time taken to reach equilibrium was dependent upon temperature.^[12] The choice of solvent can even directly affect the structure of product.^[10]

Additives can affect the rate of reaction. Unbound ligand can accelerate the reaction,^[40] and is required, in some cases, to initiate the metathesis.^[5, 16] Some reactions can be inhibited by the addition of base^[19] or metal ions.^[40]

1.2.4 Instrumentation for the observation of metathesis reactions

The techniques used to observe the metathesis reactions discussed above were as varied as the systems studied. Each technique has its own distinct advantages and disadvantages, as summarised in the table below:

Table 1.9. Advantages and disadvantages of the methods used to observe metathesis reactions.

Technique	Advantages	Disadvantages
UV-Visible spectroscopy	fast, cost-effective, in situ	only applicable to compounds with noticeable differences in absorption spectra
Nuclear Magnetic Resonance spectroscopy	in situ, fast reactions	high concentrations, long monitoring times, specific nuclei, expensive solvents
Electron-Spin Resonance spectroscopy	in situ, fast reactions	only paramagnetic compounds
Electrochemical methods	wide variety of possible compounds, extra information regarding stability and formation constants	not in situ, ease restricted by solvent choice
Gas Chromatography	low concentrations	only volatile compounds, not in situ
High-Performance Liquid Chromatography	low concentrations, wide variety of possible compounds	elution times, not in situ, need slower reactions

1.3 Objectives of this study

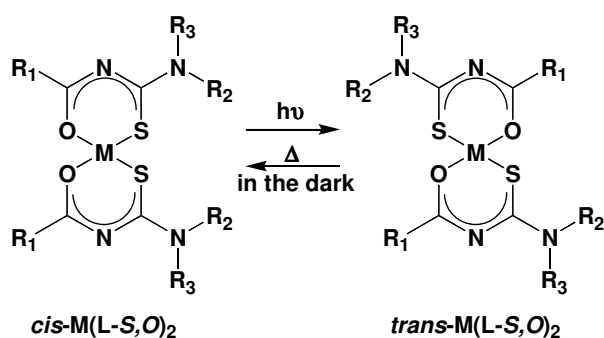


Figure 1.19. The photoinduced *cis-trans* isomerisation of *cis-M(L-S,O)₂* complexes.

M = Pd(II) or Pt(II)

It has been shown that *cis*-bis(*N,N*-dialkyl-*N'*-aroyl(acyl)thioureato)Pt(II) and Pd(II) complexes undergo a *cis* to *trans* photoinduced isomerisation reaction under intense light (Figure 1.19 adjacent).^[45] The reverse *trans* to *cis* process occurs spontaneously in the dark and it is possible that this reverse reaction occurs *via* a metathesis mechanism (see Section 4.3).

As these complexes show potential as possible molecular switches, it is important to attempt to fully understand both the forward and the reverse reaction mechanism and it was with this mind that the investigation into the chelate metathesis of these complexes was initiated.

In the light of the studies discussed in the literature review (Section 1.2) the effect of the central metal ion, the structure of the complexed ligands and the reaction medium (solvent) on the chelate metathesis reaction between *cis*-Pd(L-S,O)₂ complexes were investigated. In addition, certain literature studies incorporated the addition of acid, base or unbound ligand to the reaction mixture, and it was decided to include studies into the effects of these additives. Attempts were made to isolate or synthesise a mixed-ligand complex through a variety of synthetic methods, including the reaction between a complex and an unbound ligand in solution. In contrast to the majority of the literature studies, the chelate metathesis reaction between *cis*-Pd(L-S,O)₂ complexes was studied in dilute solutions (100 – 800 μM).

Pt(II) and Pd(II) complexes of *N,N*-dialkyl-*N'*-aroyl(acyl)thioureas can be readily separated and quantified using *rp*-HPLC and the technique was previously used to observe the photoisomerisation reaction discussed above.^[45] Considering the previous successful applications of *rp*-HPLC to these complexes,^[45, 46] this technique was chosen for the investigation into the chelate metathesis reaction between *cis*-Pd(L-S,O)₂ complexes.

1.4 High-performance liquid chromatography of metal complexes

In 1906, two articles by Russian botanist, Mikhail Tswett appeared in the journal *Berichte der Deutschen Botanischen Gesellschaft*, describing the separation of coloured pigments from an extract of leaves by passing the solution through a column of finely divided material.^[47, 48] When the leaf extract was allowed to filter down a narrow glass tube tightly packed with calcium carbonate, distinct coloured bands began to develop. Tswett called this technique chromatography from the Greek words *chroma* (colour) and *graphein* (to write).

“Like the light rays of the spectrum, the different components of a pigment mixture in the calcium carbonate column will be separated regularly from each other, and can be determined qualitatively and also quantitatively. I call such a preparation a chromatogram and the corresponding method the chromatographic method.”^[47]

Today, the term chromatography is broadly understood as the physical separation of components in a mixture due to their differing distributions between a stationary phase and a mobile phase.^[49] Chromatographic separations occur due to a series of repeated adsorptions and desorptions of the sample as it moves through the stationary phase. Individual components in the sample interact with the stationary phase to differing degrees, with those more strongly retained eluting later.

Chromatographic techniques are classified according to the nature of the stationary and mobile phases.^[50] When a solid substrate with a large active surface area, such as silica gel, is employed as the stationary phase, one speaks of adsorption chromatography. When the stationary phase is a liquid immobilised on an inactive solid support, one is using partition chromatography. In both cases, the mobile phase can be either an inert gas (gas chromatography) or a liquid of low viscosity (liquid chromatography). When making use of liquid chromatography, two additional options exist, namely ion-exchange and size-exclusion chromatography. The stationary phase in ion-exchange chromatography has either anionic or cationic sites at the surface which can interact with cat- or anions respectively from the mobile phase. Size-exclusion chromatography makes use of porous solids with a well-defined pore-size distribution. Molecules with an effective diameter larger than the defined pore

size cannot diffuse into the pores and are therefore more rapidly eluted from the column.

The techniques mentioned above employ a closed column and require pressure for the movement of the mobile phase, in contrast, thin-layer chromatography (TLC) is an open-bed technique, making use of capillary forces on a flat plate to advance the mobile phase. The stationary phase in the case of TLC consists of a thin layer of sorbent coated onto an inert, rigid plate.

The type of chromatography employed is dependent on the substances to be separated (Figure 1.20). Gas chromatography is naturally only suitable for volatile compounds with low molecular weight, while heavier, non-volatile molecules are best separated using liquid chromatography. Very large molecules require size-exclusion chromatography. Thin-layer chromatography is generally employed as a simple, rapid, qualitative technique, though quantitative analysis is possible using a scanning densitometer.

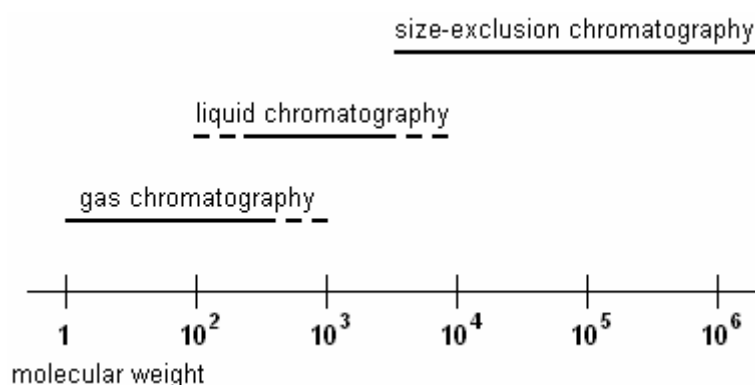


Figure 1.20. Application ranges for different classes of chromatography.

Originally, liquid chromatography was not as efficient as gas chromatography or even thin-layer chromatography. Columns were large, with an inner diameter of more than one centimetre. The mobile phase moved through the column under gravity or occasionally hydrostatic pressure and stationary phase particles were typically around 100 μm in size to accommodate a practical flow rate. These large particles decreased efficiency and increased the chance of overloading the column with sample. However, in the mid- to late-1960's, many of the principles associated with gas chromatography began to be applied to liquid chromatography. Column diameters decreased from centimetres to between two and eight millimetres, and stationary phase particle size

shrank to less than 50 μm , with a typical size of around 5-10 μm . These new columns had operating pressures of a few thousand pounds per square inch (psi). These advances, coupled with the development of more sensitive detectors led to the birth of high-performance (also known as high-pressure) liquid chromatography, or HPLC.

The first application of HPLC technology for the separation of metal chelates was undertaken by Huber and Kraak in 1972.^[51] Using a liquid-liquid chromatography system of their own construction (Figure 1.21), they managed to separate a mixture of up to six different metal β -diketonate chelates. The metals investigated were Al(III), Be(II), Co(II) and Co(IV), Cr(III), Cu(II), Fe(III), Ru(III), Zn(II) and Zr(IV), complexed to acetylacetone or trifluoroacetylacetone.

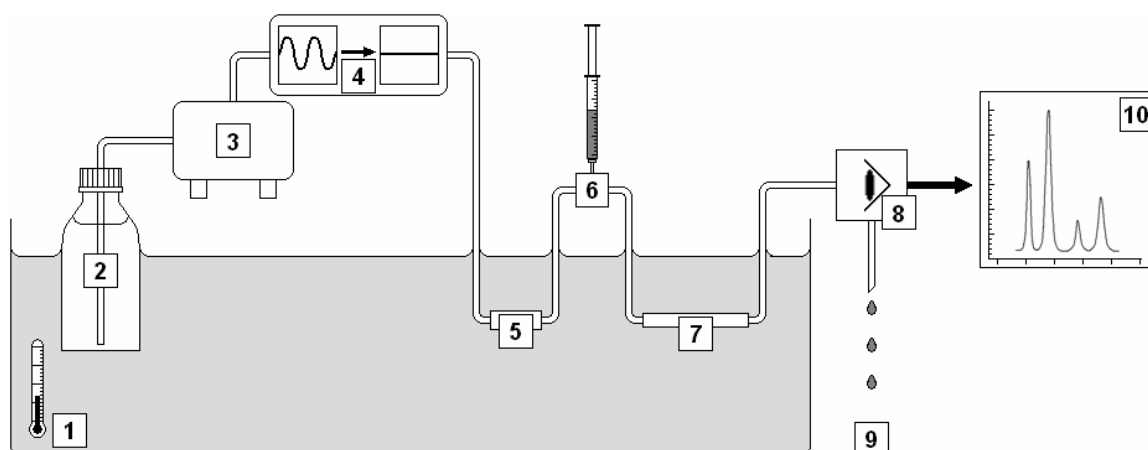


Figure 1.21. Schematic representation of Huber and Kraak's liquid chromatography system.

- 1 – Constant temperature bath (25 °C)
- 2 – Eluent reservoir
- 3 – High pressure pump
- 4 – Damping unit (eliminates pump pulsations)
- 5 – Pre-column (reduces pressure drop)
- 6 – Sampling device (precision syringe and septum-sealed injection chamber)
- 7 – Separation column
- 8 – UV detector (310 nm) with 7.5 μl flow cell (10 mm pathlength)
- 9 – Waste
- 10 – Chromatogram recorder

They based their separation column on the principles of conventional liquid-liquid extraction, where a metal is distributed between an aqueous and organic phase. A ternary mixture of 2,2,4-trimethylpentane, water and ethanol was used for both the stationary and mobile liquid by varying the relative ratios of the three components to

obtain a more polar liquid for the stationary phase and a less polar liquid for the mobile phase. The stationary liquid was loaded onto a solid support of clean, dry deactivated diatomaceous earth (5 – 10 μm) by pumping it through a 2.7 mm inner diameter borosilicate glass column packed with the support. Excess stationary liquid was displaced by pumping the less polar mobile phase through the loaded column. Various stationary and mobile phase compositions were studied in which the relative ratios of water:ethanol:2,2,4-trimethylpentane were varied. Samples were dissolved in the less polar phase and injected into the column.

Unfortunately, Huber and Kraak found that very few of the β -diketonate chelates gave symmetrical peaks, indicating that the distribution coefficients of the complexes were not constant. Additionally, as the concentration of the sample was decreased, the retention time increased, which suggested that the distribution isotherm was non-linear. They also discovered that the tris(acetylacetonato)Al(III) complex underwent dissociation and hydrolysis reactions when left in solution. A fresh solution of this complex gave one single symmetrical peak, whereas two additional separable species were observed in a three-week old solution. However, both the problem of peak asymmetry and inconsistent retention times, as well as the dissociation of the Al(III) complex could be suppressed by addition of a trace of unbound ligand to the solution (Figure 1.22).

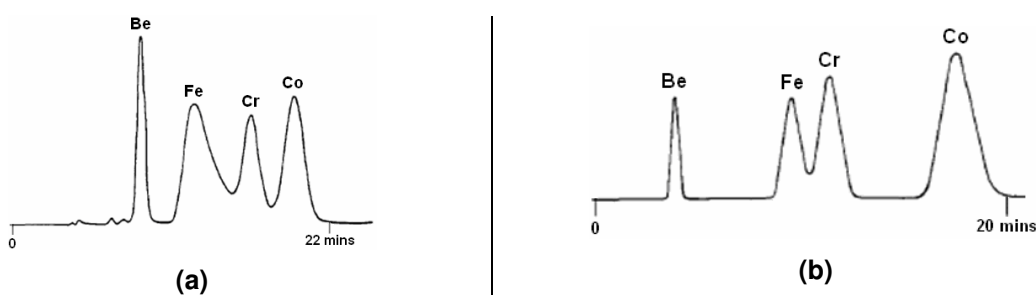


Figure 1.22. Separation of acetylacetonato complexes of Be(II), Fe(III), Cr(III) and Co(III) (a) without unbound ligand and (b) containing a trace of unbound ligand in the mobile phase.^[51]

After optimisation of the system, up to six different metal chelates could be separated in under 25 minutes (Figure 1.23 on the following page).

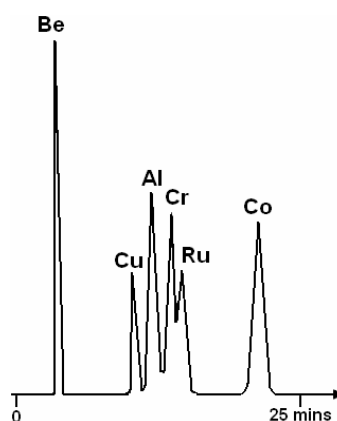


Figure 1.23. Separation of six metal acetylacetonato complexes.^[51]

Regrettably, the separation of metal complexes, though highly successful on Huber and Kraak's liquid chromatograph,^[51] could not be carried out on the early commercially available HPLC systems. The stainless steel columns, conduits and detector cells were corroded by the chlorides and bromides often present in inorganic samples and some metal complexes, such as tris(acetylacetonate)Fe(III), reacted with the finely divided normal phase silica in the column and were irreversibly adsorbed.^[52] However, with the advent of chemically modified stationary phases, such as reversed-phase silica and ion-exchangers, as well as the lining of columns with glass, HPLC became a valuable tool in inorganic chemistry.^[52]

Modern HPLC has been used to great success in, for example the separation and quantification of the mixed halo-complexes of Os(IV) and Re(IV).^[53]

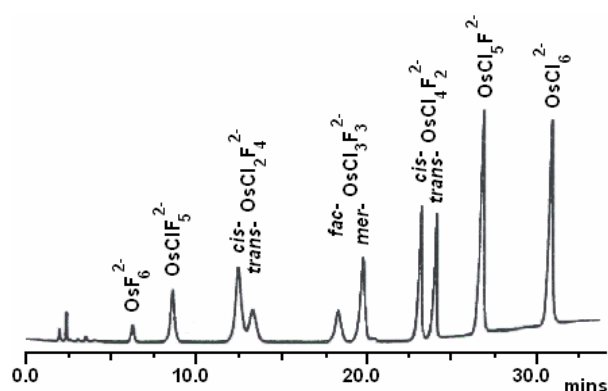


Figure 1.24. HPLC separation of mixed hexachlorofluoro Os(IV) complexes.
 Column: Nucleosil 10 Anion (4 x 250 mm)
 Mobile phase: HClO₄ gradient, 1 ml/min
 Detection: UV-Vis, 210 nm.^[53]

While these separations can also be carried out using either TLC or low pressure liquid chromatography, it is not possible to determine the concentrations of the different components using these methods. Figure 1.24 (adjacent) shows the separation of mixed hexachlorofluoro Os(IV) complexes. The *cis* and *trans*, as well as the facial and meridional isomers could be separated.

The separation and quantification of metal complexes using HPLC has a practical application for the trace determination of precious metals, such as platinum, palladium and rhodium, in process solutions.^[46] These aqueous process solutions are generally acidic with a high chloride content^[54] and contain a mixture of various chloro-aquo metal complexes. To achieve separation of the different metals, one needs to add a ligand which will quantitatively form mono-isomeric complexes of each metal within the acidic environment. By adjusting the elution conditions, the resulting complexes can then be easily separated and quantified using HPLC (Figure 1.25).

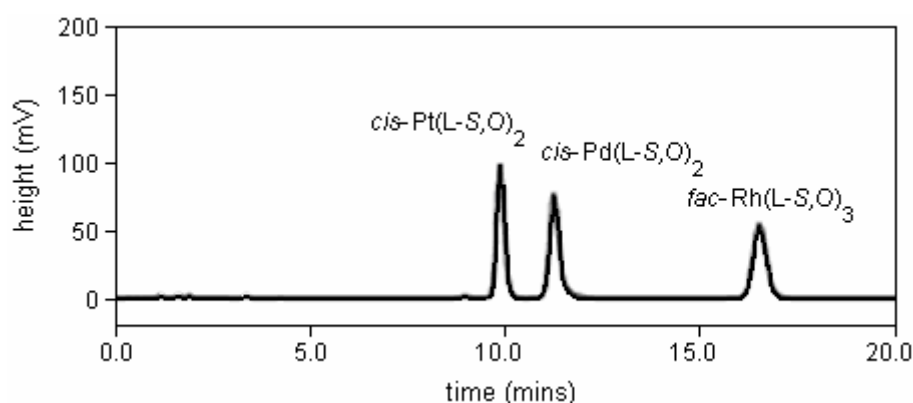


Figure 1.25. HPLC separation of Pt(II), Pd(II) and Rh(III) after complexation with *N*-pyrrolidyl-*N'*-(2,2-dimethylpropanoyl)thiourea.

Column: LUNA C₁₈-ODS (4.6 x 150 mm)

Mobile phase: 90:10 acetonitrile:0.1M acetate buffer (pH 6), 1 ml/min

Detection: UV, 254 nm.^[55]

Ideal ligands for this technique are the hydrophilic *N,N*-dialkyl-*N'*-acylthioureas, which form stable, essentially pure complexes with a variety of transition metals, but show a marked affinity for the platinum group metals under acidic conditions.^[55]

These ligands, as well as their aroyl counterparts, are remarkably versatile, not only for trace determination and other industrial applications such as preconcentration and extraction, but also within the medical field. A broader overview of these ligands is given in Section 1.5 which follows.

1.5 Coordination chemistry of *N*-alkyl- and *N,N*-dialkyl-*N'*-aroyl(acyl)thiourea ligands towards Pd(II) and other transition metals

N-alkyl- and *N,N*-dialkyl-*N'*-aroyl(acyl)thiourea ligands (Figure 1.26) are easily synthesised in a two-step, “one-pot” procedure^[56] and complexes of these ligands have shown great promise in a wide variety of applications, ranging from medicinal^[57-64] to the extraction, separation and trace determination of transition metals.^[46, 55, 65-79]

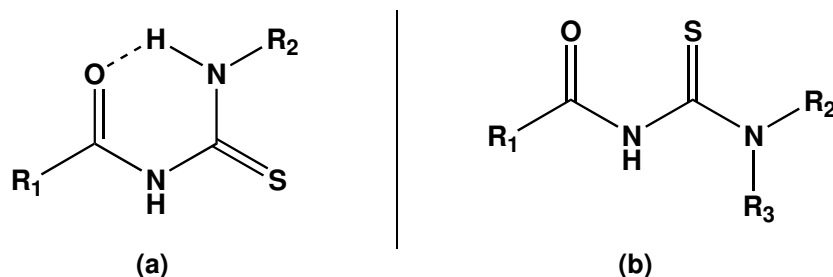
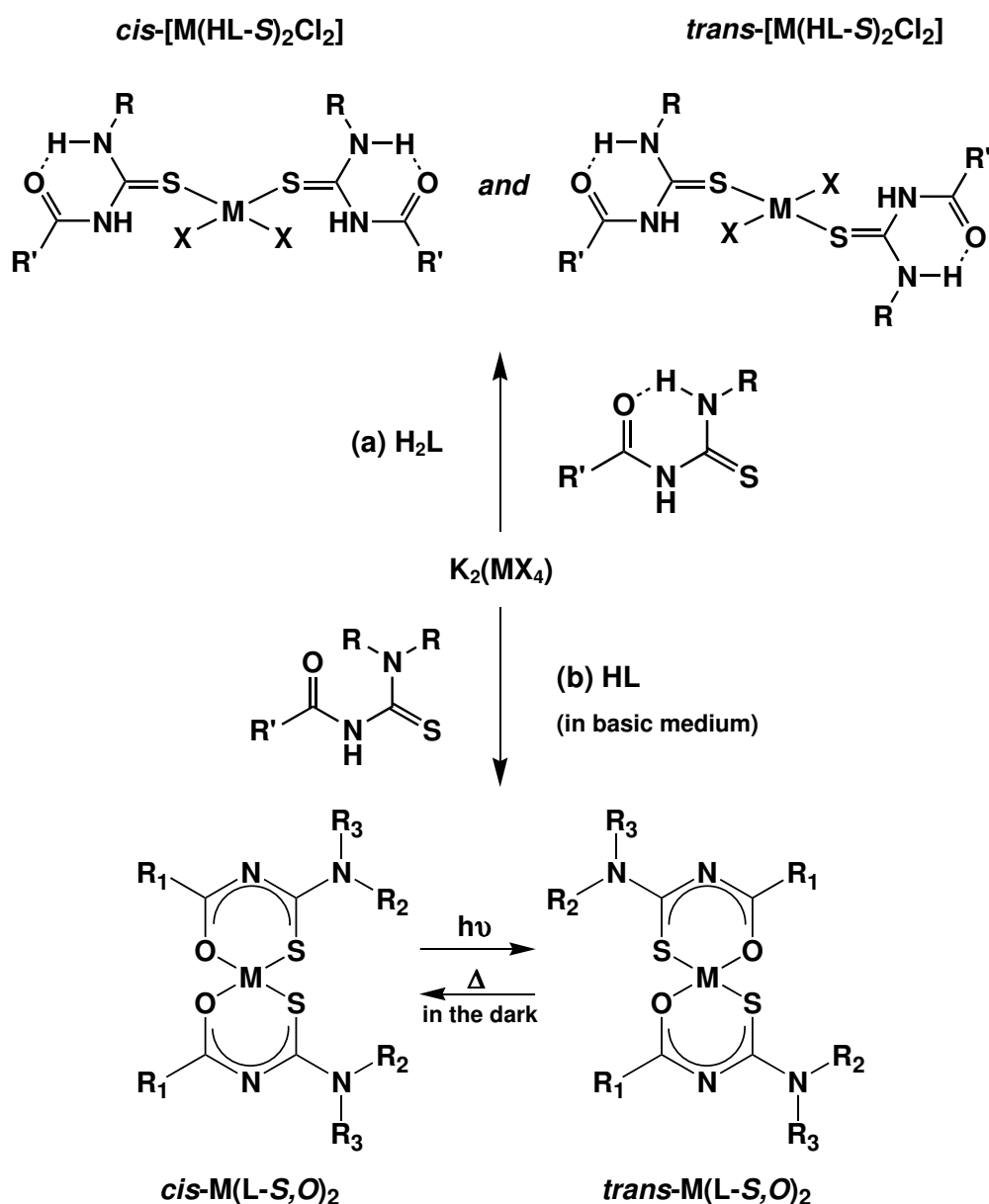


Figure 1.26. H₂L and HL ligands.

- (a) *N*-alkyl-*N'*-aroyl(acyl)thiourea (H₂L): R₁ = aryl/alkyl, R₂ = H, R₃ = alkyl
 (b) *N,N*-dialkyl-*N'*-aroyl(acyl)thiourea (HL): R₁ = aryl/alkyl, R₂ and R₃ = alkyl

These ligands readily coordinate to a wide variety of transition metals^[65, 80] in different modes^[55] (Scheme 1.4 on the following page). The H₂L ligands have only the sulphur donor atom available for coordination due to an intramolecular hydrogen bond between the carbonyl oxygen and the –C(S)NHR moiety and, when reacted with a metal halide salt such as K₂[PtX₄] (X = Cl, Br or I), form a mixture of *cis*- and *trans*-[Pt(HL-S)₂X₂] complexes (path a in Scheme 1.4).^[81-83]

The HL ligands, however can coordinate through both the oxygen and sulphur atoms in a chelating fashion, losing the thioamidic proton in the process (path b in Scheme 1.4).^[55] These complexes are predominantly in the *cis* conformation and there are many fully characterised examples available in the literature.^[46, 60, 84, 85] To date only one example of a fully characterised *trans* complex has been reported.^[86] However, it was recently discovered that the formation of the *trans* isomer from *cis*-Pt(L-S,O)₂ and *cis*-Pd(L-S,O)₂ complexes can be induced through a photochemical process, though isolation of the *trans* isomer is not possible as the isomerisation process is thermally reversible in the absence of light.^[45]



Scheme 1.4. Coordination modes of H₂L and HL to transition metal(II) ions.

Considering the chelating HL ligands in terms of Pearson's Hard Soft Acid Base (HSAB) theory,^[87, 88] one notices that they contain both a hard oxygen donor atom and a soft sulphur donor atom. This may offer some insight into why these ligands can coordinate to such a wide variety of transition metals as the hard oxygen donor atom can readily coordinate to hard metal ions such as Co(III) and Cr(III), while the soft sulphur donor prefers softer metals such as Pt(II) and Pd(II).

Beyer and Hoyer reported the potential of the benzoyl derivatives of these ligands in the liquid-liquid extraction of metal ions such as Cu(II), Hg(II), Au(III) and Pd(II),^[65] though it

was later observed by Vest *et al.* that the *N,N*-dialkyl-*N'*-benzoylthioureas (HL) were more efficient extractants than the *N*-alkyl-*N'*-benzoylthioureas (H₂L).^[68]

By adjusting the pH of the aqueous phase during the liquid-liquid extractions, König *et al.* found that *N,N*-dialkyl-*N'*-benzoylthiourea ligands would coordinate almost exclusively to platinum group metals (PGMs) in the presence of other interfering metal ions such as iron, cobalt, nickel, copper and zinc.^[71] Higher acid concentrations favoured the extraction of PGMs, and the individual platinum group metals could even, to some extent, be separated from each other through temperature and pH control during the extraction process.

Selective recovery of heavy transition metal ions is also possible through the use of functional polymeric materials such as *N*-benzoylthiourea modified dendrimers.^[67]

The use of these ligands for the separation of PGMs can be extended to the trace determination of these metals by chromatographic methods.^[46, 73-76] After complexation with an *N,N*-disubstituted-*N'*-aroyl(acyl)thiourea ligand, mixtures of PGMs can be successfully separated and quantified using high-performance thin layer chromatography (HPTLC).^[73-76] The use of fluorescent *N'*-aroylthioureas for trace determination using either HPTLC,^[78, 79] or normal- or reversed-phase TLC and HPLC,^[77] has been investigated by Schuster and co-workers. Alternatively, after complexation with a more hydrophilic *N,N*-dialkyl-*N'*-acylthiourea ligand, reversed-phase high-performance liquid chromatography (*rp*-HPLC) can be utilised for trace determination of Pt(II), Pd(II) and Rh(III) (see Figure 1.25 on page 34).^[46]

Schuster and co-workers also developed an efficient on-line system using *N,N*-diethyl-*N'*-benzoylthiourea ligands and graphite furnace absorption spectrometry, for the separation, preconcentration and trace determination of Pd(II).^[72]

An additional recently discovered practical use for these ligands is in the selective and efficient liquid membrane transport of silver ions from a mixture of Ag(I), Co(I), Ni(II), Zn(II), Cd(II) and Pb(II).^[66]

Notwithstanding the applications of these ligands in transition metal chemistry, *N*-alkyl- and *N,N*-dialkyl-*N'*-acyl(aroyl)thiourea complexes have also demonstrated biological

activity and have shown promise in medicinal applications as anti-fungal agents,^[61, 62] as well as potential treatments for cancer^[57-60] and malaria.^[63] Also, within a biological scope, the intercalation of a water-soluble mixed-ligand *N,N*-di(2-hydroxyethyl)-*N'*-benzoylthiourea—diimine Pt(II) complex into the DNA double helix, with a view to anti-cancer applications, has been recently reported.^[64]

With these many varied applications, it is prudent to attempt to understand the nature and behaviour of these ligands and complexes in solution at a fundamental, molecular level.

Chapter 2

Experimental Procedures

2.1 Synthesis and characterisation of the *cis*-bis(*N,N*-dialkyl-*N'*-aroyl(acyl)thioureato)Pd(II) complexes

2.1.1 Ligand synthesis

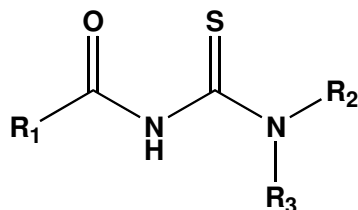
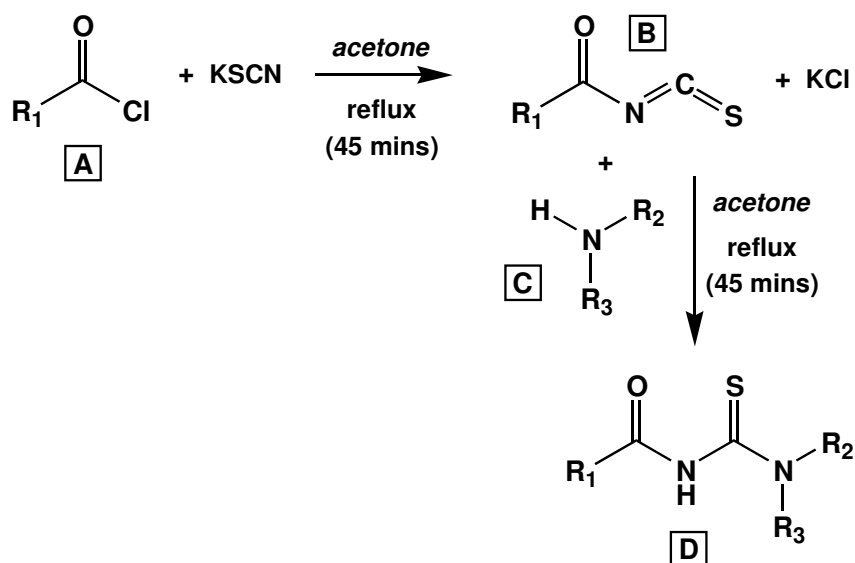


Figure 2.1. *N,N*-dialkyl-*N'*-aroyl(acyl)thiourea ligand

All ligands used (Figure 2.1 adjacent) were kindly donated by Prof K.R. Koch, Dr A.N. Westra, Dr S. Mtongana and Mr D.C. Hanekom.

The synthesis of the aforementioned ligands can be carried out using a variation of the two-step, one-pot method described by Douglass and Dains in 1934 (Scheme 2.1).^[56]



Scheme 2.1. Reaction pathway for the synthesis of *N,N*-dialkyl-*N'*-aroyl(acyl)thiourea ligands.

In a two-necked round bottom flask, 15 mmol potassium thiocyanate (pre-dried in a vacuum oven) was dissolved in 50 ml anhydrous acetone, under inert nitrogen atmosphere. Douglass and Dains discovered that anhydrous reagents resulted in higher yields of product. While stirring constantly under inert atmosphere, a solution of 15 mmol of the desired acyl/aroyl substituent (A in Scheme 2.1) in 50 ml anhydrous acetone, was added dropwise over a period of about 30 minutes. The reaction mixture,

containing acyl/aroyl isothiocyanate (B in Scheme 2.1) was then refluxed for a further 45 minutes before being cooled, under nitrogen, to room temperature.

15 mmol of the amine reagent (C in Scheme 2.1), dissolved in 50 ml anhydrous acetone, was then added dropwise over a period of 30 minutes to the reaction mixture. After being refluxed and allowed to cool for a second time, the reaction mixture was added to an excess of water and left in a fume hood to allow evaporation of the acetone. The precipitated crude product (D in Scheme 2.1) was then filtered, washed and recrystallised from an acetone/water or chloroform/ethanol mixture. This procedure usually resulted in good yields of 70-80 %.

2.1.2 Synthesis of palladium(II) complexes: $cis\text{-Pd}^{II}(\text{L-S,O})_2$

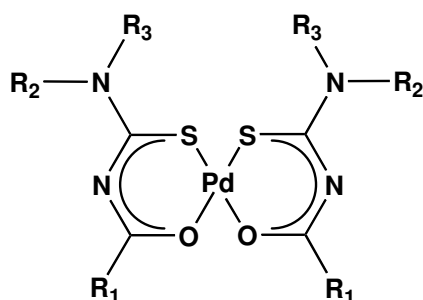
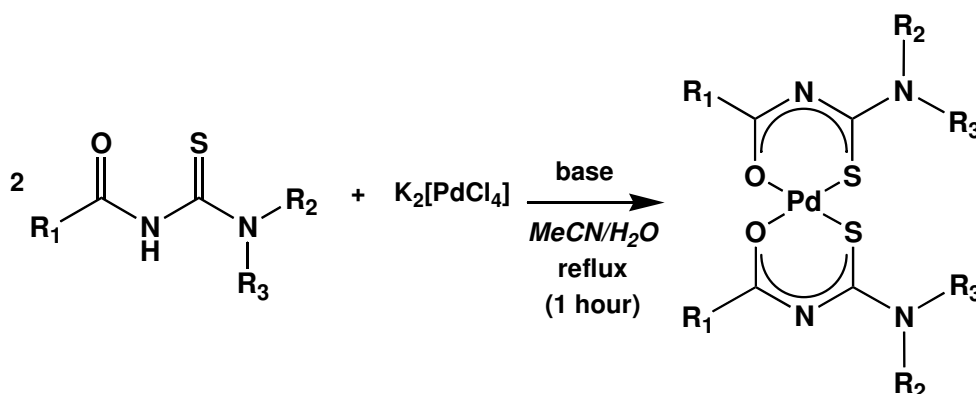


Figure 2.2. *cis*-bis(*N,N*-dialkyl-*N'*-aroyl(acyl)thioureato)Pd(II) complex.

The palladium(II) complexes (Figure 2.2) were synthesised according to the method described by Koch *et al.*^[46]



Scheme 2.2. Reaction pathway for the synthesis of *cis*-bis(*N,N*-dialkyl-*N'*-aroyl(acyl)thioureato)Pd(II) complexes.

0.5 mmol of the desired ligand and 1 mmol sodium acetate – to affect deprotonation of the ligand – were dissolved in 30 ml acetonitrile/water mixture (2:1 v/v) in a two-necked

round bottom flask and stirred at 80 °C. To this, a solution of 0.5 mmol dipotassium tetrachloropallidate, $K_2[PdCl_4]$, dissolved in 30 ml acetonitrile/water mixture (1:2 v/v), was added dropwise over a period of about 15 minutes. The reaction mixture was then stirred at 80 °C for one hour. After cooling to room temperature, excess water was added and the reaction flask sealed and placed in the refrigerator overnight. The crude product was collected by either centrifugation or filtration, and washed with water and a portion of cold ethanol. The crude product was recrystallised from either a polar mixture of acetone/water, or a more non-polar mixture such as dichloromethane/methanol or chloroform/ethanol and dried under vacuum. Generally yields of between 70-90 % were obtained.

2.1.2.1 Further purification

Exceptionally pure, clean complexes were required, as any trace impurities or unbound ligand was found to drastically affect the rate of the metathesis reaction (see Chapter 4). After an initial recrystallisation from an acetone/water mixture, examination of a TLC plate comparing complex and ligand indicated that no unreacted ligand remained. However, screening the compounds using the more-sensitive HPLC system revealed that traces of unbound ligand were in fact still present (Figure 2.3a). As both the ligands and the complexes show affinities for the same solvents, removing all traces of unbound ligand proved problematic.

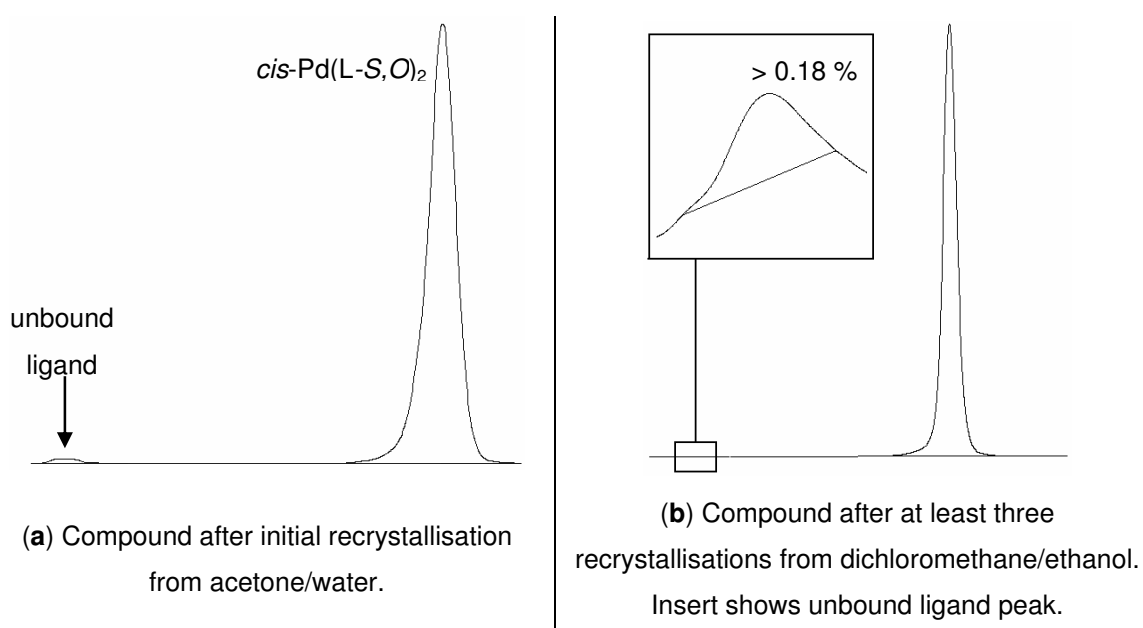


Figure 2.3. Chromatograms of the same compound before and after extensive recrystallisation.

The solvent combination which yielded the most promising results was dichloromethane/ethanol which, after approximately three successive recrystallisations, yielded compounds containing less than 0.18 % unbound ligand (Figure 2.3 b). As an additional confirmation of purity, the complexes melted within extremely narrow temperature ranges (see Section 2.1.3 below).

2.1.3 Palladium(II) complex characterisation

The complexes were characterised using ^1H and ^{13}C nuclear magnetic resonance (NMR) spectroscopy, elemental analysis, melting point analysis and liquid-chromatography-mass spectrometry (LC-MS). Crystal structures were obtained when suitable crystals could be grown. The crystal data and structure refinement data can be found in Appendix A.

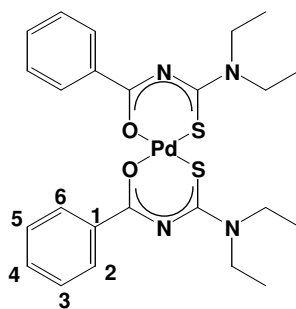
NMR spectra were recorded at 25 °C in deuterated chloroform using either a Varian INOVA 600 MHz, Varian INOVA 400 MHz or a Varian VXR 300 MHz spectrometer operating at, respectively 600, 400 or 300 MHz for ^1H and 150, 100 or 75 MHz for ^{13}C spectra. The chemical shifts were referenced relative to the residual CDCl_3 solvent proton resonance at 7.26 ppm for ^1H spectra and the centre peak of the CDCl_3 triplet at 77.0 ppm for the ^{13}C spectra. The chemical shifts are reported as ppm values, while the coupling constants are reported in Hz.

Elemental analyses were performed using a Carlo Erba EA 1108 Elemental Analyser in the microanalytical laboratory at the University of Cape Town. Melting points were obtained using an Electrothermal 9300 Digital Melting Point Apparatus.

Mass spectra were acquired on a Waters API Quattro Micro 2690 instrument operating in positive electrospray ionisation (ESI) mode with the capillary voltage set to 3.5 kV and the cone voltage to 15 V. The samples, dissolved in acetonitrile, were separated by *rp*-HPLC (see Section 2.2.2) before being introduced into the mass spectrometer.

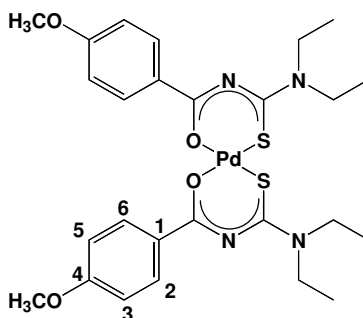
Crystal structures were obtained using a Bruker-Nonius SMART Apex Area CCD X-ray diffractometer equipped with a Mo fine-focus sealed tube and a 0.5 mm MonoCap collimator. The structures were solved and refined with SHELLXS97 and SHELLXL97^[89] respectively. The molecular graphics were rendered using XSEED.^[90]

1. *cis*-bis(*N,N*-diethyl-*N*-benzoylthioureato)palladium(II): *cis*-Pd(L¹-S,O)₂



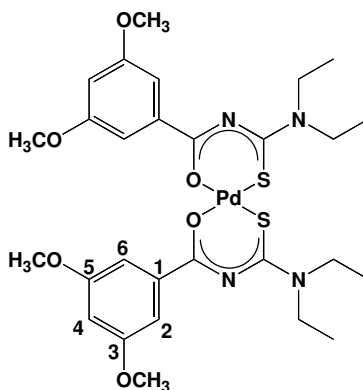
Melting point: 164.6-165.8 °C. Found: C, 50.12; H, 5.28; N, 9.34; S, 10.47 % PdC₂₄H₃₀N₄O₂S₂ requires C, 49.95; H, 5.24; N, 9.71; S, 11.11 %. δ_{H} (600 MHz, CDCl₃) 1.29 (6 H, t, ³J_{HH} 7.1, 2 CH₃), 1.34 (6 H, t, ³J_{HH} 7.1, 2 CH₃), 3.86 (8 H, q, ³J_{HH} 7.1, 4 CH₂), 7.41 (4 H, t, ³J_{HH} 7.2, C(3)H & C(5)H), 7.48 (2 H, t, ³J_{HH} 7.3, C(4)H), 8.24 (4H, d, ³J_{HH} 7.0, C(2)H & C(6)H). δ_{C} (150 MHz, CDCl₃): 12.66 (2 CH₃), 13.12 (2 CH₃), 46.04 (2 CH₂), 47.20 (2 CH₂), 127.93 (C3 & C5), 129.67 (C2 & C6), 131.44 (C4), 137.08 (C1), 170.63 (C(O)), 171.11 (C(S)). Molecular ion (M⁺) m/z: 577

2. *cis*-bis(*N,N*-diethyl-*N*-4-methoxybenzoylthioureato)palladium(II): *cis*-Pd(L²-S,O)₂



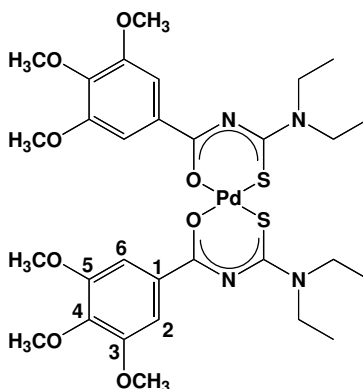
Melting point: 184.1-184.9 °C. Found: C, 48.85; H, 5.35; N, 8.44; S, 9.79 % PdC₂₆H₃₄N₄O₄S₂ requires C, 49.01; H, 5.38; N, 8.79; S, 10.07 %. δ_{H} (300 MHz, CDCl₃) 1.27 (6 H, t, ³J_{HH} 7.1, 2 CH₃), 1.32 (6 H, t, ³J_{HH} 7.1, 2 CH₃), 3.83 (4 H, q, ³J_{HH} 7.2, 2 CH₂), 3.84 (4 H, q, ³J_{HH} 7.2, 2 CH₂), 3.87 (6 H, s, OCH₃), 6.92 (4 H, d, ³J_{HH} 9.0, C(2)H & C(6)H), 8.19 (4 H, d, ³J_{HH} 9.1, C(3)H & C(5)H). δ_{C} (75 MHz, CDCl₃): 12.55 (2 CH₃), 12.92 (2 CH₃), 45.80 (2 CH₂), 47.0 (2 CH₂), 55.28 (OCH₃), 113.32 (C3 & C5), 129.94 (C1), 131.84 (C2 & C6), 162.74 (C4), 170.80 (C(S)), 171.07 (C(O)). Molecular ion (M⁺) m/z: 637

**3. *cis*-bis(*N,N*-diethyl-*N'*-3,5-dimethoxybenzoylthioureato)palladium(II):
cis-Pd(L³-S,O)₂**



Melting point: 194.8-195.4 °C. Found: C, 48.29; H, 5.51; N, 7.72; S, 8.76 % PdC₂₈H₃₈N₄O₆S₂ requires C, 48.24; H, 5.49; N, 8.04; S, 8.59 %. δ_{H} (300 MHz, CDCl₃) 1.28 (6 H, t, ³J_{HH} 7.2, 2 CH₃), 1.32 (6 H, t, ³J_{HH} 7.2, 2 CH₃), 3.82 (4 H, q, ³J_{HH} 7.1, 2 CH₂), 3.83 (12 H, s, OCH₃), 3.84 (4 H, q, ³J_{HH} 7.2, 2 CH₂), 6.58 (2 H, t, ³J_{HH} 8.9, C(4)H), 7.44 (4 H, d, ³J_{HH} 8.8, C(2)H & C(6)H). δ_{C} (75 MHz, CDCl₃): 12.26 (2 CH₃), 13.10 (2 CH₃), 46.21 (2 CH₂), 47.27 (2 CH₂), 55.35 (2 OCH₃), 103.88 (C4), 107.45 (C2 & C6), 139.17 (C1), 160.25 (C3 & C5), 169.97 (C(S)), 171.18 (C(O)). Molecular ion (M⁺) m/z: 697

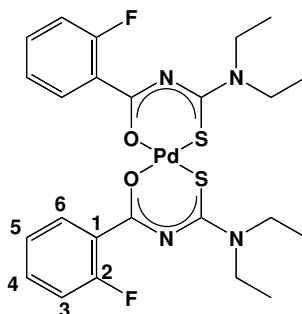
**4. *cis*-bis(*N,N*-diethyl-*N'*-3,4,5-trimethoxybenzoylthioureato)palladium(II):
cis-Pd(L⁴-S,O)₂**



Melting point: 215.7-216.8 °C. Found: C, 47.73; H, 5.65; N, 6.85; S, 8.09 % PdC₃₀H₄₂N₄O₈S₂ requires C, 47.58; H, 5.59; N, 7.40; S, 8.47 %. δ_{H} (300 MHz, CDCl₃) 1.26 (6 H, t, ³J_{HH} 7.2, 2 CH₃), 1.29 (6 H, t, ³J_{HH} 7.2, 2 CH₃), 3.80 (4 H, q, ³J_{HH} 7.1,

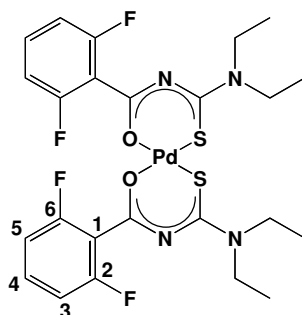
2 CH₂), 3.82 (4 H, q, ³J_{HH} 7.2, 2 CH₂), 3.86 (12 H, s, C(3)OCH₃ & C(5)OCH₃), 3.87 (6 H, s, C(4)OCH₃), 7.54 (4 H, s, C(2)H & C(6)H). δ_C(75 MHz, CDCl₃): 12.46 (2 CH₃), 12.88 (2 CH₃), 46.05 (2 CH₂), 47.18 (2 CH₂), 56.13 (OCH₃), 60.80 (OCH₃), 107.62 (C2 & C6), 132.60 (C1), 141.79 (C4), 152.74 (C3 & C5), 170.36 (C(S)), 171.22 (C(O)). Molecular ion (M⁺) m/z: 757

5. *cis*-bis(*N,N*-diethyl-*N'*-2-fluorobenzoylthioureato)palladium(II): *cis*-Pd(L⁵-S,O)₂



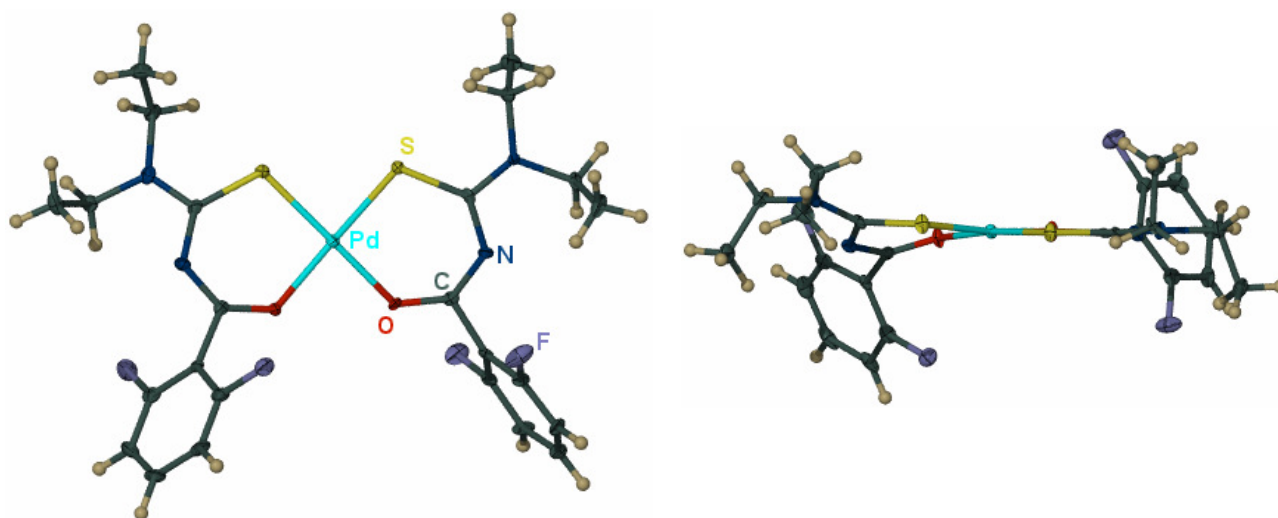
Donation. Melting point: 124.5-125.4 °C. Found: C, 46.89; H, 4.61; N, 8.64; S, 9.84 % PdC₂₄H₂₈N₄O₂S₂F₂ requires C, 47.02; H, 4.60; N, 9.14; S, 10.46 %. δ_H(400 MHz, CDCl₃) 1.22 (6 H, t, ³J_{HH} 7.1, 2 CH₃), 1.33 (6 H, t, ³J_{HH} 7.2, 2 CH₃), 3.83 (8 H, q, ³J_{HH} 7.1, 4 CH₂), 7.05 (1 H, dd, ³J_{HH} 8.3, ⁴J_{HH} 1.0, C(5)H), 7.08 (1 H, dd, ³J_{HH} 8.3, ⁴J_{HH} 1.1, C(5)H), 7.14 (2 H, td, ³J_{HH} 7.4, ⁴J_{HH} 1.2, C(4)H), 7.39 (2 H, m, due to ³J_{HF} and long range coupling to other H, C(3)H), 8.05 (2 H, td, ³J_{HH} 7.7, ⁴J_{HH} 1.9, C(6)H). δ_C(100 MHz, CDCl₃): 12.54 (2 CH₃), 12.99 (2 CH₃), 46.13 (2 CH₂), 47.00 (2 CH₂), 116.62 (C3), 116.85 (C1), 123.47 (C5), 125.68 (C6), 132.42 (C4), 161.84 (C2, ¹J_{CF} 258.12), 168.81 (C(S)), 171.10 (C(O)). Molecular ion (M⁺) m/z: 613

6. *cis*-bis(*N,N*-diethyl-*N'*-2,6-difluorobenzoylthioureato)palladium(II): *cis*-Pd(L⁶-S,O)₂

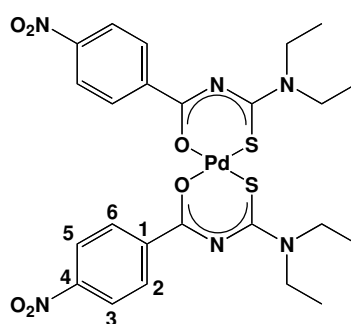


Donation. Melting point: 214.6-215.9 °C. Found: C, 44.50; H, 4.02; N, 8.05; S, 8.52 % PdC₂₄H₂₆N₄O₂S₂F₄ requires C, 44.41; H, 4.04; N, 8.63; S, 9.88 %. δ_{H} (400 MHz, CDCl₃) 1.17 (6 H, t, $^3J_{\text{HH}}$ 7.1, 2 CH₃), 1.32 (6 H, t, $^3J_{\text{HH}}$ 7.1, 2 CH₃), 3.70 (4 H, q, $^3J_{\text{HH}}$ 7.1, 4 CH₂), 3.80 (4 H, q, $^3J_{\text{HH}}$ 7.1, 2 CH₂), 6.83 (4 H, t, $^3J_{\text{HH}}$ 8.3, C(3)H & C(5)H), 7.21 (2 H, m, due to long range coupling to F and other H, C(4)H). δ_{C} (100 MHz, CDCl₃): 12.38 (2 CH₃), 12.85 (2 CH₃), 46.21 (2 CH₂), 47.07 (2 CH₂), 111.39 (C1), 111.63 (C3 & C5), 129.88 (C4), 160.34 (C2 & C6, $^1J_{\text{CF}}$ 248.30), 165.85 (C(S)), 171.09 (C(O)). Molecular ion (M⁺) m/z: 649

Crystal structure (see Appendix A for more detail)



7. *cis*-bis(*N,N*-diethyl-*N'*-4-nitrobenzoylthioureato)palladium(II): *cis*-Pd(L⁷-S,O)₂

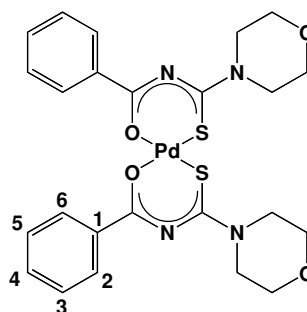


This ligand is not stable. It decomposes easily and does not readily form complexes under the standard reaction conditions.

Melting point: 240-243.5 °C (blackens/decomposes), 244.1-244.7 °C (melts). Found: C, 48.06; H, 5.41; N, 10.74; S, 8.14 % PdC₂₄H₂₈N₆O₂S₂ requires C, 43.21; H, 4.23; N, 12.60; S, 9.61 %. δ_{H} (300 MHz, CDCl₃) 1.22 (4 H, s, possible decomposition product),

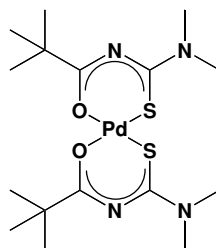
1.27 (6H, t, $^3J_{\text{HH}}$ 7.2, 2 CH₃), 1.33 (6 H, t, $^3J_{\text{HH}}$ 7.2, 2 CH₃), 1.53 (2 H, s, impurity), 3.84 (8 H, qd, $^3J_{\text{HH}}$ 7.1, $^4J_{\text{HH}}$ 2.5, 2 CH₂), 8.27 (4 H, dt, $^3J_{\text{HH}}$ 9.1, $^4J_{\text{HH}}$ 1.9, C(2)H & C(6)H), 8.35 (4 H, dt, $^3J_{\text{HH}}$ 9.1, $^4J_{\text{HH}}$ 1.9, C(3)H & C(5)H). δ_{C} (75 MHz, CDCl₃): 12.27 (2 CH₃), 12.91 (2 CH₃), 29.53 (possible decomposition product) 46.35 (2 CH₂), 47.51 (2 CH₂), 123.38 (C3 & C5), 130.55 (C2 & C6), 143.12 (C1), 149.91 (C4), 168.61 (C(S)), 172.12 (C(O)). Molecular ion (M⁺) m/z: not found

8. *cis*-bis(*N*-morpholine-*N'*-benzoylthioureato)palladium(II): *cis*-Pd(L⁸-S,O)₂



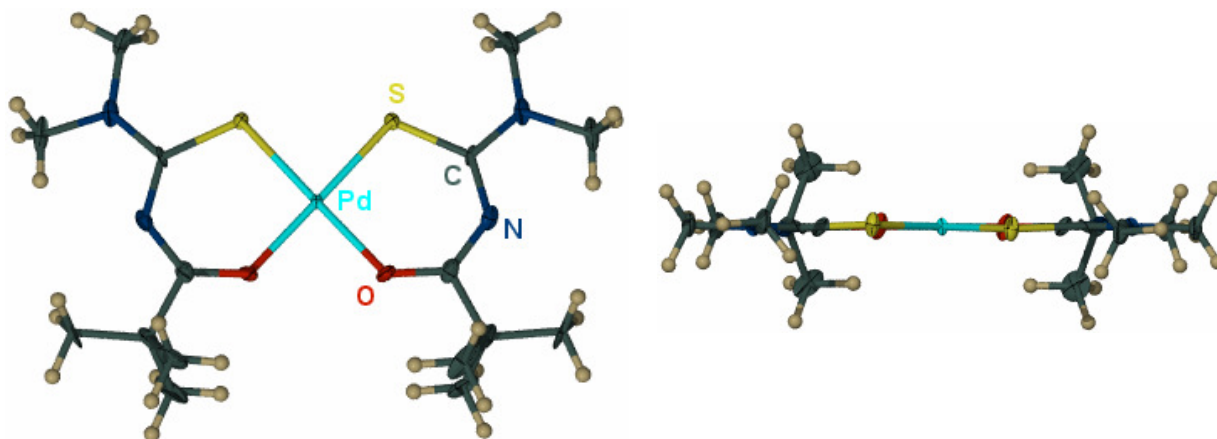
Melting point: 240-242.1 °C (blackens/decomposes), 242.4-243.5 °C (melts). Found: C, 47.55; H, 4.27; N, 8.78; S, 10.09 % PdC₂₄H₂₆N₄O₂S₂ requires C, 47.64; H, 4.33; N, 9.26; S, 10.60 %. δ_{H} (300 MHz, CDCl₃) 3.77 (8 H, t, $^3J_{\text{HH}}$ 4.0, 2 NCH₂), 4.11 (4 H, t, $^3J_{\text{HH}}$ 4.0, OCH₂), 4.21 (4 H, t, $^3J_{\text{HH}}$ 4.0, OCH₂), 7.43 (4 H, tt, $^3J_{\text{HH}}$ 7.1, $^4J_{\text{HH}}$ 1.2, C(3)H & C(5)H), 7.52 (2 H, tt, $^3J_{\text{HH}}$ 7.3, $^4J_{\text{HH}}$ 1.4, C(4)H), 8.22 (4 H, dt, $^3J_{\text{HH}}$ 7.0, $^4J_{\text{HH}}$ 1.5, C(2)H & C(6)H). δ_{C} (75 MHz, CDCl₃): 47.38 (OCH₂), 49.73 (OCH₂), 66.36 (NCH₂), 66.56 (NCH₂), 128.22 (C3 & C5), 129.95 (C2 & C6), 132.07 (C4), 136.90 (C1), 172.40 (C(S)), 172.72 (C(O)). Molecular ion (M⁺) m/z: 607

9. *cis*-bis(*N,N*-dimethyl-*N'*-2,2-dimethylpropanoylthioureato)palladium(II): *cis*-[Pd(L⁹-S,O)₂

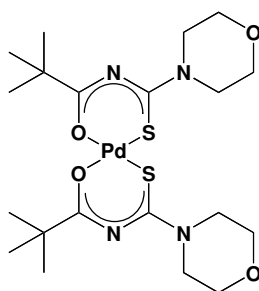


Melting point: 203.9-204.4 °C. Found: C, 40.07; H, 6.32; N, 20.89; S, 13.29 % PdC₁₆H₃₀N₄O₂S₂ requires C, 39.95; H, 6.29; N, 11.65; S, 13.33 %. δ_{H} (300 MHz, CDCl₃) 1.17 (9 H, s, 3 CH₃ (^tBu)), 3.24 (3 H, s, NCH₃), 3.29 (3 H, s, NCH₃), δ_{C} (75 MHz, CDCl₃): 28.41 (3 CH₃ (^tBu)), 40.47 (C), 41.63 (2 NCH₃), 172.39 (C(O)), 186.01 (C(S)). Molecular ion (M⁺) m/z: 481

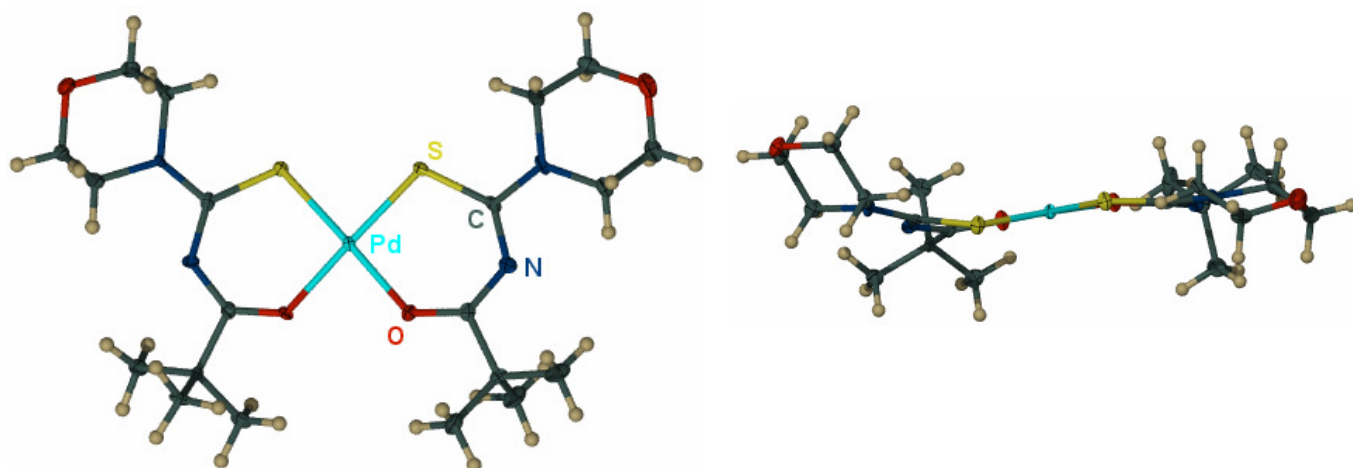
Crystal structure (see Appendix A for more detail)



10. *cis*-bis(*N*-morpholine-*N'*-2,2-dimethylpropanoylthioureato)palladium(II):
***cis*-Pd(L¹⁰-S,O)₂**



Melting point: 236-237 °C (isolated crystals blacken), 240.2-241.5 °C (melts). Found: C, 42.69; H, 6.16; N, 9.32; S, 11.17 % PdC₂₀H₃₄N₄O₂S₂ requires C, 42.76; H, 6.06; N, 9.92; S, 11.35 %. δ_{H} (300 MHz, CDCl₃) 1.16 (9 H, s, 3 CH₃ (tBu)), 3.68 (6 H, t, ³J_{HH} 4.0, 2 NCH₂), 4.02 (6 H, t, ³J_{HH} 4.0, 2 OCH₂). δ_{C} (75 MHz, CDCl₃): 28.32 (3 CH₃), 41.96 (C, ^tBu), 47.00 (OCH₂), 49.55 (OCH₂), 66.43 (2 NCH₂), 172.34 (C(S)), 187.18 (C(O)). Molecular ion (M⁺) m/z: 565

Crystal structure (see Appendix A for more detail)

2.1.3.1 Summary of compounds and abbreviated names

Complex structure	Abbreviated name	Complex structure	Abbreviated name
	<i>cis</i> -Pd(L ¹ -S,O) ₂		<i>cis</i> -Pd(L ⁶ -S,O) ₂
	<i>cis</i> -Pd(L ² -S,O) ₂		<i>cis</i> -Pd(L ⁷ -S,O) ₂
	<i>cis</i> -Pd(L ³ -S,O) ₂		<i>cis</i> -Pd(L ⁸ -S,O) ₂
	<i>cis</i> -Pd(L ⁴ -S,O) ₂		<i>cis</i> -Pd(L ⁹ -S,O) ₂
	<i>cis</i> -Pd(L ⁵ -S,O) ₂		<i>cis</i> -Pd(L ¹⁰ -S,O) ₂

Please note, in the captions of Figures, Tables and Schemes, the names of the above complexes have been abbreviated to Pd(L^A)₂ (A = 1 - 10).

2.2 Monitoring the metathesis reaction using high-performance liquid chromatography (HPLC)

Reversed-phase high-performance liquid chromatography (*rp*-HPLC) with UV-Vis detection was used to monitor the chelate metathesis reaction between two different *cis*-bis(*N,N*-dialkyl-*N'*-aroyl(acyl)thioureato)Pd(II) complexes, as illustrated in Figure 2.4.

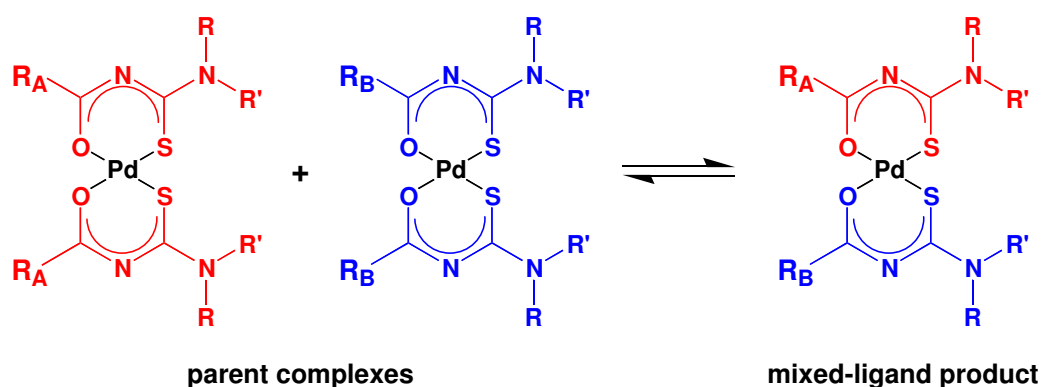


Figure 2.4. Metathesis reaction of interest.

The relatively slow rate of this metathesis reaction makes it ideal to study using HPLC. The chromatograms of this reaction were similar to the schematic chromatogram shown in Figure 2.5b, with well-defined, separated peaks, indicating that the metathesis reaction does not appear to continue whilst the sample is moving through the column.

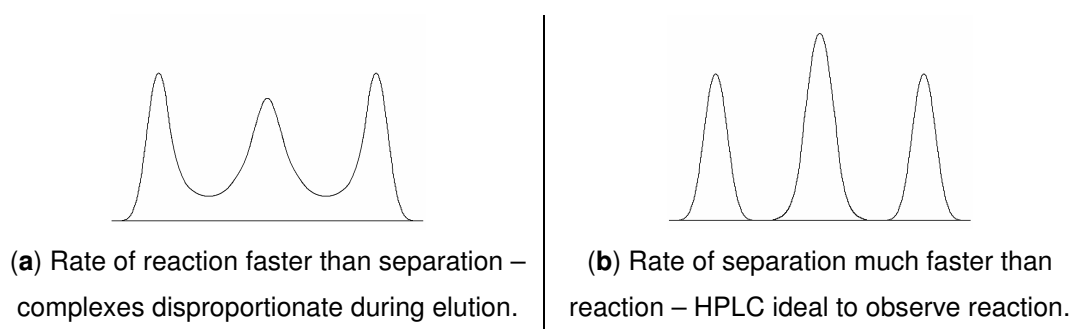


Figure 2.5. Schematic chromatograms of possible peak patterns for metathesis reactions.

If, however, the reaction were to persist during elution (Figure 2.5a), increasing the flow rate would accelerate separation and minimise contact between the three species.^[7, 16] Therefore, to confirm that the reaction does not continue on-column, the same metathesis experiment was repeated four times with flow rates of 0.25 0.5, 1 and 1.5 ml/min respectively, keeping mobile phase composition, detection wavelengths and

temperature the same. In all four cases, the peaks retained the shape seen in Figure 2.5b. The peak areas for each experiment were identical, verifying that the rate of reaction is much slower than the separation process and that, consequently, the chromatograms obtained directly represent the state of the metathesis reaction upon injection of the sample.

2.2.1 Handling and preparation of samples

Each sample was weighed on a Precisa XT 220A electronic analytical balance to an accuracy of 0.0001 g and dissolved in the appropriate solvent (Sigma-Aldrich Acetonitrile E Chromasolv[®] HPLC grade acetonitrile far-UV (34888), unless stated otherwise) in a clean, dry volumetric flask.

A specific cleaning procedure was followed to ensure that any trace impurities in the volumetric flasks were eliminated as far as possible. Firstly, to remove any metal ions, the flasks were filled with a 10 % v/v nitric acid solution and left overnight. Nitric acid was chosen above hydrochloric acid, as the strong mineral acids are known to protonate complexed acyl(aryl)thiourea ligands, leading to mixtures of *cis* and *trans* $[M^{II}(HL-S)(L-S,O)Cl]$ and $[M^{II}(HL-S)_2Cl_2]$ species.^[91, 92] After being rinsed thoroughly with distilled water, the flasks were filled with a 10 % m/v solution of KOH in ethanol and left to stand for a few hours to remove any organic substances and remove any traces of acid. The flasks were again rinsed well with distilled water and checked with a Merck Universal Indicator pH strip to ensure that all traces of acid/base had been removed. After a final rinse with reagent grade ethanol, the flasks were dried without heating, using compressed air.

Both the volumetric flasks and the HPLC sample vials were covered in aluminium foil to prevent exposure to light and thus inhibit the photoinduced *cis-trans* isomerisation these complexes can undergo.^[45]

2.2.2 HPLC procedure

All chromatography was performed on the Varian HPLC system shown below in Figure 2.6 with an Agilent Zorbax XDB C₁₈ column (4.6 x 150 mm, 5 µm particles) at 20 °C using the Galaxie Chromatography Data System (version 1.8.508.1).

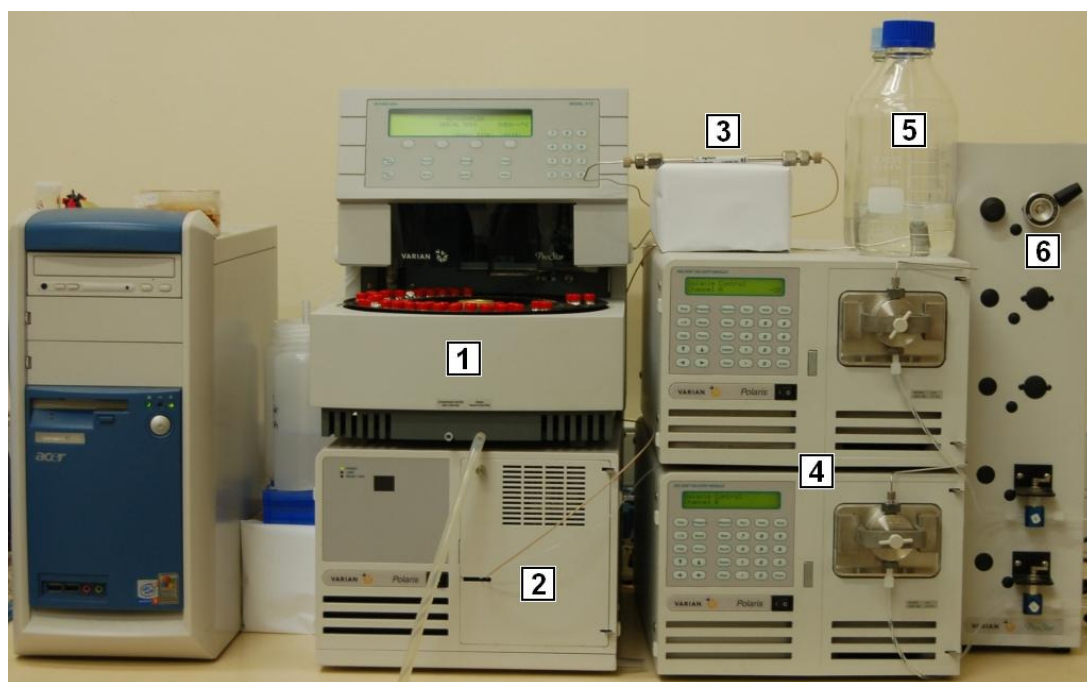


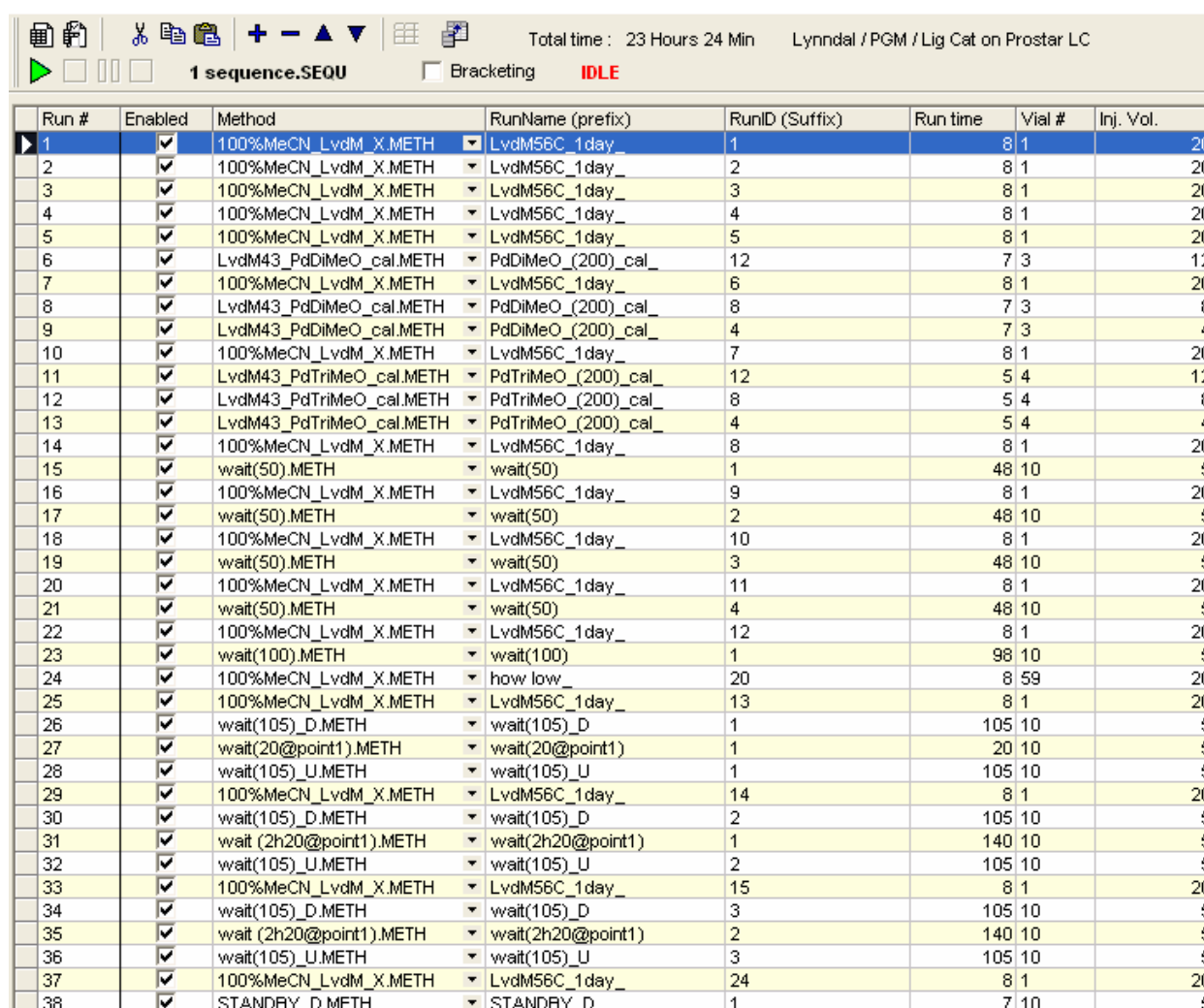
Figure 2.6. Varian HPLC system.

- 1 – Varian Prostar 420 AutoSampler
- 2 – Varian Polaris 325 UV-Vis Detector
- 3 – Agilent Zorbax XDB C₁₈ column (4.6 x 150 mm, 5 µm)
- 4 – Two Varian Polaris 210 pumps
- 5 – Eluent reservoirs
- 6 – Manual injection port

A reversed-phase column was chosen as normal-phase silica columns have been shown to initiate extensive on-column decomposition of the complexes of interest.^[93] This is presumably due to the susceptibility of these columns to traces of water and acids, as well as the inherent acidity of the surface silanol groups. The interaction of these acidic sites with the complexes may result in decomposition and the irreversible retention of the resulting highly polar products.

Samples were filtered through 0.45 μ m Micropore nitrocellulose filter units and the mobile phase filtered through a sintered filter system with 0.45 μ m membrane filter. Mobile phases were degassed by placing them in an ultrasonic bath for half an hour.

To monitor the progress of the chelate metathesis reaction over time, a sequence, such as that shown in Figure 2.7 was created using the Galaxie Chromatography Data System (version 1.8.508.1). As the Varian system (Figure 2.6) contains an autosampler, the reaction could be monitored overnight with calibration samples included in the sequence. It was possible to run up to six individual 24-hour sequences each day without any overlap.



Run #	Enabled	Method	RunName (prefix)	RunID (Suffix)	Run time	Vial #	Inj. Vol.
1	✓	100%MeCN_LvdM_X.METH	LvdM56C_1day_	1	8 1	20	20
2	✓	100%MeCN_LvdM_X.METH	LvdM56C_1day_	2	8 1	20	20
3	✓	100%MeCN_LvdM_X.METH	LvdM56C_1day_	3	8 1	20	20
4	✓	100%MeCN_LvdM_X.METH	LvdM56C_1day_	4	8 1	20	20
5	✓	100%MeCN_LvdM_X.METH	LvdM56C_1day_	5	8 1	20	20
6	✓	LvdM43_PdDiMeO_cal.METH	PdDiMeO_(200)_cal_	12	7 3	12	12
7	✓	100%MeCN_LvdM_X.METH	LvdM56C_1day_	6	8 1	20	20
8	✓	LvdM43_PdDiMeO_cal.METH	PdDiMeO_(200)_cal_	8	7 3	8	8
9	✓	LvdM43_PdDiMeO_cal.METH	PdDiMeO_(200)_cal_	4	7 3	4	4
10	✓	100%MeCN_LvdM_X.METH	LvdM56C_1day_	7	8 1	20	20
11	✓	LvdM43_PdTriMeO_cal.METH	PdTriMeO_(200)_cal_	12	5 4	12	12
12	✓	LvdM43_PdTriMeO_cal.METH	PdTriMeO_(200)_cal_	8	5 4	8	8
13	✓	LvdM43_PdTriMeO_cal.METH	PdTriMeO_(200)_cal_	4	5 4	4	4
14	✓	100%MeCN_LvdM_X.METH	LvdM56C_1day_	8	8 1	20	20
15	✓	wait(50).METH	wait(50)	1	48 10	5	5
16	✓	100%MeCN_LvdM_X.METH	LvdM56C_1day_	9	8 1	20	20
17	✓	wait(50).METH	wait(50)	2	48 10	5	5
18	✓	100%MeCN_LvdM_X.METH	LvdM56C_1day_	10	8 1	20	20
19	✓	wait(50).METH	wait(50)	3	48 10	5	5
20	✓	100%MeCN_LvdM_X.METH	LvdM56C_1day_	11	8 1	20	20
21	✓	wait(50).METH	wait(50)	4	48 10	5	5
22	✓	100%MeCN_LvdM_X.METH	LvdM56C_1day_	12	8 1	20	20
23	✓	wait(100).METH	wait(100)	1	98 10	5	5
24	✓	100%MeCN_LvdM_X.METH	how low_	20	8 59	20	20
25	✓	100%MeCN_LvdM_X.METH	LvdM56C_1day_	13	8 1	20	20
26	✓	wait(105)_D.METH	wait(105)_D	1	105 10	5	5
27	✓	wait(20@point1).METH	wait(20@point1)	1	20 10	5	5
28	✓	wait(105)_U.METH	wait(105)_U	1	105 10	5	5
29	✓	100%MeCN_LvdM_X.METH	LvdM56C_1day_	14	8 1	20	20
30	✓	wait(105)_D.METH	wait(105)_D	2	105 10	5	5
31	✓	wait(2h20@point1).METH	wait(2h20@point1)	1	140 10	5	5
32	✓	wait(105)_U.METH	wait(105)_U	2	105 10	5	5
33	✓	100%MeCN_LvdM_X.METH	LvdM56C_1day_	15	8 1	20	20
34	✓	wait(105)_D.METH	wait(105)_D	3	105 10	5	5
35	✓	wait(2h20@point1).METH	wait(2h20@point1)	2	140 10	5	5
36	✓	wait(105)_U.METH	wait(105)_U	3	105 10	5	5
37	✓	100%MeCN_LvdM_X.METH	LvdM56C_1day_	24	8 1	20	20
38	✓	STANDBY_D.METH	STANDBY_D	1	7 10	5	5

Figure 2.7. Representative sequence for one 24 hour long experiment.

The “Method” (third column in Figure 2.7) contains all the instructions necessary for the HPLC system to run the chromatogram, including parameters such as mobile phase flow rate and composition, acquisition time and detection wavelengths.

For the representative sequence seen in Figure 2.7, consecutive runs produce “snapshots” of the metathesis reaction at 10 minute intervals notwithstanding the fact that each sample run is defined as only 8 minutes long (Figure 2.7, column 6 – Run time). This is due to the fact that between two consecutive samples, the system required up to two and a half minutes to save the completed chromatogram data and load the “Method” for the next sample. The acquisition times defined in the Methods were therefore adjusted accordingly to incorporate this delay and maintain accurate time intervals.

The Varian UV-Vis detector can monitor two different wavelengths simultaneously, and these were chosen such that the two parent complexes of interest had approximately equal absorbance. The wavelengths were determined by comparing the absorbance spectra of the two individual complexes (Figure 2.8 illustrates one example. The specific wavelengths used in each experiment are listed in Appendix E). The UV-Vis spectra were obtained on an Agilent 8453 diode-array spectrophotometer.

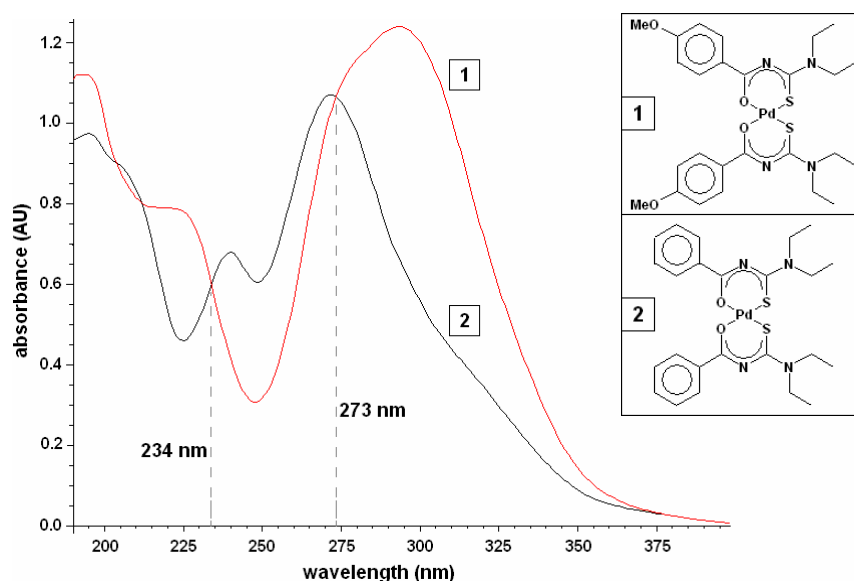


Figure 2.8. UV-Vis spectra of 20 μM solutions of two substituted *cis*-bis(*N,N*-diethyl-*N*²-benzoylthioureato) Pd(II) complexes 1 and 2, illustrating the whole number wavelengths at which the complexes possess near equal absorbance.

It was, however, not always possible to obtain identical peak areas when the chromatograms were run, as can be seen in the data in Figure 2.9 on the following page for the reaction between *cis*-Pd(L³-S,O)₂ and *cis*-Pd(L⁴-S,O)₂.

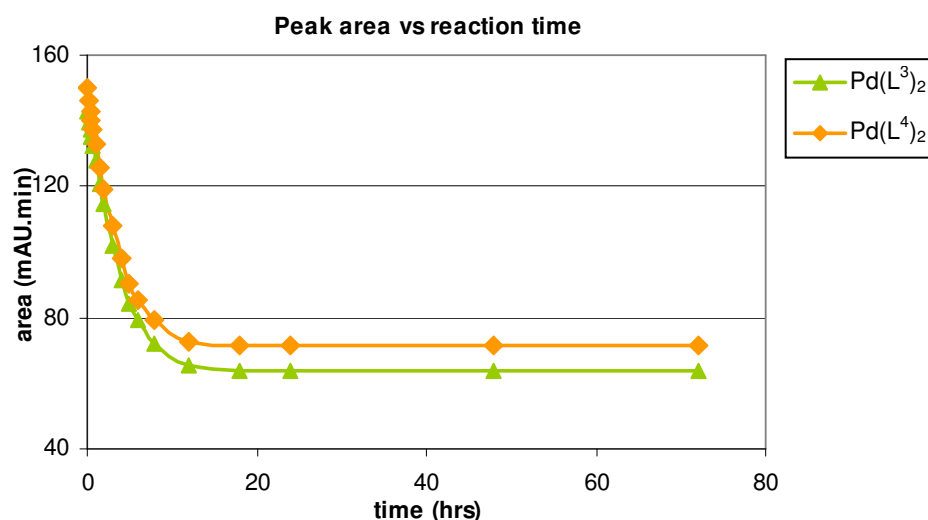


Figure 2.9. Graph of area (for 291 nm) vs. reaction time for Pd(L³)₂ and Pd(L⁴)₂.

This discrepancy was due to the fact that the UV-Vis spectra of the two parent complexes often intersected at non-whole number wavelengths (e.g. 291.42 nm), while the UV-Vis detector in the Varian HPLC system was only capable of monitoring whole number wavelengths (e.g. 291.0 nm). This difference of only a few tenths of a wavelength was sufficient to cause a small difference in peak area between the two parent complexes of around 8 mAU.min. However, for every individual experiment, each parent complex solution was calibrated separately at both observation wavelengths, so these slight differences in absorbance were not problematic.

All samples were eluted at an isocratic flow rate of 1 ml per minute with either 100 % acetonitrile or 95:5 volume % acetonitrile:milli-Q water, depending on how well the two complexes could be separated. It was not necessary to use a buffer solution as the complexes are uncharged in the solvents under investigation. Chromatograms obtained with and without a 0.1 M acetic acid/sodium acetate buffer (pH \approx 6) in the mobile phase were identical.

Unless stated otherwise in the text, 800 μ L of each complex solution was mixed in a 2 ml wide-opening HPLC sample vial and immediately placed in the autosampler tray. A 20 μ l sample was taken from the vial and injected into the column at set time intervals to obtain a representative chromatogram of the extent of the metathesis reaction. Before the first sample could be injected, however, the HPLC instrument had to load the required "Method", resulting in a slight delay of not more than fifteen seconds between starting the sequence and the first injection. Therefore, all chromatograms referred to

as $t = 0$, in fact represent the state of the metathesis system after a few seconds reaction time.

The data from each chromatogram, such as retention times and peak heights and areas could be copied and collected into an Excel spreadsheet for further analysis (see Section 2.3 for more detail).

2.2.3 LC-MS procedure

LC-MS analysis was carried out on a Waters 2695 Liquid Chromatograph–Waters API Quattro Micro 2690 Mass Spectrometer system operating in positive electrospray ionisation (ESI) mode. The same column and conditions used in the HPLC experiments (see Section 2.2.2 above) were utilised to separate the metal chelate complexes before introduction into the mass spectrometer. A trace of formic acid was added to the mobile phase to prevent sodium adduct formation.

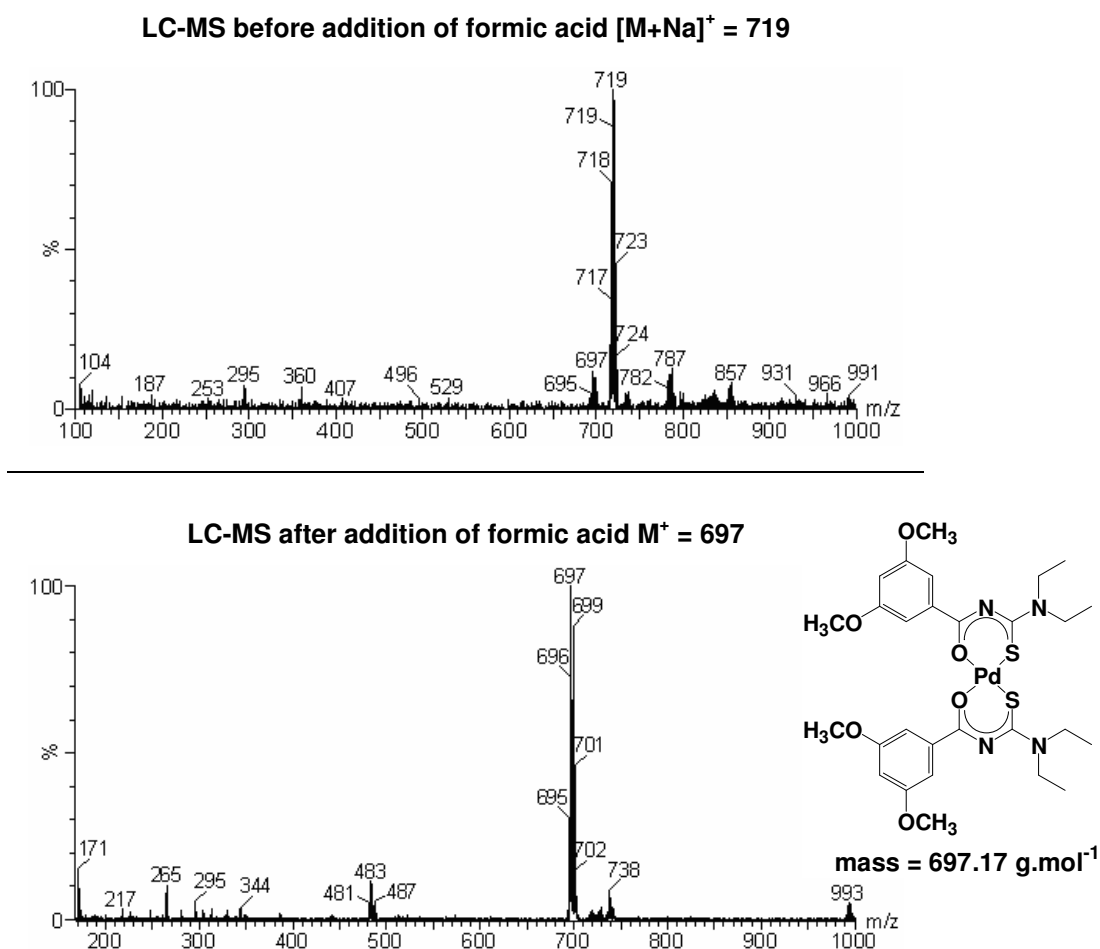


Figure 2.10. Mass spectra of the same compound before (above) and after addition of formic acid to the mobile phase. The inset shows the structure of the compound along with its mass.

2.3 Calculations

2.3.1 Calibration and calculation of concentrations and percentages

The example discussed here is of the calculations for the metathesis reaction between $cis\text{-Pd}(\text{L}^3\text{-S},\text{O})_2$ and $cis\text{-Pd}(\text{L}^4\text{-S},\text{O})_2$; however all experiments were processed in the same manner. As the experiments were designed to monitor the metathesis reaction over time, it was necessary to gather the data from each individual chromatogram into a single spreadsheet for each experiment. For both observation wavelengths (as noted in Section 2.2.2, chosen such that the parent complexes had almost equal absorbance), the raw data was copied from the Galaxie Chromatography Data System (version 1.8.508.1) and pasted directly into the spreadsheet. The Galaxie software could be configured to automatically calculate parameters such as the height, width, area and relative percentage of the peaks (Figure 2.11).

Run #	Time	Compound Name	Retention Time (mins)	Peak Height (mAU)	Peak Area (mAU.min)	Relative Peak Area (%)	Peak Width (mins)
1	0 mins	$\text{Pd}(\text{L}^4)_2$	3.82	519	74.5	46.60	0.22
		<i>mixed-lig</i>	4.59	3.8	0.7	0.46	0.26
		$\text{Pd}(\text{L}^3)_2$	5.01	506.6	84.6	52.94	0.26

Figure 2.11. Raw data from a single run, as copied from the Galaxie software.

As the mixed-ligand product could not be physically separated from the reaction mixture, it was not possible to obtain a calibration curve for the mixed-ligand complex. Therefore, the concentration of the mixed-ligand product had to be calculated from the decrease in the concentrations of the parent complexes.

To obtain the calibration graphs for each individual parent complex, different volumes of the solution of interest were injected into the HPLC system and the area of the peak recorded. As any sample is diluted immediately by the mobile phase upon injection, it is not the volume, but the number of μmoles injected that is being monitored.

In most experiments, 20 μl samples of the reaction mixture were injected, which corresponds to a 10 μl volume of each parent complex. (When solutions of higher

concentration were used, the injected volumes were reduced accordingly to prevent column and detector overload.) The peak area calibration graphs exhibited near perfect linearity up to an injection volume of 15 μl (Table 2.1 and Figure 2.12). Errors arising from the calibration graphs will be discussed in Section 2.3.2.

Table 2.1. Calibration data for a 400 μM solution of $\text{Pd}(\text{L}^4)_2$.

Volume Injected (μl)	Number of moles injected (μmol)	Peak Area	
		230 nm	291 nm
2	8.00E-04	24.5	26.1
3	1.20E-03	37.9	40.0
5	2.00E-03	67.8	70.7
7	2.80E-03	95.1	98.0
10	4.00E-03	136.8	137.7
15	6.00E-03	201.3	192.5

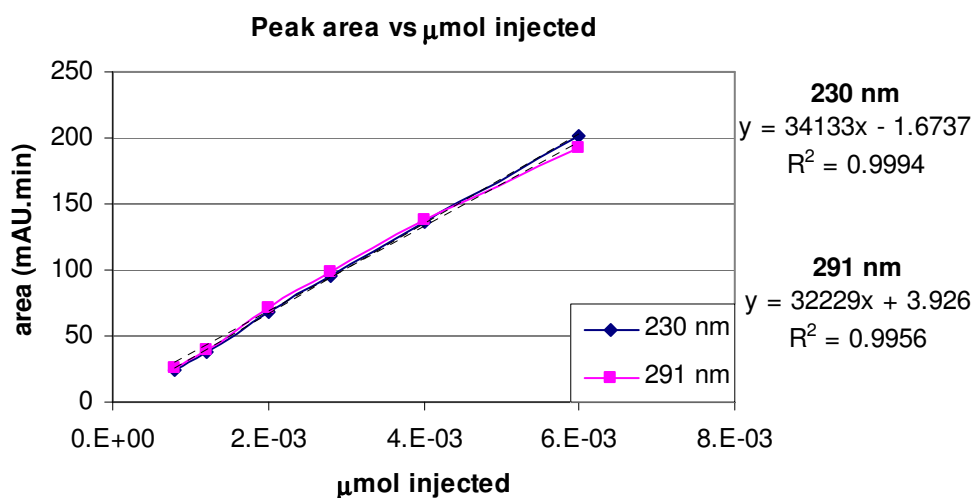


Figure 2.12. Calibration graph for a 400 μM solution of $\text{Pd}(\text{L}^4)_2$, showing the regression lines fitted to the data.

Scheme 2.3 on page 61, illustrates a summary of the calculations for the number of moles and concentration of the parent complexes, as well as the mixed-ligand product for the first 30 minutes of reaction between equal volumes of 400 μM $\text{cis-Pd}(\text{L}^3\text{-S},\text{O})_2$ and 400 μM $\text{cis-Pd}(\text{L}^4\text{-S},\text{O})_2$ solutions. The calculation procedures were identical for all time intervals recorded and for all experiments.

Scheme 2.3. Calculation of number of moles, concentration and percentage of each species present in solution.

Because

$$\text{Pd(L}^{\text{A}}\text{)}_2 + \text{Pd(L}^{\text{B}}\text{)}_2 \rightleftharpoons 2 \text{Pd(L}^{\text{A}}\text{)(L}^{\text{B}}\text{)}$$

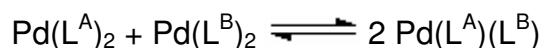
	Mixed-ligand Product				<i>2*ave(parents) initial</i>	<i>n product = 2*ave(parents)</i>	[product] μM	% product
	Pd(L ⁴) ₂		Pd(L ³) ₂					
<i>Initial Areas (mAU.min):</i>	147.95	141.00	149.75	144.60				
<i>Initial number of mol (μmol):</i>	4.10E-03	4.08E-03	4.16E-03	4.01E-03	8.18E-03			
	<i>from Pd(L⁴)₂</i>		<i>from Pd(L³)₂</i>					
<i>Time (hrs)</i>	<i>230 nm</i>	<i>291 nm</i>	<i>230 nm</i>	<i>291 nm</i>				
0	9.70E-06	1.16E-05	9.72E-06	1.11E-05	2.10E-05	1.05	0.26	
0.17	8.18E-05	5.78E-05	7.64E-05	7.21E-05	1.44E-04	7.20	1.76	
0.33	1.48E-04	9.83E-05	1.40E-04	1.28E-04	2.57E-04	12.86	3.15	
0.50	1.95E-04	1.39E-04	1.99E-04	1.61E-04	3.47E-04	17.35	4.24	

$$100 \times \frac{n_{\text{product}}}{(n_{\text{parent 1}} + n_{\text{parent 2}} + n_{\text{product}})}$$

Difference between initial number of moles (···) and number of moles after 10 minutes reaction time (← →).

	Parent - Pd(L ⁴) ₂						Parent - Pd(L ³) ₂					
	230 nm			291 nm			230 nm			291 nm		
<i>Gradient of Calibration Line</i>	36065			34585			35995			36048		
<i>Time (hrs)</i>	Area	μmol	[Pd(L ⁴) ₂] μM	Area	μmol	[Pd(L ⁴) ₂] μM	Area	μmol	[Pd(L ³) ₂] μM	Area	μmol	[Pd(L ³) ₂] μM
0	147.60	4.09E-03	204.63	140.60	4.07E-03	203.27	149.40	4.15E-03	207.53	144.20	4.00E-03	200.01
0.17	145.00	4.02E-03	201.03	139.00	4.02E-03	200.95	147.00	4.08E-03	204.20	142.00	3.94E-03	196.96
0.33	142.60	3.95E-03	197.70	137.60	3.98E-03	198.93	144.70	4.02E-03	201.00	140.00	3.88E-03	194.19
0.50	140.90	3.91E-03	195.34	136.20	3.94E-03	196.91	142.60	3.96E-03	198.08	138.80	3.85E-03	192.52

The first step in the calculation procedure was to obtain the initial areas and concentrations of the parent complexes from the calibration graphs. Next, for every time interval, the number of μmoles of each parent complex present in solution was subtracted from the corresponding initial number of μmoles before reaction. The average of these values for each of the two parent complexes at both wavelengths was multiplied by two to obtain the number of μmoles of the mixed-ligand product, as:



The number of μmoles was then divided by the volume of the injected sample (usually $20 \mu\text{l}$) to calculate the concentration of the complexes at each time interval.

The percentage mixed-ligand complex or parent complex present at any point in time could be obtained by dividing the number of moles of the complex of interest by the sum of the number of moles of all species present in solution (i.e. both parent complexes and mixed-ligand product):

$$\text{percentage complex present} = 100 \times \frac{n_{\text{complex}}}{(n_{\text{Pd}(\text{L}^{\text{A}})_2} + n_{\text{Pd}(\text{L}^{\text{B}})_2} + n_{\text{Pd}(\text{L}^{\text{A}})(\text{L}^{\text{B}})})}$$

As the HPLC system did not lend itself to ideal temperature control conditions, equilibrium constants were only obtained for $\pm 20 \text{ }^\circ\text{C}$. Equilibrium constants were calculated using the usual formula:

$$K = \frac{[\text{Pd}(\text{L}^{\text{A}})(\text{L}^{\text{B}})]^2}{[\text{Pd}(\text{L}^{\text{A}})_2][\text{Pd}(\text{L}^{\text{B}})_2]}$$

As with any refinement of data, the resulting values were not without error. Any number of errors may occur during the execution of an experiment and calibration graphs are seldom perfectly linear. The possible sources of error will be discussed in the following section (Section 2.3.2).

2.3.2 Possible sources of error

In many of the HPLC experiments discussed in the subsequent chapters, a large amount of data is summarised in a single graph. Because of this, error bars have been omitted from individual data points, as their presence is distracting and cumbersome when comparing the data. All experiments followed the same well defined procedures and protocols – both in the gathering of data and the calculations – to ensure reproducible results and minimise possible errors. All possible sources of error will be briefly be discussed and summarised in this section.

External environmental factors

When planning an experiment, one of the first factors that needs to be taken into account is the effect that the external environment has on the reactions – in other words, the environment outside of the reaction vessel. For example, temperature can affect the rates of most chemical reactions, including the equilibria between sample and stationary phase within the HPLC column. In an HPLC separation, elevated temperatures accelerate the repeated adsorption and desorption of the sample as it moves through the stationary phase, usually resulting in shorter retention times.^[50] As both the metathesis reaction as well as the method of observation could be affected by temperature fluctuations, the air-conditioned laboratory was maintained at a constant temperature of 20 °C (± 1).

Another factor which must be considered during the study of *cis*-bis(*N,N*-dialkyl-*N'*-aroyl(acyl)thioureato) metal(II) complexes is the effect of light. Under intense light, a photochemical *cis-trans* isomerisation of these complexes can take place.^[45] In the subdued ambient lighting conditions in the laboratory, such isomerisation is less likely, but to exclude any possible effect of light on the complexes, both the volumetric flasks and the HPLC vials were covered in aluminium foil.

Handling and preparation of samples

Trace amounts of impurity were found to affect the rate of the metathesis reaction (see Chapter 4 for more details), and therefore all volumetric flasks and HPLC vials were cleaned and dried thoroughly, as described in Section 2.2.1.

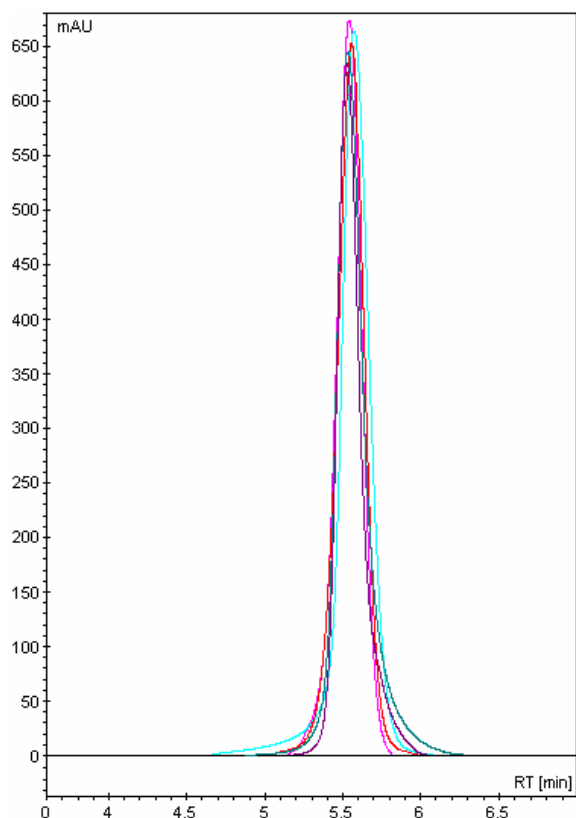


Figure 2.13. Overlaid chromatograms of 10 μl volumes of different 400 μM solutions of $\text{Pd}(\text{L}^3)_2$.

During the preparation of a sample, error could arise in the weighing of the compounds. However, this error is negligible, as can be seen in the adjacent Figure 2.13, which shows the overlaid chromatograms of a number of different 400 μM solutions of the same compound, $\text{cis-Pd}(\text{L}^3\text{-S},\text{O})_2$. Each individual solution was injected a number of times to ensure reproducibility (see Reproducibility on the following page). The heights and areas of the peaks are near identical, indicating that the masses of compound weighed in each case were almost equal. The mean area of the 10 μl volumes pictured is 141.18 mAU.min, with a standard deviation of 3.76 mAU.min. This corresponds to a relative error of 2.66 %

$$\left(\% \text{error} = 100 * \frac{\text{standard deviation}}{\text{mean value}} \right) \text{ between}$$

the different weighed samples.

Where possible, the mass of compound needed to produce solutions of higher or lower concentration was kept constant and the volume of solvent was varied. This convention was adopted in order to maximise the number of experiments which could be performed using a single batch of synthesised compound. In many cases, the data from a number of separate experiments was to be compared and, therefore, consistency in the compounds used was of paramount importance.

The samples of solution to be mixed in the HPLC vials were measured using micropipettes which were calibrated gravimetrically before each experiment. A small beaker containing distilled water was placed on the analytical balance and a set volume removed using the micropipette. The difference in the mass of the water and beaker before and after the sample was removed, combined with the density of water at the measured laboratory temperature, provided the volume of liquid sampled by the pipette.

Gravimetric calibration of micropipettes is more accurate than sole reliance on the marked volumes on the micropipette.

Reproducibility

As discussed above, utmost care was taken in assuring reproducibility in the preparation of the solutions. However, whenever an analytical instrument is used to perform measurements, the reproducibility of these measurements must be considered. To test this reproducibility, identical samples containing three different compounds, from a single HPLC vial were injected into the instrument in succession. The samples were all subject to the same environmental conditions and all eluted using the same “Method” (see Section 2.2.2 for more information on “Methods”). It was found that the maximum relative error on these replicates was approximately 0.71 % (see Appendix B1 for calculations).

While the error in the replicates was so small as to be negligible, it was not always possible to obtain perfectly reproducible experimental results as seen in Figure 2.14.

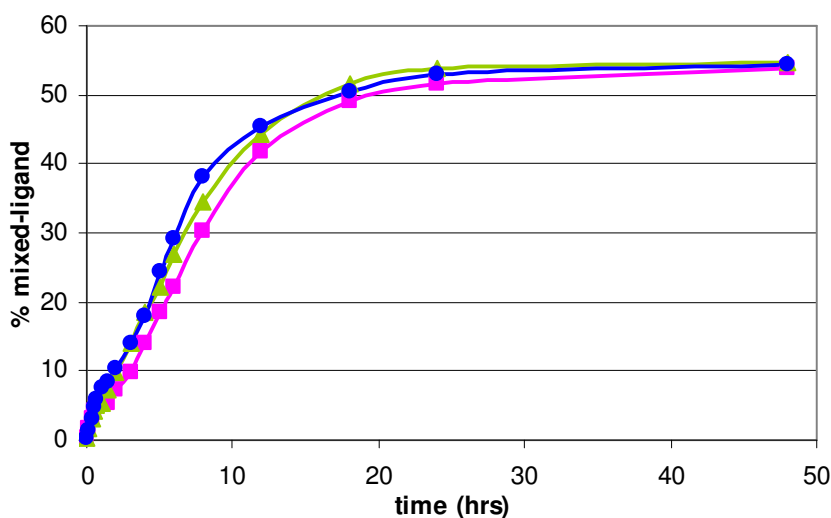


Figure 2.14. Data from the repeated experiments.

Figure 2.14 illustrates the results of the same experiment, performed on three separate occasions, using different freshly-prepared 400 μM $\text{cis-Pd}(\text{L}^3\text{-S},\text{O})_2$ and $\text{cis-Pd}(\text{L}^4\text{-S},\text{O})_2$ solutions. While all three experiments reached the same equilibrium distribution of complexes within the same amount of time (48 hours), the rates at which this equilibrium was achieved differ somewhat. Excluding the beginning of the reaction (where the concentration of the mixed-ligand product is very low) and the end of the

reaction (where there was no more than a 2 % relative percentage difference), the average relative difference between the repeated experiments was 11.16 %. This could perhaps be due, in part, to subtle differences in the ambient temperature or slight differences in the initial concentrations of the parent complexes on the three occasions, or the unavoidable presence of traces of impurities.

Calibration graphs

The calculation of the number of μmoles and concentration of a species from the raw data is entirely dependant upon the calibration graphs which, in the case of this project, relate the number of μmoles injected to the UV-Vis detector response (see Figure 2.12 on page 60).

The most noticeable area of concern was the fact the calibration graphs did not pass precisely through zero. At the wavelengths chosen, acetonitrile does not have any significant absorbance, therefore the instrument signal for a blank sample should be zero. However, when one calculates the 95 % confidence interval of the intercept (see Appendix C for the calculations), we see that zero falls within this interval and therefore, we can conclude that the intercept does not differ significantly from zero.^[94] As all the calibration points lie on the fitted straight line (the R^2 value is greater than 0.99), it was not necessary to calculate the hyperbolic confidence limits for the entire line.^[95]

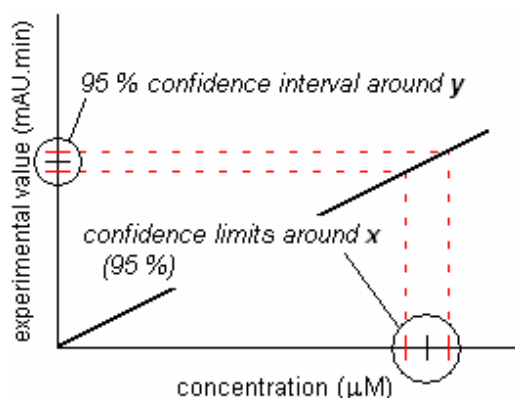


Figure 2.15. Confidence limits around a concentration value calculated from the calibration graph.

To estimate the error for a concentration calculated using the calibration graph, it is necessary to obtain the confidence limits around this concentration value. This can be done by merely substituting the upper and lower values of the 95 % confidence interval around the y -value (measured peak area) into the regression line equation. These two values give the upper and lower confidence limits around the x -value (calculated concentration) as can be seen in Figure 2.15 adjacent.

Using this method, it was found that the error on the calculated concentration values was not more than 0.46 % (see Appendix B2 for calculations).

Estimate of total error

Taking into account all possible sources of error, an estimation of the total error can be made by using the formula: $\text{total error} = \sqrt{a^2 + b^2 + c^2 + \dots}$ where each letter represents an error arising from an individual source. This yields a total maximum error of approximately 11.6 % for data points in the middle of the reaction (see Reproducibility on page 65). The error at the start of the reaction is a little higher due to the low concentration of product formed which results in relatively small differences in the area of the parent complex peaks in consecutive chromatograms. As the reaction nears equilibrium, the magnitude of the errors decreases (Figure 2.16).

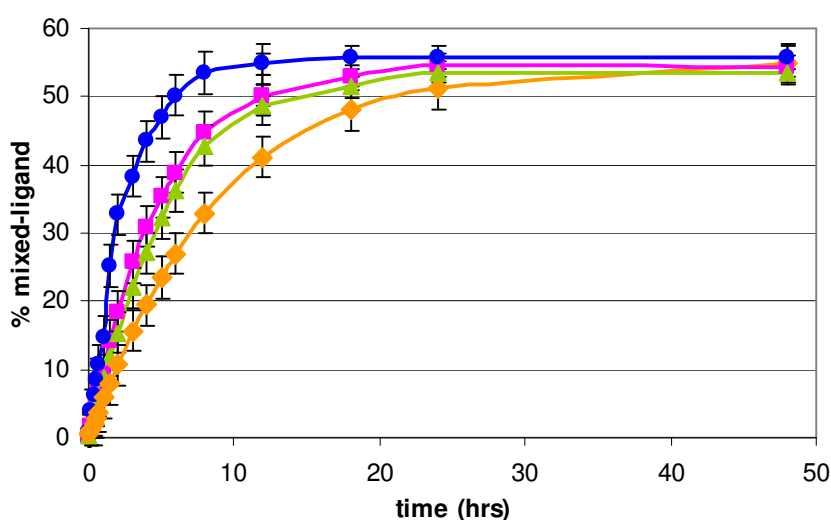


Figure 2.16. Representative data set, including error bars. The overall relative error is approximately 11.6 %.

Chapter 3

Conditions under which metathesis occurs

3.1 The identification of mixed-ligand complexes

When two Ni(II), Pd(II) or Pt(II) *cis*-bis-chelates of different *N,N*-dialkyl-*N'*-aroyl(acyl)thiourea ligands were mixed, a chelate metathesis reaction occurred, resulting in a mixed-ligand product (Figure 3.1).

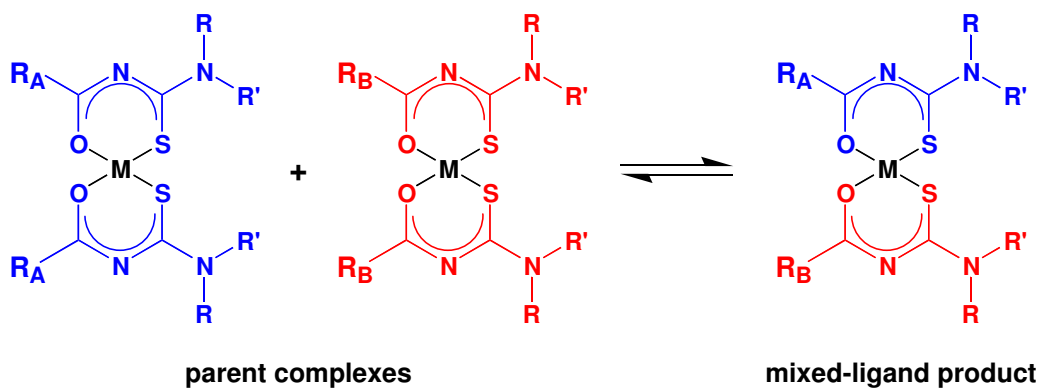


Figure 3.1. Metathesis reaction of interest, M = Ni(II) Pd(II) or Pt(II).

This metathesis reaction occurred in single metal as well as mixed-metal systems, reaching a steady state, or equilibrium, with both the parent complexes and the mixed-ligand product being observed. NMR spectra (Section 3.1.1) and liquid chromatograms/mass spectra (Section 3.1.2) revealed the presence of these mixed-ligand complexes in solution and as additional confirmation, a mixed-ligand complex was also observed in the solid state (Section 3.1.3).

All HPLC experiments discussed in this chapter were carried out at 20 °C, using freshly-dissolved solutions of the parent compounds (400 μ M in concentration, unless stated otherwise in the text). Please refer to Section 4.2.2 for more detail regarding the age of the solutions.

3.1.1 *Nuclear magnetic resonance spectra (NMR) of mixed-ligand complexes*

^1H NMR spectroscopy is a relatively fast technique and, though the complexes of interest all had similar structures, the differences in the electronic environment of the benzoyl protons were sufficient for these protons to resonate at distinct frequencies. Figure 3.2 shows NMR spectra for the metathesis reaction between *cis*-bis(*N,N*-diethyl-*N'*-4-methoxybenzoylthioureato)Ni(II) ($cis\text{-Ni}(\text{L}^2\text{-S},\text{O})_2$) and *cis*-bis(*N,N*-diethyl-*N'*-3,4,5-trimethoxybenzoylthioureato)Ni(II) ($cis\text{-Ni}(\text{L}^4\text{-S},\text{O})_2$) in

deuterated chloroform.* The aromatic region between 6.75 and 7.55 ppm has been magnified to show the singlet peaks of the L^4 ligand protons and the doublet peaks resulting from the L^2 ligand protons *ortho* to the methoxy substituent. The upper spectrum was recorded as soon as possible after the solutions of the two parent complexes had been mixed whilst the lower spectrum was recorded once the reaction had reached equilibrium.

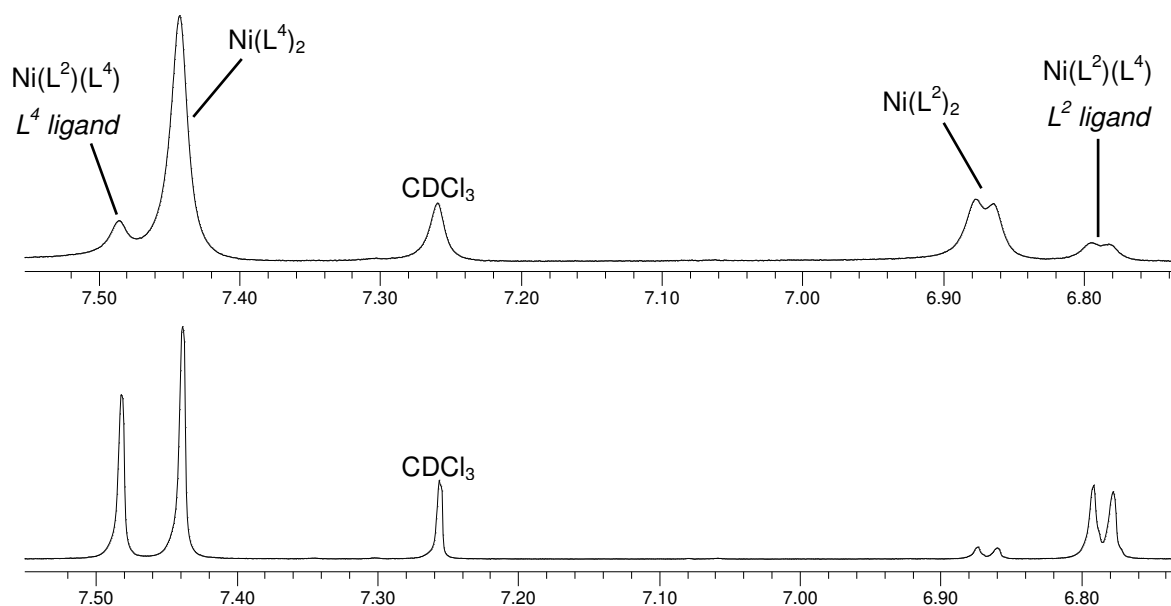


Figure 3.2. Aromatic region of ^1H NMR spectra for the reaction between $\text{Ni}(\text{L}^2)_2$ and $\text{Ni}(\text{L}^4)_2$, immediately after mixing (upper spectrum) and at equilibrium (lower spectrum).

The peaks corresponding to the mixed-ligand product increase in height while the peaks corresponding to the two parent complexes decrease in height as the reaction progresses, illustrating the formation of the mixed-ligand product.

Similar results were observed with Pd(II) complexes. Figure 3.3 on the following page illustrates a time-arrayed acquisition for the metathesis reaction between *cis*-Pd(L^3 -S,O) $_2$ and *cis*-Pd(L^4 -S,O) $_2$. The growth of the peaks corresponding to the mixed-ligand species over time is clearly visible.

* Many thanks to Ms J. M. McKenzie for the NMR experimental data.

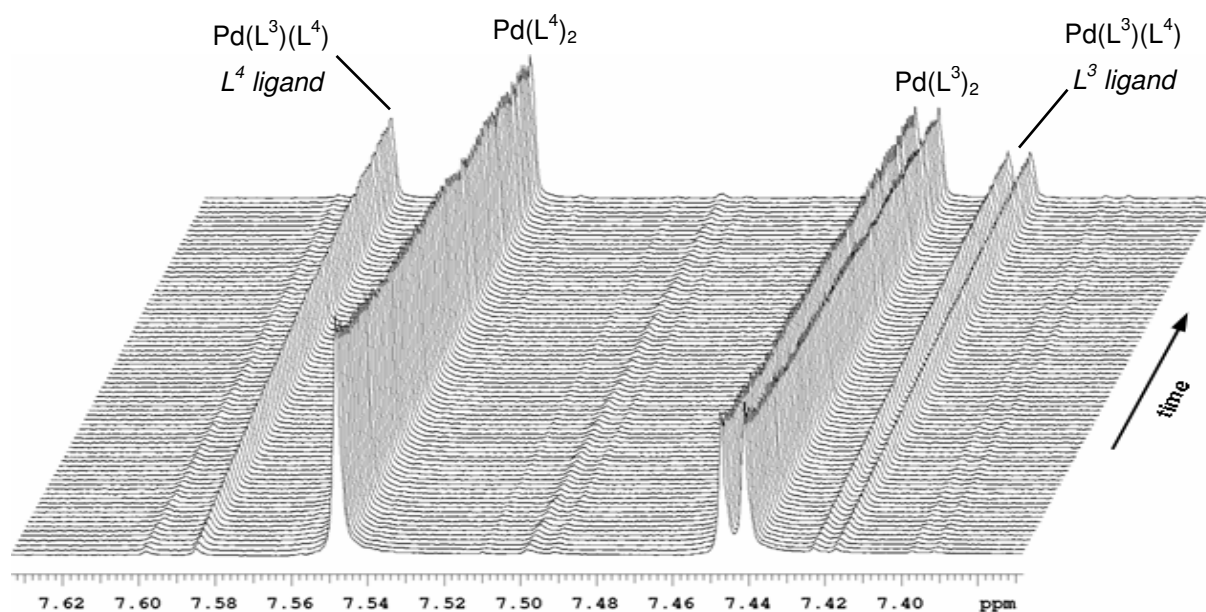


Figure 3.3. Time-arrayed acquisition for the metathesis reaction between $\text{Pd}(\text{L}^3)_2$ and $\text{Pd}(\text{L}^4)_2$.

Notwithstanding the straightforward identification of the mixed-ligand complexes from NMR spectra, this technique was not suitable for our study. The solubility of the complexes in the primary solvent of interest, acetonitrile, was not high enough to obtain sufficient concentrations for NMR measurements. For the micromolar concentration ranges under investigation, HPLC was a more efficient technique.

3.1.2 Liquid chromatographs-mass spectra (LC-MS) of mixed-ligand complexes

The metathesis reaction between two different $\text{cis-Pd}(\text{L-S},\text{O})_2$ or $\text{cis-Pt}(\text{L-S},\text{O})_2$ complexes produces three distinct peaks on the chromatogram corresponding to the two parent complexes, $\text{Pd}(\text{L}^A)_2$ and $\text{Pd}(\text{L}^B)_2$, and the mixed-ligand product $\text{Pd}(\text{L}^A)(\text{L}^B)$, which has a retention time (t_R) midway between the parent complexes (Figure 3.4).

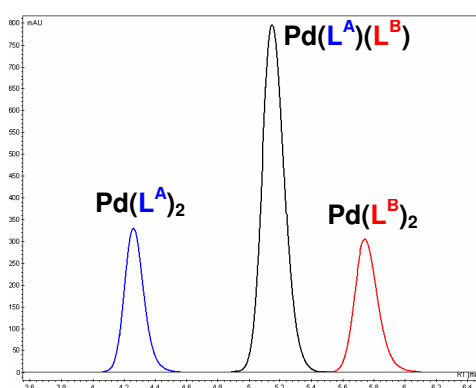


Figure 3.4. Representative chromatogram illustrating the three species present.

Ni(II) complexes of *N,N*-dialkyl-*N'*-acyl(aryl)thioureas, however, decompose whilst moving through the column, resulting in irreversibly retained compounds which make HPLC analysis impossible.^[96]

To confirm the identities of the peaks observed in the chromatograms, electrospray LC-MS analysis was employed. The Pd(II) and Pt(II) chelates were instantly recognisable in the mass spectra from their distinct isotope distribution patterns and, in each case, the molecular ion in the mass spectrum corresponded exactly to the calculated mass. Figure 3.5 illustrates the isotope distribution patterns for Pd and Pt, whilst Figure 3.6 shows the mass spectrum of a mixed-ligand Pt(II) complex.

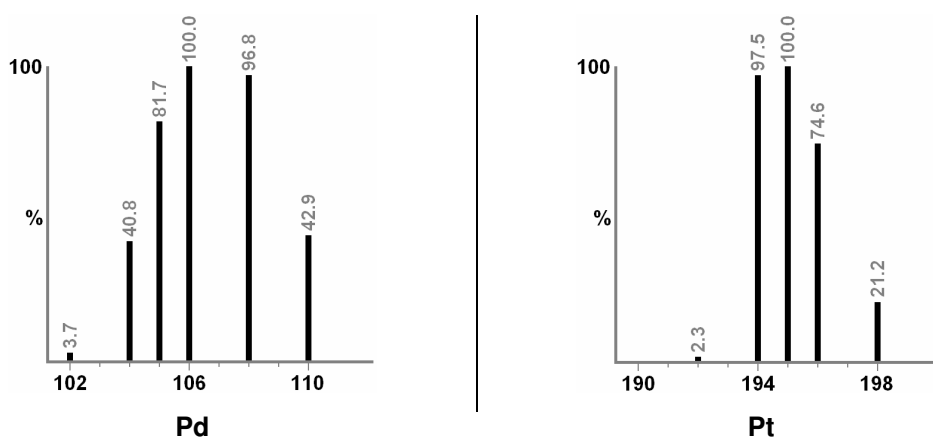


Figure 3.5. Isotope distribution patterns for Pd and Pt.^[97]

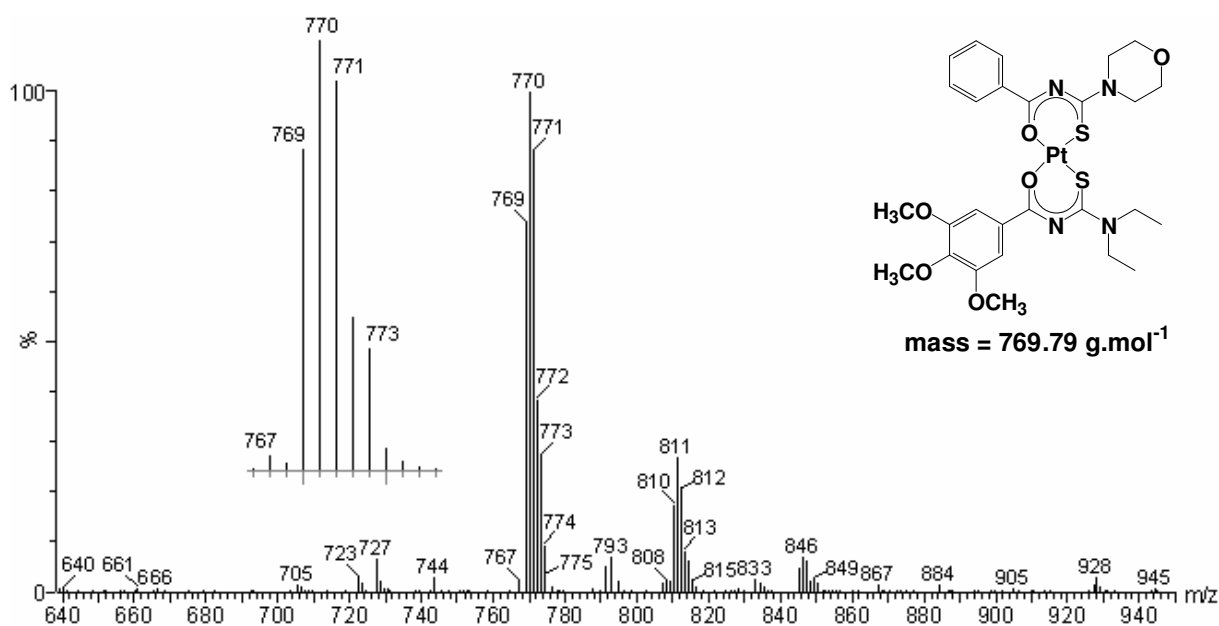


Figure 3.6. Mass spectrum of mixed-ligand Pt(L⁴)(L⁸) complex showing expansion of the isotope pattern. (The signal at *m/z* 811 corresponds to a solvent adduct [M+CH₃CN]⁺. This could either be present in the original solution [see Scheme 3.1], or formed within the MS ion source.)

In the molecular ion of each complex, there are a number of smaller peaks not present in the metal isotope pattern (Figure 3.5) which can be attributed to the isotope contributions of the elements present in the organic ligand of the complex – carbon, hydrogen, nitrogen, oxygen and sulphur. There are also a number of additional metal-containing signals, apart from the molecular ion, in the mass spectra which are likely due to products formed within the ion source of the instrument.

3.1.3 Crystal structure of the mixed-ligand *cis*-Pd(L³-S,O)(L⁴-S,O) complex

Good fortune permitted that a suitable crystal grew in a sealed, refrigerated NMR tube.* The structure was obtained using the procedure described in Section 2.1.2.1.

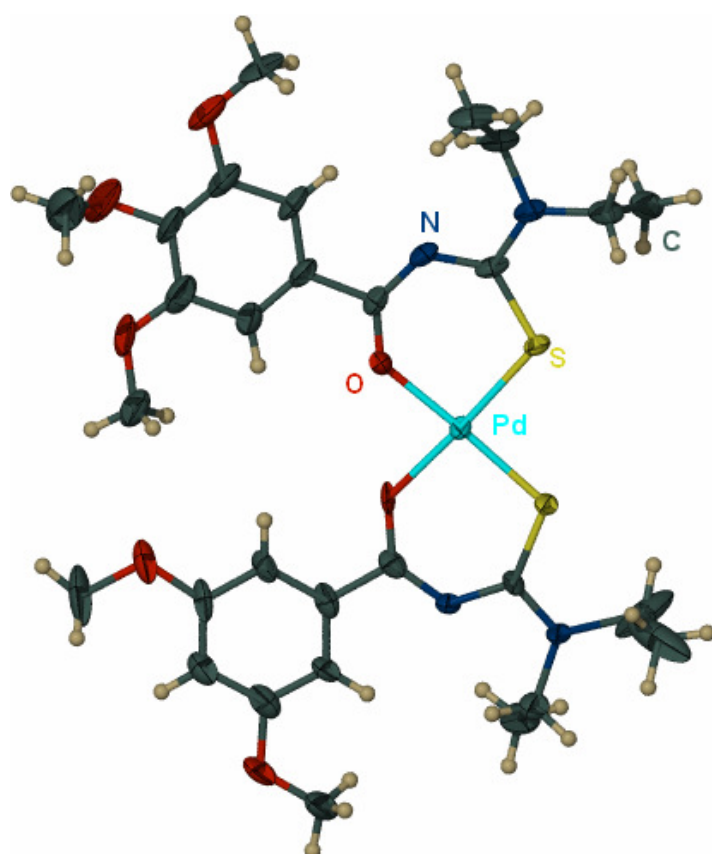


Figure 3.7. Crystal structure of the mixed-ligand Pd(L³)(L⁴) complex.

The bond lengths and angles in the mixed-ligand complex pictured here adjacent (Figure 3.7) are comparable to similar *cis*-bis(*N,N*-dialkyl-*N'*-aroylthioureato)Pd(II) complexes.

However, as this structure was fairly disordered, with an R factor of 0.1501, the modelling of the structure was not sufficient to permit a direct comparison between the bond lengths and angles of the mixed-ligand complex and those of the corresponding parent complexes.

* Many thanks to J. M. McKenzie for the raw crystal structure data.

3.2 Chelate metathesis in Pd(II), Pt(II) and mixed-metal systems

As was mentioned previously, it was found that chelate metathesis was a general phenomenon for all combinations of two Pd(II) or Pt(II) complexes of different ligands in both single metal and mixed-metal systems.

The metathesis reaction occurred over a wide range of concentrations from the millimolar concentration range, down to very dilute 1 μM solutions (Figure 3.8). Though the peaks in the chromatogram of this low concentration reaction are small (between 1.15 and 7.3 mAU in height) and some impurities and baseline noise are evident, the three peaks, corresponding to the two parent complexes and the mixed-ligand product, are still clearly visible.

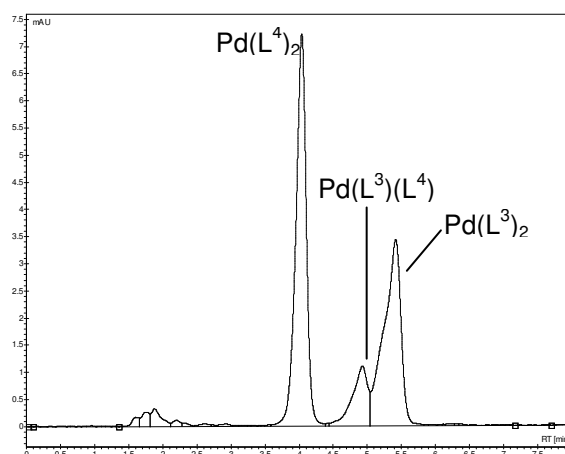


Figure 3.8. Chromatogram of metathesis reaction in a mixture of equal volumes of 1 μM $\text{Pd}(\text{L}^3)_2$ and 1 μM $\text{Pd}(\text{L}^4)_2$ solutions.

A small percentage of mixed-ligand complex is visible even at these very low concentrations.

After a period of time, an equilibrium, or steady state, between the two parent complexes and the mixed-ligand product was reached in all systems. The equilibrium distribution and the time required to reach this equilibrium were dependant upon both the central metal ion and the structure of the chelated ligands. Predictably, the rate of reaction differed significantly between the single metal Pd(II) systems and systems containing Pt(II) – either single-metal or mixed-metal Pd(II)-Pt(II) systems.

3.2.1 Chelate metathesis in *cis*-Pd(L-S,O)₂ complexes

The metathesis reaction between two different *cis*-Pd(L-S,O)₂ complexes reached equilibrium, in most cases, within two days with no detectable complex decomposition (Figure 3.9). (More detail on the Pd(II) systems may be found in Section 3.4.)

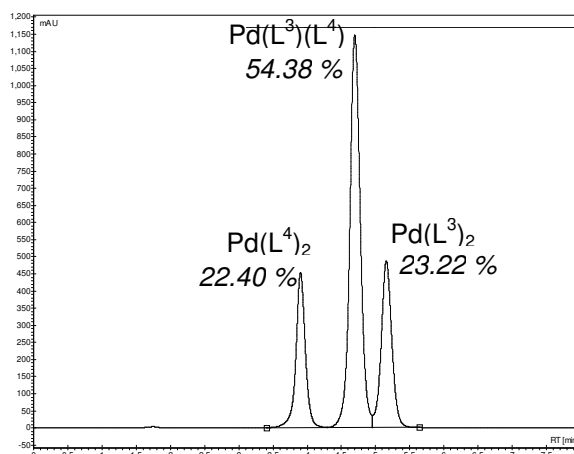


Figure 3.9. Equilibrium chromatogram of metathesis reaction between Pd(L³)₂ and Pd(L⁴)₂ after two days. No decomposition of the complexes is evident. The equilibrium distribution is included on the chromatogram with each percentage value next to the appropriate peak.

Decomposition did, however occur when solutions of Pd(II) complexes were left to stand for a number of months (Figure 3.10). However, this decomposition of the complexes accounts for less than 6 % of the total peak area.

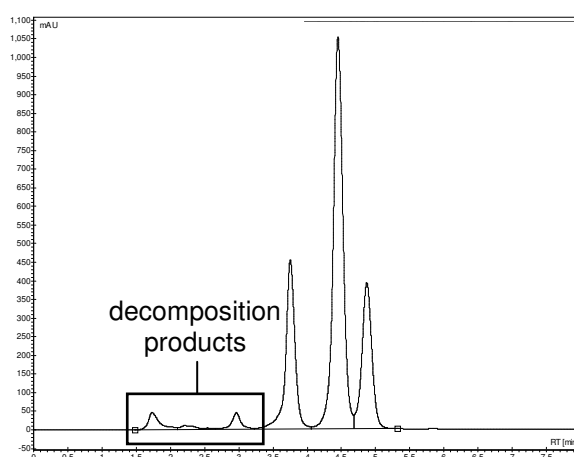


Figure 3.10. Chromatogram of solution of Pd(L³)₂ and Pd(L⁴)₂ after 3 months. Some decomposition of the complexes is evident (1.5 – 3.3 mins t_R).

Some of these decomposition products could be identified using LC-MS and corresponded to unbound ligand (1.8 minutes t_R) and a metal containing species with a mass corresponding to a partially solvated complex (*circa* 3 minutes t_R) of the form shown in Figure 3.11 adjacent.

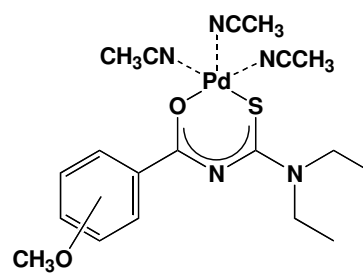


Figure 3.11. Proposed solvated Pd(L)(CH₃CN)₃ complex.

Chelate metathesis also occurred between three different *cis*-Pd(L-S,O)₂ complexes in solution. Figure 3.12 below illustrates the metathesis reaction between *cis*-Pd(L²-S,O)₂, *cis*-Pd(L³-S,O)₂ and *cis*-Pd(L⁴-S,O)₂ in acetonitrile. All three parent complexes as well as the three mixed-ligand products are observed in solution.

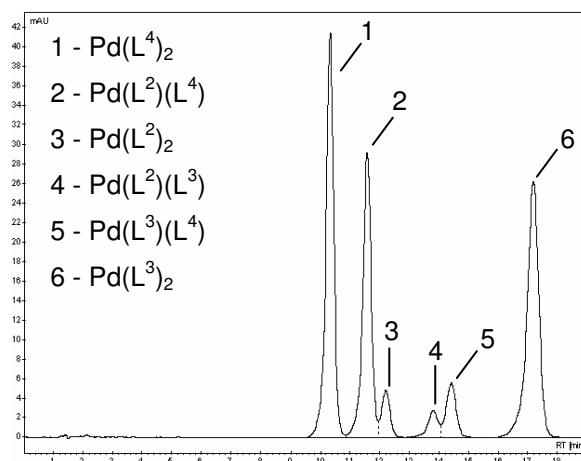


Figure 3.12. Metathesis reaction between three complexes: Pd(L²)₂, Pd(L³)₂ and Pd(L⁴)₂.

Please note: the heights and areas of the peaks in this chromatogram are not proportional to the concentration of each species in solution owing to differences in UV absorbance of the complexes.

3.2.2 Chelate metathesis in *cis*-Pt(L-S,O)₂ complexes

Systems containing Pt(II) complexes required around three months to reach equilibrium, as opposed to around two days for the corresponding Pd(II) systems. After three weeks, the complexes had already begun to undergo some decomposition. (As a result of this decomposition, it was not possible to determine the relative percentage of each complex present at equilibrium.) Additional peaks began to appear on the chromatogram between 1.5 minutes and 2.5 minutes retention time, as well as between the parent complex and mixed-ligand product at 3.15 minutes (Figure 3.13). The decomposition of the complexes accounted for around 8% of the total peak area.

Similar results were observed in other combinations of Pt(II) complexes. Although an LC-MS analysis of these solutions was undertaken, it was not possible to positively identify any of the decomposition products.

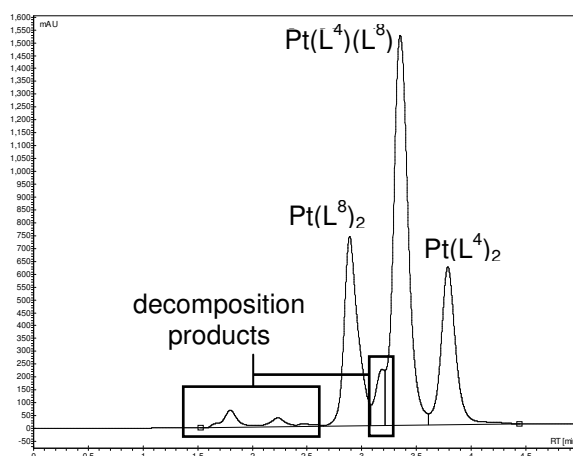


Figure 3.13. Equilibrium chromatogram of metathesis reaction between $\text{Pt}(\text{L}^4)_2$ and $\text{Pt}(\text{L}^8)_2$ after three months. Some decomposition of the complexes is evident.

3.2.3 Chelate metathesis in mixed-metal Pd(II)-Pt(II) systems

In the mixed-metal Pd(II)-Pt(II) systems, it is possible to form six different complexes (highlighted for clarity):



At equilibrium, all six possible complexes are visible on the chromatogram along with some decomposition products due to the fact that, as in the case of the single-metal Pt(II) systems, this system took three months to establish an equilibrium (Figure 3.14 on the following page). (Due to decomposition of the complexes, it was not possible to accurately determine the relative percentage of each complex present at equilibrium.) Notwithstanding the fact that the Pd(II) and Pt(II) compounds of the same ligand are isostructural, it is possible to achieve a separation of these compounds even under 100 % acetonitrile elution conditions.^[46] (Better separations are possible with a higher percentage of milli-Q (MQ) water in the mobile phase, but at the expense of elution time.) Interestingly, the Pt(II) complexes always elute ahead of their Pd(II) counterparts.^[46]

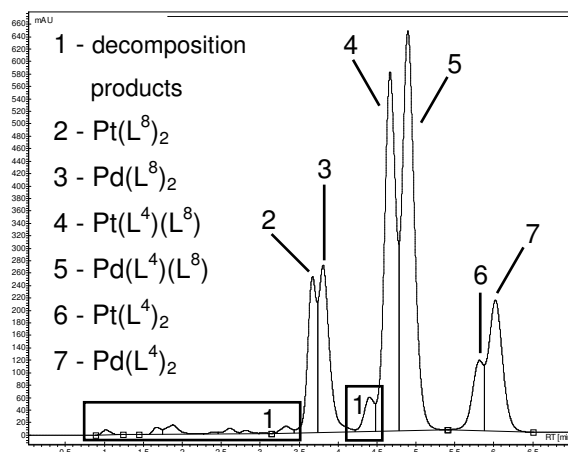


Figure 3.14. Equilibrium chromatogram of metathesis reaction between $\text{Pd}(\text{L}^4)_2$ and $\text{Pt}(\text{L}^8)_2$ after three months. Some decomposition of the complexes is evident.

The reaction between $\text{Pd}(\text{L}^A)_2$ and $\text{Pt}(\text{L}^B)_2$ proceeds in two parts. The mixed-ligand product for each metal, $\text{Pd}(\text{L}^A)(\text{L}^B)$ and $\text{Pt}(\text{L}^A)(\text{L}^B)$ – which requires exchange of one ligand – forms first (Figure 3.15). The complexes in which both ligands have been exchanged, $\text{Pd}(\text{L}^B)_2$ and $\text{Pt}(\text{L}^A)_2$ (numbers 3 and 6 in Figure 3.14 above), only began to appear on the chromatogram after some ten weeks.

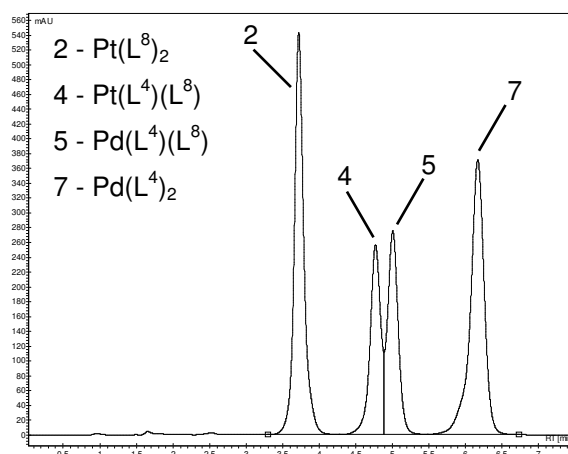


Figure 3.15. Chromatogram of metathesis reaction between $\text{Pd}(\text{L}^4)_2$ and $\text{Pt}(\text{L}^8)_2$ after 3 weeks. Only the mixed-ligand product for each metal and the Pd(II) and Pt(II) parent complexes, are observed.

Although chelate metathesis is a general phenomenon for Ni(II), Pd(II) and Pt(II) complexes of N,N-dialkyl-N'-acyl(aryl)thioureas, all further experiments focused on the Pd(II) complexes, as the timescale for the Pt(II) complexes to reach equilibrium was too long and the Ni(II) complexes were not suitable for study using HPLC.

3.3 Attempted synthesis of a mixed-ligand complex

Isolating the mixed-ligand complex from the reaction mixture would have been especially beneficial as calibration graphs could have been obtained and the behaviour of this complex in solution, with its possible disproportionation into its two corresponding parent complexes, could have been monitored. Unfortunately, none of the attempts to synthesise or isolate a mixed-ligand complex were successful.

Three different paths were investigated in the endeavour to obtain a mixed-ligand *cis*-Pd(L³-S,O)(L⁴-S,O) complex. The first method involved refluxing a mixture of the two parent complexes in acetonitrile for one week in the hope of driving the equilibrium far to the right (see Figure 3.1 on page 69) and producing mainly the mixed-ligand product. The system in question took two days at room temperature to reach equilibrium. However, after a full week at reflux, less mixed-ligand complex, as well as some complex decomposition, was observed in the reflux sample when compared to the room temperature sample (Figure 3.16), rendering this method unsuccessful.

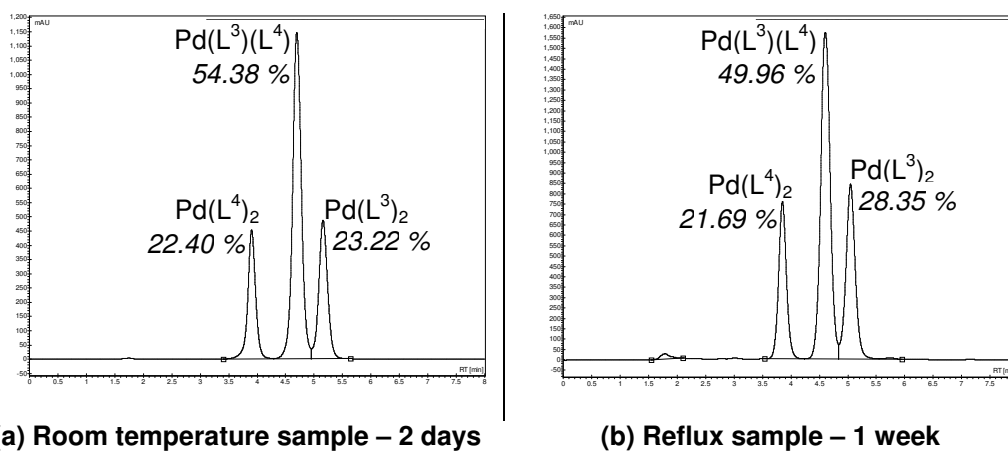


Figure 3.16. Chromatograms of reaction between Pd(L³)₂ and Pd(L⁴)₂ at (a) room temperature (equilibrium) or (b) under reflux.

With the failure of the reflux method, an attempt was made to synthesise a mixed-ligand complex from the starting materials. There are two available methods to synthesise *N,N*-dialkyl-*N'*-aroyl(acyl)thiourea bis-complexes. The first synthetic method is the “hot” method described in Section 2.1.2 on page 41, but in this case, carried out using a 50/50 mole ratio of the two ligands HL³ and HL⁴. The second is a “cold” method, carried out at room temperature without addition of heat, adapted from the method described by Mautjana *et al.* (see Appendix D1).^[46]

In both the “hot” and “cold” methods, the crude product was not recrystallised for fear of the potential mixed-ligand complex undergoing redistribution. However, neither the “hot” nor the “cold” method produced mixed-ligand compound exclusively. Instead, when the precipitates were dissolved in acetonitrile and immediately injected into the HPLC system, the chromatograms revealed a mixture of the three complexes – *cis*-Pd(L³-S,O)₂, *cis*-Pd(L⁴-S,O)₂ and *cis*-Pd(L³-S,O)(L⁴-S,O) – as well as traces of unbound ligand and the partially-solvated complexes proposed in Figure 3.11 (page 76), and a number of other unidentifiable species (Figure 3.17). While the “hot” synthetic method produced similar results to the reflux method discussed above (Figure 3.16b), the “cold” synthetic method did in fact produce around 7 % more mixed-ligand complex than the room temperature metathesis reaction. Recrystallisation did not result in a higher relative yield of mixed-ligand complex, though the polarity of the solvent did affect the relative distributions of the three complexes. The chromatograms and relative distributions of the recrystallised mixture synthesised *via* the “hot” method may be found in Appendix D2. The data from a similar experiment performed using HL¹/HL² may be found in Appendix D3.

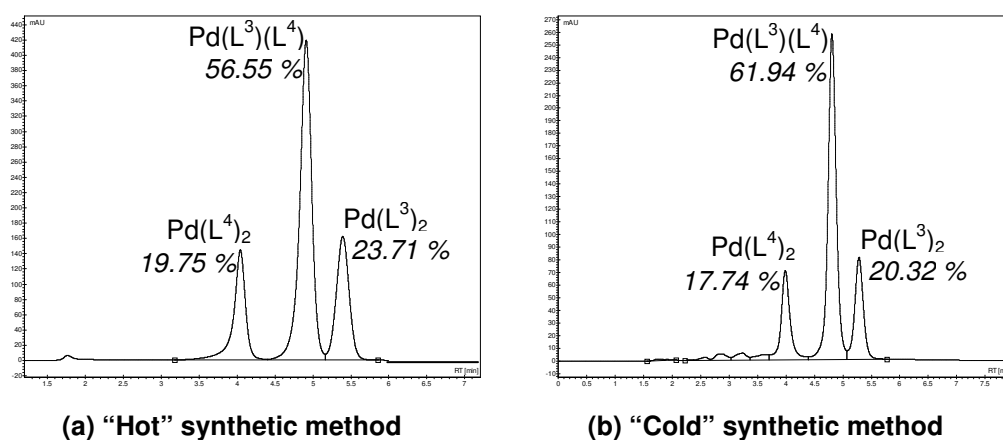


Figure 3.17. The distribution of complexes from the two synthetic methods.

In lieu of the lack of success in the synthesis of a mixed-ligand complex, preparative chromatography may offer an alternative route in isolating the product complex from the reaction mixture. A large-bore reversed-phase column and fraction collector would be necessary to isolate the mixed-ligand complexes, as *N,N*-dialkyl-*N'*-aroyl(acyl)thiourea bis-complexes decompose on-column when in contact with the normal-phase silica gel typically utilised in more traditional preparative chromatography.^[93] Unfortunately time did not permit an in-depth investigation into preparative chromatography as a means to separate the three complexes. This technique should be considered for future studies.

3.4 The effect of ligand structure on metathesis

As was mentioned previously, the equilibrium distribution and the time required to reach this equilibrium in the chelate metathesis reactions under investigation were dependant upon the structure of the chelated ligands.

Due to the fact that the Pt(II) complexes required months to reach a steady state and the Ni(II) complexes were unsuitable for study using HPLC, these experiments focused on the Pd(II) complexes. All experiments discussed in this section were performed using equal volumes of 400 μ M solutions of the Pd(II) complexes of interest. A sample was injected into the HPLC system immediately after mixing and then at 24-hour intervals to monitor the extent of the chelate metathesis reaction.

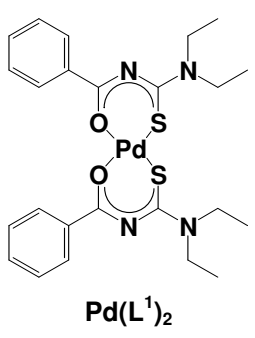
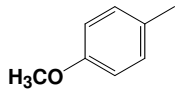
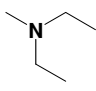
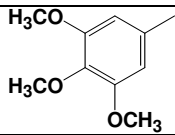
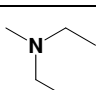
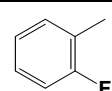
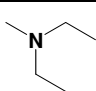
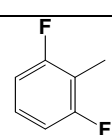
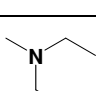
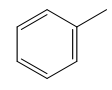
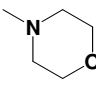
3.4.1 Effect of substitution on the benzoyl ring of aroylthiourea Pd(II) complexes on the extent and rate of the metathesis reaction

The first set of experiments investigated the effect of substitution on the benzoyl ring of the aforementioned aroyl-complexes. A solution of *cis*-Pd(L¹-S,O)₂ was mixed with, respectively, solutions of *cis*-Pd(L²-S,O)₂, *cis*-Pd(L⁴-S,O)₂, *cis*-Pd(L⁵-S,O)₂ and *cis*-Pd(L⁶-S,O)₂, as well as with *cis*-Pd(L⁸-S,O)₂. The combinations, along with the structures of the relevant complexes are summarised in Table 3.1 on the following page.

An attempt was made to include *cis*-Pd(L⁷-S,O)₂ – the nitro-substituted benzoyl complex – but unfortunately all chromatograms of this complex contained multiple peaks and were not reproducible. This is most likely due to the decomposition of *cis*-Pd(L⁷-S,O)₂ in solution (see Section 2.1.2.1).

The detection wavelengths for each combination were chosen so that the two parent complexes had near equal absorption (see Section 2.2.2). A full list of wavelengths for all the combinations of *cis*-Pd(L-S,O)₂ complexes studied can be found in Appendix E.

Table 3.1. Substituted-benzoyl complexes mixed with $\text{Pd}(\text{L}^1)_2$.

 $\text{Pd}(\text{L}^1)_2$	Complex Abbreviation	Benzoyl Substituent	Thioamine Substituent	Reference Number (see Figure 3.18)
	$\text{cis-Pd}(\text{L}^2\text{-S},\text{O})_2$			# 2
	$\text{cis-Pd}(\text{L}^4\text{-S},\text{O})_2$			# 4
	$\text{cis-Pd}(\text{L}^5\text{-S},\text{O})_2$			# 5
	$\text{cis-Pd}(\text{L}^6\text{-S},\text{O})_2$			# 6
	$\text{cis-Pd}(\text{L}^8\text{-S},\text{O})_2$			# 8

In all cases the metathesis reaction took between two and three days to reach equilibrium, the only exception being the reaction between $\text{cis-Pd}(\text{L}^1\text{-S},\text{O})_2$ and $\text{cis-Pd}(\text{L}^6\text{-S},\text{O})_2$, which required about three weeks to reach equilibrium. The equilibrium constants for each combination differed significantly and are arranged from smallest to largest in Figure 3.18 below.

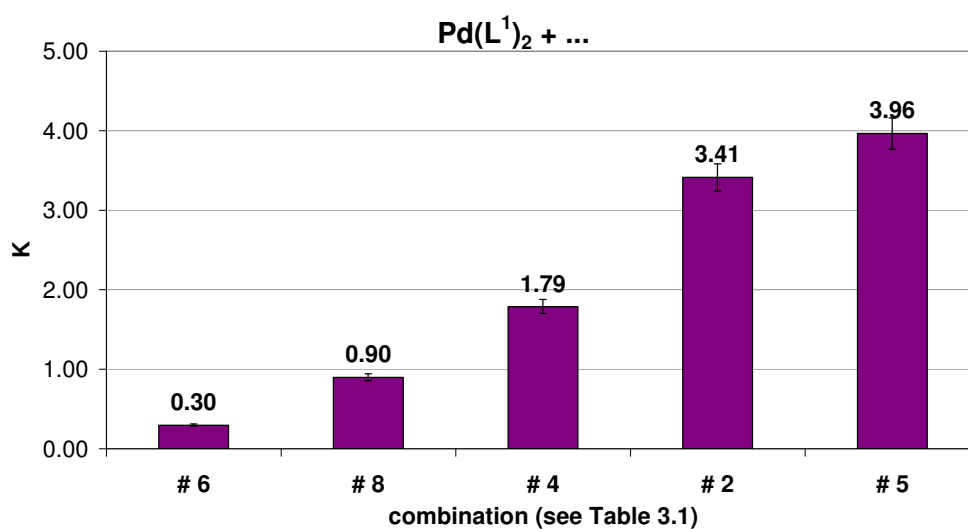


Figure 3.18. Equilibrium constants for various combinations of $\text{Pd}(\text{L}^1)_2$ with other substituted benzoyl complexes.

The error in the equilibrium constant calculation was estimated at 5%. This was determined using the mean value and standard deviation of thirty experiments carried out using $cis\text{-Pd}(\text{L}^3\text{-S},\text{O})_2$ and $cis\text{-Pd}(\text{L}^4\text{-S},\text{O})_2$.

3.4.2 Investigation into the extent and rate of reaction for a combinations of a variety of $cis\text{-Pd}(\text{L-S},\text{O})_2$ complexes

These experiments were continued using many different combinations of the $cis\text{-Pd}(\text{L-S},\text{O})_2$ complexes available. The results are summarised below in Figure 3.19. The results from the previous set of experiments (Figure 3.18) have also been included to give a more complete picture.

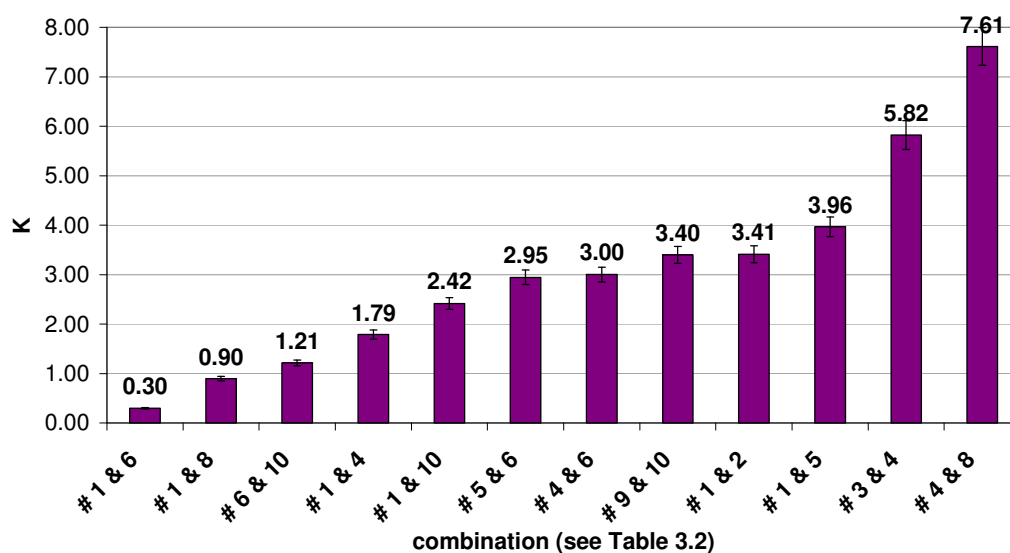


Figure 3.19. Equilibrium constants for various combinations of $\text{Pd}(\text{L})_2$ complexes.

Table 3.2. Reference numbers for the combinations of complexes in Figure 3.19.

Please refer to page 51 for the structures of these compounds.

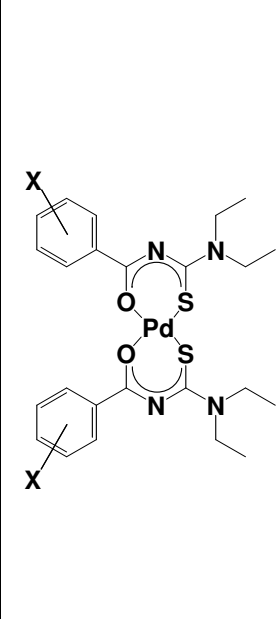
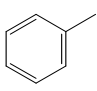
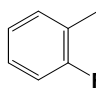
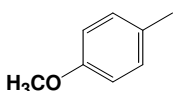
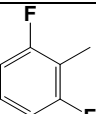
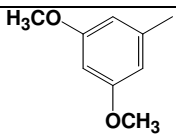
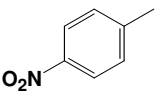
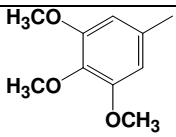
Reference Number	Complex	Reference Number	Complex
# 1	$cis\text{-Pd}(\text{L}^1\text{-S},\text{O})_2$	# 6	$cis\text{-Pd}(\text{L}^6\text{-S},\text{O})_2$
# 2	$cis\text{-Pd}(\text{L}^2\text{-S},\text{O})_2$	# 7	$cis\text{-Pd}(\text{L}^7\text{-S},\text{O})_2$
# 3	$cis\text{-Pd}(\text{L}^3\text{-S},\text{O})_2$	# 8	$cis\text{-Pd}(\text{L}^8\text{-S},\text{O})_2$
# 4	$cis\text{-Pd}(\text{L}^4\text{-S},\text{O})_2$	# 9	$cis\text{-Pd}(\text{L}^9\text{-S},\text{O})_2$
# 5	$cis\text{-Pd}(\text{L}^5\text{-S},\text{O})_2$	# 10	$cis\text{-Pd}(\text{L}^{10}\text{-S},\text{O})_2$

All combinations of the aroyl complexes (with the exception of $cis\text{-Pd}(\text{L}^1\text{-S},\text{O})_2$ and $cis\text{-Pd}(\text{L}^6\text{-S},\text{O})_2$) took between two and four days to reach equilibrium. Combinations which included acyl complexes (numbers 9 and 10) required between one and two weeks to attain equilibrium.

It is clear that the structure of the complexed ligands affects both the extent to which chelate metathesis happens and the rate of the reaction. The fact that the acyl complexes required longer to reach equilibrium suggests that the delocalisation of electrons in the aroyl complexes might play a role in the rate of the reaction by stabilising any potential negative charge on uncomplexed donor atoms during the exchange of ligands. This stabilising effect does not, however, necessarily allow more mixed-ligand product to form – for example, in the reaction between the aroyl complexes $cis\text{-Pd}(\text{L}^1\text{-S},\text{O})_2$ and $cis\text{-Pd}(\text{L}^8\text{-S},\text{O})_2$, only around 16 % of the each parent complex underwent metathesis.

Intuitively, one would tend to assume that the electron-donating or -withdrawing nature of the substituents on the benzoyl rings (Table 3.3) would affect the extent of the metathesis reaction, with electron-donating groups strengthening the Pd-O bond, making metathesis less likely and electron-withdrawing groups having the opposite effect. This, however, proved not to be the case.

Table 3.3 Substituents on the benzoyl ring of the $cis\text{-bis}(N,N\text{-diethyl-}N'\text{-aroyl-thioureato})\text{Pd}(\text{II})$ complexes.

	Substituent	Effect	Substituent	Effect	
		-			electron-withdrawing, -I
		electron-donating, -I, +R			electron-withdrawing, -I
		electron-donating, -I, +R			electron-withdrawing, -I, -R
		electron-donating, -I, +R			

Depending on their structure, the substituents on the benzoyl ring have either an inductive effect (+I or -I) or a resonance effect (+R or -R) as seen in Table 3.3. An inductive effect is the donation or withdrawal of electrons through a σ -bond due to either the electronegativity of the substituent or the polarity of the bonds in the substituent. Resonance effects occur when a p-orbital on the aromatic ring overlaps with a p-orbital on the substituent and electrons are donated or withdrawn through this π -bond.^[98]

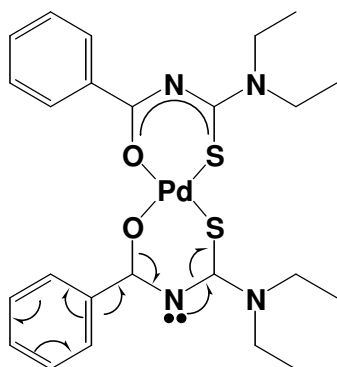


Figure 3.20. Delocalisation through the $\text{Pd}(\text{L}_2)_2$ complexes. Substituents on the benzoyl-ring have been omitted for clarity.

However, due to extensive delocalisation throughout the aroyl complexes (Figure 3.20), it was not possible to accurately predict the effect of the ring-substituents on the electron distribution over the coordinating atoms and the metal centre.

Electron density in the coordination sphere of the metal determines the strength of the metal-oxygen and metal-sulphur bonds and it is possible that the strength of these bonds could determine both the extent and rate of metathesis for these complexes. The trends observed in these experiments will, however, require further study.

Due to their high equilibrium constant ($K = 5.82 \pm 0.27$) and the reasonable time of two days needed to reach equilibrium, the combination of $\text{cis-Pd}(\text{L}^3\text{-S},\text{O})_2$ and $\text{cis-Pd}(\text{L}^4\text{-S},\text{O})_2$ was chosen for all subsequent experiments (Figure 3.21). Though $\text{cis-Pd}(\text{L}^4\text{-S},\text{O})_2$ and $\text{cis-Pd}(\text{L}^8\text{-S},\text{O})_2$ gave a greater percentage mixed-ligand complex, the three days needed to reach equilibrium made this combination unattractive.

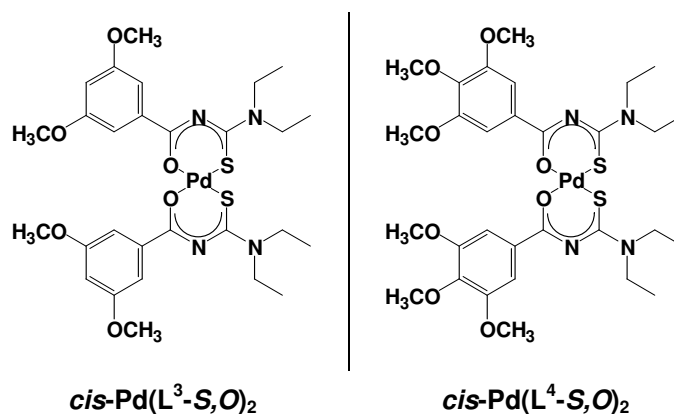
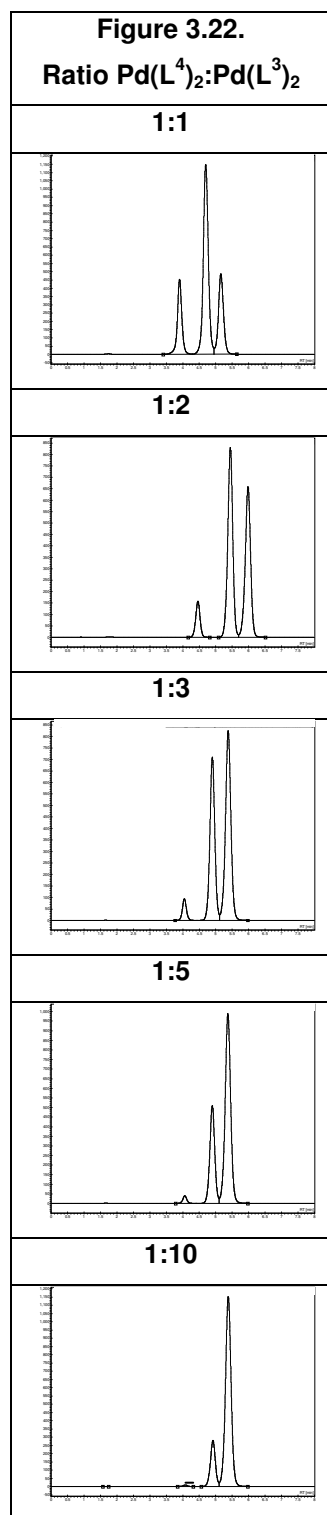


Figure 3.21. Complexes used in all subsequent experiments.

3.5 Varying the ratio of the two complexes in solution

Varying the ratio of the two reacting complexes in solution can offer insight into the relative stability of the complexes in solution by examining whether one or the other is preferentially consumed in the reaction.



However, in acetonitrile, for all the ratios investigated, a fraction of both parent complexes remain in solution as can be seen in the equilibrium chromatograms for various combinations in Figure 3.22 adjacent. In "1:10", a trace of *cis*-Pd(L⁴-S,O)₂ still remains in solution, notwithstanding a tenfold excess of *cis*-Pd(L³-S,O)₂.

The equilibrium distributions were identical when *cis*-Pd(L⁴-S,O)₂ was in excess, as illustrated by Figure 3.23. All combinations reached equilibrium within 24 hours.

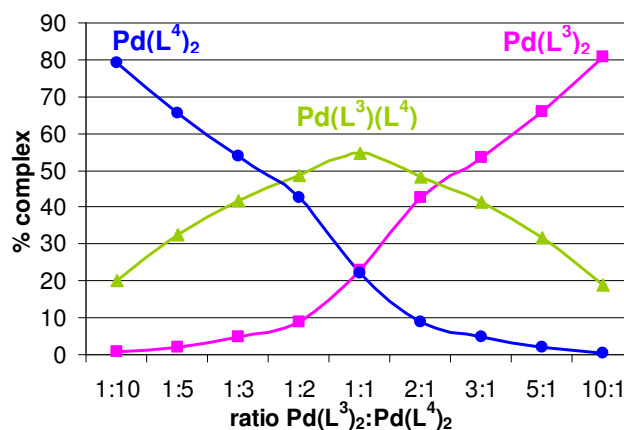


Figure 3.23. Graphical representation of equilibrium distributions for chromatograms seen in Figure 3.22 adjacent.

As a fraction of both parent complexes remain in solution, irrespective of the ratio, as well as the fact that the trends seen in Figure 3.23 are identical, suggests that the stability constants of these two complexes in acetonitrile are near-equal.

3.6 The effect of solvent on chelate metathesis

The properties of the medium in which any reaction takes place – the solvent – can influence both the extent to which a reaction takes place as well as the rate of the reaction. These properties include the polarity, acidity and donor-acceptor ability of the solvent molecule.^[99]

The chelate metathesis reaction between *N,N*-dialkyl-*N'*-aroyl(acyl)thioureato Pd(II) bis-complexes was examined in a number of solvents, ranging from polar protic to non-polar aprotic solvents. The solvents investigated are listed in Table 3.4 along with their donor numbers (D_N)^[99] and their dielectric constants (ϵ_r).^[100] Dielectric constants are a measure of polarity and the values listed below (ϵ_r) refer to the relative permittivity of the solvent – a dimensionless quantity. Water has been included for comparative purposes.

Table 3.4. Solvents used in this investigation and their properties.

Solvent	D_N (kcal.mol ⁻¹)	ϵ_r
benzene	0.1	2.283
toluene	0.1	2.379
chloroform	4.0	4.807
1,4-dioxane	10.8	2.219
acetone	12.5	21.01
acetonitrile	14.1	36.64
water	18.0	80.10
methanol	30.0	33.00
ethanol	32.0	25.30

The donor number (D_N) relates to the Lewis basicity of the solvent. In other words, the ability of the solvent to donate an electron pair from one of its donor atoms to form a coordinate bond with an acceptor atom in a solute molecule.^[99] The particular scale used here was developed by Gutmann and Wychera in 1966. The donor number is defined as the negative of the standard heat of reaction ($-\Delta H^\circ$ kcal.mol⁻¹) for the formation of the 1:1 adduct between the donor solvent and the electron acceptor antimony(V) pentachloride in the inert solvent 1,2-dichloroethane.^[101] Antimony(V) pentachloride was chosen as the probe for this reaction as it is considered to be on the

border between hard and soft acceptors. The Gutmann and Wychera scale is not ideal, as the calorimetric measuring equipment is not widely available and it has not been possible to extend the scale to all available solvents. However, this scale is widely accepted in Europe and subsequent studies have found many spectroscopic quantities that are linearly related to it.^[99, 102-106]

For these experiments, $cis\text{-Pd}(\text{L}^3\text{-S},\text{O})_2$ and $cis\text{-Pd}(\text{L}^4\text{-S},\text{O})_2$ were chosen as in acetonitrile they exhibited the highest equilibrium constant ($K = 5.82 \pm 0.27$) and the reaction reached equilibrium within a reasonable period of two days. For comparative purposes, all experiments, save those in benzene, were carried out at 20 °C using 400 μM solutions of the two complexes dissolved in the solvent of interest and observed using HPLC. The benzene experiments were observed using ^1H NMR at 25 °C with solutions in the millimolar concentration range.* In the case of the two alcohol solvents, methanol and ethanol, the solubility of the complexes was too low, so a 50/50 (v/v) mixture of acetonitrile/alcohol was used.

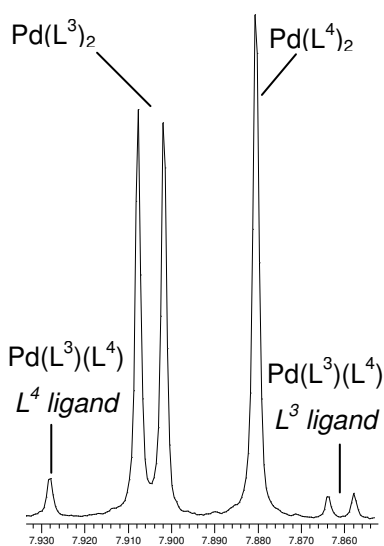


Figure 3.24. Aromatic region of ^1H NMR spectrum of $\text{Pd}(\text{L}^3)_2$ and $\text{Pd}(\text{L}^4)_2$ in benzene after 24 hours reaction time.

The property of the solvent which appeared to have the greatest effect on the chelate metathesis reaction was its Lewis basicity, expressed by the donor number (D_N). While metathesis did take place to some extent in all the solvents investigated, the extent and rate of the reaction increased with increasing donor number of the solvent.

In the solvents with the lowest donor numbers – benzene and toluene – barely any mixed-ligand complex formed as can be seen from the NMR data for deuterated benzene in Figure 3.24 adjacent. Even after 24-hours reaction time, the peaks corresponding to the mixed-ligand product are very small when compared to the peaks in the analogous Ni(II) metathesis reaction in acetonitrile (Figure 3.2).

* Many thanks to Ms J.M McKenzie for the NMR data.

The rate, as well as the extent of the metathesis reaction could be greatly increased if a trace of unbound ligand was added to the reaction mixture (Figure 3.25).

The addition of deuterated acetonitrile, on the other hand, had only a small effect on the extent and rate of the metathesis reaction and did not produce the results observed in the combinations of acetonitrile with 1,4-dioxane or acetone (Figure 3.27b and Figure 3.29b).

Analogous results to the benzene experiment were observed when the metathesis reaction was carried out in toluene.

Similarly, in 1,4-dioxane ($D_N = 10.8 \text{ kcal.mol}^{-1}$), very little mixed-ligand product formed. Figure 3.26a shows the chromatogram for the metathesis reaction in 1,4-dioxane after three weeks. (The region between 2.5 and 7.5 minutes t_R has been expanded to exclude the large solvent peaks.)

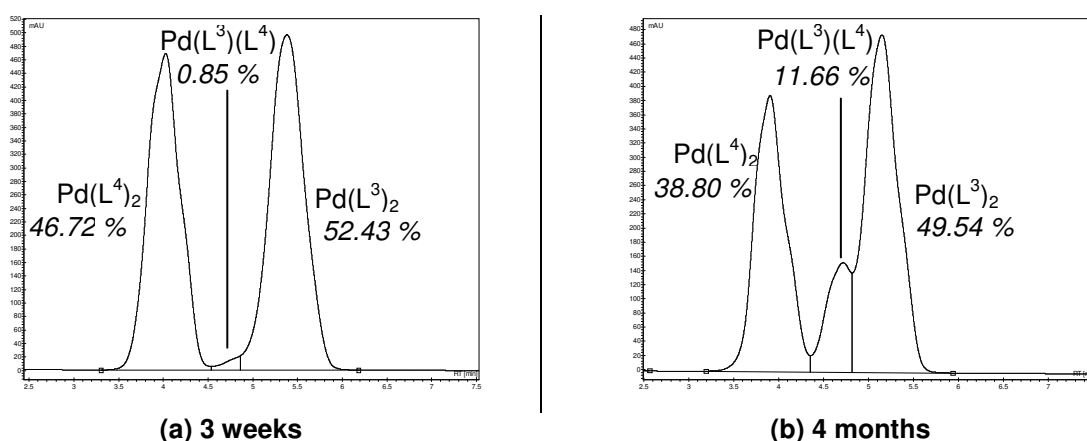


Figure 3.26. Metathesis reaction between $\text{Pd}(\text{L}^3)_2$ and $\text{Pd}(\text{L}^4)_2$ in 1,4-dioxane after (a) three weeks and (b) four months.

The peak corresponding to the mixed-ligand product is barely visible between the two parent complex peaks – less than 0.5 % of each parent complex underwent metathesis. Even after four months (Figure 3.26b), the metathesis reaction in 1,4-dioxane had not

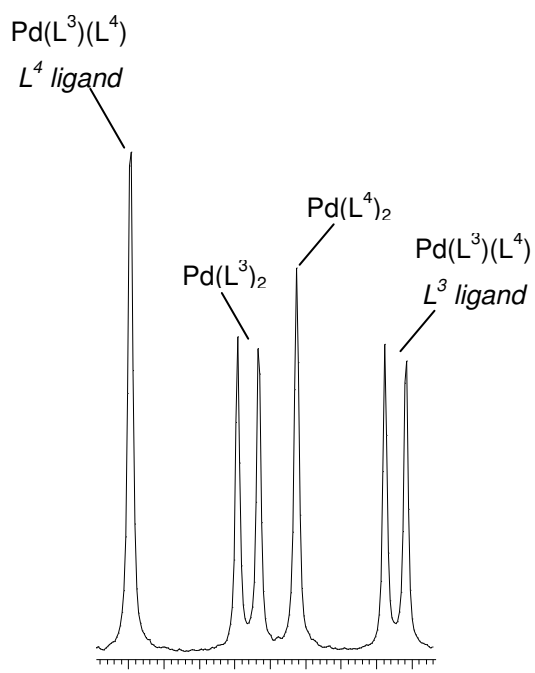


Figure 3.25. Aromatic region of ^1H NMR spectrum of $\text{Pd}(\text{L}^3)_2$ and $\text{Pd}(\text{L}^4)_2$ in benzene after addition of unbound ligand.

reached the equilibrium distribution seen in the acetonitrile solutions (see Figure 3.9 on page 75).

The broad, uneven shape of the peaks was due to the fact that the sample was dissolved in 1,4-dioxane, whereas the mobile phase in the HPLC system was acetonitrile. While these two solvents are miscible, the difference in polarity (ϵ_R) – 2.219 for 1,4-dioxane *versus* 36.64 for acetonitrile – is significant enough to distort the peak shapes. The more non-polar character of 1,4-dioxane makes it a stronger solvent than acetonitrile in *rp*-HPLC. This, coupled to the differences in viscosity between the two solvents ($\eta = 1.18$ cP 1,4-dioxane^[107] while $\eta = 0.35$ cP for acetonitrile^[108] at 25 °C), results in a process known as “viscous fingering”^[109] which may also contribute to the distorted peak shapes. Avoiding these problems would require that the mobile phase be changed from acetonitrile to 1,4-dioxane. Such an undertaking would be a time-consuming and impractical course of action for only a limited number of 1,4-dioxane samples.

While the metathesis reaction did not occur significantly in pure 1,4-dioxane, it could be encouraged by either addition of a trace of unbound ligand (Figure 3.27a) or addition of acetonitrile to form a 50/50 v/v solution (Figure 3.27b).

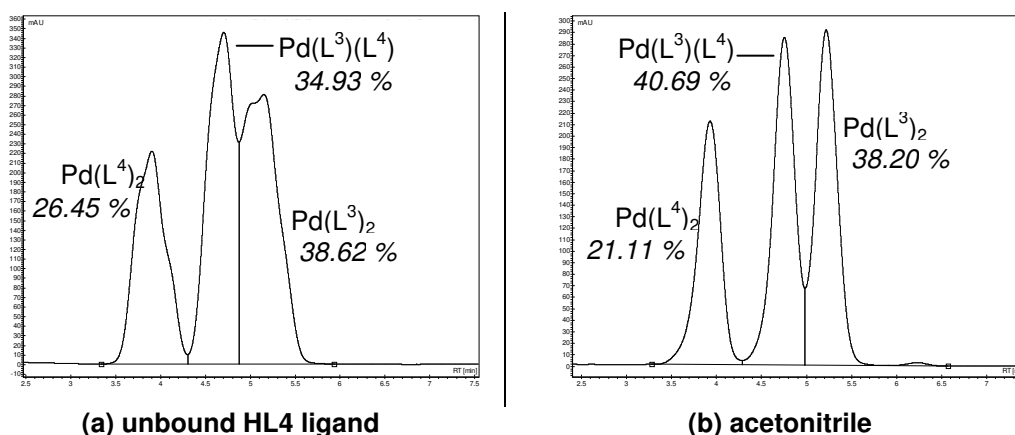


Figure 3.27. Metathesis reaction between Pd(L³)₂ and Pd(L⁴)₂ in 1,4-dioxane solution after addition of (a) unbound ligand (after one week) or (b) acetonitrile (after four months).

While neither case reached the equilibrium seen in pure acetonitrile, the additives nevertheless had an effect. The addition of acetonitrile ($D_N = 14.1$ kcal.mol⁻¹) increased the donating ability of the solvent and allowed more mixed-ligand product to form than was seen in pure 1,4-dioxane within a comparable time period. When a trace of

unbound ligand was added (10 % mole ratio – see Section 4.2.3 for more detail) thirty-five times more mixed-ligand product formed than was observed within a comparable time period in pure 1,4-dioxane. The effect of unbound ligand on the metathesis reaction will be discussed in greater detail in Section 4.2.3.

Acetone, with a donor number of $12.5 \text{ kcal.mol}^{-1}$, is more alike in donor ability to acetonitrile than 1,4-dioxane, yet again, very little mixed-ligand product was observed initially (Figure 3.28a).

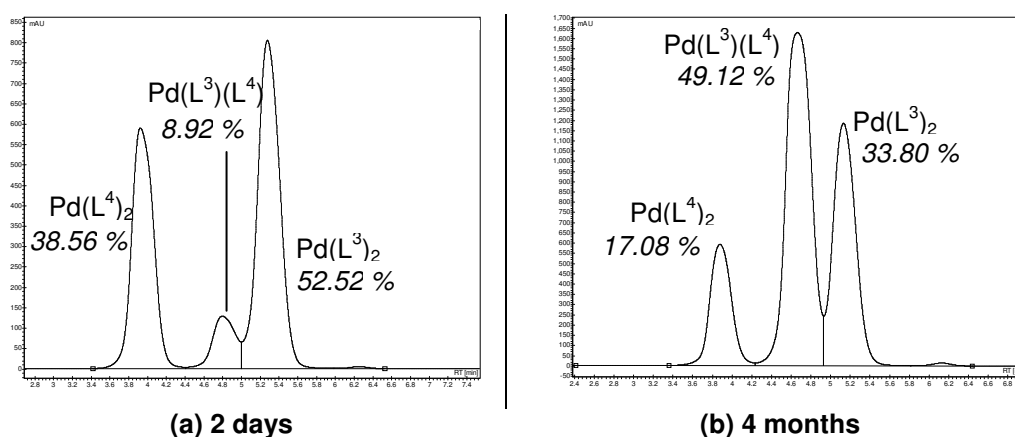


Figure 3.28. Metathesis reaction between $\text{Pd}(\text{L}^3)_2$ and $\text{Pd}(\text{L}^4)_2$ in acetone after (a) two days and (b) four months.

As in the 1,4-dioxane experiments, the addition of a trace of unbound ligand or dilution to a 50/50 acetone/acetonitrile solution resulted in a higher relative percentage mixed-ligand complex (Figure 3.29a and b respectively). These distributions are similar to the equilibrium observed in pure acetonitrile (Figure 3.9 on page 75).

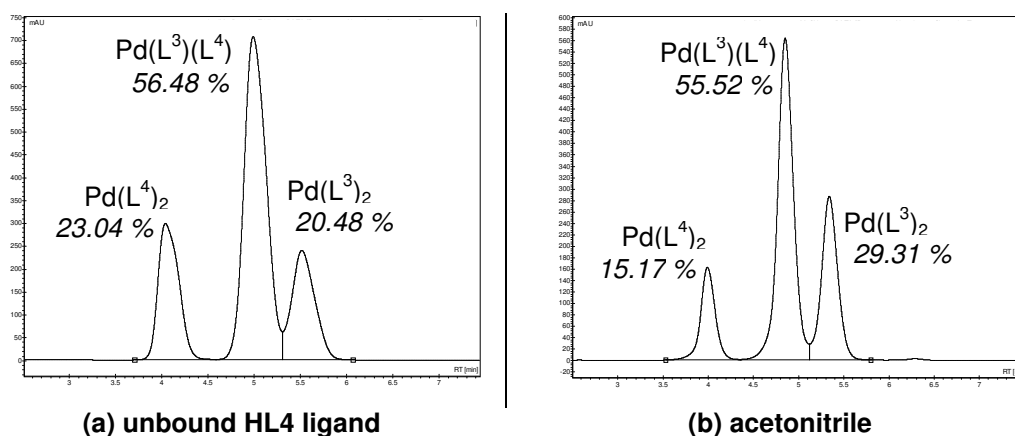


Figure 3.29. Metathesis reaction between $\text{Pd}(\text{L}^3)_2$ and $\text{Pd}(\text{L}^4)_2$ in acetone solution after addition of (a) unbound ligand (after one day) or (b) acetonitrile (after one day).

Methanol and ethanol, of all the solvents investigated, have the highest donor numbers ($D_N = 30.0$ and $32.0 \text{ kcal.mol}^{-1}$ respectively) and the alcohol/acetonitrile mixtures gave the most promising results (Figure 3.30a and b on the following page). These systems reached equilibrium within only 24 hours (versus 48 hours in pure acetonitrile). The dielectric constants of these solvent systems are lower than pure acetonitrile, and in both instances, $\text{cis-Pd(L}^4\text{-S}_2\text{O)}_2$ was favoured slightly (see Section 3.7 for further examples of this phenomenon). Some complex decomposition was also observed. However, the relative percentage mixed-ligand complex was higher than in the metathesis reaction in pure acetonitrile (Figure 3.9).

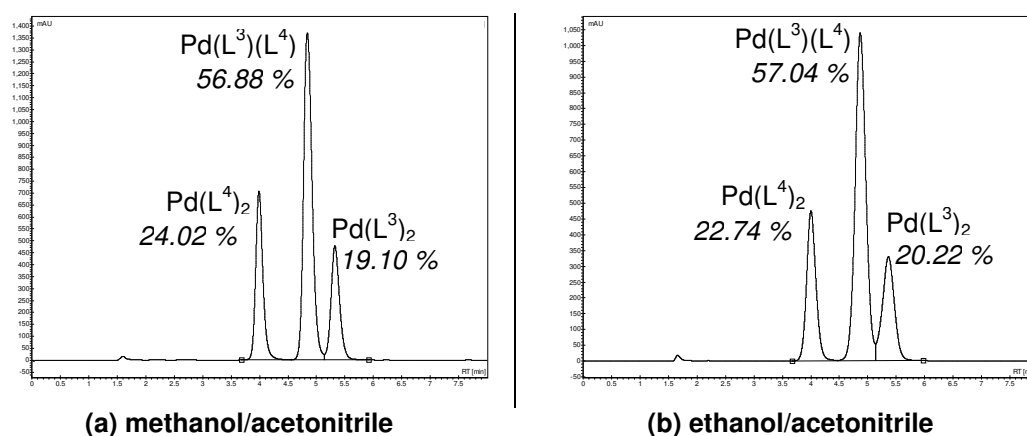
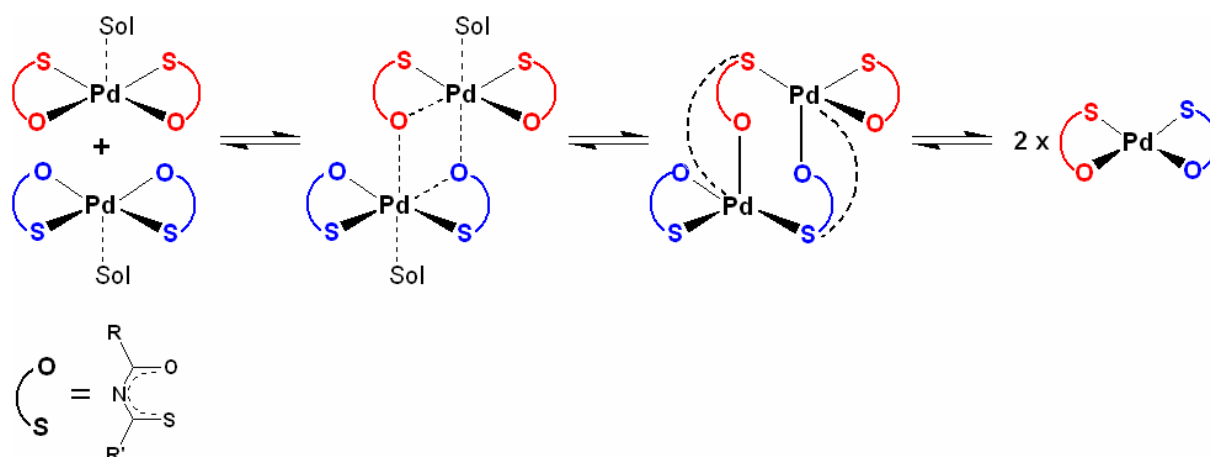


Figure 3.30. Metathesis reaction between $\text{Pd(L}^3\text{)}_2$ and $\text{Pd(L}^4\text{)}_2$ in alcohol/acetonitrile solutions after 24-hours reaction time.

The solvating ability of a solvent is dependant upon polarity, but also upon the ability of the solvent molecules to interact in a more specific manner with the solute molecules. Polar interactions between solvent and solute are non-specific and are based on multipoles, induced dipoles and dispersion forces (very weak attraction forces between molecules owing to the inevitable uneven electron distributions in molecules).^[110] On the other hand, more specific interactions – such as the donation of a non-bonding electron pair of the solvent towards forming a coordinate bond with an acceptor atom in the solute, resulting in a direct solvation – are often much stronger than the non-specific polar interactions between solvent and solute.^[99]

The fact that the extent of reaction, as well as the rate, increased with increasing donor number suggested that the metathesis reaction might take place via a solvent-stabilised intermediate (Scheme 3.1). The Pd-O bond is not as strong as the Pd-S bond,^[111] so it is likely that this bond will break first. The empty position in the coordination sphere of

the metal can be filled by a lone electron-pair from a solvent molecule. It has also been shown that Pd(II) complexes are inclined to form weak bonds in the apical position, most often occupied by a solvent molecule.^[111-113]



Scheme 3.1. Possible mechanism for the metathesis reaction, showing solvent-stabilised intermediate.

A solvent with a higher donor number can more readily donate an electron lone-pair to a complex with an incomplete coordination sphere to stabilise the species. Additionally, the fact that no large peaks eluted along with the solvent front supports the hypothesis that these complexes do not dissociate completely when undergoing metathesis. As a highly non-polar C₁₈ HPLC column and a polar acetonitrile mobile phase was used, any ionic or charged species would remain unretained and elute together with the mobile phase. No such peaks were observed in the chromatograms of freshly prepared solutions.

Additionally, Figure 3.26b (1,4-dioxane) and Figure 3.28b (acetone), which show the chromatograms after four months reaction time, strongly suggest that the solvent plays a role not only in the extent of the metathesis reaction, but also in the rate of reaction.

3.7 Ligand exchange between a complex and an unbound ligand

To obtain a solution containing mixed-ligand complex there are two available options: either mixing two different $cis\text{-Pd}(\text{L-S},\text{O})_2$ complexes (see Section 3.4) or exchanging a bound ligand with an unbound ligand ^[14] as illustrated in Figure 3.31.

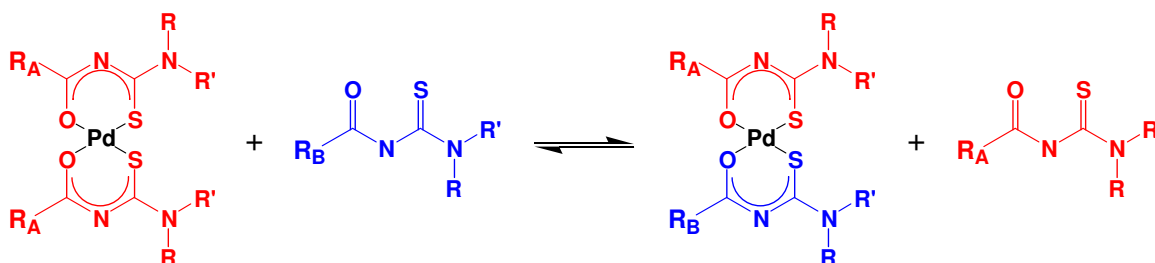


Figure 3.31. Exchange between a complex and a different unbound ligand.

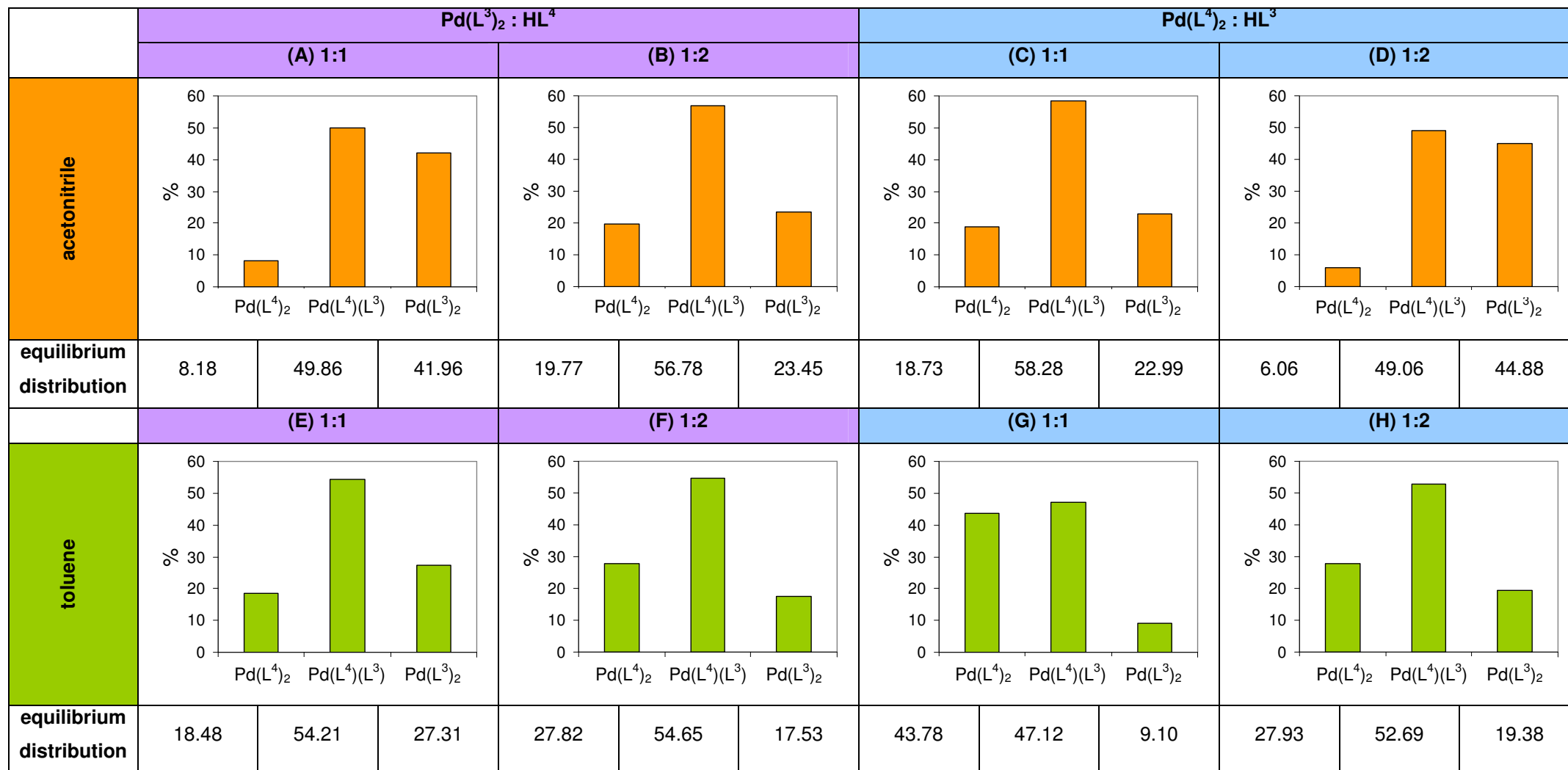
Again, due to their high equilibrium constant, $cis\text{-Pd}(\text{L}^3\text{-S},\text{O})_2$ and $cis\text{-Pd}(\text{L}^4\text{-S},\text{O})_2$ were the complexes of choice to investigate this phenomenon (see Figure 3.21 above). Both combinations of $cis\text{-Pd}(\text{L}^3\text{-S},\text{O})_2$ with HL^4 and $cis\text{-Pd}(\text{L}^4\text{-S},\text{O})_2$ with HL^3 were investigated employing a 1:1 as well as a 1:2 complex to unbound ligand mole ratio. As the nature of the solvent had a profound effect on the metathesis reaction (see Section 3.6), these experiments were carried out in a donating, polar solvent (acetonitrile) and then repeated in a non-donating, non-polar solvent (toluene). (In the discussions which follow, $cis\text{-Pd}(\text{L-S},\text{O})_2$ has been shortened to $\text{Pd}(\text{L})_2$ for clarity.)

It was found that the reaction between one complex and a different unbound ligand was much faster than the chelate metathesis reaction between two complexes. In acetonitrile these mixtures were already at equilibrium upon the first injection and in toluene, the reaction took only half an hour to reach equilibrium. The very low donor number of toluene ($D_N = 0.1 \text{ kcal}\cdot\text{mol}^{-1}$) may explain why this reaction did not immediately reach equilibrium (see Section 3.6 for a more detailed discussion).

A graphical representation of the equilibrium distributions for these “complex and unbound ligand” experiments is summarised in Figure 3.32 on the following page. The graphs are plotted with $\text{Pd}(\text{L}^4)_2$ first on the x-axis, followed by the mixed-ligand product and finally $\text{Pd}(\text{L}^3)_2$ so as to mimic the chromatograms (see Figure 3.9 on page 75).

Figure 3.32 Graphs of the equilibrium distributions in the “complex and unbound ligand” experiments in acetonitrile and toluene.

The relative percentage distribution of $\text{Pd}(\text{L}^4)_2$, $\text{Pd}(\text{L}^3)(\text{L}^4)$ and $\text{Pd}(\text{L}^3)_2$ at equilibrium is listed under each graph.



Even in the cases where sufficient unbound ligand is available for all of the complexes to potentially exchange both ligands (the 1:2 mole ratio experiments), the original parent complex is still to be found in the solutions.

The equilibrium distributions of graphs A and B for $\text{Pd}(\text{L}^3)_2/\text{HL}^4$ in acetonitrile (Figure 3.32) are somewhat intuitive: a 1:1 mole ratio of complex to unbound ligand (graph A) provides only enough unbound HL^4 ligand for each $\text{Pd}(\text{L}^3)_2$ complex to potentially exchange one ligand to produce the mixed-ligand complex $\text{Pd}(\text{L}^3)(\text{L}^4)$. Additionally, it is also possible for a $\text{Pd}(\text{L}^3)_2$ complex to exchange both its bound ligands with the unbound HL^4 in solution to form $\text{Pd}(\text{L}^4)_2$. With the addition of only one equivalent of HL^4 , 49.86 % of the parent $\text{Pd}(\text{L}^3)_2$ complex was converted into the mixed-ligand product while only a small percentage (8.18 %) of the $\text{Pd}(\text{L}^3)_2$ exchanged both ligands. When a 1:2 mole ratio of complex to unbound ligand was added, enough unbound ligand was present in solution to allow all of the $\text{Pd}(\text{L}^3)_2$ to potentially exchange both bound ligands. However, instead of a complete conversion to $\text{Pd}(\text{L}^4)_2$, a near-identical equilibrium distribution seen for chelate metathesis of the two complexes was observed (see Figure 3.9 on page 75).

However, when $\text{Pd}(\text{L}^4)_2/\text{HL}^3$ was examined in acetonitrile (C and D in Figure 3.32), there was a clear bias towards the $\text{Pd}(\text{L}^3)_2$ product. When two equivalents of unbound HL^3 ligand were added (graph D), 44.88 % of the $\text{Pd}(\text{L}^4)_2$ complexes exchanged both ligands to form $\text{Pd}(\text{L}^3)_2$. Even a 1:1 mole ratio (graph C) produced significantly more of the product complexes (mixed-ligand and $\text{Pd}(\text{L}^3)_2$ in this case) than did the corresponding $\text{Pd}(\text{L}^3)_2/\text{HL}^4$ combination (graph A).

In toluene, a similar bias towards $\text{Pd}(\text{L}^4)_2$ was observed. In fact, the graphs for $\text{Pd}(\text{L}^3)_2/\text{HL}^4$ in acetonitrile (A and B) and $\text{Pd}(\text{L}^4)_2/\text{HL}^3$ in toluene (G and H) are near-perfect mirror images of each other.

All separations were carried out on a reversed-phase C_{18} -column, which separates components solely on the basis of hydrophobicity^[50] – the retention of a compound increases with increasing hydrophobic character. As a result of this, the relative polarities of the two parent complexes may be estimated by merely comparing the retention times of the complexes. The *cis*- $\text{Pd}(\text{L-S,O})_2$ complexes and their mixed-ligand analogues were neutral, consequently the complex eluting first is the more polar, while

the one eluting later is the less polar (more hydrophobic) of the two. $cis\text{-Pd}(\text{L}^4\text{-S},\text{O})_2$ has three $-\text{OCH}_3$ substituents on the benzoyl ring and has a retention time of around 3.9 minutes whereas $cis\text{-Pd}(\text{L}^3\text{-S},\text{O})_2$ has only two $-\text{OCH}_3$ substituents and a retention time of around 5.3 minutes (when eluted with 100 % acetonitrile). The difference in the polarity of the complexes extends to the unbound ligands as well, with HL^4 more polar than HL^3 .

When a complex exchanges one of its bound ligands, L^A , for an unbound one from solution HL^B , the bound ligand is protonated and released into solution as HL^A . (These protonated ligands were observed in the LC-MS data for these solutions.) It is clear from the data in Figure 3.32 on page 95, that in the polar acetonitrile solutions, the less polar $cis\text{-Pd}(\text{L}^3\text{-S},\text{O})_2$ and more polar HL^4 are favoured. Likewise, in non-polar toluene, the more polar $cis\text{-Pd}(\text{L}^4\text{-S},\text{O})_2$ and less polar HL^3 are favoured.

When the ligands are complexed to the Pd(II) centre, extensive delocalisation throughout the complex (see Figure 3.20 on page 85) can assist in dissipating any localised concentration of charge. In the unbound ligand, on the other hand, such extensive delocalisation is not possible. Therefore, it may be that the more polar HL^4 ligand is better stabilised in polar acetonitrile, while in toluene, the same is true of the less polar HL^3 ligand. This phenomenon will, however, require a more in-depth investigation.

3.7.1 Ligand exchange between a complex and its identical ^{13}C -labelled ligand: NMR evidence

The fact that metathesis between the two complexes $\text{Pd}(\text{L}^A)_2$ and $\text{Pd}(\text{L}^B)_2$ occurs can be partly explained by entropy. Reaction between two dissimilar parent complexes produced three different complexes in solution (the two parent complexes and the mixed-ligand product) which increased the molecular disorder and consequently, increased the entropy of the system. Likewise, reaction between a complex, $\text{Pd}(\text{L}^A)_2$, and an unbound ligand, HL^B , resulted in five different species in solution – the three complexes, $\text{Pd}(\text{L}^A)_2$, $\text{Pd}(\text{L}^A)(\text{L}^B)$ and $\text{Pd}(\text{L}^B)_2$ as well as both unbound ligands, HL^A and HL^B .

If a solution of an identical ligand, HL^A , is added to a solution of a complex, $Pd(L^A)_2$, the products produced in their exchange are identical in structure to the original reactants. Therefore there is no increase in the molecular disorder of the system and the reaction cannot be driven by entropy. Nevertheless, this reaction does indeed take place and was observed in ^{13}C NMR spectra for the reaction between $cis-Pd(L^1-S,O)_2$ and a ^{13}C -enriched HL^1 ligand (Figure 3.33).

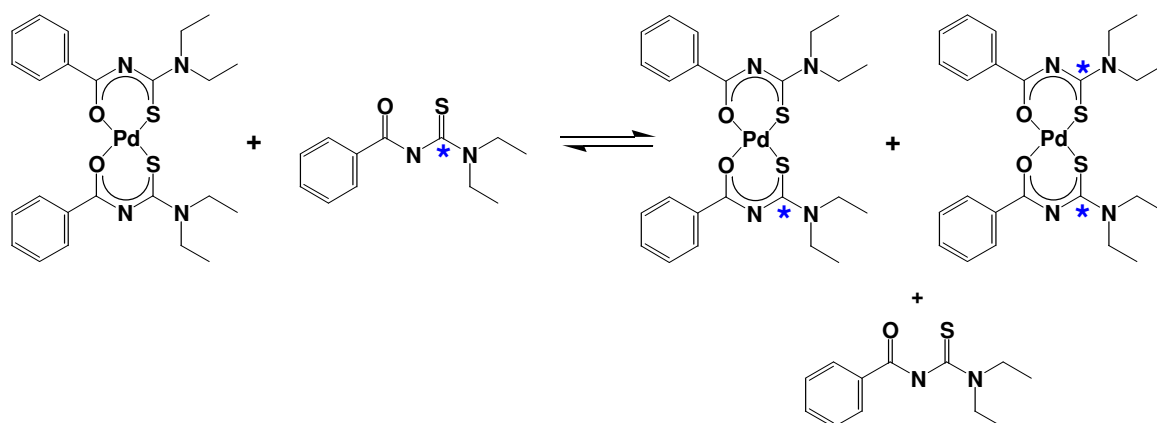


Figure 3.33. Exchange between $Pd(L^1)_2$ and HL^1 which is ^{13}C -enriched at the sulphur-carbonyl (*).

The NMR spectra were recorded in deuteriochloroform. As ^{13}C NMR is less sensitive than 1H NMR due to the low natural abundance of the ^{13}C nucleus (only 1.08%), as well as the small magnetogyric ratio of the ^{13}C nucleus (67.28 radians/tesla),^[114] higher concentrations of the compound of interest are necessary to obtain spectra within a reasonable period of time. Though the majority of the HPLC experiments were performed using acetonitrile solutions, both $cis-Pd(L-S,O)_2$ and HL are more soluble in chloroform than in acetonitrile. Therefore, to obtain the more concentrated solutions necessary for NMR measurements, deuteriochloroform was chosen for this experiment.

^{13}C NMR spectra were recorded for both $cis-Pd(L^1-S,O)_2$ and HL^1 individually, as well as for a mixture of the two compounds. The spectrum of the $cis-Pd(L^1-S,O)_2$ complex is shown below in Figure 3.34, including an expansion of the carbonyl and sulphur-carbonyl region of the spectrum. The height of each peak in the spectrum is typical for proton-decoupled spectra of $cis-Pd(L-S,O)_2$ complexes with the carbonyl (170.63 ppm) and sulphur-carbonyl (171.11 ppm) peaks roughly equal in intensity. (For a full assignment of this spectrum, please refer to Section 2.1.2.1.)

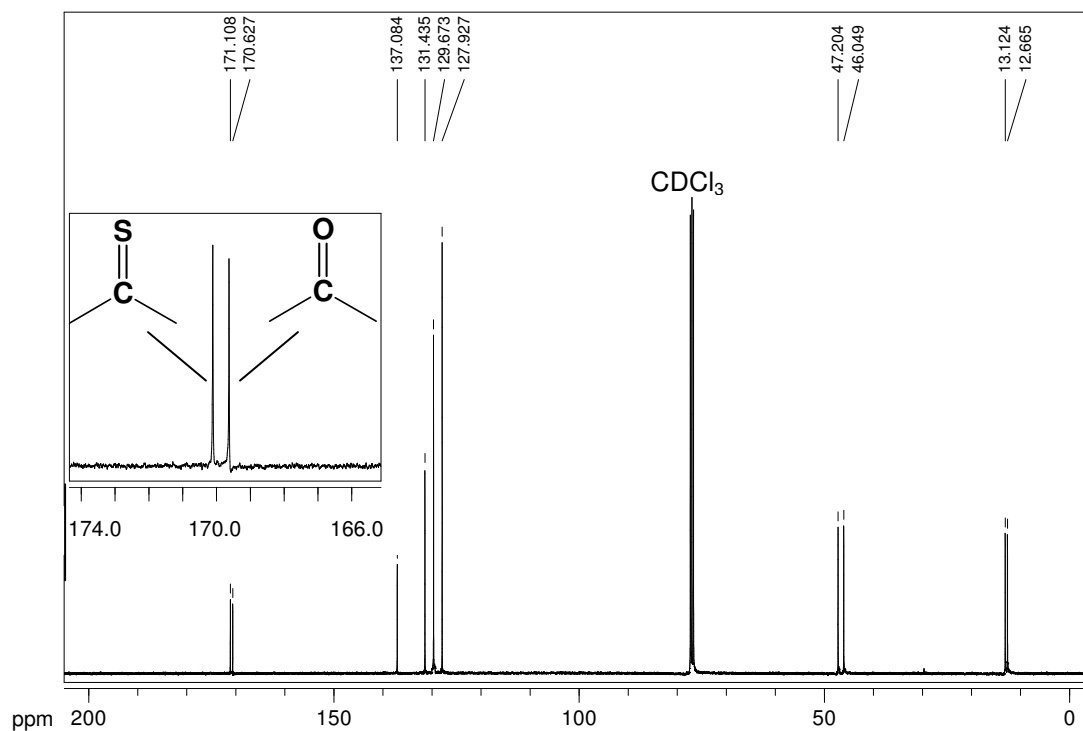


Figure 3.34. ^{13}C NMR spectrum of $\text{Pd}(\text{L}^1)_2$ highlighting the carbonyl peak (170.63 ppm) and sulphur-carbonyl peak (171.11 ppm).

In the ^{13}C NMR spectrum of the ^{13}C -enriched HL^1 ligand, the enriched sulphur-carbonyl peak at 179.24 ppm dwarfs the rest of the spectrum, including the tiny carbonyl peak at 163.71 ppm (Figure 3.35).

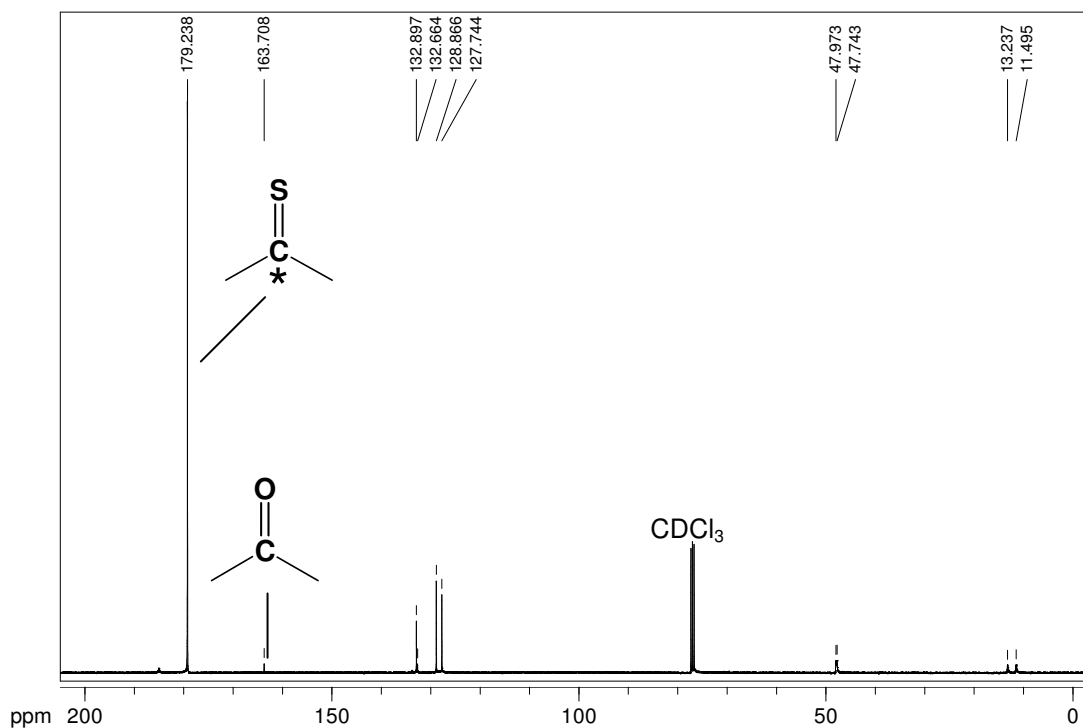


Figure 3.35. ^{13}C NMR spectrum of HL^1 highlighting the carbonyl peak (163.71 ppm) and the ^{13}C -enriched sulphur-carbonyl peak (179.24 ppm).

When equimolar cis -Pd(L¹-S,O)₂ complex and ¹³C-enriched HL¹ ligand solutions were mixed in a 1:1 ratio, evidence of both the complex and ligand could be observed in the carbonyl and sulphur-carbonyl region (Figure 3.36). Peaks attributable to the complex appeared at 171.10 ppm (sulphur-carbonyl) and 170.62 ppm (carbonyl), denoted by S_C and O_C respectively in Figure 3.36. It was immediately clear from the increased intensity of the sulphur-carbonyl peak of the complex that a number of the ¹³C-enriched ligands had been incorporated into a complex, releasing non-enriched ligand into solution. The ligand peaks appeared at 179.20 ppm (sulphur-carbonyl) and 163.67 ppm (carbonyl), denoted by S_L and O_L respectively in Figure 3.36. The difference in the relative intensities of the sulphur-carbonyl and carbonyl peaks attributable to the HL¹ ligand was not so dramatic in the spectrum of the mixture (Figure 3.36) as it was in the individual spectrum (Figure 3.35). This indicates that both ¹³C-enriched as well as non-enriched ligand was present in the solution.

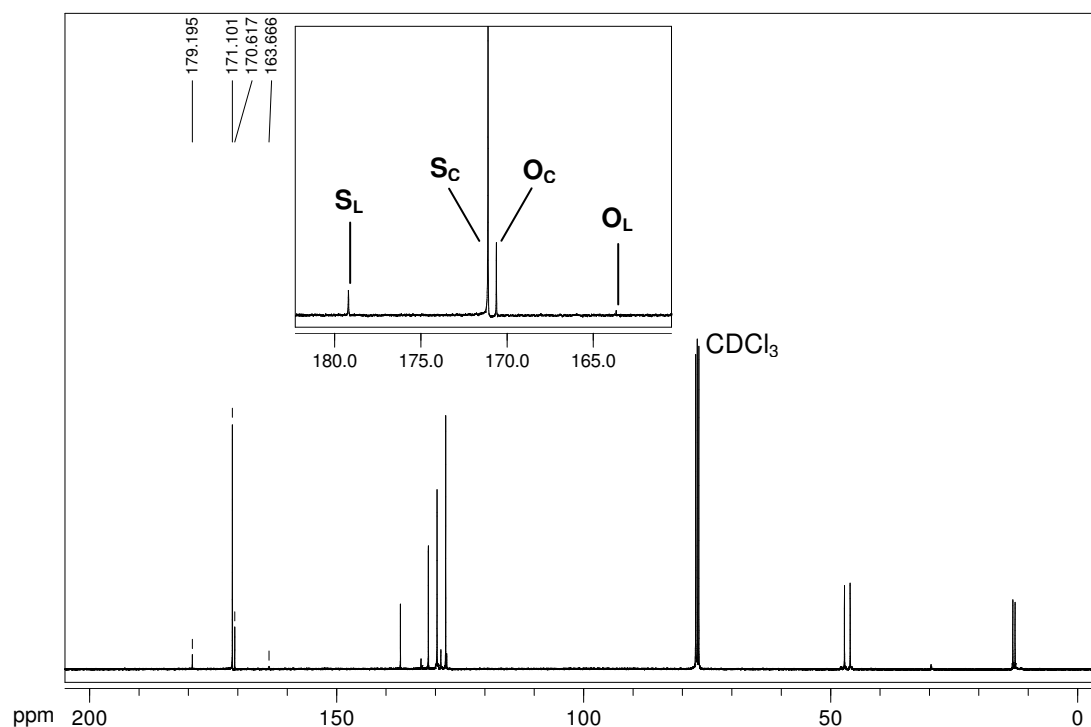


Figure 3.36. ¹³C NMR spectrum of the mixture of Pd(L¹)₂ and ¹³C-enriched HL¹, highlighting the carbonyl and sulphur-carbonyl region in the insert.

As decoupled ¹³C-NMR spectra cannot be used to calculate concentrations, it was not possible to determine the percentage unbound ¹³C-labeled ligand that had been incorporated into a complex.

Chapter 4

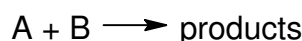
Factors which affect the rate of metathesis

4.1 Determining the rate characteristics of a reaction

The rate of a chemical reaction may be determined by plotting the change in concentration of a reactant or a product against time.^[115] Many conventional analytical methods may be employed to obtain the concentrations of interest. For relatively slow reactions, spectrophotometric or electrochemical methods are typically employed to monitor the rate. Very fast reactions, where the reaction is 50 % complete within ten seconds or less, and reactions which appear to occur instantaneously – the precipitation of a salt or acid-base neutralisations for instance – require special techniques such as stop-flow, relaxation or competition methods.^[116]

Many factors can affect the rate of a reaction, including the nature of the reactants, the mechanism of reaction, concentration, temperature, reaction medium, light or the presence of a catalyst.^[115, 116]

The dependence of the rate upon the concentrations of the species is reflected in the rate law and reaction order. For example, in the straightforward reaction:



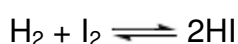
where the initial concentrations of A and B are the same, the rate of formation of the products over time is equal to the decrease in concentration of the reactants. The differential rate law is:

$$-\frac{d[A]}{dt} = -\frac{d[B]}{dt} = k[A][B]$$

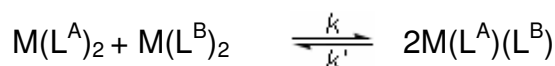
As the rate law is dependent upon the concentration of both A and B, this is a second-order reaction. The constant, k is known as the characteristic rate constant for the reaction and is a constant value, independent of concentration and only affected by temperature. It remains unchanged throughout the reaction and provides a more suitable measure of reaction velocity than experimentally measured rates, as well as providing information concerning the mechanism of the reaction.

Often, for straightforward reactions, the rate law and reaction order can be conveniently acquired from the method of initial rates. In this method, the rate at the beginning of a reaction is measured for a number of different starting concentrations of the reagents. The method of initial rates is often used in conjunction with the isolation method, in which all but one reagent is in excess. By assuming that the concentration of the excess reagents stays virtually constant, the rate law assumes the form of a first-order process which greatly simplifies calculations. As an example, for a process which may have a rate law in the form of $v = k[A]^a[B]^b$ (where v indicates the overall rate), the initial rate law, when reagent B is in excess, becomes: $v_0 = k[A_0]^a$. Taking the logarithm of both sides and plotting the logarithm of the initial rates against the logarithms of the initial concentrations of A should give a straight line with slope a . The numerical value of this slope gives the order of the reaction in [A]. Repeating the experiment with reagent A in excess will give the value of b . Once the values in the rate equation have been obtained, the rate constant may be found by merely substituting the experimental data into the equation.^[117]

However, when a reaction is reversible, the products actively take part in the reaction immediately upon being formed and the above-mentioned method is no longer viable. Nevertheless, a numerical method does exist to calculate both forward and reverse rate constants in the case of reversible reactions. The method was developed towards the end of the 19th century by Bodenstein^[118-120] to calculate rate constants for the reaction:



This method was used in 1980 by Moriyasu and Hashimoto to calculate the forward (k) and reverse (k') rate constants for the metathesis reaction:



where M = Ni(II) or Cu(II) and L = a dithiocarbamate ligand.^[7, 16] As in the experiments discussed in this thesis, they made use of HPLC to obtain their data. More detailed descriptions of their experiments may be found in Section 1.2.1.1. The analysis by Moriyasu and Hashimoto involved the following procedure. The first step in calculating the rate constants is to formulate the differential rate laws for the forward reaction – the formation of the mixed-ligand product (equation 1a on the following page):

$$\frac{d[\text{MA}_2]}{dt} = \frac{d[\text{MB}_2]}{dt} = k'[\text{MAB}]^2 - k[\text{MA}_2][\text{MB}_2] \quad (1a)$$

and the reverse reaction – the disproportionation of the mixed-ligand product back into the parent complexes:

$$\frac{d[\text{MAB}]}{dt} = k[\text{MA}_2][\text{MB}_2] - k'[\text{MAB}]^2 \quad (1b)$$

This, as has been noted, is a reversible reaction and thus the contributions of both the forward and the reverse reaction must be included in each rate law as these reactions occur simultaneously throughout the reaction period. Unfortunately these differential rate laws are now impossible to solve as they contain both the forward and reverse rate constants, as well as being dependant upon the concentration of both parent complexes and the mixed-ligand product. Through algebraic manipulation of the equations and exploitation of the fact that the ratio of the forward and reverse rate constants is equal to the equilibrium constant ($K = k/k'$), this problem may be neatly circumvented (see Appendix F for the calculations).

When $K = 4$, as was the case in the experiments of Moriyasu and Hashimoto,^[7, 16] the manipulated rate equations can be reduced to:

$$-\ln\left(1 - \frac{2x}{a_0}\right) = ka_0t \quad (2a)$$

$$-\ln\left(1 - \frac{y}{a_0}\right) = ka_0t \quad (2b)$$

Where $[\text{MA}_2] = [\text{MB}_2] = x$ and $[\text{MAB}] = y$ and the initial concentrations $[\text{MA}_2]_{t0} = [\text{MB}_2]_{t0} = a_0$. A plot of these equations renders a straight-line graph from which the value of the forward rate constant (k) can easily be calculated from the slope (Figure 4.1 on the following page). The reverse rate constant (k'), is obtained from the relationship $k' = k/K$, where the equilibrium constant, K , is in this case equal to 4.

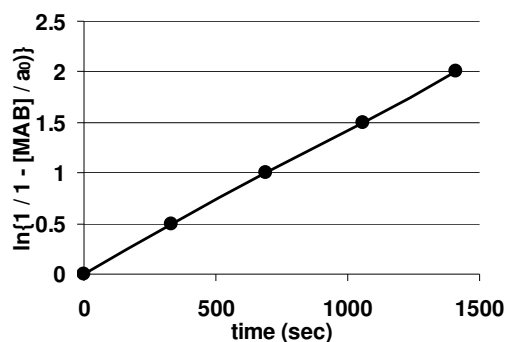


Figure 4.1. Plot of equation 2b for the experiment by Moriyasu and Hashimoto discussed in Section 1.2.1.1.^[16]

However, if $K \neq 4$, k and k' are estimated using the following equation:^[118-120]

$$k = \left(\frac{2}{mt} \right) \cdot \left(\ln \frac{\left(\frac{2a_0 - m}{1 - 4/K} \right)^{-y}}{\left(\frac{2a_0 + m}{1 - 4/K} \right)^{-y}} + \ln \left(\frac{2a_0 - m}{2a_0 + m} \right) \right) \quad m = 4a_0 \sqrt{1/K}$$

A table must be drawn up of the time intervals and the corresponding experimentally measured concentrations. Each set of data, as well as the equilibrium constant, must be substituted into the equation. To obtain a value for the forward rate constant, the average of these calculated k -values is taken. The forward rate constant and the equilibrium constant may then be used to calculate the reverse rate constant.

4.1.1 Rate of reaction in the chelate metathesis of *cis*-Pd(L-S,O)₂ complexes

As has been mentioned previously, the chelate metathesis reactions between *cis*-Pd(L-S,O)₂ complexes were studied using HPLC. While the technique can be used to detect very small quantities of analyte, it was unfortunately restricted due to the time needed to elute the sample from the column. In the case of the chelate metathesis reactions under investigation, chromatograms could only be obtained at ten-minute intervals (see Section 2.2.2). When comparing three identical experiments repeated on three separate occasions, the reaction rates differed by as much as 11.16% (see Section 2.3.2). (The equilibrium constants, however, remained reproducible over a number of experiments.) Therefore, all experiments which were to be compared were

carried out concurrently using the same solutions of the parent complexes to minimise error.

Consequently, while it is possible to estimate the reaction rates and rate constants, in the sections that follow, these rates will be discussed relative to each other, as definite numerical values do not give any further information or insight into the process. There may also be the possibility of unknown side reactions which will render Bodenstein's method, which is only relevant to a reversible reaction of the type $A + B \rightleftharpoons 2AB$, unsuitable.^[118-120]

In the equilibrium studies (see Section 3.4) it was found that the reaction between $cis\text{-Pd}(\text{L}^3\text{-S},\text{O})_2$ and $cis\text{-Pd}(\text{L}^4\text{-S},\text{O})_2$ was complete within a reasonable period of two days and had the highest equilibrium constant and therefore, these two complexes were chosen for the rate investigations (Figure 4.2). All experiments were performed with acetonitrile solutions of the parent complexes – see Section 3.6, as well as Sections 4.2.4 and 4.2.5 for more information on the effect of the solvent on the reaction.

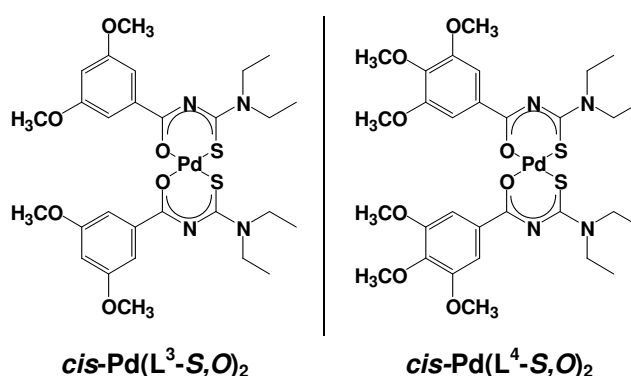


Figure 4.2. Complexes used for all the investigations into reaction rate.

All data will be reported as the relative percentage mixed-ligand product present in solution. Percentage was chosen over concentration or number of moles as slight differences in the initial concentrations of the parent complexes are inevitable. A full explanation of the calibration procedures and the formulas used to calculate these percentage values can be found in Section 2.3.1. In most of the figures, more than one set of data has been plotted on the same set of axes, so error bars have been omitted for clarity. A full discussion regarding the magnitude of possible errors, as well as a representative graph can be found in Section 2.3.2.

4.2 Factors which affect the rate of the chelate metathesis reaction

4.2.1 *The effect of concentration*

4.2.1.1 Initial unsuccessful concentration-dependence study

The very first study undertaken into the rate of the chelate metathesis reaction between the *cis*-Pd(L-S,O)₂ complexes, focused on the effect of concentration with the intention of perhaps elucidating the rate law. Initially, an acetonitrile stock solution of each parent complex, with concentration 800 μM was made and the other concentrations of interest – 400, 200, 100, 50 and 20 μM – diluted down from this solution as needed. The compounds used to make up the stock solutions had not yet been submitted to the rigorous recrystallisations described in Section 2.1.2. The experiments were performed over a period of three days – two sequences per day, each monitoring a reaction for an 18 hour period. The results which emerged from this set of experiments could at best, be described as erratic, with no discernable patterns found in the data (Figure 4.3).

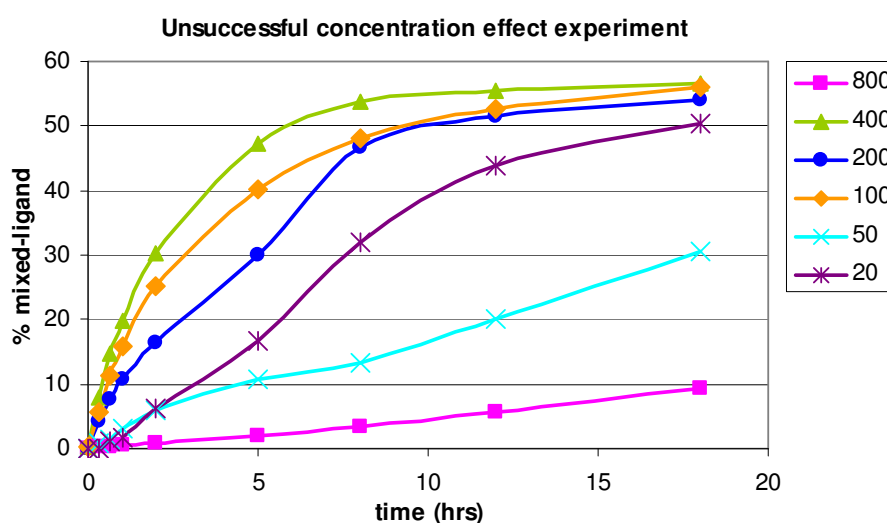


Figure 4.3. First set of experiments studying the effect of concentration on rate, showing erratic results. Regarding the labelling of these graphs, the curve marked e.g. “800”, refers to the experiment in which equal volumes of 800 μM *cis*-Pd(L³-S,O)₂ and *cis*-Pd(L⁴-S,O)₂ solutions were mixed.

The experiments were therefore repeated a week later with the same stock solutions used in the first experiment, to confirm reproducibility. In this second set of experiments, the rate of reaction in all the solutions now appeared to be the same (Figure 4.4 on the following page).

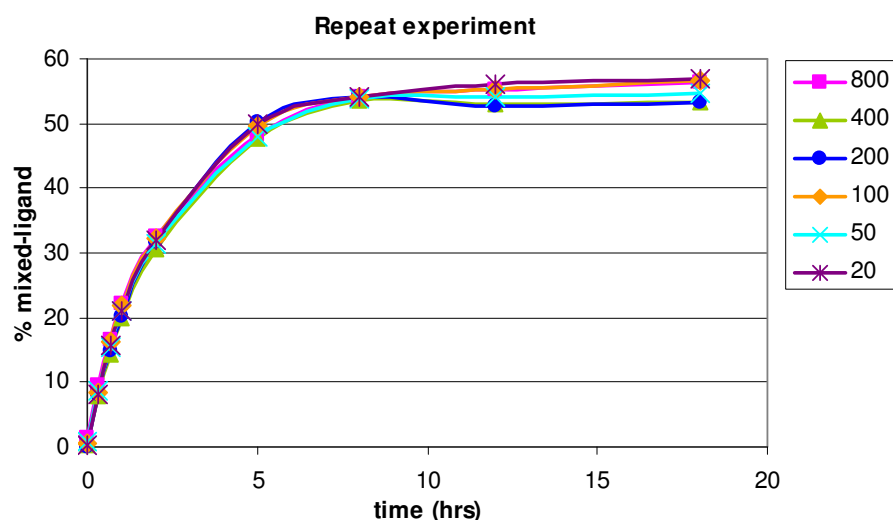


Figure 4.4. Repeat of the concentration-dependence experiments. The reaction rate in all the solutions was the same.

4.2.1.2 Successful concentration-dependence study

A similar set of experiments was, in the light of the results above, repeated using freshly-prepared acetonitrile solutions, with the amount of compound necessary for each solution weighed separately. Moreover the starting compounds had been recrystallised many times until no impurities could be detected in the chromatograms (see Section 2.1.2 for more detail). This revised concentration-effect experiment focused on concentrations of 800, 400, 200 and 100 μM for the parent complexes. Lower concentrations were not viable due to the fact that either very small amounts of compound or very large volumes of expensive acetonitrile were needed. The results of this experiment are summarised in Figure 4.5.

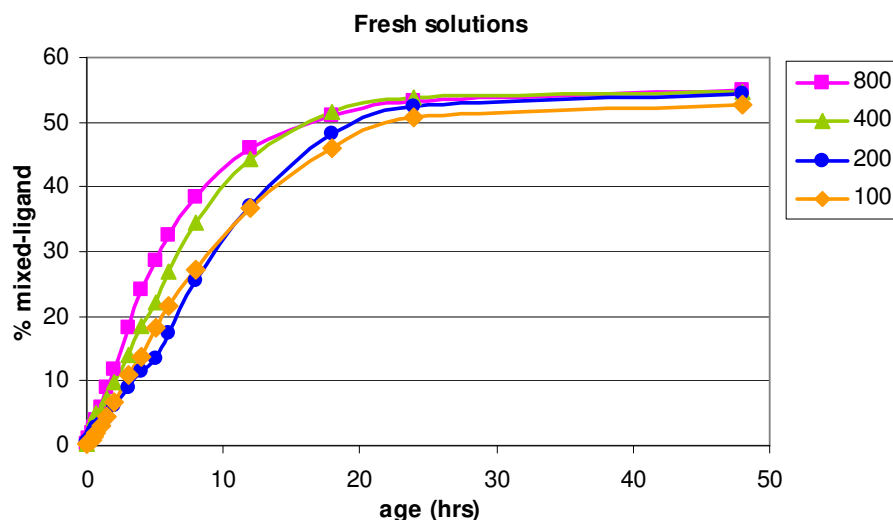


Figure 4.5. Revised concentration-dependence experiment, using freshly dissolved solutions.

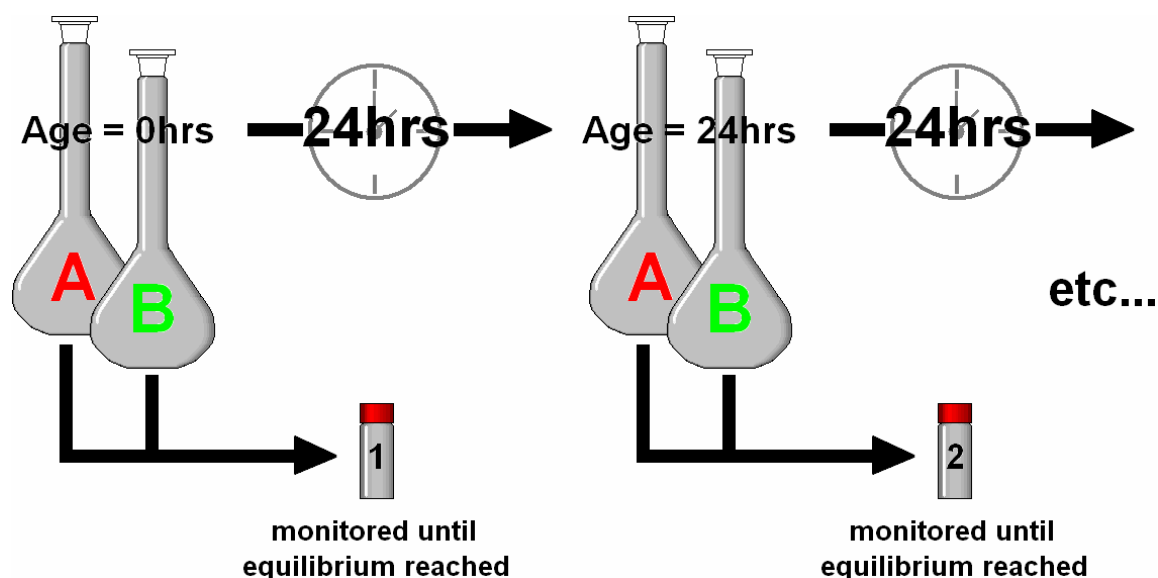
Although the rates of reaction for the four concentrations (800-100 μM) were similar, the mixture of 800 μM *cis*-Pd(L³-S,O)₂ and 800 μM *cis*-Pd(L⁴-S,O)₂ exhibited a slightly faster reaction rate, followed closely by the 400 μM solutions. The 200 μM and 100 μM solutions reacted at a comparable rate.

The most basic model for reaction kinetics assumes that each time a bimolecular collision occurs, there is a reaction.^[116] On this assumption, the higher the concentration, the more molecules are available and the more collisions can occur. More collisions mean a higher rate of reaction. The data from the experiments with the fresh solutions suggest that this mechanism may indeed play a role. However, with an eight-fold difference in initial concentrations, one would expect a greater variation in the relative rates of reaction. This suggests that other additional factors may also contribute to the rate of the metathesis reaction.

The results from the unsuccessful concentration-effect experiment (Section 4.2.1.1) suggested that the “age” of the solutions upon mixing may also play a role in determining the rate of the metathesis reaction. Therefore, it was decided to study the effect of the “age” of solutions from the time of their preparation, using the most pure, recrystallised compounds available.

4.2.2 The effect of age

To study the effect of age on the rate of the metathesis reaction, the freshly-prepared solutions used in the concentration experiment discussed in Section 4.2.1.2, were left to “age” for fixed times. After a sample had been taken from the solution of each parent complex (flasks A and B in Scheme 4.1), mixed in a vial and monitored using HPLC, the foil-covered volumetric flasks were left in the cupboard at 20 °C. After 24 hours, a second set of samples was taken from the same flasks containing the individual complex solutions. This second set of samples, once mixed in an HPLC vial, should show how the rate would be affected if the solutions were 24 hours old upon mixing. This procedure was repeated for solutions which were 48 hours, 72 hours, 120 hours (5 days) and 168 hours (1 week) old (Scheme 4.1 on the following page).



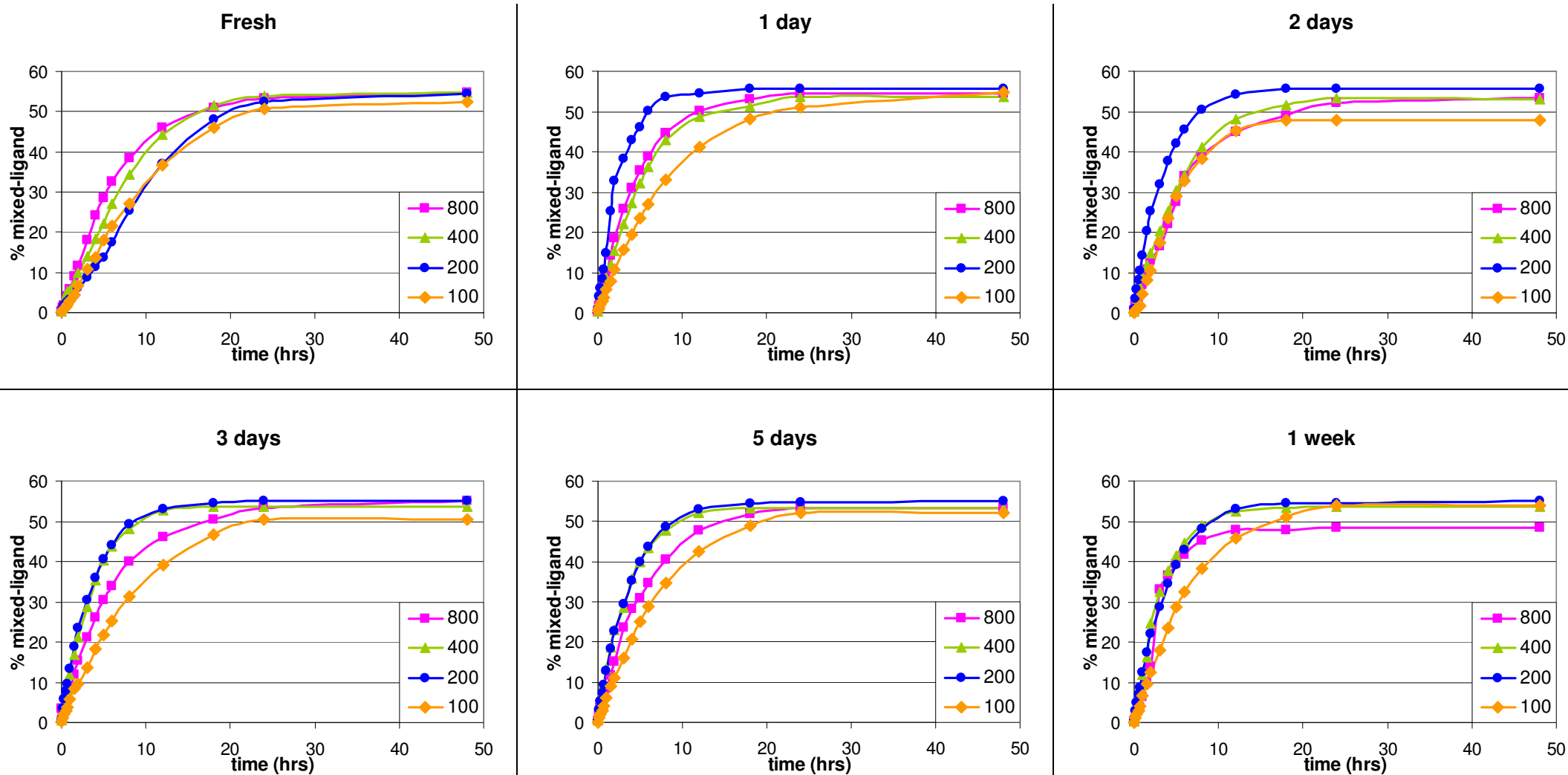
Scheme 4.1. Schematic representation of the procedure for the age-dependence experiments.

The volumetric flasks, as well as the HPLC vials were covered in aluminium foil to prevent photoinduced *cis-trans* isomerisation.^[45]

The effect of the “age” of the solutions was studied for four different initial concentrations: 800, 400, 200 and 100 μM and the data from these experiments is summarised in Figure 4.6 on the following page. The fresh-prepared solutions discussed in Section 4.2.1.2 have also been included for comparative purposes. Each graph shows data from one aging experiment (i.e. the fresh solutions, those left to age for 24 hours etc.), with the four different concentrations plotted on one set of axes (Figure 4.6 on the following page).

Regarding the labelling of the graphs in Figure 4.6: the graph marked, for example, “800”, refers to the experiment where equal volumes of 800 μM acetonitrile solutions of *cis*-Pd(L³-S,O)₂ and *cis*-Pd(L⁴-S,O)₂ were mixed.

(Continued on page 112.)

Figure 4.6. The effect of the “age” of the solutions upon mixing on the rate of metathesis of $cis\text{-Pd}(\text{L}^3\text{-S},\text{O})_2$ and $cis\text{-Pd}(\text{L}^4\text{-S},\text{O})_2$ in acetonitrile at 20° C.

(Continued from page 110.)

The freshly prepared solutions, which have already been discussed in the previous section, reacted with predictable rates – the higher the concentration, the faster the overall reaction rate. However, even after being left for only one day to age, there was a marked difference in the patterns observed with the lower concentration solutions “overtaking” the highest concentration solution (see for example “1 day” in Figure 4.6 on the previous page). In most cases, all concentrations reached a near-equal equilibrium distribution after a maximum of two days reaction time. (For a numerical list of the equilibrium constants and times taken to reach equilibrium for this set of experiments, please refer to Appendix G.)

Additionally, the rate of reaction increased with the increasing “age” of the solutions upon mixing. A maximum reaction rate was reached after three days “aging” time. Figure 4.7 below illustrates the difference in reaction rates for the mixtures of 400 μM $\text{cis-Pd}(\text{L}^3\text{-S},\text{O})_2$ and $\text{cis-Pd}(\text{L}^4\text{-S},\text{O})_2$ solutions. Similar trends were observed in the other concentrations under investigation.

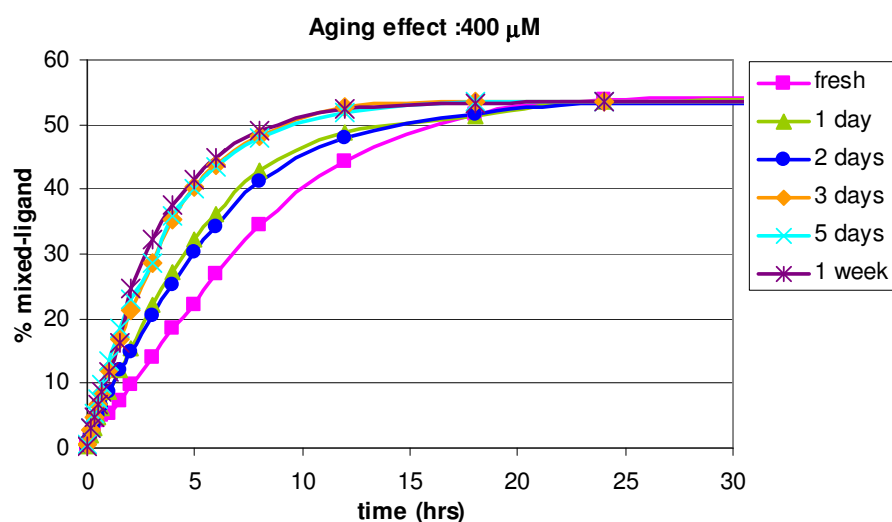


Figure 4.7. Graph showing the increase in reaction rate for “aged” solutions.

This example is for the mixtures of 400 μM $\text{Pd}(\text{L}^3)_2$ and $\text{Pd}(\text{L}^4)_2$ solutions.

The area between 0 and 30 hours has been expanded for clarity (equilibrium is attained after 48 hours).

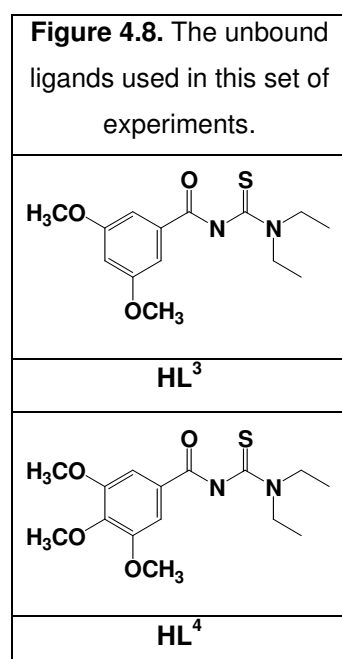
It appears that the “age” of the solutions upon mixing does indeed play a role in the overall rate of reaction, but the non-logical, sometimes counter-intuitive trends suggest that the metathesis reaction between $\text{cis-Pd}(\text{L-S},\text{O})_2$ complexes is a far more complicated process than originally assumed.

When a metal complex remains in solution for an extended period of time, it is possible that changes in the structure of the complex will occur due to complex dissociation, the interaction between the solvent molecules and the complex, or solvolysis reactions. A ligand may become partially, or entirely detached from the complex with the vacant positions in the coordination sphere of the metal occupied by solvent molecules. It is also possible that uncomplexed ligand may undergo solvolysis reactions. (Some of these decomposition products could be identified using LC-MS analysis and are discussed in Section 3.2.)

With this hypothesis in mind, it was decided to investigate what effect the presence of traces of unbound ligand in solution would have on the rate of the metathesis reaction. This study was carried out to potentially gaining a better understanding of “aging” effect.

4.2.3 The effect of the addition of unbound ligand

In the metathesis reactions under investigation, solutions of two different *cis*-Pd(L-S,O)₂ complexes are mixed – in the case of these rate studies, *cis*-Pd(L³-S,O)₂ and *cis*-Pd(L⁴-S,O)₂. Each solution was allowed to age individually, so upon mixing, two different unbound ligands are potentially present in the solution. The simplest scenario assumes that equal amounts of both ligands have been released into solution as aging occurs.



However, due to slight structural differences in the ligands, this may not be strictly accurate. Therefore this investigation included, both a 50/50 (mole ratio) mixture of HL³ and HL⁴ (Figure 4.8 adjacent) as well as each unbound ligand individually.

Additionally, it was necessary to determine whether the unbound ligand actively participated in the reaction or whether it acted in a purely catalytic role, increasing the rate of the reaction without actually being consumed during the reaction (see Section 4.2.3.1).^[116]

The effect of unbound ligand on the rate of the metathesis of $cis\text{-Pd}(\text{L-S},\text{O})_2$ complexes was studied by adding a solution of unbound ligand to the freshly-prepared complex solutions. Fresh solutions were used in order to minimise the amount of unbound ligand present due to solvation or dissociation. Aliquots of the unbound ligand solutions were added to the mixtures of 400 μM $cis\text{-Pd}(\text{L}^3\text{-S},\text{O})_2$ and $cis\text{-Pd}(\text{L}^4\text{-S},\text{O})_2$ solutions to obtain 1.25, 2.5, 5 and 10 mol% unbound ligand in the reaction mixtures. By way of explanation, 100 μl of an 800 μM unbound ligand solution (0.08 μmoles of ligand) was added to 1 ml of each of the 400 μM $cis\text{-Pd}(\text{L}^3\text{-S},\text{O})_2$ and $cis\text{-Pd}(\text{L}^4\text{-S},\text{O})_2$ solutions (0.4 μmoles of each $cis\text{-Pd}(\text{L-S},\text{O})_2$ complex). In other words, the reaction mixture contains 0.08 μmoles of unbound ligand for every 0.8 μmol of complex, or a ratio of 10 mol%.

The data for the metathesis reaction after addition of a 50/50 (mole ratio) mixture of HL^3 and HL^4 is summarised in Figure 4.9 on the following page. The small peaks at around 1.8 minutes retention time were identified by LC-MS as the unbound ligand. The first chromatogram, obtained directly after mixing ($t = 0$ hours), as well as the equilibrium chromatogram and time taken to reach equilibrium is shown. The relative percentage of each compound is reported under the appropriate chromatogram. There was a slight favouring of the less polar $cis\text{-Pd}(\text{L}^3\text{-S},\text{O})_2$ complex (see Section 3.7 for more detail on this phenomenon).

While a fresh mixture of complexes without any added ligand takes two days to reach equilibrium (see Section 3.4), these mixtures reached equilibrium within two hours or less. The addition of unbound ligand significantly accelerated the metathesis reaction and doubling the amount of unbound ligand almost exactly halved the time required to reach equilibrium. When 1.25 mol% of the mixture of unbound HL^3 and HL^4 was added, the metathesis system took two hours to reach equilibrium. In doubling the amount of unbound ligand to 2.5 mol%, equilibrium was reached within only one hour. With 5 mol% the system was at equilibrium within half an hour and when 10 mol% was added, the system required only 20 minutes to reach equilibrium. (As chromatograms could only be recorded at 10 minute intervals, it is possible that the 10 mol% system may have already attained equilibrium after 15 minutes.)

(Continued on page 116)

mol% unbound ligand added				Figure 4.9. Data from addition of 50/50 (mole ratio) mixture of HL ³ and HL ⁴ solution to the mixture of Pd(L ³) ₂ and Pd(L ⁴) ₂ .											
				1.25 mol%			2.5 mol%			5 mol%			10 mol%		
Chromatogram (t = 0)															
				% Distribution			47.17	5.03	47.80	44.85	9.26	45.89	41.07	15.39	43.54
Pd(L ⁴) ₂	Pd(L ³)(L ⁴)	Pd(L ³) ₂													
Chromatogram (equilibrium)															
				Time taken to reach equilibrium			2 hours			1 hour			30 minutes		
% Distribution				20.88	54.57	24.55	20.44	55.13	24.41	19.65	55.84	24.51	21.74	54.92	23.34

(Continued from page 114.)

The data for the metathesis reactions after addition of the individual ligand solutions – HL^3 or HL^4 respectively – is summarised below in Table 4.1 with a graph of the data for HL^4 plotted in Figure 4.10.

Table 4.1. Data for the acceleration of the reaction upon addition of the individual unbound ligand solutions.

		mol% unbound ligand added							
		1.25 mol%		2.5 mol%		5 mol%		10 mol%	
		% distribution	t = 0	equilibrium 1.5 hrs	t = 0	equilibrium 40 mins	t = 0	equilibrium 20 mins	t = 0
HL^3	Pd(L4) ₂	45.97	19.35	43.30	19.11	36.00	17.68	30.08	15.86
	Pd(L4)(L3)	5.57	54.89	9.39	55.03	19.72	54.55	26.97	54.24
	Pd(L3) ₂	48.46	25.76	47.31	25.86	44.28	27.77	42.95	29.90
HL^4	% distribution	t = 0	equilibrium 3 hrs	t = 0	equilibrium 1.5 hrs	t = 0	equilibrium 40 mins	t = 0	equilibrium 20 mins
	Pd(L4) ₂	47.61	19.72	46.37	20.94	43.49	19.89	40.43	21.03
	Pd(L4)(L3)	3.77	57.84	6.22	55.05	11.39	55.99	18.62	55.60
	Pd(L3) ₂	48.62	22.44	47.41	24.01	45.12	24.12	40.95	23.37

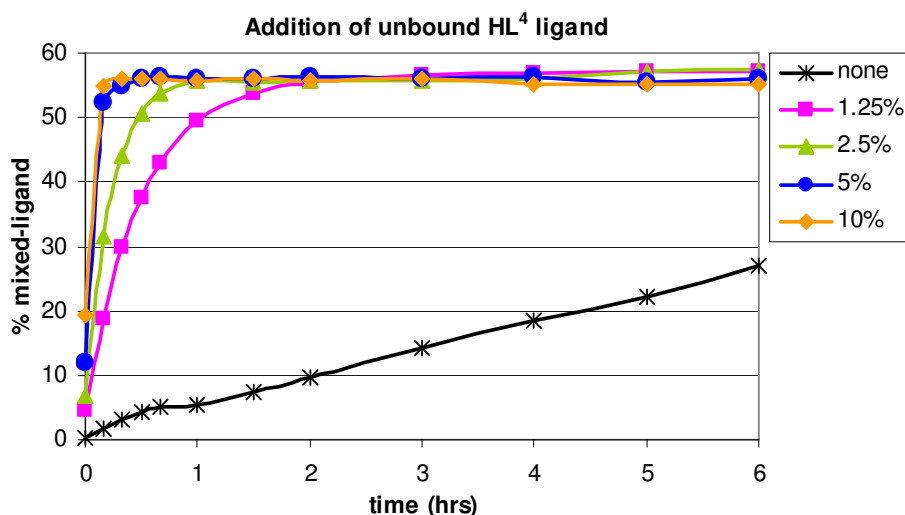


Figure 4.10. The effect of unbound HL^4 ligand added to a mixture of freshly dissolved $Pd(L^3)_2$ and $Pd(L^4)_2$ solutions. The graph shows the data for the first 6 hours of reaction.

It is interesting to note that the metathesis of complexes with added HL^3 ligand reached equilibrium within approximately half the time of those containing HL^4 ligand. This may be due to the favouring of the less polar HL^3 ligand and *cis*- $Pd(L^3-S,O)_2$ complex in the

polar acetonitrile solution (see Section 3.6 for more detail). The times required to reach equilibrium for the mixture of the two ligands lie exactly between those for the individual ligand systems. For example, the 5 mol% HL³ and HL⁴ mixture required 30 minutes to reach equilibrium, compared with 20 minutes (HL³) and 40 minutes (HL⁴) respectively for the individual ligand solutions.

It is clear that the addition of traces of unbound ligand to the reaction mixtures significantly increased the rate of the metathesis reaction. Traces of unbound ligand were observed in the LC-MS data for solutions made from the less pure complexes (see Figure 2.3 on page 42) and in solutions left to age for extended periods (see Figure 3.10 on page 75). This may help to explain the erratic trends observed in the initial unsuccessful concentration effect experiment discussed in Section 4.2.1.1 as well as offer an insight into the slight acceleration of the reaction

4.2.3.1 Addition of a different unbound ligand

When the added unbound ligand corresponds to one or both of the complexes in solution, it cannot be determined from the chromatograms whether the unbound ligand is acting merely as a catalyst or whether it is actively taking part in the reaction. In order to determine a possible mechanism, a ligand HL^C, which forms a Pd(II) complex with a substantially different retention time to *cis*-Pd(L^A)₂ and *cis*-Pd(L^B)₂ must be added to the solution.

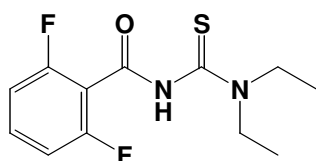


Figure 4.11. HL⁶ ligand.

The complexes *cis*-Pd(L³-S,O)₂ and *cis*-Pd(L⁴-S,O)₂ have retention times of 3.7 and 5.0 minutes respectively when eluted with 100 % acetonitrile, making HL⁶ (Figure 4.11 adjacent) and its corresponding complex, *cis*-Pd(L⁶-S,O)₂ (which has a retention time of 2.6 minutes) ideal for this investigation.

The data from this experiment is plotted in Figure 4.12 on the following page. The HL⁶ ligand produced much the same acceleration in the metathesis reaction as did addition of HL⁴ (Figure 4.10), with the solutions containing 1.25 mol% and 2.5 mol% HL⁶ reaching equilibrium within the same three hour and 1.5 hour time-periods respectively. In contrast to the other unbound ligand experiments, the 5 mol% and 10 mol% solutions did not fit strictly into the “doubling the unbound ligand halves time to equilibrium”-

pattern, requiring one hour (5 mol%) and 30 minutes (10 mol%) respectively to reach equilibrium. A possible reason for this observation is discussed on page 119.

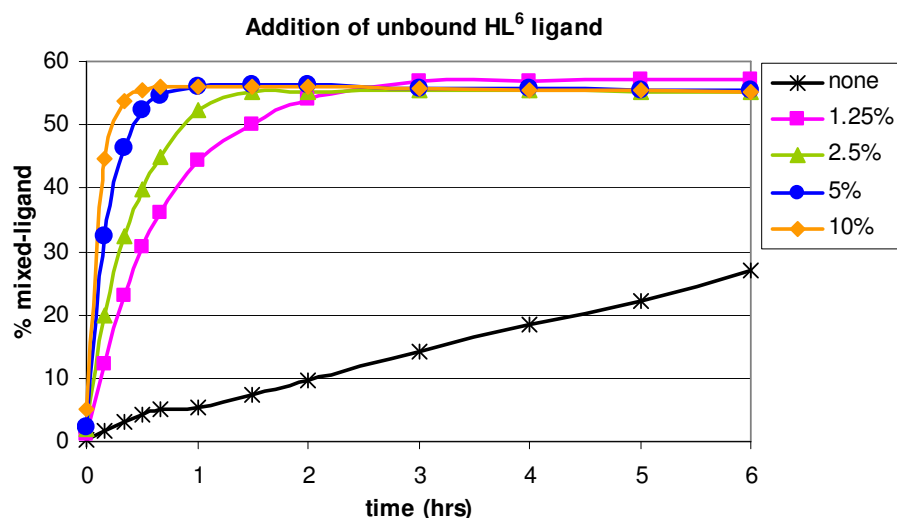


Figure 4.12. The effect of unbound HL^6 ligand added to a mixture of freshly dissolved $\text{Pd}(\text{L}^3)_2$ and $\text{Pd}(\text{L}^4)_2$ solutions. The percentage $\text{Pd}(\text{L}^3)(\text{L}^4)$ formed is plotted.

Figure 4.13 shows the chromatogram obtained immediately after mixing $\text{cis-Pd}(\text{L}^3\text{-S},\text{O})_2$, $\text{cis-Pd}(\text{L}^4\text{-S},\text{O})_2$ and 10 mol% HL^6 solution (chosen for clarity). The section between 2.8 and 3.7 minutes retention time has been enlarged to show the two mixed-ligand species, $\text{Pd}(\text{L}^4)(\text{L}^6)$ and $\text{Pd}(\text{L}^3)(\text{L}^6)$. The presence of these species indicate that the unbound ligand does, in fact, take part in the reaction from the outset.

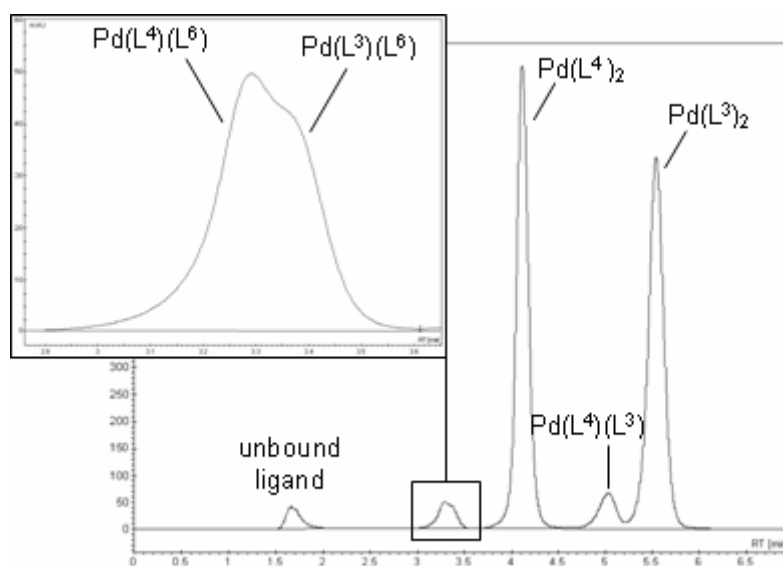


Figure 4.13. Chromatogram immediately after mixing $\text{Pd}(\text{L}^3)_2$ and $\text{Pd}(\text{L}^4)_2$ solutions with 10 mol% HL^6 solution.

In the higher concentration solutions (5 mol% and 10 mol% HL⁶), there was sufficient unbound HL⁶ ligand present in solution to form trace amounts of the *cis*-Pd(L⁶-S,O)₂ complex within the first few seconds of the reaction. At equilibrium, the peak corresponding to *cis*-Pd(L⁶-S,O)₂ was clearly visible on the chromatogram as can be seen in Figure 4.14, which shows an expansion of the region between 2.5 and 4.0 minutes retention time. The chromatogram of the 10 mol% solution was chosen for clarity, as the peak was most pronounced in the solution with the highest concentration unbound HL⁶ ligand.

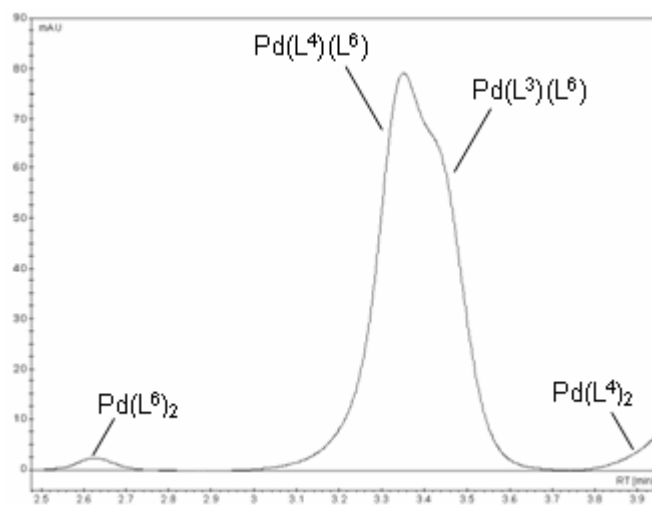
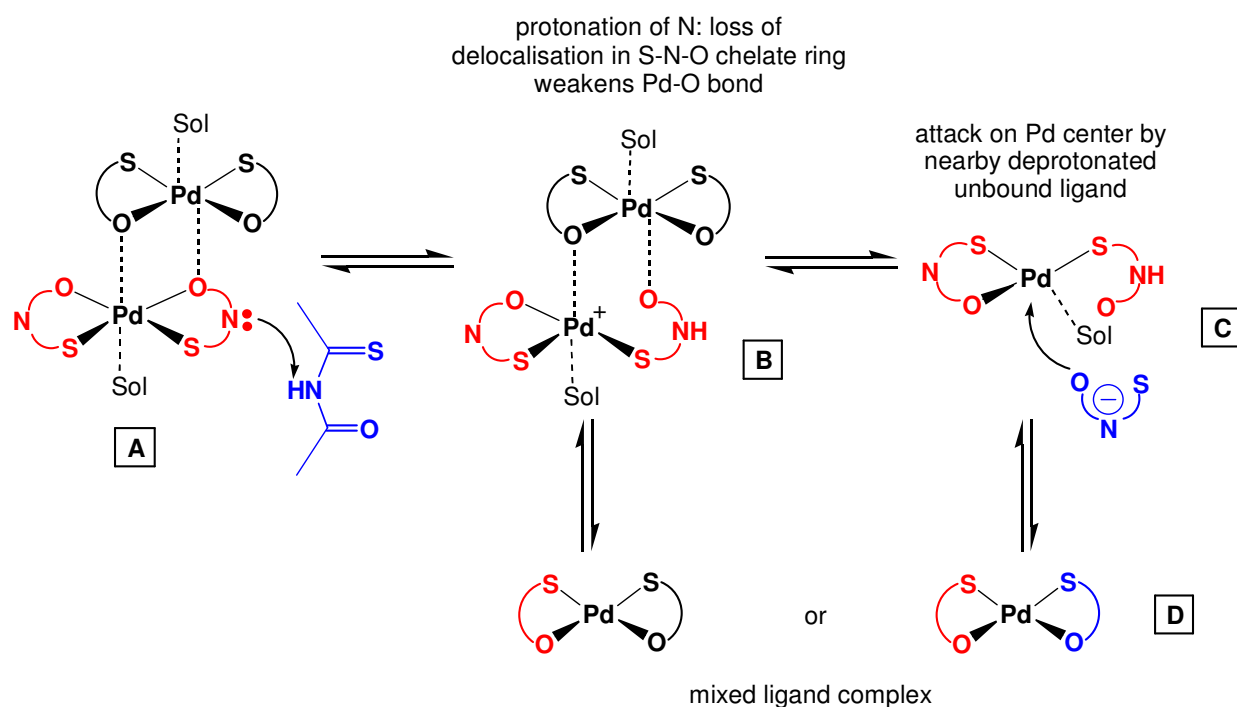


Figure 4.14. Expansion (2.5 – 4 mins t_R) of the equilibrium chromatogram of the mixture of Pd(L³)₂ and Pd(L⁴)₂ solutions with 10 mol% HL⁶ solution.

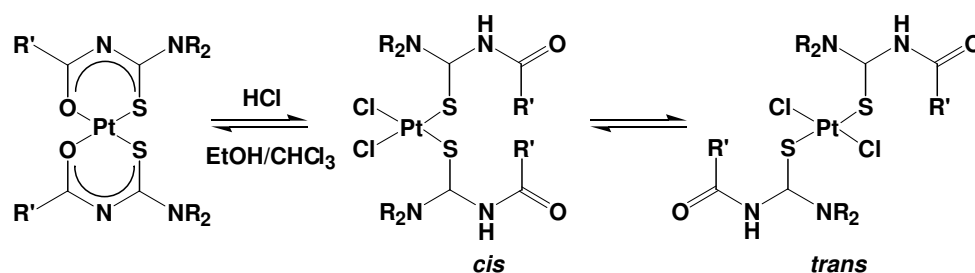
The formation of the *cis*-Pd(L⁶-S,O)₂ complex may help to explain the slightly slower rate of formation of the mixed-ligand Pd(L⁴-S,O)(L³-S,O) complex in the 5 and 10 mol% solutions of HL⁶ when compared to the corresponding HL⁴ solutions as mentioned on page 118 (Figure 4.10 and Figure 4.12). Less of the mixed-ligand Pd(L⁴-S,O)(L³-S,O) complex can form if there is competition between the chelate metathesis reaction of *cis*-Pd(L³-S,O)₂ and *cis*-Pd(L⁴-S,O)₂ and the formation of the *cis*-Pd(L⁶-S,O)₂ complex (see Scheme 4.2).

The fact that the unbound ligand actively participates in the reaction from the outset and does not merely act as a catalyst allows for the postulation of a mechanism for the acceleration of the metathesis reaction in the presence of unbound ligand as shown in Scheme 4.2 on the following page. (Please also refer to Scheme 3.1 on page 93)



Scheme 4.2. Proposed simplified mechanism for the acceleration of the reaction due to unbound ligand.

In this proposed mechanism, a proton-exchange occurs between the nitrogen atom of a complexed ligand and the protonated nitrogen atom of an unbound ligand (A in Scheme 4.2). This unbound ligand may be either a ligand corresponding to one of the two complexes present in solution, or a different *N,N*-dialkyl-*N'*-acyl(aryl)thiourea ligand. The protonation of the complexed ligand results in a loss of delocalisation in the chelate ring and a subsequent weakening of the Pd-O bond (B in Scheme 4.2). The bond between Pd and O is not as strong as a corresponding bond between Pd and S.^[111] It has also been shown that when a complexed ligand of a (*N,N*-dialkyl-*N'*-acyl(aryl)thioureato)Pt(II) complex is protonated by a strong acid such as HCl, the metal-oxygen bond is broken, while the metal-sulphur bond remains intact (Scheme 4.3). The vacant positions in the coordination sphere of Pt(II) are occupied by chloride ions.^[91, 92]



Scheme 4.3. The effect of addition of concentrated HCl to a solution of *cis*-Pt(L-S,O)₂.^[91, 92]

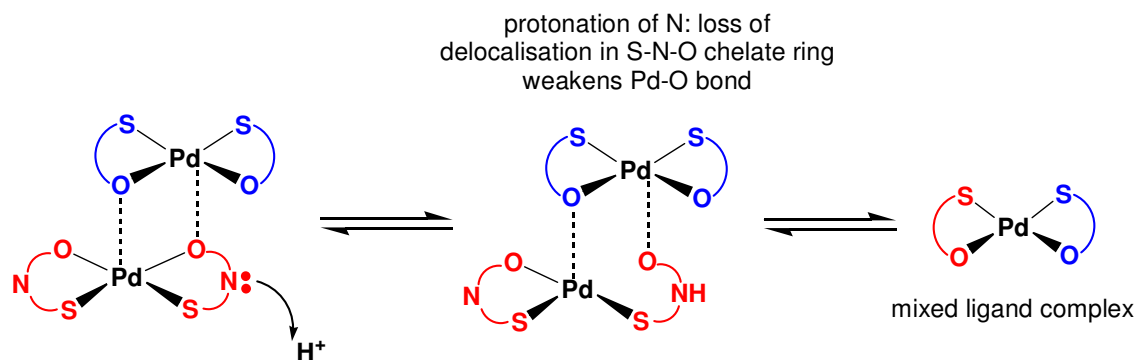
At this stage, there are two possible paths which may be followed. Either the deprotonated unbound ligand can directly attack the Pd(II) centre (C in Scheme 4.2) or the two associated Pd(II) complexes can exchange their complexed ligands (D in Scheme 4.2) as was seen in Scheme 3.1 on page 93.

The postulation of this mechanism raises the question as to whether the acceleration of the metathesis reaction was due to the specific interactions between the complex and the unbound ligand (Scheme 4.2) or whether a similar acceleration could be obtained through merely the addition of protons from a Brønsted acid (such as acetic acid).

4.2.4 The effect of the addition of a Brønsted acid

As with the study of the effect of unbound ligand on reaction rate, solutions of 1.25, 2.5, 5 and 10 mol% acetic acid in acetonitrile were added to the mixtures of 400 μM *cis*-Pd(L³-S,O)₂ and *cis*-Pd(L⁴-S,O)₂ solutions. Acetic acid was chosen above a mineral acid such as HCl, as these strong acids are known to protonate the complexed ligands, leading to mixtures of *cis* and *trans* [M^{II}(HL-S)(L-S,O)Cl] and [M^{II}(HL-S)₂Cl₂] species in solution (see Scheme 4.3).^[91, 92] It was not possible to measure the pH of the acid solutions as the concentrations of acid were too low (10 to 80 μM) to be detected by the instruments available.

If the acceleration in the metathesis reaction is, indeed, due to the presence of protons in solution, the mechanism will be similar to that discussed in Section 4.2.3.1. The nitrogen atom of the complexed ligand abstracts a proton from the solution, leading to a loss of delocalisation in the chelate ring and a weakening of the Pd-O bond. The weakening of this bond promotes the exchange of ligands between the associated complexes, allowing the formation of two equivalents of mixed-ligand complex (Scheme 4.4 on the following page).



Scheme 4.4. Possible mechanism for the acceleration of the reaction due to protons.

However, when the data from this experiment is plotted (Figure 4.15), only the higher concentrations of acid (5 and 10 mol%) appeared to accelerate the reaction, with the solutions reaching equilibrium in six and 12 hours respectively. When 1.25 or 2.5 mol% acid was added however, the metathesis reaction was actually slowed down, requiring 72 hours to reach equilibrium – 24 hours longer than a reaction mixture with no acid added.

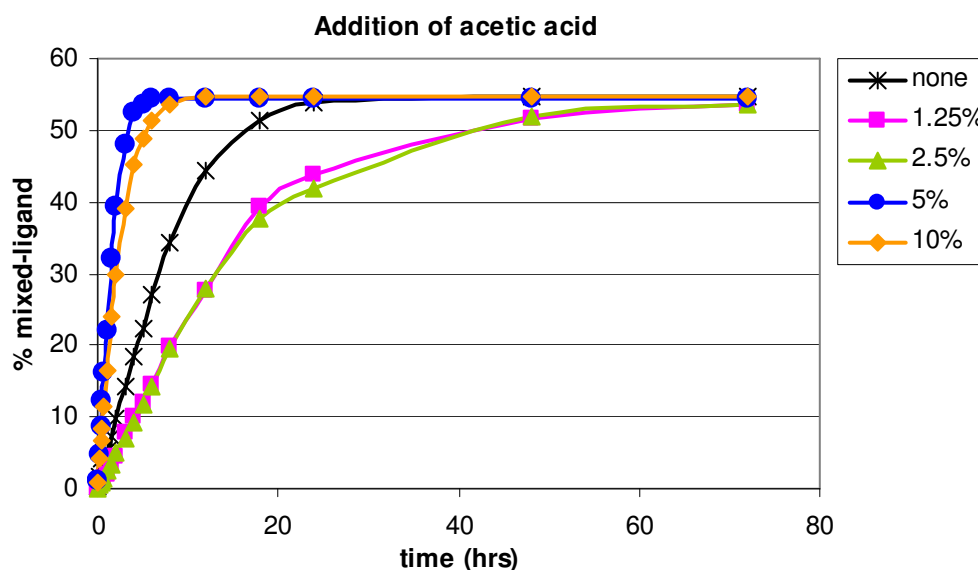


Figure 4.15. The effect of acid added to a mixture of freshly dissolved $\text{Pd}(\text{L}^3)_2$ and $\text{Pd}(\text{L}^4)_2$ solutions.

The reaction mixtures containing higher concentrations of added acetic acid did indeed exhibit the acceleration in reaction postulated by the mechanism in Scheme 4.4 although the effect of added acid was not as dramatic as that observed in the addition of unbound ligand. This is presumably due to the fact that in the latter case, the deprotonated unbound ligand in the vicinity of the Pd(II) centre can immediately attack and replace a complexed ligand (C in Scheme 4.2). Acetate ions – oxygen donor

ligands – will not bind strongly to Pd(II).^[111] Additionally, the acceleration in reaction may in part have been due to a slight increase in the donating ability of the solvent. Acetic acid may, in itself, also be considered a solvent and has a donor number (D_N) of $20.0 \text{ kcal.mol}^{-1}$, compared to the $14.1 \text{ kcal.mol}^{-1}$ of acetonitrile.^[99] In Section 3.6, it was shown that the higher the donor number of a solvent, or mixture of solvents, the faster the metathesis reaction.

However, when a lower concentration of acid was added (1.25 and 2.5 mol%), the metathesis reaction was slowed, indicating a different process at work. It is possible, in the light of the mechanisms postulated in Scheme 4.2 and Scheme 4.4, that the metathesis reaction between *cis*-Pd(L-S,O)₂ complexes may be either initiated or catalysed by the protons from the traces of acid or water which are inevitably to be found in even the purest solvent; or by the traces of unbound ligand present in the compounds even after numerous recrystallisations (see Section 2.1.2). The slower rate of the metathesis reaction could perhaps be due to the interaction of an added component (such as acetic acid in this case) with the water, acid or traces of unbound ligand in the solutions.

It is known that acetic acid can form dimers (Figure 4.16 adjacent), both in the gas phase and in aprotic solvents.^[121] As the pK_a of acetic acid in acetonitrile is 21.57^[122] (compared to 4.76 in water^[123]), dissociation of the acid molecules into H^+ and CH_3COO^- ions is not favoured and most of the molecules will be bound in dimers.

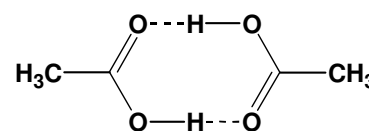


Figure 4.16. Acetic acid dimer.

However, it has been shown that water molecules can be incorporated into this dimer through hydrogen bonds by initiating the breaking of one of the $O-H\cdots O$ bonds in the dimer.^[121] These bound water molecules are now unable to supply the protons which may have assisted in initiating or catalysing the metathesis reaction. It may also be possible that the acetic acid molecules can hydrogen-bond to the thioamidic proton of an unbound *N,N*-dialkyl-*N'*-acyl(aryl)thiourea ligand. By trapping the unbound ligand within hydrogen bonds, the acetic acid effectively prevents the ligand from initiating or catalysing the metathesis reaction (as was seen in Section 4.2.3).

4.2.5 The effect of the addition of a Brønsted base

As the addition of acid had an effect on the rate of the reaction, it was decided to investigate the effect of base. Sodium acetate was chosen as it was used during the synthesis of the *cis*-Pd(L-S,O)₂ compounds (Section 2.1.2) and traces may remain in the compounds if they are not purified sufficiently. Again, as in the unbound ligand and acid experiments, solutions of sodium acetate dissolved in acetonitrile were added to mixtures of fresh solutions of the metal complexes obtain base:complex ratios of 1.25, 2.5, 5 and 10 mol%.

In general, the effect of base on the rate of the metathesis reaction was not as striking as that of either acid or unbound ligand (Figure 4.17). The acceleration in the rate of metathesis for the solutions containing higher concentrations of base (5 and 10 mol%) was negligible. The reaction mixture containing 2.5 mol% base showed a similar results to the corresponding 2.5 mol% acid solution. When a 1.25 mol% solution of base was added however, a severe retardation of the rate of metathesis was observed (the magenta curve in Figure 4.17).

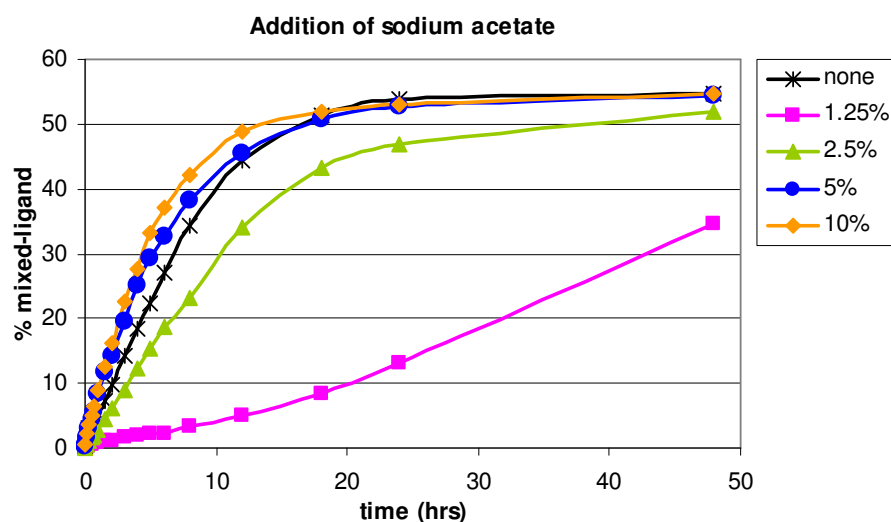
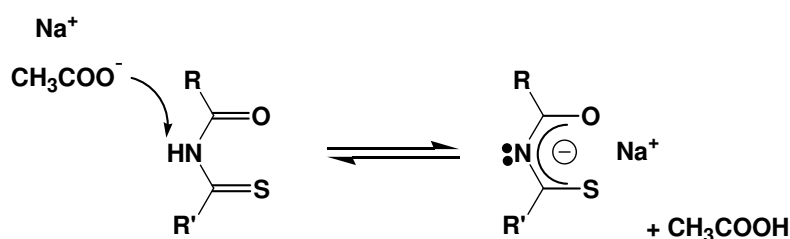


Figure 4.17. The effect of base added to a mixture of freshly dissolved Pd(L³)₂ and Pd(L⁴)₂ solutions.

The minor acceleration in the metathesis reaction when the higher concentrations of base were added may be due to the slight increase in the donating ability of the solvent imparted by the base (see Section 4.2.4 above).

The deceleration in the metathesis reaction may be, again, due to the interaction between the added base and the traces of water, acid or unbound ligand in the solution. The Arrhenius theory of dissociation states that the lower the concentration of an electrolyte, the more molecules are dissociated.^[124] It is known from the synthesis of the *N,N*-dialkyl-*N'*-acyl(aryl)thiourea complexes (see Section 2.1.2) that the negatively-charged CH_3COO^- ions of the sodium acetate readily deprotonate thiourea ligands, resulting in uncharged acetic acid (see Section 4.2.4 above) and a negatively charged deprotonated thiourea ligand (Scheme 4.5). However, as acetonitrile cannot solvate ions well,^[123] the negatively charged ligand could possibly ion-pair with the positively charged Na^+ ions. Though no known complex of this type has been reported, its formation in acetonitrile is plausible.



Scheme 4.5. One possible mechanism for the deceleration of the reaction upon addition of base.

A similar mechanism is possible with traces of acid or water. The deprotonation and ion-pairing mechanism effectively removes any source of protons from the reaction, effectively preventing the initiation or catalysis of the metathesis reaction by protons. A possible reason why the deceleration was more pronounced in the low concentration base solutions in relation to the acid solutions, is that the forces between charged particles (as in the ion pairing in the base mechanism) are stronger than the dipole-dipole interaction that makes up a hydrogen-bond (as in the hydrogen-bonding in the acid mechanism).^[124]

4.3 Metathesis and the photoisomerisation reaction

When a solution of a *cis*-bis(*N,N*-dialkyl-*N*-acyl(aro)ylthioureato)M(II) complex (where M = Pd(II) or Pt(II)) is exposed to intense light, a photoinduced *cis* to *trans* isomerisation occurs.^[45] Left in the dark, the *trans* complexes revert back to the *cis* configuration exclusively within a period of time. This process is readily observed with *rp*-HPLC as seen in Figure 4.18 which shows overlaid chromatograms of an irradiated solution of *cis*-bis(*N,N*-diethyl-*N*'-3,5-dimethoxybenzoylthioureato)Pd(II) (*cis*-Pd(L³-S,O)₂) from t = 0 (directly after removal of the intense light source); to t = 18 hours, by which time all *trans* complexes had reverted back to *cis*.

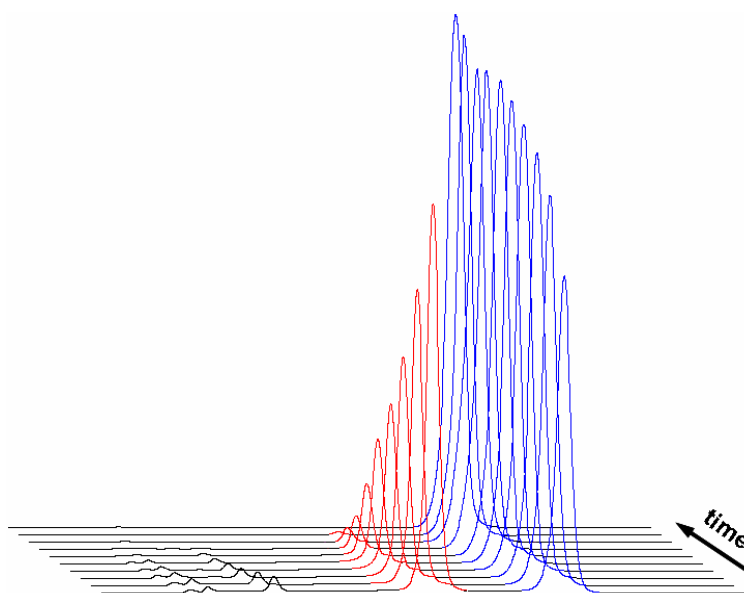


Figure 4.18. Overlaid chromatograms of the reversion of *trans*-Pd(L³)₂ (red) to *cis*-Pd(L³)₂ (blue) in the dark after one hour of irradiation. Possible photodecomposition products are observed between 1.5 and 3 minutes retention time. This system required 18 hours to revert back to the *cis* complex exclusively.

A number of additional peaks were observed between 1.5 and 3 minutes retention time on the chromatogram. These smaller peaks diminished with time and, along with the *trans* peak, were no longer detectable after 18 hours. This indicated that these smaller peaks could be photodecomposition products. Though the identity of these peaks need to be confirmed by LC-MS analysis, a comparison of the retention times of the photodecomposition peaks with known species in solution indicated that one of the decomposition products may be unbound ligand (which had a retention time of around 1.8 minutes under the current LC conditions).

It was postulated in Section 1.3 (see Figure 1.19 on page 28), that the reverse *trans* to *cis* reaction (in the dark) of the *cis-trans* isomerisation of *cis*-M(L-S,O)₂ complexes^[45] may be a metathesis reaction (Figure 4.19).

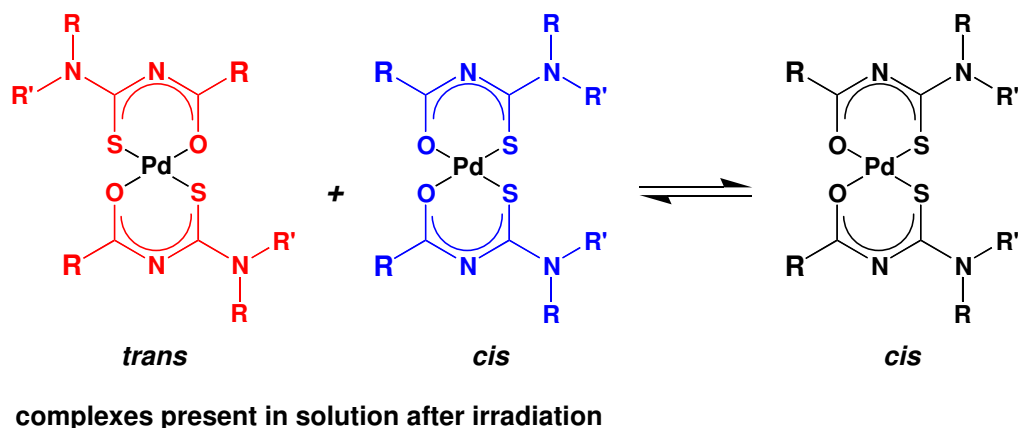


Figure 4.19. Reverse *trans* to *cis* reaction in the dark, postulated as a metathesis reaction.

In this hypothesis, the *trans* and *cis* species in solution (after irradiation) interact in much the same way as the two parent complexes in a chelate metathesis reaction. The complexes exchange bound ligands, but, as the *cis* configuration is thermodynamically favoured, the resulting product is a *cis* complex. (Density functional theory (DFT) calculations have confirmed the greater thermodynamic stability of the *cis* configuration.^[125])

If it is indeed the case that the reverse reaction is a metathesis process, then the rate of the reverse *trans* to *cis* reaction should be affected by the same factors as chelate metathesis reactions.

It was shown in Sections 4.2.3 and 4.2.4 that the presence of unbound ligand or sufficient acetic acid in the reaction mixture significantly accelerated chelate metathesis between two different *cis*-Pd(L-S,O)₂ complexes. With this in mind, four vials of a freshly-prepared *cis*-Pd(L³-S,O)₂ acetonitrile solution were irradiated with intense white light (150W quartz-halogen lamp from a conventional slide projector) for one hour before being covered in aluminium foil to restrict further exposure to light and placed in the sample tray of the HPLC system. The samples were monitored, in the dark, until the peak corresponding to the *trans* species could no longer be detected and only the *cis* peak remained on the chromatogram. (*cis*-Pd(L³-S,O)₂ was chosen as previous experiments indicated this compound gave the best separation of the *cis* and *trans*

species under 100 % acetonitrile elution conditions.^[126] To three of the *cis*-Pd(L³-S,O)₂ samples, 10 mol% aliquots of the known accelerants were added – unbound HL³ ligand either before or after irradiation, or acetic acid after irradiation.

The results from this set of experiments are summarised in Figure 4.20 below. . For clarity, only the area between t = 0 to 6 hours is displayed. The time required for each sample to revert back to solely the *cis* complex is colour-coded in the inset. (The percentage *trans* complex present at each time interval (y-axis) was calculated using a similar procedure to that described in Section 2.3.1, though in this case, using the calibration data and difference in area of the *cis* peak at the two detection wavelengths.)

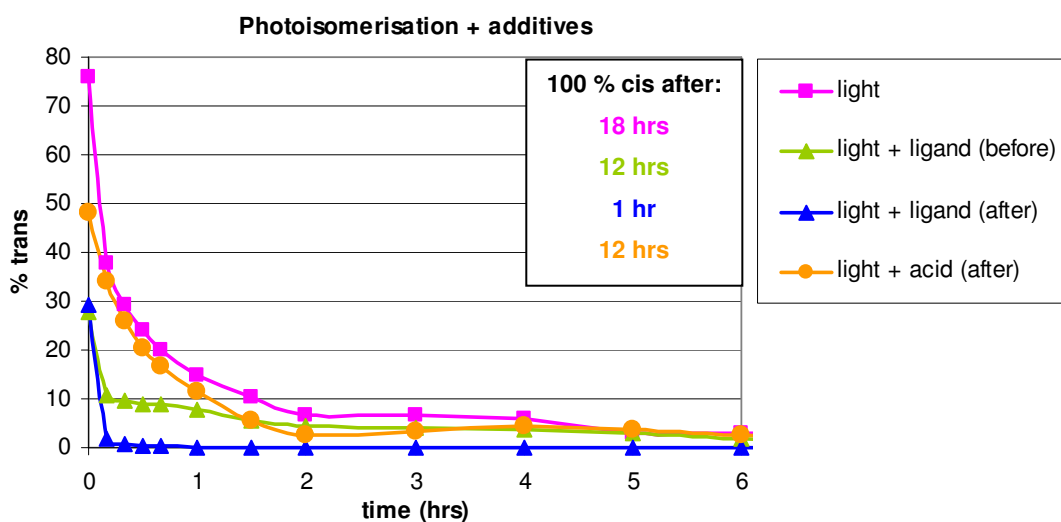


Figure 4.20. The reversion of *trans*-Pd(L³)₂ to *cis*-Pd(L³)₂ over time.

The area between 0 and 6 hours on the graph has been expanded and the time required for all *trans* to revert to *cis* for each experiment, colour-coded in the inset.

In the absence of any additives (magenta curve in Figure 4.20), 75.91 % of the *cis*-Pd(L³-S,O)₂ complexes isomerised to the *trans* species after irradiation and the solution required around 18 hours to revert back to the *cis* species exclusively (see Figure 4.18). These results differ somewhat from those previously obtained,^[45, 126] most likely due to the fact that, in this case, a freshly-prepared solution of an extensively purified compound was used (see Sections 2.1.2.1 and 4.2.2).

In the solutions containing additives however, less *trans* complex was present initially, immediately after irradiation and these solutions reverted back to exclusively *cis* species within a shorter period of time (Figure 4.20).

Unbound HL³ ligand, added *after* irradiation (blue curve in Figure 4.20) had the greatest accelerating effect, with all *trans* complex having reverted to *cis* after only one hour. In contrast, in the solution to which unbound ligand had been added *before* irradiation (green curve in Figure 4.20), 12 hours were required for complete reversion of *trans* to *cis*. However, the relative percentage *trans* complex present initially ($t = 0$) was similar for both the solution to which the ligand had been added before irradiation (27.78 %) and that to which ligand had been added after irradiation (29.25 %).

In the light of these results, it is possible that the reverse *trans* to *cis* reaction (*sans* additives) may be initiated or catalysed by traces of unbound ligand liberated by the possible photodecomposition reactions. Additionally, it has been shown that Pd(L-S,O)₂ complexes can exchange their bound ligands with unbound ligands from solution (see Section 3.7) and it may be possible that a similar process could also play a role in the reverse *trans* to *cis* reaction both with and without the further addition of unbound ligand.

Due to the fact that the complexes can exchange bound ligands for unbound ligands from solution, a 10 mol% addition of acetic acid – which was shown to increase the rate of a chelate metathesis reaction (Section 4.2.4) – was made to one of the irradiated samples. As can be seen in the orange curve in Figure 4.20, only 48.08 % *trans* complex was present initially and the addition of acetic acid caused an increase in the rate of the *trans* to *cis* reaction. The acceleration was not as striking as that seen upon addition of unbound ligand, which is consistent with the results observed for the chelate metathesis reactions (Sections 4.2.3 and 4.2.4). The acceleration of the *trans* to *cis* reaction with the addition of acetic acid, however, lends some credence to the hypothesis that the reverse “dark” reaction could indeed be a chelate metathesis reaction.

Further, in-depth studies into the photoisomerisation/metathesis relationship are however, necessary. The difference in rate between the solutions to which unbound ligand was added before or after irradiation also requires investigation. Additionally, it will be beneficial to attempt to identify the transient photodecomposition products *via* LC-MS analysis.

Chapter 5

Concluding remarks and recommendations

5.1 Concluding remarks

A variety of *cis*-bis(*N,N*-dialkyl-*N*-acyl(aro)ylthioureato)Pd(II) complexes were easily synthesised in a one-pot procedure (Section 2.1.2) and fully characterised using melting point analysis, ^1H and ^{13}C NMR, elemental analysis and LC-MS (Section 2.1.3).

Six-membered chelate rings, such as those in the *cis*-M(L-S,O)₂ complexes (M = Ni(II), Pd(II) or Pt(II)) under investigation in this thesis, are generally considered to be amongst the most stable configurations in metal complexes.^[26] However, it was found that complexes of an assortment of *N,N*-dialkyl-*N*-acyl(aro)ylthiourea ligands readily undergo facile chelate metathesis reactions at room temperature in a variety of solvents. The mixed-ligand products of the metathesis reaction were observed in solution as well as in the solid state (Section 3.1). It was, however, unfortunately not possible to isolate or synthesise a mixed-ligand complex exclusively (Section 3.3).

The metathesis reactions reached a steady state or equilibrium between the two parent complexes and the mixed-ligand product after a certain period of time. Even with a ten-fold excess of one of the parent complexes, all three complexes – Pd(L^A)₂, Pd(L^B)₂ and Pd(L^A)(L^B) – were still to be found in solution (Section 3.5). With a one-to-one ratio of the two parent complexes, the extent of the reaction (equilibrium distribution) was affected by the substituents on the ligands (Section 3.4) as well as the reaction medium (Section 3.6). Both the extent and the rate of the metathesis reaction was promoted in more polar solvents with a higher Lewis basicity (represented by the donor number D_N). Acetonitrile and acetonitrile/alcohol mixtures gave the best results, but the metathesis reaction could be encouraged in solvents with a lower D_N through the addition of a trace of unbound ligand or dilution with acetonitrile (to a 50/50 v/v mixture).

In addition to the chelate metathesis reaction, the thiourea complexes also underwent ligand exchange between a complex and unbound ligand in both acetonitrile and toluene solutions (Section 3.7). Again, even with sufficient unbound ligand available in solution for all the complexes to exchange both ligands, all three complexes were still present in solution. This set of experiments revealed that the choice of solvent determined which complex is favoured in solution. In identical experiments performed in polar acetonitrile and in non-polar toluene, it was found that the more polar *cis*-bis(*N,N*-diethyl-*N*-3,4,5-trimethoxybenzoylthioureato)Pd(II) complex was favoured in

non-polar toluene, while the less polar *cis*-bis(*N,N*-diethyl-*N*-3,5-dimethoxybenzoylthioureato)Pd(II) was favoured in polar acetonitrile. Additionally, NMR experiments revealed that the thiourea complexes can undergo exchange with their identical (¹³C-labeled) ligand in solution (Section 3.7.1).

The relative rate of the metathesis reaction between *cis*-Pd(L-S,O)₂ complexes was affected by a number of factors. The rate varied predictably with the known lability of the central metal ion – Pd(II) > Pt(II) (Section 3.2), while the substituents on the complexed ligands (Section 3.4) and the reaction medium (Section 3.6) also played a role in the rate of reaction. In a more polar, more donating solvent system (higher D_N), the metathesis reaction was more rapid. In addition, a number of unanticipated effects played a role in the metathesis reaction, which suggested that the reaction is not as straightforward as originally assumed. Certain effects were intuitive, such as the effect of concentration – the rate of reaction increased with increasing concentration (Section 4.2.1). Other effects were unexpected, such as the effect of the “age” of the solutions upon mixing (Section 4.2.2) – the rate of reaction increased with increasing age of the solutions, reaching a maximum after three days aging time.

Additives and/or impurities present in solution also had an effect on the relative rate of the metathesis reaction. The most notable was the presence of small quantities of unbound ligand. In this context, four different combinations of unbound ligand were investigated (Section 4.2.3) along with a simple Brønsted acid and base (Sections 4.2.4 and 4.2.5). All concentrations of added unbound ligand accelerated the reaction with a similar effect observed for additions of 5 or 10 mole% solutions of acid or base. Lower concentrations of acid or base caused a decrease reaction rate relative to a solution without any added acid or base. Mechanisms were postulated for the acceleration of the reaction due to unbound ligand and acid. The investigations into reaction rate highlighted the importance of especially pure complexes, which lead to the strong focus on purification and many successive recrystallisations of the synthesised complexes (Section 2.1.2.1).

Preliminary studies indicated that the chelate metathesis reactions for these *cis*-M(L-S,O)₂ complexes may hold significant implications for the *trans* to *cis* isomerisation of such Pd(II) and Pt(II) complexes following their photoinduced isomerisation from *cis* to *trans* (Section 4.3).^[45]

5.2 Recommendations for further study

The studies discussed in this thesis have shed some light on a number of factors which influence the chelate metathesis reactions between *cis*-M(L-S,O)₂ complexes in solution. However, certain aspects will require further study in order to fully understand all the processes and mechanisms involved in this multifaceted reaction.

Firstly, in order to study the mixed-ligand product complexes in more detail, preparative chromatography, utilising a large-bore reversed-phase column and fraction collector must be investigated as a means to separate these complexes from the reaction mixture.

The equilibrium distributions observed in the study into the effect of ligand substituents on the metathesis reaction (Section 3.4), requires a more in-depth investigation to clarify the trends observed. In addition, an investigation into the effect of temperature on the metathesis reaction would be beneficial as preliminary NMR studies have indicated a correlation between temperature and the rate of the metathesis reaction. Additionally, further investigation into the deceleration of the chelate metathesis reaction upon addition of small quantities (1.25 or 2.5 mol%) of a Brønsted acid or base (Sections 4.2.4 and 4.2.5) requires further investigation. A study into the effect of uncomplexed metal ions on the rate of reaction may also give some insight to the mechanism of reaction.

The relationship between chelate metathesis and the *cis-trans* photoisomerisation reaction (Section 4.3) also requires additional study, including the possible identification of the photodecomposition products.

References

- [1] *IUPAC Compendium of Chemical Terminology, Electronic Edition*, copyright IUPAC, **2007**, <http://goldbook.iupac.org/M03878.html>, accessed 25/04/2007, last updated 01/01/2007.
- [2] *Metathesis Reaction (Chemistry)*, copyright Wikipedia, [http://en.wikipedia.org/wiki/Metathesis_reaction_\(chemistry\)](http://en.wikipedia.org/wiki/Metathesis_reaction_(chemistry)), accessed 02/02/2007, last updated 31/01/2007.
- [3] A. M. Rouhi, *Chemical and Engineering News*, **2002**, (80), 29.
- [4] *Nobel Prize Winners 2005*, copyright Nobel_Web_AB, **2007**, <http://nobelprize.org/nobelprizes/chemistry/laureates/2005/>, accessed 05/05/2007, last updated 01/01/2007.
- [5] J. C. Lockhart and W. J. Mossop, *Journal of the Chemical Society: Dalton Transactions*, **1973**, 19.
- [6] J. C. Lockhart and W. J. Mossop, *Journal of the Chemical Society: Dalton Transactions*, **1973**, 662.
- [7] M. Moriyasu and Y. Hashimoto, *Bulletin of the Chemical Society of Japan*, **1980**, (53), 3590.
- [8] T. Ohya, K. Iwamoto and M. Sato, *Journal of the Chemical Society: Dalton Transactions*, **1985**, 987.
- [9] R.-M. Olk, W. Dietzsch, J. Kahlmeier, P. Jörchel, R. Kirmse and J. Sieler, *Inorganica Chimica Acta*, **1997**, (254), 375.
- [10] N. D. Yordanov and A. Dimitrova, *Inorganic Chemistry Communications*, **2005**, (8), 113.
- [11] R. Chant, A. R. Hendrickson, R. L. Martin and N. M. Rohde, *Inorganic Chemistry*, **1975**, (14), 1894.
- [12] A. Davison, J. A. McCleverty, E. T. Shawl and E. J. Wharton, *Journal of the American Chemical Society*, **1967**, (89), 830.
- [13] J. A. McCleverty, D. G. Orchard and K. Smith, *Journal of the Chemical Society: Inorganic, Physical, Theoretical*, **1971**, 707.
- [14] T. R. Miller and I. G. Dance, *Journal of the American Chemical Society*, **1973**, (95), 6970.
- [15] M. Moriyasu and Y. Hashimoto, *Bulletin of the Chemical Society of Japan*, **1981**, (54), 3374.
- [16] M. Moriyasu and Y. Hashimoto, *Chemistry Letters*, **1980**, 117.
- [17] O. Liška, G. Guiochon and H. Colin, *Journal of Chromatography*, **1979**, (171), 145.
- [18] O. Liška, J. Lehotay, E. Brandšteterová and G. Guiochon, *Journal of Chromatography*, **1979**, (171), 153.
- [19] A. L. Balch, *Inorganic Chemistry*, **1971**, (10), 388.
- [20] W. D. Kerber, D. L. Nelsen, P. S. White and M. R. Gagné, *Journal of the Chemical Society: Dalton Transactions*, **2005**, 1948.
- [21] A. C. Adams and E. M. Larson, *Inorganic Chemistry*, **1966**, (5), 228.
- [22] J. J. Fortman and R. E. Sievers, *Inorganic Chemistry*, **1967**, (6), 2022.
- [23] T. J. Pinnavaia and R. C. Fay, *Inorganic Chemistry*, **1966**, (5), 233.
- [24] T. J. Pinnavaia and S. O. Nweke, *Inorganic Chemistry*, **1969**, (8), 639.
- [25] T. Wang and P. C. Uden, *Journal of Chromatography*, **1990**, (517), 185.
- [26] A. E. Martell and R. D. Hancock, *Metal Complexes in Aqueous Solutions*, Plenum Press, New York, **1996**.
- [27] R. H. Holm, L. H. Pignolet and R. A. Lewis, *Journal of the American Chemical Society*, **1971**, (93), 360.
- [28] M. C. Palazzotto, D. J. Duffy, B. L. Edgar, L. Que and L. H. Pignolet, *Journal of the American Chemical Society*, **1973**, (95), 4537.
- [29] L. Que and L. H. Pignolet, *Inorganic Chemistry*, **1974**, (13), 351.
- [30] M. Moriyasu and Y. Hashimoto, *Analytical Letters*, **1978**, (A11), 593.
- [31] H. Sigel, *Angewandte Chemie, International Edition*, **1975**, (14), 394.
- [32] O. Liška, J. Lehotay, E. Brandšteterová, G. Guiochon and H. Colin, *Journal of Chromatography*, **1979**, (172), 379.
- [33] N. D. Yordanov and D. Shopov, *Inorganica Chimica Acta*, **1971**, (5), 579.
- [34] N. D. Yordanov and D. Shopov, *Journal of the Chemical Society: Dalton Transactions*, **1976**, 883.

- [35] A. Davison, N. Edelstein, R. H. Holm and A. H. Maki, *Journal of the American Chemical Society*, **1963**, (85), 2029.
- [36] A. L. Balch, I. G. Dance and R. H. Holm, *Journal of the American Chemical Society*, **1968**, (90), 1139.
- [37] C. Faulmann, J.-P. Legros, P. Cassoux, J. Cornelissen, L. Brossard, M. Inokuchi, H. Tajima and M. Tokomto, *Journal of the Chemical Society: Dalton Transactions*, **1989**, 249.
- [38] J. C. Wang and J. P. Fackler, *Acta Crystallographica, Section C*, **1989**, (45), 951.
- [39] J. Stach, R. Kirmse, U. Abram, W. Dietzsch, J. H. Noordik, K. Spee and C. P. Keijzers, *Polyhedron*, **1984**, (3), 433.
- [40] D. C. Olson and D. W. Margerum, *Journal of the American Chemical Society*, **1962**, (84), 680.
- [41] D. C. Olson and D. W. Margerum, *Journal of the American Chemical Society*, **1963**, (85), 297.
- [42] J. D. Carr and D. W. Margerum, *Journal of the American Chemical Society*, **1966**, (88), 1645.
- [43] D. W. Margerum and J. D. Carr, *Journal of the American Chemical Society*, **1966**, (88), 1639.
- [44] T. Katsuyama and T. Kumai, *Bulletin of the Chemical Society of Japan*, **1975**, (48), 3581.
- [45] D. Hanekom, J. M. McKenzie, N. M. Derix and K. R. Koch, *Chemical Communications*, **2005**, 767.
- [46] A. N. Mautjana, J. D. S. Miller, A. Gie, S. A. Bourne and K. R. Koch, *Journal of the Chemical Society: Dalton Transactions*, **2003**, 1952.
- [47] M. Tswett, *Berichte der Deutschen botanischen Gesellschaft*, **1906**, (24), 316.
- [48] M. Tswett, *Berichte der Deutschen botanischen Gesellschaft*, **1906**, (24), 385.
- [49] C. F. Poole and S. A. Schuette, *Contemporary practice of chromatography*, Elsevier, Amsterdam, **1984**.
- [50] H. Engelhardt, *High performance liquid chromatography - Chemical laboratory practice*, Springer-Verlag, Berlin, **1979**.
- [51] J. F. K. Huber and J. C. Kraak, *Analytical Chemistry*, **1972**, (44), 1554.
- [52] M. Lederer, *Chromatography for inorganic chemistry*, John Wiley & Sons Ltd, Chichester, **1994**.
- [53] P. Obergfell and H. Müller, *Fresenius Zeitschrift für Analytische Chemie*, **1987**, (314), 758.
- [54] R. I. Edwards, W. A. M. te Riele and G. J. Bernfeld, *Gmelin Handbook of Inorganic Chemistry, 8th edition, Supplemental Volume A1*, Springer-Verlag, Berlin, **1986**.
- [55] K. R. Koch, *Coordination Chemistry Reviews*, **2001**, (216-217), 473.
- [56] I. B. Douglass and F. B. Dains, *Journal of the American Chemical Society*, **1934**, (56), 719.
- [57] U. Bierbach and N. Farrel, *Journal of Inorganic Biochemistry*, **1995**, (59), 233.
- [58] A. Rodger, K. K. Patel, K. J. Sanders, M. S. Datt, C. Sacht and M. J. Hannon, *Journal of the Chemical Society: Dalton Transactions*, **2002**, 3656.
- [59] C. Sacht and M. S. Datt, *Polyhedron*, **2000**, (19), 1347.
- [60] C. Sacht, M. S. Datt, S. Otto and A. Roodt, *Journal of the Chemical Society: Dalton Transactions*, **2000**, 727.
- [61] R. del-Campo, J. J. Criado, E. Garcia, M. R. Hermosa, A. Jimenez-Sanchez, J. L. Manzano, E. Monte, E. Rodriguez-Fernandez and F. Sanz, *Journal of Inorganic Biochemistry*, **2002**, (89), 74.
- [62] E. Rodriguez-Fernandez, E. Garcia, M. R. Hermosa, A. Jimenez-Sanchez, M. M. Sanchez, E. Monte and J. J. Criado, *Journal of Inorganic Biochemistry*, **1999**, (75), 181.
- [63] T. Egan, K. R. Koch, P. L. Swan, C. Clarkson, D. A. v. Schalkwyk and P. J. Smith, *Journal of Medicinal Chemistry*, **2004**, (47), 2926.
- [64] Y.-S. Wu, K. R. Koch, V. R. Abratt and H. H. Klump, *Archives of Biochemistry and Biophysics*, **2005**, (440), 28.
- [65] P. Mühl, K. Gloe, F. Dietze, E. Hoyer and L. Beyer, *Zeitschrift für Chemie*, **1986**, (26), 81.
- [66] H. G. Berhe, S. A. Bourne, M. W. Bredenkamp, C. Esterhuysen, M. M. Habtu, K. R. Koch and R. C. Luckay, *Inorganic Chemical Communications*, **2006**, (9), 99.
- [67] A. Rether and M. Schuster, *Reactive and Functional Polymers*, **2003**, (57), 13.

- [68] P. Vest, M. Schuster and K. H. Koenig, *Fresenius Zeitschrift für Analytische Chemie*, **1989**, (335), 759.
- [69] M. Dominguez, E. Antico, L. Beyer, A. Aguirre, S. Garcia-Granda and V. Salvado, *Polyhedron*, **2002**, (21), 1429.
- [70] M. Merdivan, A. Gungor, S. Savasci and R. S. Aygun, *Talanta*, **2000**, (53), 141.
- [71] K.-H. König, M. Schuster, B. Steinbrech, G. Schneeweis and R. Schlodder, *Fresenius Zeitschrift für Analytische Chemie*, **1985**, (321), 457.
- [72] M. Schuster and M. Schwarzer, *Analytica Chimica Acta*, **1996**, (328), 1.
- [73] K.-H. König, M. Schuster, G. Schneeweis and B. Steinbrech, *Fresenius Zeitschrift für Analytische Chemie*, **1984**, (319), 66.
- [74] K.-H. König, M. Schuster, G. Schneeweis and B. Steinbrech, *Fresenius Zeitschrift für Analytische Chemie*, **1985**, (325), 321.
- [75] M. Schuster, *Fresenius Zeitschrift für Analytische Chemie*, **1992**, (342), 791.
- [76] M. Schuster, B. Kugler and K.-H. König, *Fresenius Zeitschrift für Analytische Chemie*, **1990**, (338), 717.
- [77] E. Unterreitmaier and M. Schuster, *Analytica Chimica Acta*, **1995**, (309), 339.
- [78] M. Schuster and E. Unterreitmaier, *Fresenius Zeitschrift für Analytische Chemie*, **1993**, (346), 630.
- [79] M. Schuster and M. Sandor, *Fresenius Zeitschrift für Analytische Chemie*, **1996**, (356), 326.
- [80] L. Beyer, E. Hoyer, J. Liebscher and H. Hartmann, *Zeitschrift für Chemie*, **1981**, (21), 81.
- [81] S. Bourne and K. R. Koch, *Journal of the Chemical Society: Dalton Transactions*, **1993**, 2071.
- [82] K. R. Koch, Y. Wang and A. Coetzee, *Journal of the Chemical Society: Dalton Transactions*, **1999**, 1013.
- [83] A. N. Westra, C. Esterhuysen and K. R. Koch, *Acta Crystallographica, Section C*, **2004**, (C60), m395.
- [84] G. Fitzel, L. Beyer, J. Sieler, R. Richter, J. Kaiser and E. Hoyer, *Zeitschrift für Anorganische und Allgemeine Chemie*, **1977**, (433), 237.
- [85] A. Irving, K. R. Koch and M. Matoetoe, *Inorganica Chimica Acta*, **1993**, (206), 193.
- [86] K. R. Koch, J. d. Toit, M. R. Caira and C. Sacht, *Journal of the Chemical Society: Dalton Transactions*, **1994**, 785.
- [87] R. G. Pearson, *Journal of Chemical Education*, **1968**, (45), 581.
- [88] R. G. Pearson, *Journal of Chemical Education*, **1968**, (45), 643.
- [89] G. M. Sheldrick, *SHELXS97 and SHELXL97*, 1997, University of Göttingen, Germany.
- [90] J. L. Atwood and L. J. Barbour, *Crystal Growth and Design*, **2003**, (3), 3.
- [91] K. R. Koch and S. Bourne, *Journal of Molecular Structure*, **1998**, (441), 11.
- [92] K. R. Koch, T. Grimmbacher and C. Sacht, *Polyhedron*, **1998**, (17), 267.
- [93] M. Matoetoe, *M.Sc Thesis*, University of Cape Town, **1990**.
- [94] J. N. Miller, *Analyst*, **1991**, (116), 3.
- [95] J. S. Hunter, *Journal of the Association of Official Analytical Chemists*, **1981**, (64), 574.
- [96] K. R. Koch, *et al.*, *Unpublished results*.
- [97] *Isotope Patterns*, copyright WebElements™ 1993-2007 Mark Winter [The University of Sheffield and WebElements Ltd], <http://www.webelements.com>, accessed 17/05/2007, last updated.
- [98] J. McMurry, *Organic Chemistry, 5th edition*, Brooks/Cole, Pacific Grove, **2000**.
- [99] Y. Marcus, *The Properties of Solvents*, John Wiley and Sons Ltd, Chichester, **1998**.
- [100] *CRC Handbook of Chemistry and Physics, 87th edition, 2006-2007*, CRC Press - Taylor and Francis Group, Florida, **2006**.
- [101] V. Gutmann and E. Wychera, *Inorganic and Nuclear Chemistry Letters*, **1966**, (2), 257.
- [102] R. W. Soukup and R. Schmid, *Journal of Chemical Education*, **1985**, (62), 459.
- [103] M. J. Kamlet and R. W. Taft, *Journal of the American Chemical Society*, **1976**, (98), 377.
- [104] M. J. Kamlet and R. W. Taft, *Journal of the American Chemical Society*, **1976**, (98), 2886.

- [105] M. J. Kamlet, J.-L. M. Abboud, M. H. Abraham and R. W. Taft, *Journal of Organic Chemistry*, **1983**, (48), 2877.
- [106] I. Koppel and V. Palm, *Organic Reactions (Tartu)*, **1976**, (11), 121.
- [107] M. Haro, V. Rodríguez, P. Cea, M. C. López and C. Lafuente, *International Journal of Thermophysics*, **2004**, (25), 669.
- [108] *Acetonitrile Physical Properties*, copyright Sigma-Aldrich, **2008**,
http://www2.sigmaaldrich.com/suite7/Area_of_Interest/Research_Essentials/Solvents/Acetonitrile_Center/Physical_Properties.html, accessed 25/02/2008, last updated 2008.
- [109] S. Keunchkarian, M. Reta, L. Romero and C. Castells, *Journal of Chromatography*, **2006**, (1119), 20.
- [110] *Intermolecular Forces*, copyright AUS-e-TUTE, **2007**, <http://www.ausetute.com.au/intermof.html>, accessed 25/08/2007, last updated.
- [111] S. E. Livingstone in *Comprehensive Inorganic Chemistry, Vol. 3* (Ed.: J. C. Bailar), Pergamon Press, Oxford, **1973**.
- [112] C. M. Harris, S. E. Livingstone and I. H. Reece, *Journal of the Chemical Society*, **1959**, 1505.
- [113] S. E. Livingstone and B. Wheelahan, *Australian Journal of Chemistry*, **1964**, (17), 219.
- [114] D. Pavia, G. Lampman and G. Kriz, *Introduction to spectroscopy, 3rd edition*, Harcourt College Publishers, Orlando, **2001**.
- [115] B. Stevens, *Chemical kinetics for general students of chemistry*, Chapman and Hall Ltd, London, **1970**.
- [116] L. Arnaut, S. Formosinho and H. Burrows, *Chemical kinetics: from molecular structure to chemical reactivity*, Elsevier, Amsterdam, **2007**.
- [117] P. W. Atkins, *Physical chemistry, 6th ed.*, Oxford University Press, Oxford, **1999**.
- [118] M. Bodenstein, *Zeitschrift für physikalische Chemie*, **1894**, (13), 56.
- [119] M. Bodenstein, *Zeitschrift für physikalische Chemie*, **1897**, (22), 1.
- [120] M. Bodenstein, *Zeitschrift für physikalische Chemie*, **1898**, (29), 295.
- [121] J. Chocholoušová, J. Vacek and P. Hobza, *Journal of Physical Chemistry A*, **2003**, (107), 3086.
- [122] H. Bartnicka, I. Bojanowska and M. K. Kalinowski, *Australian Journal of Chemistry*, **1991**, (44), 1077.
- [123] J. March, *Advanced organic chemistry: Reactions, mechanisms and structure, 4th ed.*, Wiley-Interscience, New York, **1992**.
- [124] G. M. Barrow, *Physical Chemistry, 3rd ed.*, McGraw-Hill Kogakusha, Tokyo, **1973**.
- [125] M. R. Burger, *Unpublished results*, **2007**.
- [126] D. C. Hanekom, *M.Sc Thesis*, University of Stellenbosch, **2005**.

Appendices

Appendix A – Crystal structure and refinement data for *cis*-Pd(L⁶-S,O)₂, *cis*-Pd(L⁹-S,O)₂, *cis*-Pd(L¹⁰-S,O)₂ and Pd(L³-S,O)(L⁴-S,O)

		<i>cis</i> -Pd(L ⁶ -S,O) ₂ (page 47)	<i>cis</i> -Pd(L ⁹ -S,O) ₂ (page 49)	<i>cis</i> -Pd(L ¹⁰ -S,O) ₂ (page 50)	<i>cis</i> -Pd(L ³ -S,O)(L ⁴ -S,O) (page 73)	
Molecular formula		C ₂₄ H ₂₆ F ₄ N ₄ O ₂ PdS ₂	C ₁₆ H ₃₀ N ₄ O ₂ PdS ₂	C ₂₀ H ₃₄ N ₄ O ₄ PdS ₂	C ₂₉ H ₄₀ N ₄ O ₇ PdS ₂	
Formula weight (g.mol⁻¹)		649.01	480.96	565.03	727.17	
Crystal system		Orthorhombic	Orthorhombic	Monoclinic	Orthorhombic	
Space group		<i>Pbca</i>	<i>Pbcn</i>	<i>P2₁/n</i>	<i>Pbca</i>	
Unit cell dimensions	(Å)	a	12.3706 (11)	9.7113 (12)	10.657 (2)	16.272 (2)
		b	18.8355 (17)	21.183 (3)	10.361 (2)	13.1455 (17)
		c	22.0840 (19)	10.3483 (13)	21.850 (5)	29.774 (4)
	(°)	α	90.00	90.00	90.00	90.00
		β	90.00	90.00	91.597 (4)	90.00
		γ	90.00	90.00	90.00	90.00
Volume (Å³)		5145.7 (8)	2128.8 (5)	2411.7(8)	6368.9 (14)	
μ (mm⁻¹)		0.943	1.084	0.976	0.765	
Z		8	4	4	8	
Temperature (K)		100 (2)	100 (2)	100 (2)	446 (2)	
Reflections collected / unique		30700 / 6130 (R _{int} = 0.1360)	12150 / 2516 (R _{int} = 0.0766)	14447 / 5557 (R _{int} = 0.1087)	37983 / 7578 (R _{int} = 0.1523)	
θ range for data collection (°)		2.1625 – 20.1885	2.307 – 23.758	2.1755 – 17.7135	2.4165 – 19.1745	
Goodness-of-fit on F²		1.046	1.257	0.990	1.206	
Final R [I > 2σ(I)] (all data)		0.0661	0.0754	0.0661	0.1501	
wR₂ [I ≥ 2σ(I)] (all data)		0.1089	0.1351	0.1093	0.2351	
Largest residual e-density	peak	1.478	1.236	1.375	1.641	
	hole	-1.370	-1.556	-1.126	-0.956	

Appendix B1 – Calculation of error on instrument signal replicates[§]

Data for repeated injections of an equilibrium mixture of *cis*-Pd(L³-S,O)₂ and *cis*-Pd(L⁴-S,O)₂. The data for *cis*-Pd(L³-S,O)₂ at 291 nm results in the largest relative percentage error of 0.71 % (as reported on page 65).

Replicate #	230		291	
	Pd(L ³) ₂	Pd(L ⁴) ₂	Pd(L ³) ₂	Pd(L ⁴) ₂
1	89	95.4	90.5	97.8
2	89.2	95.4	91.4	98.4
3	89.4	95.1	91.3	99.3
4	89.7	95	91.6	99.2
5	89.9	94.4	92.3	98.8
mean	89.44	95.06	91.42	98.7
std dev	0.3647	0.4099	0.6458	0.6164
relative % error	0.41	0.43	0.71	0.62

Appendix B2 – Estimation of error around calculated concentration values[§]

The data for *cis*-Pd(L³-S,O)₂ at 291 nm (0.71 rel % error) above was taken as the “worst case scenario”. The 95 % confidence interval around the instrument signal (y-value) was calculated to be 0.80284. Adding or subtracting $0.40142 \left(\frac{\text{confidence interval}}{2} \right)$ from the mean y-value of 91.42 gives the upper and lower values respectively of the confidence limits around a measured instrument signal. These confidence limit values were substituted into each of the four calibration graph equations $y = mx + c$ (see table below). The relative error in the x-values was calculated using: $\text{rel \% error} = 100 \cdot \frac{\text{confidence interval}}{2 \cdot \text{mean}}$

mean y-value	confidence interval 95%	calibration equation	230 nm				291 nm			
			Pd(L ³) ₂		Pd(L ⁴) ₂		Pd(L ³) ₂		Pd(L ⁴) ₂	
91.42	0.80284	m	36120		34133		37355		32229	
y_{min}	91.02	c	-0.481		-1.674		-2.788		3.926	
y_{max}	91.82		x_{min}	x_{max}	x_{min}	x_{max}	x_{min}	x_{max}	x_{min}	x_{max}
			2.53E-03	2.56E-03	2.72E-03	2.74E-03	2.51E-03	2.53E-03	2.70E-03	2.73E-03
		confidence interval	2.22E-05		2.35E-05		2.15E-05		2.49E-05	
		relative % error	0.44		0.43		0.43		0.46	

[§] Many thanks to Ms M.R. Burger for the spreadsheet used in these calculations

Appendix C – Calculation of 95 % confidence interval for calibration graphs^[94]

In order to calculate the 95 % confidence interval, it is necessary to first obtain an estimate of the random errors on the slope and intercept of the linear regression line $y = mx + c$ using the following equations:

$$\begin{array}{l|l}
 \text{Slope:} & \text{Intercept:} \\
 s_m = \frac{s_{y/x}}{\sqrt{\sum_i (x_i - \bar{x})^2}} & s_c = s_{y/x} \sqrt{\frac{\sum_i x_i^2}{n \sum_i (x_i - \bar{x})^2}} \\
 \hline
 \text{Where } s_{y/x} = \sqrt{\frac{\sum_i (y_i - \hat{y}_i)^2}{n-2}} &
 \end{array}$$

x_i and y_i represent each individual set of data points from the experimentally measured calibration line, while \hat{y} is the corresponding point on the calculated regression line. \bar{x} is the x-value of the centroid of the regression line.

The standard deviations of the slope and the intercept can be obtained from the equations:

$$\begin{array}{l|l}
 \text{Standard deviation of the slope:} & \text{Standard deviation of the intercept:} \\
 m \pm ts_m & c \pm ts_c
 \end{array}$$

where the value of t is chosen at the 95 % confidence interval for $n - 2$ degrees of freedom.

These calculated confidence limits can be used to determine whether the experimentally measured calibration points differ significantly from the calculated linear regression line. For instance, to ascertain whether the intercept of the calibration line differs appreciably from 0, one merely needs to establish whether the 95 % confidence interval around the intercept a , includes 0. For the intercepts of the calibration lines shown in Figure 2.12 on page 60 ($t = 2.45$):

	230 nm		291 nm
	$y = - 1.6737 + 34133x$		$y = 3.926 + 32229x$
$s_c =$	1.31		3.36
$ts_c =$	3.217		8.232

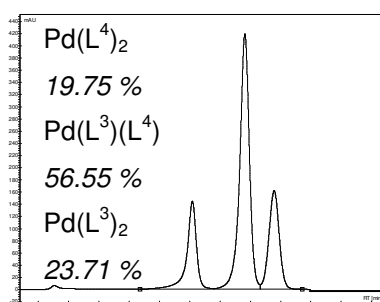
For both the 230 and 291 nm calibration lines, the confidence intervals around the intercepts do indeed include 0, making it valid to use only the slope of the calibration line for calculations.

Appendix D1 – “Cold” synthetic method adapted from Mautjana *et al.*^[46]

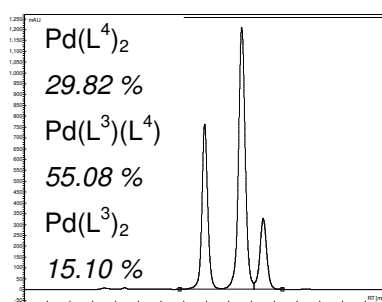
In the “cold” synthetic method, 0.03 mmol $K_2[PdCl_4]$ and 0.03 mmol of each ligand, HL^3 and HL^4 , along with 0.12 mmol sodium acetate, in 15 ml of a 50/50 v/v mixture of acetonitrile and water was shaken in a separating funnel. The mixture was left to stand for an hour and occasionally agitated. The crude complex settled out of solution as a light brown, powdery precipitate. 10 ml saturated sodium chloride solution (5.8 M) was then added bring about a salt-induced phase separation. The water-rich lower layer was discarded and the precipitate, suspended in the acetonitrile-rich upper layer, was separated by filtration and washed with water before being rinsed with a portion of cold ethanol and dried under vacuum.

Appendix D2 – Chromatograms and distributions of recrystallised crude synthesised product of Pd(II) salt with HL^3/HL^4 .

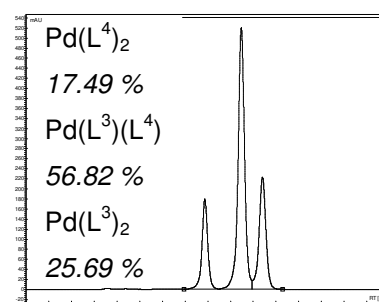
The more polar $cis-Pd(L^4-S,O)_2$ is favoured in the polar recrystallisation and the less polar $cis-Pd(L^3-S,O)_2$ in the non-polar recrystallisation.



(a) Crude product



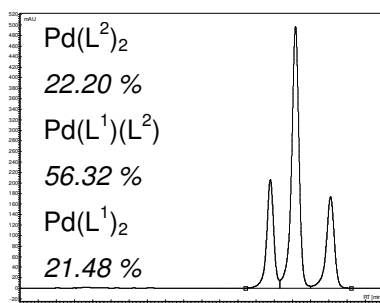
(b) Recrystallised from polar acetone/water



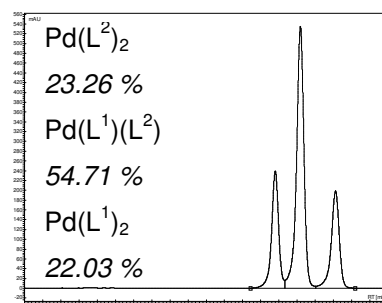
(c) Recrystallised from non-polar chloroform/ethanol

Appendix D3 – Chromatograms and distributions of crude and recrystallised synthesised product of Pd(II) salt with HL^1/HL^2 .

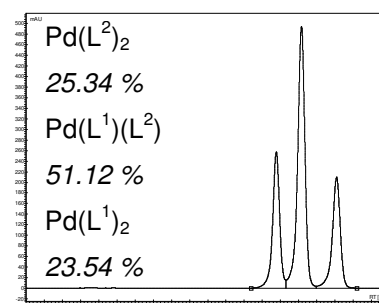
There is no favouring of one complex in this set of experiments.



(a) Crude product



(b) Recrystallised from polar acetone/water



(c) Recrystallised from non-polar chloroform/ethanol

Appendix E – Detection wavelengths

Please refer to the table on page 51 for the structures of these complexes.

Combination		Wavelengths (nm)	
Parent 1	Parent 2	λ_1	λ_2
$\text{Pd}(\text{L}^1)_2$	$\text{Pd}(\text{L}^2)_2$	234	273
$\text{Pd}(\text{L}^1)_2$	$\text{Pd}(\text{L}^4)_2$	238	281
$\text{Pd}(\text{L}^1)_2$	$\text{Pd}(\text{L}^5)_2$	220	238
$\text{Pd}(\text{L}^1)_2$	$\text{Pd}(\text{L}^6)_2$	216	232
$\text{Pd}(\text{L}^1)_2$	$\text{Pd}(\text{L}^8)_2$	222	255
$\text{Pd}(\text{L}^1)_2$	$\text{Pd}(\text{L}^{10})_2$	222	291
$\text{Pd}(\text{L}^3)_2$	$\text{Pd}(\text{L}^4)_2$	230	291
$\text{Pd}(\text{L}^4)_2$	$\text{Pd}(\text{L}^6)_2$	243	274
$\text{Pd}(\text{L}^4)_2$	$\text{Pd}(\text{L}^8)_2$	234	293
$\text{Pd}(\text{L}^5)_2$	$\text{Pd}(\text{L}^6)_2$	229	254
$\text{Pd}(\text{L}^6)_2$	$\text{Pd}(\text{L}^{10})_2$	277	297
$\text{Pd}(\text{L}^9)_2$	$\text{Pd}(\text{L}^{10})_2$	237	273

These wavelengths were all chosen such that the parent complexes had near-equal absorbance. All wavelengths were rounded off to the nearest whole number value as the Varian HPLC system could only monitor whole number wavelengths (see Section 2.2.2 for more detail).

Appendix F – Bodenstein's numerical method ^[118-120] (see Section 4.1)

For the reversible reaction: $M(L^A)_2 + M(L^B)_2 \xrightleftharpoons[k']{k} 2M(L^A)(L^B)$

The rate laws are:

$$\frac{d[MA_2]}{dt} = \frac{d[MB_2]}{dt} = k'[MAB]^2 - k[MA_2][MB_2] \quad (1a)$$

$$\frac{d[MAB]}{dt} = k[MA][MB] - k'[MAB]^2 \quad (1b)$$

Setting $[MA_2] = [MB_2] = x$ and $[MAB] = y$ for clarity, equations 1a and 1b become:

$$\frac{dx}{dt} = k' \cdot y^2 - k \cdot x^2 \quad (2a)$$

$$\frac{dy}{dt} = k \cdot x^2 - k' \cdot y^2 \quad (2b)$$

Assuming that the initial concentrations of the two parent complexes are exactly equal (a_0), the concentration of the mixed-ligand product, MAB can be represented by: $y = 2(a_0 - x)$ and the concentration of the parent complexes, MA_2 and MB_2 , represented by: $x = a_0 - \frac{y}{2}$. Substituting these new relationships as well as for the reverse rate constant ($k' = \frac{k}{K}$) produces equations in only one variable (k and K are constants):

$$\begin{aligned} \frac{dx}{dt} &= 4 \frac{k}{K} \cdot (a_0 - x)^2 - k \cdot x^2 \\ &= \left(\frac{4}{K} - 1 \right) k x^2 - \frac{8a_0}{K} k x + \frac{4a_0^2}{K} k \end{aligned} \quad (3a)$$

$$\begin{aligned} \frac{dy}{dt} &= k \cdot \left(a_0 - \frac{y}{2} \right)^2 - \frac{k}{K} \cdot y^2 \\ &= - \left(\frac{4}{K} - 1 \right) \frac{ky^2}{4} - a_0 ky + a_0^2 k \end{aligned} \quad (3b)$$

When $K = 4$, as was the case in Moriyasu and Hashimoto's experiments,^[7, 16] these equations may be integrated to produce:

$$-\ln\left(1 - \frac{2x}{a_0}\right) = ka_0 t \quad (4a)$$

$$-\ln\left(1 - \frac{y}{a_0}\right) = ka_0 t \quad (4b)$$

If $K \neq 4$, the equation on page 105 must be used.

Appendix G – Equilibrium constants and time taken to reach equilibrium for concentration/aging experiments (see Figure 4.6 on page 111)

Concentration	800	400	200	100
Age upon mixing: Fresh				
K	5.90	5.82	5.76	4.94
time to equilibrium (hrs)	48	48	48	48
Age upon mixing: 1 day				
K	5.79	5.35	5.96	5.37
time to equilibrium (hrs)	24	24	24	48
Age upon mixing: 2 days				
K	4.71	5.26	6.36	3.38
time to equilibrium (hrs)	24	24	18	24
Age upon mixing: 3 days				
K	5.97	5.34	5.79	4.22
time to equilibrium (hrs)	48	18	18	24
Age upon mixing: 5 days				
K	4.65	5.28	5.81	4.79
time to equilibrium (hrs)	18	18	18	24
Age upon mixing: 7 days				
K	3.40	5.21	5.83	5.63
time to equilibrium (hrs)	18	18	18	24

Index of figures, tables and schemes

List of Figures

Figure 1.1. Olefin metathesis.	2
Figure 1.2. <i>N,N</i> -dialkyl- <i>N</i> -aroyl(acyl)thiourea ligand.....	4
Figure 1.3. bis(<i>N,N</i> -disubstituted dithio- or diselenocarbamato)metal(II) complex (E = S or Se)	5
Figure 1.4. Two-dimensional TLC separation of mixture of (a) bis(<i>N,N</i> -diethyldithiocarbamato)Ni(II) (c) bis(<i>N,N</i> -dihexyldithiocarbamato)Ni(II) and (b) their mixed ligand complex.....	6
Figure 1.5. Chromatograms of the individual parent complexes as well as the mixture of the two.	6
Figure 1.6. Reaction between a bis(<i>N,N</i> -dialkyl dithiocarbamato)Ni(II) complex and a Ni(II) complex of a different ligand.	7
Figure 1.7. bis(<i>cis</i> -1,2 disubstituted dithiolato)metal(II) complex.	10
Figure 1.8. The three complexes in solution present immediately after mixing.	13
Figure 1.9. Diagram illustrating the relationship between the ten possible dimeric complexes and the three monomeric complexes. The two different ligands are indicated by + and -. ^[19]	13
Figure 1.10. (a) Vicinal and (b) geminal dichalcogen complexes studied by Olk <i>et al.</i> M = Cu, Ni or Pd. ^[9]	14
Figure 1.11. UV-Vis spectra of the two parent Ni(II) complexes	15
Figure 1.12. Crystal structure of the anionic mixed-ligand Pd(II) complex studied by Olk <i>et al.</i> ^[9] The counter-ion has been omitted	16
Figure 1.13. Structure of (a) bis(dithiolato)Ni(II) complex and (b) bis(α -diiminato)Ni(II) complex.....	17
Figure 1.14. α -diimine ligands studied by Miller and Dance.	17
Figure 1.15. The complexes studied by Ohya <i>et al.</i>	19
Figure 1.16. Dependence of K on the dielectric constant of the solvent. ^[8]	20
Figure 1.17. Metathesis reactions between metal complexes of these N/O donor ligands were studied..	21
Figure 1.18. Substituted Ni(II) complexes studied by Lockhart and Mossop.	22
Figure 1.19. The photoinduced <i>cis-trans</i> isomerisation of <i>cis</i> -M(L-S,O) ₂ complexes. M = Pd(II) or Pt(II) .	28
Figure 1.20. Application ranges for different classes of chromatography.	30
Figure 1.21. Schematic representation of Huber and Kraak's liquid chromatography system.	31
Figure 1.22. Separation of acetylacetonato complexes of Be(II), Fe(III), Cr(III) and Co(III)	32
Figure 1.23. Separation of six metal acetylacetonato complexes	33
Figure 1.24. HPLC separation of mixed hexachlorofluoro Os(IV) complexes.....	33
Figure 1.25. HPLC separation of Pt(II), Pd(II) and Rh(III) after complexation with	34
Figure 1.26. H ₂ L and HL ligands.	35
Figure 2.1. <i>N,N</i> -dialkyl- <i>N</i> -aroyl(acyl)thiourea ligand.....	40
Figure 2.2. <i>cis</i> -bis(<i>N,N</i> -dialkyl- <i>N</i> -aroyl(acyl)thioureato)Pd(II) complex.	41
Figure 2.3. Chromatograms of the same compound before and after extensive recrystallisation.....	42
Figure 2.4. Metathesis reaction of interest.	52

Figure 2.5. Possible chromatogram patterns for metathesis reactions.....	52
Figure 2.6. Varian HPLC system.....	54
Figure 2.7. Representative sequence for one 24 hour long experiment.....	55
Figure 2.8. UV-Vis spectra of 20 μM solutions of two substituted <i>cis</i> -bis(<i>N,N</i> -diethyl- <i>N'</i> -benzoylthioureato) Pd(II) complexes 1 and 2, illustrating the whole number wavelengths at which the complexes possess near equal absorbance.....	56
Figure 2.9. Graph of area (for 291 nm) vs. reaction time for Pd(L ³) ₂ and Pd(L ⁴) ₂	57
Figure 2.10. Mass spectra of the same compound before (above) and after addition of formic acid to the mobile phase. The inset shows the structure of the compound along with its mass.	58
Figure 2.11. Raw data from a single run, as copied from the Galaxie software.	59
Figure 2.12. Calibration graph for a 400 μM solution of Pd(L ⁴) ₂ , showing the regression lines fitted to the data.....	60
Figure 2.13. Overlaid chromatograms of 10 μl volumes of different 400 μM solutions of Pd(L ³) ₂	64
Figure 2.14. Data from the repeated experiments.	65
Figure 2.15. Confidence limits around a concentration value calculated from the calibration graph.....	66
Figure 2.16. Representative data set, including error bars. The overall relative error is approximately 11.6 %.	67
Figure 3.1. Metathesis reaction of interest, M = Ni(II) Pd(II) or Pt(II).	69
Figure 3.2. Aromatic region of ¹ H NMR spectra for the reaction between Ni(L ²) ₂ and Ni(L ⁴) ₂ , immediately after mixing (upper spectrum) and at equilibrium (lower spectrum).	70
Figure 3.3. Time-arrayed acquisition for the metathesis reaction between Pd(L ³) ₂ and Pd(L ⁴) ₂	71
Figure 3.4. Representative chromatogram illustrating the three species present.....	71
Figure 3.5. Isotope distribution patterns for Pd and Pt. ^[97]	72
Figure 3.6. Mass spectrum of mixed-ligand Pt(L ⁴)(L ⁸) complex showing expansion of the isotope pattern.	72
Figure 3.7. Crystal structure of the mixed-ligand	73
Figure 3.8. Chromatogram of metathesis reaction in a mixture of equal volumes of.....	74
Figure 3.9. Equilibrium chromatogram of metathesis reaction between Pd(L ³) ₂ and Pd(L ⁴) ₂ after two days. No decomposition of the complexes is evident. The equilibrium distribution is included on the chromatogram with each percentage value next to the appropriate peak.	75
Figure 3.10. Chromatogram of solution of Pd(L ³) ₂ and Pd(L ⁴) ₂ after 3 months.....	75
Figure 3.11. Proposed solvated Pd(L)(CH ₃ CN) ₃ complex.....	76
Figure 3.12. Metathesis reaction between three complexes: Pd(L ²) ₂ , Pd(L ³) ₂ and Pd(L ⁴) ₂	76
Figure 3.13. Equilibrium chromatogram of metathesis reaction between Pt(L ⁴) ₂ and Pt(L ⁸) ₂ after three months. Some decomposition of the complexes is evident.	77
Figure 3.14. Equilibrium chromatogram of metathesis reaction between Pd(L ⁴) ₂ and Pt(L ⁸) ₂ after three months. Some decomposition of the complexes is evident.	78

Figure 3.15. Chromatogram of metathesis reaction between Pd(L ⁴) ₂ and Pt(L ⁸) ₂ after 3 weeks.....	78
Figure 3.16. Chromatograms of reaction between Pd(L ³) ₂ and Pd(L ⁴) ₂ at (a) room temperature (equilibrium) or (b) under reflux.....	79
Figure 3.17. The distribution of complexes from the two synthetic methods.....	80
Figure 3.18. Equilibrium constants for various combinations of Pd(L ¹) ₂ with other substituted benzoyl complexes.....	82
Figure 3.19. Equilibrium constants for various combinations of Pd(L) ₂ complexes.....	83
Figure 3.20. Delocalisation through the Pd(L) ₂ complexes.....	85
Figure 3.21. Complexes used in all subsequent experiments.....	85
Figure 3.22. Ratio Pd(L ⁴) ₂ :Pd(L ³) ₂	86
Figure 3.23. Graphical representation of equilibrium distributions for chromatograms seen in Figure 3.22 adjacent.....	86
Figure 3.24. Aromatic region of ¹ H NMR spectrum of Pd(L ³) ₂ and Pd(L ⁴) ₂ in benzene after 24 hours reaction time.....	88
Figure 3.25. Aromatic region of ¹ H NMR spectrum of Pd(L ³) ₂ and Pd(L ⁴) ₂ in benzene after addition of unbound ligand.....	89
Figure 3.26. Metathesis reaction between Pd(L ³) ₂ and Pd(L ⁴) ₂ in 1,4-dioxane after (a) three weeks and (b) four months.....	89
Figure 3.27. Metathesis reaction between Pd(L ³) ₂ and Pd(L ⁴) ₂ in 1,4-dioxane solution after addition of (a) unbound ligand (after one week) or (b) acetonitrile (after four months).....	90
Figure 3.28. Metathesis reaction between Pd(L ³) ₂ and Pd(L ⁴) ₂ in acetone after (a) two days and (b) four months.....	91
Figure 3.29. Metathesis reaction between Pd(L ³) ₂ and Pd(L ⁴) ₂ in acetone solution after addition of (a) unbound ligand (after one day) or (b) acetonitrile (after one day).....	91
Figure 3.30. Metathesis reaction between Pd(L ³) ₂ and Pd(L ⁴) ₂ in alcohol/acetonitrile solutions after 24-hours reaction time.....	92
Figure 3.31. Exchange between a complex and a different unbound ligand.....	94
Figure 3.32. Graphs of the equilibrium distributions in the “complex and unbound ligand” experiments in acetonitrile and toluene.....	95
Figure 3.33. Exchange between Pd(L ¹) ₂ and HL ¹ which is ¹³ C-enriched at the sulphur-carbonyl (*).	98
Figure 3.34. ¹³ C NMR spectrum of Pd(L ¹) ₂ highlighting the carbonyl peak (170.63 ppm) and sulphur-carbonyl peak (171.11 ppm).....	99
Figure 3.35. ¹³ C NMR spectrum of HL ¹ highlighting the carbonyl peak (163.71 ppm) and the ¹³ C-enriched sulphur-carbonyl peak (179.24 ppm).....	99
Figure 3.36. ¹³ C NMR spectrum of the mixture of Pd(L ¹) ₂ and ¹³ C-enriched HL ¹ , highlighting the carbonyl and sulphur-carbonyl region in the insert.....	100

Figure 4.1. Plot of equation 2b for the experiment by Moriyasu and Hashimoto discussed in Section 1.2.1.1. ^[16]	105
Figure 4.2. Complexes used for all the investigations into reaction rate.....	106
Figure 4.3. First set of experiments studying the effect of concentration on rate, showing erratic results.	107
Figure 4.4. Repeat of the concentration-dependence experiments. The reaction rate in all the solutions was the same.	108
Figure 4.5. Revised concentration-dependence experiment, using freshly dissolved solutions.....	108
Figure 4.6. The effect of the “age” of the solutions upon mixing on the rate of metathesis of <i>cis</i> -Pd(L ³ -S,O) ₂ and <i>cis</i> -Pd(L ⁴ -S,O) ₂ in acetonitrile at 20° C.....	111
Figure 4.7. Graph showing the increase in reaction rate for “aged” solutions.	112
Figure 4.8. The unbound ligands used in this set of experiments.....	113
Figure 4.9. Data from addition of 50/50 (mole ratio) mixture of HL ³ and HL ⁴ solution to the mixture of Pd(L ³) ₂ and Pd(L ⁴) ₂	115
Figure 4.10. The effect of unbound HL ⁴ ligand added to a mixture of freshly dissolved Pd(L ³) ₂ and Pd(L ⁴) ₂ solutions. The graph shows the data for the first 6 hours of reaction.	116
Figure 4.11. HL ⁶ ligand.....	117
Figure 4.12. The effect of unbound HL ⁶ ligand added to a mixture of freshly dissolved Pd(L ³) ₂ and Pd(L ⁴) ₂ solutions. The percentage Pd(L ³)(L ⁴) formed is plotted.	118
Figure 4.13. Chromatogram immediately after mixing Pd(L ³) ₂ and Pd(L ⁴) ₂ solutions with 10 mol% HL ⁶ solution.	118
Figure 4.14. Expansion (2.5 – 4 mins t _R) of the equilibrium chromatogram of the mixture of Pd(L ³) ₂ and Pd(L ⁴) ₂ solutions with 10 mol% HL ⁶ solution.	119
Figure 4.15. The effect of acid added to a mixture of freshly dissolved Pd(L ³) ₂ and Pd(L ⁴) ₂ solutions....	122
Figure 4.16. Acetic acid dimer.....	123
Figure 4.17. The effect of base added to a mixture of freshly dissolved Pd(L ³) ₂ and Pd(L ⁴) ₂ solutions. .	124
Figure 4.18. Overlaid chromatograms of the reversion of <i>trans</i> -Pd(L ³) ₂ (red) to <i>cis</i> -Pd(L ³) ₂ (blue) in the dark after one hour of irradiation. Possible photodecomposition products are observed between 1.5 and 3 minutes retention time. This system required 18 hours to revert back to the <i>cis</i> complex exclusively.	126
Figure 4.19. Reverse <i>trans</i> to <i>cis</i> reaction in the dark, postulated as a metathesis reaction.....	127
Figure 4.20. The reversion of <i>trans</i> -Pd(L ³) ₂ to <i>cis</i> -Pd(L ³) ₂ over time.	128

List of Tables

Table 1.1. Possible products from olefin metathesis reactions. ^[3]	3
Table 1.2. Complexes reacted with the bis-(<i>N,N</i> -dialkyl dithiocarbamate)Ni(II) complexes. ^[15]	8
Table 1.3. Selected results from the study by Davison <i>et al.</i> ^[12]	11

Table 1.4. Selected results from the study by Balch. ^[19]	12
Table 1.5. Selected results from the study by Miller and Dance (using route 1). ^[14]	18
Table 1.6. Dielectric constant of solvent vs. equilibrium constant of metathesis reaction. ^[8]	20
Table 1.7. Selected results from the thermodynamic studies by Lockhart and Mossop. ^[5]	23
Table 1.8. Selected results from the kinetic studies by Lockhart and Mossop. ^[6]	25
Table 1.9. Advantages and disadvantages of the methods used to observe metathesis reactions.	27
Table 2.1. Calibration data for a 400 μM solution of $\text{Pd}(\text{L}^4)_2$	60
Table 3.1. Substituted-benzoyl complexes mixed with $\text{Pd}(\text{L}^1)_2$	82
Table 3.2. Reference numbers for the combinations of complexes in Figure 3.19.....	83
Table 3.3 Substituents on the benzoyl ring of the <i>cis</i> -bis(<i>N,N</i> -diethyl- <i>N'</i> -aroyl-thioureato) $\text{Pd}(\text{II})$ complexes.	84
Table 3.4. Solvents used in this investigation and their properties.	87
Table 4.1. Data for the acceleration of the reaction upon addition of the individual unbound ligand solutions.....	116

List of Schemes

Scheme 1.1. The release of an unbound diseleno ligand into solution.....	9
Scheme 1.2. Formation of the 5-coordinate complexes.....	9
Scheme 1.3. Two distinct types of ligand exchange possible for the $\text{Pt}(\text{II})$ and $\text{Pd}(\text{II})$ complexes of dppe and substituted salicylaldimines. ^[20]	26
Scheme 1.4. Coordination modes of H_2L and HL to transition metal(II) ions.....	36
Scheme 2.1. Reaction pathway for the synthesis of <i>N,N</i> -dialkyl- <i>N'</i> -aroyl(acyl)thiourea ligands.....	40
Scheme 2.2. Reaction pathway for the synthesis of <i>cis</i> -bis(<i>N,N</i> -dialkyl- <i>N'</i> -aroyl(acyl)thioureato) $\text{Pd}(\text{II})$ complexes.	41
Scheme 2.3. Calculation of number of moles, concentration and percentage of each species present in solution.	61
Scheme 3.1. Possible mechanism for the metathesis reaction, showing solvent-stabilised intermediate.	93
Scheme 4.1. Schematic representation of the procedure for the age-dependence experiments.....	110
Scheme 4.2. Proposed simplified mechanism for the acceleration of the reaction due to unbound ligand.	120
Scheme 4.3. The effect of addition of concentrated HCl to a solution of <i>cis</i> - $\text{Pt}(\text{L-S},\text{O})_2$. ^[91, 92]	120
Scheme 4.4. Possible mechanism for the acceleration of the reaction due to protons.	122
Scheme 4.5. One possible mechanism for the deceleration of the reaction upon addition of base.	125